Fast Mathematical Algorithms & Hardware Corporation

Vladimir Rokhlin
Ronald R. Coifman
Victor Wickerhauser

1020 Sherman Avenue
Hamden, CT 06514
(203) 288-9444

Project Title :

FAST MULTIPOLE METHODS FOR SCATTERING COMPUTATIONS

FINAL TECHNICAL REPORT October 1994

DARPA # 7894
Monitored by AFOSR Contract No F49620-91-C0084
Contractor FMA&H Corporation
Effective Date of contract 9.1 .1991
Contract expiration date 8.31.94
Total Contract $527,802

Principal Investigators : Ronald R Coifman 203 432 4175
Vladimir Rokhlin 203 432 6490
Program Manager : Dr Arje Nachman 202 767 5025

REPORT DOCUMENTATION PAGE

Form Approved
OMB No. 0704-0188

1. AGENCY USE ONLY (Leave blank)	2. REPORT DATE	3. REPORT TYPE AND DATES COVERED
		FINAL/01 SEP 91 TO 31 AUG 94

4. TITLE AND SUBTITLE
FAST MULTIPOLE METHODS FOR SCATTERING COMPUTATIONS

5. FUNDING NUMBERS
7894/09
F49620-91-C-0084

6. AUTHOR(S)
RONALD R. COIFMAN AND VLADIMIR ROKHLIN

7. PERFORMING ORGANIZATION NAME(S) AND ADDRESS(ES)
FAST MATHEMATICAL ALGORITHMS & HARDWARE CORPORATION
1020 SHERMAN AVENUE
HAMDEN, C T 06514

8. PERFORMING ORGANIZATION REPORT NUMBER
AFOSR-TR- 95 0102

9. SPONSORING/MONITORING AGENCY NAME(S) AND ADDRESS(ES)
AFOSR/NM
110 DUNCAN AVE, SUTE B115
BOLLING AFB DC 20332-0001

10. SPONSORING/MONITORING AGENCY REPORT NUMBER
F49620-91-C-0084

11. SUPPLEMENTARY NOTES

12a. DISTRIBUTION/AVAILABILITY STATEMENT
APPROVED FOR PUBLIC RELEASE: DISTRIBUTION IS UNLIMITED

12b. DISTRIBUTION CODE

The purpose of this phase of the project was to develop fast algorithms for computations of electromagnetic scattering (radar), and assist in the implementation and development of fast engineering software using these algorithms by the team at Hughes Research Laboratories.

Present methods for computing radar cross sections and other scattering crossections are severely limited by prohibitive processing and memory requirements. New fundamental FAst Multipole Methods developed over the last few years by Rokhlin (for2-d scattering) held the promise for breaking this computational bottleneck, the goal set out in this project was to extend the work to higher dimensions and to complete the computational infrastructure needed for converting these algorithms to engineering tools.

The codes and algorithms obtained in this joint effort between HRL and FMAH have already changed the state of the art in this area of electromagnetics simulations and promise to revolutionize computational design technology. We have verified that these algorithms provide the expected improvements and scaling.

14. SUBJECT TERMS

17. SECURITY CLASSIFICATION OF REPORT	18. SECURITY CLASSIFICATION OF THIS PAGE	19. SECURITY CLASSIFICATION OF ABSTRACT	20. LIMITATION OF ABSTRACT
UNCLASSIFIED	UNCLASSIFIED	UNCLASSIFIED	SAR(SAME AS REPORT)

NSN 7540-01-280-5500

FINAL REPORT summary

The purpose of this phase of the project was to develop fast algorithms for computations of electromagnetic scattering (radar), and assist in the implementation and development of fast engineering software using these algorithms by the team at Hughes Research Laboratories.

Present methods for computing radar cross sections and other scattering crossections are severely limited by prohibitive processing and memory requirements. New fundamental Fast Multipole Methods developed over the last few years by Rokhlin (for 2-d scattering) held the promise for breaking this computational bottleneck, the goal set out in this project was to extend the work to higher dimensions and to complete the computational infrastructure needed for converting these algorithms to engineering tools .

The codes and algorithms obtained in this joint effort between HRL aand FMAH have already changed the state of the art in this area of electromagnetic simulations and promise to revolutionize computational design technology. We have verified that these algorithms provide the expected improvements and scaling (see reports for detailed technical presentation).

During the last three years, several technical developments took place. Following is a summary discussion of such developments.

1. The most significant algorithmic development of the first phase has been the construction of the complete three-dimensional version of the Fast Multipole Method for the Helmholtz equation (see me, CRW). As expected, it required a certain amount of serious analytical work. However, at a certain point, the complete theory was constructed, and the whole project assumed a purely technical character, much like its two-dimensional counterpart. This was the only algorithmic step that could actually fail, and once we made it, the overall project became significantly simpler. (see report 1)

2. As expected, we combined the two-dimensional FMM with a wavelet-style scheme, obtaining a version of the FMM that is almost entirely insensitive to the increase in the number of nodes on the sub-wavelength scale. The algorithm has been implemented at FMAH, . The Hughes group is about to start incorporating the scheme into its codes, while the FMAH group is extending it to three dimensions. This development

permits us to perform calculations with extremely high accuracy (essentially, with machine precision) at a very limited additional cost.

3. Somewhat unexpectedly, we discovered that the existing FMM for the Helmholtz equation can be significantly improved (see report). More specifically, there exists a single-stage FMM with the asymptotic CPU time estimate $O(N^{4/3})$, as opposed to the prior estimates of $O(N^{3/2})$, with N the total number of nodes on the boundary of the scatterer. When a multi-stage FMM is used, the result is a considerably faster algorithm. The method has been implemented at FMAH in two dimensions, and the resulting scheme has the break-even point with the direct method at $N \sim 500$, which is beginning to approach the efficiency of the FMM for the Laplace equation. The Hughes group is in the process of incorporating this improvement into their codes, and a detailed report is in preparation.

4. A detailed investigation has been undertaken of the behaviour of the FMM when the boundaries of the scatterers are reasonably smooth (see report 2). This resulted in the discovery of the "Coifman-Meyer basis", a remarkable basis in which the integral operators of scattering theory (and many other operators of interest) are sparse. This development is of significant general interest, since it can be viewed as a localized version of the Fourier Transform - an object known to be very desirable in many areas of applied mathematics.

5. Several algorithms have been constructed for the direct (non-iterative) solution of integral equations with dense kernels (see [Jones, Ma, Rokhlin], [Starr, Rokhlin], [Starr]). While none of these results is specifically applicable to the Helmholtz equation, together they develop an apparatus that can (and will) be applied to the scattering problems.

6. An important technical step in the numerical solution of an integral equation is the choice of the discretization. When the kernel of the integral equation is singular, the latter involves the choice (or the construction) of an efficient quadrature formula for functions with appropriate singularities. Somewhat surprisingly, the existing quadratures leave much to be desired in the context of the integral equations of scattering theory, both in two and three dimensions. As a part of our project, we have expended a significant amount of effort to improve the quadratures for functions with singularities of relevant types. [see report].

Faster Single-Stage Multipole Method for the Wave Equation *

Ronald Coifman
Vladimir Rokhlin
Fast Mathematical Algorithms and Hardware Corp.

Stephen Wandzura
Hughes Research Labs

Abstract

The fast multipole method (FMM) provides a sparse decomposition of the impedance matrix arising from a discretization of an integral equation equivalent to the wave equation with radiation boundary condition. Mathematically, the sparse factorization is made possible by a diagonal representation of translation operators for multipole expansions. Physically, this diagonal representation corresponds to the complete determination of fields in the source-free region by the far fields alone.

Because the diagonal form of the translation operator is not a well behaved function, it must be filtered in numerical practice. (This does not constitute a practical limitation to the accuracy of the results obtained with the method because of the superalgebraic convergence of the multipole expansions.) In the originally published version of the FMM, the filtering was accomplished by a simple truncation of the

*This research was supported by the Advanced Research Projects Agency of the Department of Defense and was monitored by the Air Force Office of Scientific Research under Contracts No. F49620-91-C-0064 and F49620-91-C-0084. The United States Government is authorized to reproduce and distribute reprints for governmental purposes notwithstanding any copyright notation hereron.

multipole expansion of the translation operator. This sharp cutoff results in an oscillatory transfer function that is non-negligible over the entire unit sphere (i.e., in all far-field directions). Physically, the transfer function represents the effect a bounded source has on a well-separated observation region, expressed in terms of the far field of the source. This suggests that a suitable transfer function might be non-negligible only in the direction of the separation vector. It turns out that such a transfer function may be obtained by applying a smooth cutoff to the multipole expansion. Although such a transfer function requires the tabulation of far fields in a denser set of directions, the overall computational and storage requirements for a single-stage FMM are reduced to $\mathcal{O}(N^{4/3})$ from $\mathcal{O}(N^{3/2})$.

1 Review of FMM

The fast multipole method (FMM) for the wave equation[1, 2] gives a prescription for a sparse decomposition of the (impedance) matrix obtained by discretization of the integral kernel

$$G(\mathbf{x}-\mathbf{x}') = \frac{e^{ik|\mathbf{x}-\mathbf{x}'|}}{4\pi\,|\mathbf{x}-\mathbf{x}'|}\,. \tag{1}$$

Mathematically, this decomposition ensues from the diagonal form of the translation operator in the far-field representation[3]. For brevity, this summary relies heavily on the exposition and notation of [2].

Briefly, the FMM works by decomposing the interactions into near-field and far-field parts. This is done by dividing the scatterer into groups and classifing each pair of groups as near or far. The matrix representing the near-field part is sparse by virtue of locality. The far-field part may be factored by using

$$\frac{e^{ik|\mathbf{X}+\mathbf{d}|}}{|\mathbf{X}+\mathbf{d}|} \approx \frac{ik}{4\pi}\int d^2\hat{k}\, e^{i\mathbf{k}\cdot\mathbf{d}}\mathcal{T}_L(kX, \hat{k}\cdot\hat{X})\,, \tag{2}$$

where the $\mathcal{T}$ is the diagonal representation of the translation operator:

$$\mathcal{T}_L(\kappa, \cos\theta) \equiv \sum_{l=0}^{L} i^l(2l+1)h_l^{(1)}(\kappa)P_l(\cos\theta)\,, \tag{3}$$

and X is the distance between the two members of a group pair. In the previously published version of the FMM, the sharp cutoff at $l = L$ caused the transfer function $\mathcal{T}$ to be non-negligible over a wide range of angle. As we show below, examination of $\mathcal{T}$ reveals that it may be modified so that it has support only in a narrow range of $\cos\theta$ near 1. The only cost of this modification is a denser sampling of far-field radiation patterns from the groups.

2 The Translation Operator

The transfer function $\mathcal{T}_L(\kappa, \cos\theta)$ represents the interaction between bounded source distributions separated by distance κ/k (where k is the free-space wavenumber) and θ is the angle between the displacement vector of the centers of the groups and a direction at which the far-field of the source distribution is computed. Since we expect the fields radiated from a bounded region to a well separated observation region to be given only in terms of the far-field in directions that point toward the observation region, we might expect that $\mathcal{T}_L(\kappa, \cos\theta)$ would be strongly peaked for $\cos\theta \approx 1$. Furthermore, since convergence of the multipole expansions requires $L \approx kD$, where D is the diameter of the regions, we might also expect that the peak have a width $\delta\theta \propto L/\kappa$. Numerical examination of $\mathcal{T}$ reveals that this is indeed the case; however, there are rather large oscillatory tails outside the peak. In Figure 1, $\mathcal{T}_{10}(30, \cos\theta)$ is plotted. This is the transfer function that one would use for rather small (compared to a wavelength) groups separated by 4.8 wavelengths. The oscillatory tails are reminiscent of *leakage* in power spectrum estimation using the FFT[4]. This suggests that by using a smooth "window function" to compute $\mathcal{T}$ rather than a sharp cutoff, that leakage to large angles may be reduced. In fact, this is the case; even a simple-minded cosine window function, giving

$$\tilde{\mathcal{T}}_L(\kappa, \cos\theta) = \mathcal{T}_L(\kappa, \cos\theta) + \sum_{l=L+1}^{2L} i^l (2l+1) \left[1 - \sin^2 \frac{(l-L)\pi}{2L}\right] h_l^{(1)}(\kappa) P_l(\cos\theta)\,, \quad (4)$$

produces the localized transfer function plotted in Figure 2. Naturally, because we are taking more terms in the multipole expansion of $\mathcal{T}$, we must

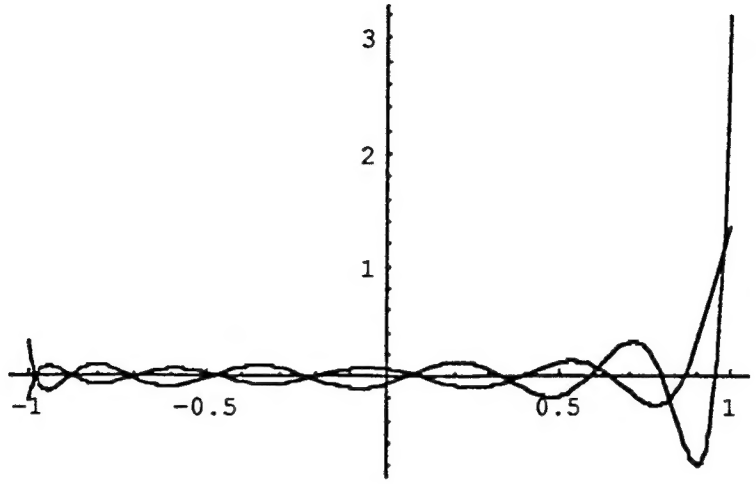

Figure 1: Real and imaginary parts of transfer function $\mathcal{T}$ of $\cos\theta$ for $L = 10$, $\kappa = 30$.

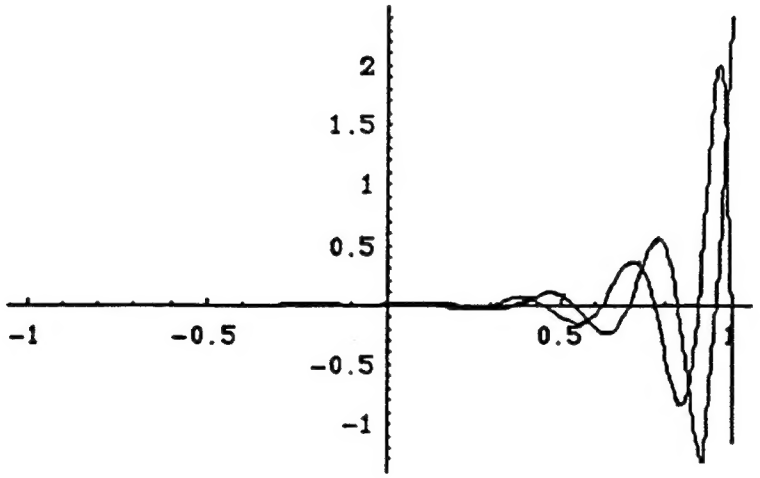

Figure 2: Real and imaginary parts of the localized transfer function $\tilde{\mathcal{T}}$ of $\cos\theta$ for $L = 10$, $\kappa = 30$.

sample the far fields in a denser set of directions appropriate to a quadrature rule for spherical integrations exact for a larger set of spherical harmonics. The trigonometric window function in Eq. (4) is only for purposes of illustration; more efficient windows should be used in practice.

3 Complexity Reduction

A detailed analysis, to be published elsewhere, reveals that the window function of l can be chosen to minimize the support in solid angle of $\mathcal{T}$. This analysis confirms the intuition, implied above, that the solid angle of support of the resulting transfer function is about $\pi(kD)^2/(4\kappa^2)$, where D is the diameter of the groups. In the $\mathcal{O}\left(N^{3/2}\right)$ FMM, the operation count of the translation operator application is $\propto KM^2$, where M is the number of groups and K is the number of far-field directions tabulated. It might now seem that this count should be multiplied by a factor $\propto (kD)^2/(4\kappa^2) \propto 1/M$, giving a total count $\propto (K/M)M^2 \propto N$, which is independent of M. This is incorrect, however, because it implies that by decreasing the size of the groups that the number of directions at which the far-field is used can be reduced without limit. Actually, since we must know the far-field of each group in at least one direction for each other group, the number of directions must go to a constant for very small groups. The total operation count for application of the translation operators is thus $(bN/M^2 + c)\,M^2$, where b and c are implementation dependent constants. (Actually, a more careful analysis gives a factor of $\ln M$ in the b term, but it has no effect on the behavior for large N.) Minimizing the sum of this with the operation count for the other steps in the FMM (aN^2/M, where a is another constant), one sees that, for large problems, b is irrelevant, and the total operation count is minimized by choosing

$$M = \left(\frac{aN^2}{2c}\right)^{1/3}, \tag{5}$$

so that the total operation count is $\mathcal{O}\left(N^{4/3}\right)$. For smaller problems, where the c term does not dominate, the operation count varies roughly as $N \ln N$.

References

[1] V. Rokhlin, "Rapid solution of integral equations of scattering theory in two dimensions," *Journal of Computational Physics*, 86(2):414–439, 1990.

[2] R. Coifman, V. Rokhlin, and S. Wandzura, "The fast multipole method: A pedestrian prescription," *IEEE Antennas and Propagation Society Magazine*, 35(3):7–12, June 1993.

[3] V. Rokhlin, "Diagonal form of translation operators for the Helmholtz equation in three dimensions," *Applied and Computational Harmonic Analysis*, 1(1):82–93, December 1993.

[4] W. H. Press, B. P. Flannery, S. Teukolsky, and W. T. Vetterling, *Numerical Recipes — The Art of Scientific Computing*, Cambridge University Press, Cambridge, 1986.

In [6], a far-reaching generalization of the classical Gaussian quadrature rules is introduced, replacing the polynomials with a wide class of functions. While the rules of [6] possess most of the desirable properties of the classical Gaussian integration formulae (positivity of the weights, etc.), it is not clear from [6] how such quadrature rules can be obtained numerically. In this paper, we present a numerical scheme for the generation of such generalized Gaussian quadratures. The algorithm is applicable to a variety of functions, including smooth functions as well as functions with endpoint singularities. The performance of the algorithm is demonstrated with several numerical examples.

Generalized Gaussian Quadrature Rules For Systems of Arbitrary Functions

J. Ma†, V. Rokhlin†, and S. Wandzura‡

Research Report YALEU/DCS/RR-990
October, 1993

† Research supported in part by DARPA under Contract F49620/91/C/0084, and in part by ONR under Grant N00014-89-J-1527.

‡ Hughes Aircraft Co., California.

Keywords: *Numerical Integration, Quadrature rule, Gaussian Quadrature*

1 Introduction

Classical Gaussian quadrature rules are extremely efficient when the functions to be integrated are well approximated by polynomials. When the functions to be integrated are very different from polynomials, Gaussian quadratures do not perform well; a particularly difficult problem involves the integration of functions of the form

$$f(x) = \sum_{i=1}^{n} \alpha_i \cdot \varphi_i, \tag{1}$$

where each of the functions φ_i has its own singularity at one of the ends of the interval, and the function f can only be evaluated *in toto*, the coefficients α_i being unavailable. This problem is encountered in the solution of integral equations with singular kernels, in the numerical complex analysis, in the numerical solution of elliptic partial differential equations on regions with corners, and in many other situations. While such problems are normally dealt with by means of various ad hoc procedures (see, for example, [1], [7]), these schemes lack the rapid convergence, stability, and elegance of the Gaussian rules.

In fact, in [6], a far-reaching generalization of the classical Gaussian quadratures is introduced, replacing the polynomials with functions from an extremely wide class. The quadrature rules of [6] possess most of the desirable properties of the classical Gaussian integration formulae, such as positivity of the weights, rapid convergence, mathematical elegance, etc. Unfortunately, it is not clear from [6] how such quadrature rules can be obtained numerically.

In this paper, we present a numerical scheme for the construction of such generalized Gaussian quadratures. The algorithm is applicable to a variety of functions, including smooth functions (not necessarily polynomials), as well as functions with end-point singularities.

The paper is organized as follows. In Section 2, we summarize the relevant results from [6], and in Section 3, we restate some numerical methods to be used in this paper. In Section 4, we develop analytical apparatus to be used in the numerical construction of the generalized Gaussian quadrature rules, then we extend those analytical tools to functions with end-point singularities in Section 5. The actual numerical algorithm is presented in Section 6, and the performance of the algorithm is demonstrated with numerical examples in Section 7.

2 Mathematical Preliminaries

In this section, we summarize several classical results from [6] to be used in Sections 4 and 5.

2.1 Chebychev Systems

Definition 2.1 *(Chebyshev System)*

A finite sequence of functions $\{\varphi_1, \varphi_2, \cdots, \varphi_m\}$ *will be referred to as a* Chebyshev system *if and only if each of them is continuous on* $[a, b]$*, and the determinants*

$$\det \begin{pmatrix} \varphi_1(x_1) & \varphi_1(x_2) & \cdots & \varphi_1(x_m) \\ \varphi_2(x_1) & \varphi_2(x_2) & \cdots & \varphi_2(x_m) \\ \vdots & \vdots & & \vdots \\ \varphi_m(x_1) & \varphi_m(x_2) & \cdots & \varphi_m(x_m) \end{pmatrix} \tag{2}$$

are non-zero for any set of m *points* $x_1, x_2, \cdots, x_m \in [a, b]$ *such that* $x_i \neq x_j$ *for any* $i \neq j$*.*

Following are several important cases of Chebyshev systems (for more examples, see [6]).

Example 2.1 *For any natural* m*, the functions* $1, x, x^2, \cdots, x^m$ *constitute a Chebyshev system. Moreover, if* α_1*,* α_2*,* $\cdots$*,* α_m *is a sequence of distinct real numbers, then the system* $\{x^{\alpha_i}\}$ *is a Chebyshev system on any interval* $[a, b] \subset (0, \infty)$*.*

Example 2.2 *For any* n *distinct real numbers* $\alpha_1, \alpha_2, \cdots, \alpha_n$*, the functions* $e^{\alpha_1 x}$*,* $xe^{\alpha_1 x}$*,* $e^{\alpha_2 x}$*,* $xe^{\alpha_2 x}$*,* $\cdots$*,* $e^{\alpha_n x}$*,* $xe^{\alpha_n x}$ *constitute a Chebyshev system on any interval* $[a, b] \subset (-\infty, \infty)$*.*

Definition 2.2 *(Hermite System)*

A finite sequence of functions $\{\varphi_1, \varphi_2, \cdots, \varphi_{2n}\}$ *will be referred to as an* Hermite system *on the interval* $[a, b]$ *if and only if* $\varphi_i \in C^1[a, b]$ *for all* $i = 1, 2, \cdots, 2n$*, and the determinants*

$$\det \begin{pmatrix} \varphi_1(x_1) & \varphi_1'(x_1) & \varphi_1(x_2) & \varphi_1'(x_2) & \cdots & \varphi_1(x_n) & \varphi_1'(x_n) \\ \varphi_2(x_1) & \varphi_2'(x_1) & \varphi_2(x_2) & \varphi_2'(x_2) & \cdots & \varphi_2(x_n) & \varphi_2'(x_n) \\ \vdots & \vdots & \vdots & \vdots & & \vdots & \vdots \\ \varphi_{2n}(x_1) & \varphi_{2n}'(x_1) & \varphi_{2n}(x_2) & \varphi_{2n}'(x_2) & \cdots & \varphi_{2n}(x_n) & \varphi_{2n}'(x_n) \end{pmatrix} \tag{3}$$

are non-zero for any set of $2n$ *points* $x_1, x_2, \cdots, x_{2n} \in [a, b]$ *such that* $x_i \neq x_j$ *for any* $i \neq j$*.*

Definition 2.3 *(Extended Hermite System)*

A finite sequence of functions $\{\varphi_1, \varphi_2, \cdots, \varphi_{2n}\}$ *will be referred to as an* extended Hermite system *if it is both Chebyshev and Hermite.*

Remark 2.1 *The Extended Hermite systems are a slight generalization of the extended Chebychev systems of [6].*

Following are several important cases of extended Hermite systems (for more examples, see [6]).

Example 2.3 *For any natural n, the functions $1, x, x^2, \cdots, x^{2n}$ constitute an extended Hermite system. Moreover, if α_1, α_2, $\cdots$, α_{2n} is a sequence of distinct real numbers, then the system*

$$x^{\alpha_1}, x^{\alpha_2}, \cdots, x^{\alpha_{2n}} \tag{4}$$

is an extended Hermite system on any interval $[a, b] \subset (0, \infty)$.

Example 2.4 *An important special case of the proceeding example is the finite sequence of functions*

$$1, x^{\alpha}, x, x^{1+\alpha}, x^2, x^{2+\alpha}, \cdots, x^{n-1}, x^{n-1+\alpha} \tag{5}$$

with α an arbitrary non-integer real number.

2.2 Gaussian Quadratures

We will be considering integrals of the form

$$\int_a^b \omega(x)\varphi(x)dx, \tag{6}$$

where $\omega : [a, b] \to R^1$ is a non-negative function to be referred to as the weight function, and $\varphi : [a, b] \to R^1$ is a function from a suitably chosen class. A quadrature rule is an expression of the form

$$T_n(\varphi) = \sum_{i=1}^{n} w_i \cdot \varphi(x_i), \tag{7}$$

with $x_i \in [a, b]$ and $w_i \in R^1$ for all $i = 1, 2, \cdots, n$. The points x_i and coefficients w_i are referred to as the nodes and weights of the quadrature formula (7), respectively, while the expression (7) itself is viewed as an approximation to the integral (6). Normally, quadrature formulae are chosen to be exact on certain chosen sets of functions, most frequently, polynomials up to some fixed order m. An $n-$point quadrature formula is referred to as a Gaussian quadrature if and only if it integrates exactly all polynomials of orders up to $2n - 1$.

We will generalize the notion of the classical Gaussian quadrature somewhat, by introducing the following definition.

Definition 2.4 *(Gaussian Quadrature)*
Suppose that

$$\{\varphi_1, \varphi_2, \cdots, \varphi_{2n}\} \tag{8}$$

is a set of integrable functions $[a, b] \to R^1$. We will say that the $n-$point quadrature rule (7) is Gaussian with respect to the system (8) if and only if it integrates exactly all of the functions (8). In other words, a Gaussian rule is an $n-$point rule that is exact for $2n$ pre-chosen functions. We will refer to the nodes and weights of a Gaussian quadrature as the Gaussian nodes and weights, respectively.

Remark 2.2 *Obviously, a classical Gaussian quadrature rule is a Gaussian quadrature rule for which*

$$\begin{aligned} \varphi_1(x) &= 1, \\ \varphi_2(x) &= x, \\ \cdots &\quad \cdots \\ \varphi_{2n}(x) &= x^{2n-1}. \end{aligned} \tag{9}$$

The principal result we use from [6] is the following theorem.

Theorem 2.1 *(Karlin-Studden)*
Suppose that the functions $\{\varphi_1, \varphi_2, \cdots, \varphi_{2n}\}$ *constitute a Chebyshev system on the interval* $[a, b]$. *Then there exists a unique n-point quadrature rule (7) that is Gaussian with respect to the functions* $\{\varphi_1, \varphi_2, \cdots, \varphi_{2n}\}$. *Furthermore, all the weights* $w_1, w_2, \cdots, w_n$ *of the quadrature are positive.*

As for smooth functions, Gaussian quadrature rules also exist for a variety of functions with end-point singularities. The following theorem is an immediate consequence of Theorem 2.1.

Theorem 2.2 *Suppose that functions* $\varphi_i : (a, b] \to R^1$ *are continuous, and integrable on* $[a, b]$ *for all* $i = 1, 2, \cdots, 2n$. *Suppose also that the function* $w(x) > 0$ *is continuous on* $(a, b]$ *and integrable on* $[a, b]$. *Suppose further that functions* ψ_i *are defined by the formula*

$$\psi_i(x) = \frac{\varphi_i(x)}{w(x)}, \tag{10}$$

and that

$$\lim_{x \to a} \psi_i(x) < \infty \tag{11}$$

for all $i = 1, 2, \cdots, 2n$. *Suppose finally that the functions* $\{\psi_1, \psi_2, \cdots, \psi_{2n}\}$ *defined by (10) constitute a Chebyshev system on the closed interval* $[a, b]$.

Then there exists a unique n-point quadrature rule (7) that is Gaussian with respect to the functions $\{\varphi_1, \varphi_2, \cdots, \varphi_{2n}\}$. *Furthermore, all the weights* $w_1, w_2, \cdots, w_n$ *of the quadrature are positive.*

Proof: The theorem is proved by applying Theorem 2.1 to the new weight function

$$\tilde{\omega}(x) = \omega(x) \cdot w(x), \tag{12}$$

and the new set of functions $\{\psi_1, \psi_2, \cdots, \psi_{2n}\}$. ■

Example 2.5 *For any natural n, and real number* $0 < \alpha < 1$, *the unique n-point quadrature on the interval* $[0, 1]$ *with respect to the functions*

$$1, x^{-\alpha}, x, x^{1-\alpha}, x^2, x^{2-\alpha}, \cdots, x^{n-1}, x^{n-1-\alpha}. \tag{13}$$

can be obtained via the following Chebyshev system (see Example 2.3)

$$x^{\alpha}, 1, x^{1+\alpha}, x, x^{2+\alpha}, x^2, \cdots, x^{n-1+\alpha}, x^{n-1} \tag{14}$$

on the interval $[0, 1]$ *with the weight function* $\tilde{\omega}(x) = \omega(x) \cdot x^{\alpha}$.

3 Numerical Preliminaries

In this section, we collect the relevant numerical tools to be used in Sections 4 and 5. They can be found, for example, in [3], [4], [5].

3.1 Nested Chebyshev Approximation

For any non-negative integer n, the Chebyshev polynomial T_n of order n is defined by the formula

$$T_n(\cos\theta) = \cos(n\theta). \tag{15}$$

Clearly, $|T_n(x)| \leq 1$ for $x \in [-1,1]$.

The Chebyshev polynomials constitute an orthonormal basis for $L^2[-1,1]$ with respect to the inner product

$$(f,g) = \int_{-1}^{1} \frac{1}{\sqrt{1-x^2}} \cdot f(x) \cdot g(x) dx. \tag{16}$$

Therefore, any function $f \in C^0[-1,1]$ can be represented by an expansion

$$f(x) = \sum_{i=0}^{\infty} a_i \cdot T_i(x), \tag{17}$$

with the coefficients a_i given by

$$a_i = (f, T_i). \tag{18}$$

Lemma 3.1 states that the Chebyshev series (17) converges rapidly for sufficiently smooth functions. Its proof can be found, for example, in [5].

Lemma 3.1 *Suppose that n and k are natural numbers, and that $f \in C^k[-1,1]$. Suppose further that the coefficients $a_0, a_1, \cdots, a_n$ are defined the formula (18). Then for any $x \in [-1,1]$,*

$$\left| f(x) - \sum_{i=0}^{n} a_i \cdot T_i(x) \right| = O(\frac{1}{n^{k-1}}). \tag{19}$$

In particular, if $f \in C^\infty$, then the expansion (17) converges to f superalgebraically.

Observation 3.1 *For functions with end-point singularities, such as $f(x) = \ln x$, we can build a structure on the given interval, consisting of subintervals clustering near the end points (see Figure 3.1), and then use the Chebyshev expansion (17) to approximate the functions on each subinterval. On each of the subintervals, the Chebyshev expansion converges superalgebraiclly.*

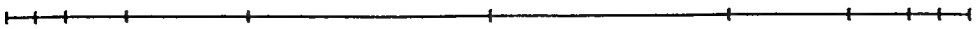

Figure 1: Subintervals clustering near the end-points

3.2 Nonlinear Equations

We will be considering systems of nonlinear equations of the form

$$F(\mathrm{x}) = 0, \tag{20}$$

where $\mathrm{x} = (x_1, \cdots, x_n)^T \in R^n$, and the mapping $F : R^n \to R^n$ is of the form

$$F(\mathrm{x}) = \begin{pmatrix} f_1(x_1, \cdots, x_n) \\ f_2(x_1, \cdots, x_n) \\ \vdots \\ f_n(x_1, \cdots, x_n) \end{pmatrix}. \tag{21}$$

Definition 3.1 *The Jacobian matrix of mapping F in (21) is defined by the formula*

$$DF(\mathrm{x}) = \begin{pmatrix} \frac{\partial f_1}{\partial x_1} & \cdots & \frac{\partial f_1}{\partial x_n} \\ \vdots & & \vdots \\ \frac{\partial f_n}{\partial x_1} & \cdots & \frac{\partial f_n}{\partial x_n} \end{pmatrix}. \tag{22}$$

The following two lemmas about the solution of systems of nonlinear equations (20) are well-known (see [3], [8], for example).

Lemma 3.2 *(Newton's Method)*

Suppose that $F : R^n \to R^n$ is continuously differentiable in an open convex set $D \subset R^n$, and the mapping $G : R^n \to R^n$ is defined by the formula

$$\mathrm{y} = \mathrm{x} - (DF(\mathrm{x}))^{-1} F(\mathrm{x}). \tag{23}$$

Suppose also that $\mathrm{x}^* \in R^n$ is the zero of F, and there exists $\beta > 0$ such that

$$||DF(\mathrm{x}^*)^{-1}|| \leq \beta. \tag{24}$$

Suppose further that there exist two positive numbers r and γ such that $\mathrm{x} \in D$ for any x such that $||\mathrm{x} - \mathrm{x}^*|| < r$, and

$$||DF(\mathrm{x}) - DF(\mathrm{y})|| \leq \gamma ||\mathrm{x} - \mathrm{y}|| \tag{25}$$

for any x, y such that $||\mathrm{x} - \mathrm{x}^*|| < r$, $||\mathrm{y} - \mathrm{x}^*|| < r$. Suppose finally that x_0 is an arbitrary point in R^n, and the sequence $\mathrm{x}_1, \mathrm{x}_2, \cdots$, of points in R^n is defined by the formula

$$\mathrm{x}_{k+1} = G(\mathrm{x}_k) \tag{26}$$

for all $k = 0, 1, 2, \cdots$.

Then there exist $\epsilon > 0$ *and* $\alpha > 0$ *such that the sequence generated by (26) converges to* x^*, *and*

$$||x_{k+1} - x^*|| \leq \alpha ||x_k - x^*||^2 \tag{27}$$

for any x_0 *such that* $||x_0 - x^*|| < \epsilon$.

Lemma 3.3 *(Modified Newton's Method)*

Suppose that under the assumptions of Lemma 3.2, x^* *is the zero of the mapping* $F : D \to R^n$. *Suppose also that*

$$A_0, A_1, A_2, \cdots \tag{28}$$

is a sequence of $n \times n$ *nonsingular matrices, and the mapping* $G : R^n \to R^n$ *is defined by the formula*

$$y = x - A_k^{-1} F(x). \tag{29}$$

Suppose further that there exists a positive real number M *such that*

$$||A_k - DF(x_k)|| \leq M \cdot ||F(x_k)||. \tag{30}$$

Suppose finally that x_0 *is an arbitrary point in* R^n, *and the sequence* $x_1, x_2, \cdots$, *of points in* R^n *is defined by the formula*

$$x_{k+1} = G(x_k) \tag{31}$$

for all $k = 0, 1, 2, \cdots$.

Then there exist $\epsilon > 0$ *and* $\alpha > 0$ *such that the sequence generated by (31) converges to* x^*, *and*

$$||x_{k+1} - x^*|| \leq \alpha ||x_k - x^*||^2 \tag{32}$$

for any x_0 *such that* $||x_0 - x^*|| < \epsilon$,

3.3 Continuation Method

The Newton algorithm for the solution of systems of non-linear equations is an extremely powerful technique, provided that a satisfactory initial point is available. In many cases, a starting point is not available directly, but can be obtained by the process known as the continuation method (otherwise referred to as the homotopy method). Following is a brief description of the technique.

Suppose that we are trying to solve a system of non-linear equations

$$F(x) = 0, \tag{33}$$

with $F : R^n \to R^n$ satisfying the conditions of Lemma 3.3, except for the initial point x_0, which is not available. Suppose further that we *do* have access to a mapping $G : [0, 1] \times R^n \to R^1$, satisfying the following conditions.

1. The mapping $F_0 : R^n \to R^n$ defined by the formula

$$F_0(\mathrm{x}) = G(0, \mathrm{x}) \tag{34}$$

has a simple structure, so that the solution of the equation

$$F_0(\mathrm{x}) = 0 \tag{35}$$

is unique and known.

2. For all $\mathrm{x} \in R^n$,

$$G(1, \mathrm{x}) = F(\mathrm{x}). \tag{36}$$

3. For all $t \in [0, 1]$, the equation

$$G(t, \mathrm{x}) = 0 \tag{37}$$

has a unique solution $\mathrm{x}(t) \in R^n$, and satisfies the conditions of Lemma 3.3 in the neighborhood of $\mathrm{x}(t)$.

4. x is a continuous (or better, Lipschitz) function of t.

Under the above conditions, the following procedure yields the solution of the equation (33).

1. For a sufficiently large m, construct the points $t_i = (i-1)/(m-1)$ on the interval $[0, 1]$, with $i = 1, 2, \cdots, m$, and consider the solutions of the equation (33) for $t = t_i$ with $i = 1, 2, \cdots, m$.

2. Clearly, we know the solution $\mathrm{x}(0)$ of the equation,

$$G(t_i, \mathrm{x}) = 0 \tag{38}$$

when $i = 1$, and for all $i = 2, 3, \cdots, m$, we solve the equation (37) by means of Lemma 3.3, using $\mathrm{x}(t_{i-1})$ as the initial approximation.

3. Since $t_n = 1$, the result of the final step of this process is the solution of the equation (33).

A detailed discussion of the continuation techniques can be found in [4], where the convergence of the above scheme is proven (in a much more general environment) for all sufficiently large m.

4 Analytical Apparatus

In this section, we develop analytical tools to be used in the numerical construction of the Gaussian quadratures whose existence follows from Theorem 2.1.

4.1 Construction of Gaussian Quadratures

The following lemma is an immediate consequence of Definition 2.3 of extended Hermite systems.

Lemma 4.1 *Suppose that the functions* $\{\varphi_1, \varphi_2, \cdots, \varphi_{2n}\}$ *constitute an Hermite system on the interval* $[a, b]$, *and* $x_1, x_2, \cdots, x_n$ *are* n *points on the interval* $[a, b]$ *such that* $x_i \neq x_j$ *for any* $i \neq j$. *Then there exist such unique coefficients* $\alpha_{i,j}$, $\beta_{i,j}$, $i = 1, 2, \cdots, n$, $j = 1, 2, \cdots, 2n$ *that*

$$\begin{cases} \sigma_i(x_k) &= 0, \\ \sigma_i'(x_k) &= \delta_{ik}, \end{cases} \tag{39}$$

$$\begin{cases} \eta_i(x_k) &= \delta_{ik}, \\ \eta_i'(x_k) &= 0, \end{cases} \tag{40}$$

for all $i = 1, 2, \cdots, n$, $k = 1, 2, \cdots, n$, *with* $\delta_{i,k}$ *denoting the Kronecker symbol, and the functions* σ_i, η_i *defined by the formulae*

$$\sigma_i(x) = \sum_{j=1}^{2n} \alpha_{i,j} \cdot \varphi_j(x), \tag{41}$$

and

$$\eta_i(x) = \sum_{j=1}^{2n} \beta_{i,j} \cdot \varphi_j(x). \tag{42}$$

Furthermore, there exist unique coefficients a_{ij}, b_{ij} *with* $i = 1, 2, \cdots, 2n$, $j = 1, 2, \cdots, n$, *such that*

$$\varphi_i(x) = \sum_{j=1}^{n} a_{i,j} \cdot \sigma_j(x) + b_{i,j} \cdot \eta_j(x) \tag{43}$$

for all $i = 1, 2, \cdots, 2n$.

In other words, there exist unique linear combinations $\sigma_1, \sigma_2, \cdots, \sigma_n$, $\eta_1, \eta_2, \cdots, \eta_n$ *of the functions* $\varphi_1, \varphi_2, \cdots, \varphi_{2n}$ *satisfying the conditions (39), (40), (43). Conversely, the functions* $\varphi_1, \varphi_2, \cdots, \varphi_{2n}$ *are linear combinations of the functions* $\sigma_1, \sigma_2, \cdots, \sigma_n$, $\eta_1, \eta_2, \cdots, \eta_n$.

Theorem 4.1 below is the principal analytical tool of this paper. It establishes the necessary and sufficient conditions under which a quadrature is Gaussian with respect to a given Hermite system.

Theorem 4.1 *Suppose that functions*

$$\varphi_1, \varphi_2, \cdots, \varphi_{2n} \tag{44}$$

constitute an Hermite system on the interval $[a, b]$. *Then the nodes* $x_1, x_2, \cdots, x_n$ *on* $[a, b]$ *are Gaussian with respect to the functions (44) if and only if*

$$\int_a^b \omega(x)\sigma_i(x)dx = 0 \tag{45}$$

for all $i = 1, 2, \cdots, n$. *In this case, the Gaussian weights* $w_1, w_2, \cdots, w_n$ *are given by the formula*

$$w_i = \int_a^b \omega(x)\eta_i(x)dx, \tag{46}$$

with functions $\sigma_1, \sigma_2, \cdots, \sigma_n$, $\eta_1, \eta_2, \cdots, \eta_n$, *in (45), (46) are defined by formulae (39) - (42).*

Proof: First, we show that for any Gaussian quadrature rule (7), the conditions (45), (46) are satisfied. Indeed, since it integrates exactly all of the functions $\varphi_1, \varphi_2, \cdots, \varphi_{2n}$, it also integrates exactly all their linear combinations $\sigma_1, \sigma_2, \cdots, \sigma_n$, $\eta_1, \eta_2, \cdots, \eta_n$. Now, (45), (46) follow immediately from (39), (40).

Suppose now that the nodes $x_1, x_2, \cdots, x_n$ are such that the conditions (45) are satisfied, and the coefficients $w_1, w_2, \cdots, w_n$ are defined by the formula (46). We will show that the n-point quadrature (7) is Gaussian with respect to the system (44).

Due to Lemma 4.1, there exist coefficients $\alpha_{i,j}$, $\beta_{i,j}$, $i = 1, 2, \cdots, n$, $j = 1, 2, \cdots, 2n$ such that

$$\varphi_i = \sum_{j=1}^{n}(a_{ij}\sigma_j + b_{ij}\eta_j) \tag{47}$$

for any $i = 1, 2, \cdots, 2n$. Thus

$$\int_a^b \omega(x)\varphi_i(x)dx = \sum_{j=1}^{n} a_{ij}\int_a^b \omega(x)\sigma_j(x)dx + b_{ij}\int_a^b \omega(x)\eta_j(x)dx. \tag{48}$$

Combing (48) with (45), (46), we have

$$\int_a^b \omega(x)\varphi_i(x)dx = \sum_{j=1}^{n} b_{ij}w_j. \tag{49}$$

On the other hand, combining (39), (40), and (48), we obtain

$$\begin{aligned}\sum_{j=1}^{n} w_j\varphi_i(x_j) &= \sum_{j=1}^{n} w_j \sum_{k=1}^{n}(a_{ik}\sigma_k(x_j) + b_{ik}\eta_k(x_j)) \\ &= \sum_{j=1}^{n} b_{ij}w_j. \end{aligned} \tag{50}$$

Combining (49) and (50), we finally get

$$\int_a^b \omega(x)\varphi_i(x)dx = \sum_{j=1}^{n} w_j\varphi_i(x_j). \tag{51}$$

for all $i = 1, 2, \cdots, 2n$. ■

Theorem 4.2 below follows immediately from Theorem 4.1. It describes the Gaussian nodes as the solution of a system of non-linear equations.

Theorem 4.2 *Suppose that the functions* $\{\varphi_1, \varphi_2, \cdots, \varphi_n\}$ *constitute an Hermite system, and functions* $\{\sigma_1, \sigma_2, \cdots, \sigma_n\}$ *and* $\{\eta_1, \eta_2, \cdots, \eta_n\}$ *are defined by the formulae (39), (40), (41), and (42). Suppose further that* S *is a subset of* R^n *consisting of all finite sequences* $\{x_1, x_2, \cdots, x_n\}$ *such that* $x_i \neq x_j$ *whenever* $i \neq j$ *. Suppose finally that the mapping* $F : S \rightarrow R^n$ *is defined by the formula*

$$\begin{pmatrix} x_1 \\ x_2 \\ \vdots \\ x_n \end{pmatrix} \longrightarrow \begin{pmatrix} \int_a^b \omega(x)\sigma_1(x)dx \\ \int_a^b \omega(x)\sigma_2(x)dx \\ \vdots \\ \int_a^b \omega(x)\sigma_n(x)dx \end{pmatrix}. \tag{52}$$

Then $\{x_1, x_2, \cdots, x_n\}$ *are the Gaussian nodes with respect to the system of functions* $\{\varphi_1, \varphi_2, \cdots, \varphi_n\}$ *if and only if*

$$F(x_1, \cdots, x_n) = 0. \tag{53}$$

4.2 Computation of Gaussian Quadratures

In this subsection, we observe that the modified Newton method in Subsection 3.2 assumes a particularly simple form when it is applied to the system of equations (53), and establish Theorem 4.5, the principal numerical tool of this paper. Theorem 4.5 shows that an extremely simple iterative scheme converges quadratically for the system of equations (53).

Theorem 4.4 below provides an analytical expression for the Jacobian matrix of the mapping F defined by the formula (52). Theorem 4.3 is the consequence of Lemmas 4.2 and 4.3, and will be used in the proof of Theorem 4.4. Theorem 4.5 follows immediately form Lemma 3.3, Corollary 4.2, and Theorem 4.4.

Lemma 4.2 *Suppose that functions* $\{\varphi_1, \varphi_2, \cdots, \varphi_{2n}\}$ *form an extended Hermite system with* $\varphi_i \in C^3[a, b]$ *for all* $i = 1, 2, \cdots, 2n$. *Suppose also that*

$$x_1, x_2, \cdots, x_n \tag{54}$$

are n *distinct points on the interval* $[a, b]$, *and functions*

$$\sigma_1, \sigma_2, \cdots, \sigma_n, \eta_1, \eta_2, \cdots, \eta_n \tag{55}$$

are determined by the set of points (54) via formulae (39) and (40). Suppose further that l *is an integer such that* $1 \leq l \leq n$, *and* δ *is a real number such that*

$$x_1, \cdots, x_{l-1}, x_l + \delta, x_{l+1} \cdots, x_n \tag{56}$$

are n *distinct points on interval* $[a, b]$. *Suppose finally that the functions*

$$\tilde{\sigma}_1, \tilde{\sigma}_2, \cdots, \tilde{\sigma}_n, \tilde{\eta}_1, \tilde{\eta}_2, \cdots, \tilde{\eta}_n \tag{57}$$

are determined by the set of points (56) via formulae (39) and (40).

Then there exist coefficients α_{il} and β_{il} with $i = 1, 2, \cdots, n$, such that

$$\tilde{\sigma}_i(x) = \sigma_i(x) + \alpha_{il} \cdot \sigma_l(x) + \beta_{il} \cdot \eta_l(x) \tag{58}$$

for all $i \neq l$, $i = 1, 2, \cdots, n$, and

$$\tilde{\sigma}_l(x) = \alpha_{ll} \cdot \sigma_l(x) + \beta_{ll} \cdot \eta_l(x). \tag{59}$$

Proof: Due to Lemma 4.1, there exist unique coefficients α_{ij}, β_{ij} with $i = 1, 2, \cdots, 2n$, $j = 1, 2, \cdots, n$, such that for all $i = 1, 2, \cdots, 2n$,

$$\tilde{\sigma}_i(x) = \sum_{j=1}^{n} (\alpha_{ij} \cdot \sigma_j(x) + \beta_{ij} \cdot \eta_j(x)) \tag{60}$$

for any $x \in [a, b]$. Differentiating (60), we have

$$\tilde{\sigma}_i'(x) = \sum_{j=1}^{n} \left(\alpha_{ij} \cdot \sigma_j'(x) + \beta_{ij} \cdot \eta_j'(x)\right). \tag{61}$$

For the functions (57), the conditions (39), (40) assume the form

$$\begin{cases} \tilde{\sigma}_i(x_l + \delta) &= 0, \\ \tilde{\sigma}_i'(x_l + \delta) &= \delta_{il}, \end{cases} \tag{62}$$

and

$$\begin{cases} \tilde{\sigma}_i(x_k) &= 0, \\ \tilde{\sigma}_i'(x_k) &= \delta_{ik} \end{cases} \tag{63}$$

for all $i = 1, 2, \cdots, n$, $k = 1, 2, \cdots, n$, and $k \neq l$.

For any $k \neq l$, evaluating (60) at x_k and applying conditions (39), (40), (63), we obtain

$$\beta_{ik} = 0 \tag{64}$$

for all $i = 1, 2, \cdots, n$.

Similarly, for any $k \neq l$, evaluating (61) at x_k and applying conditions (39), (40), (63), we have

$$\alpha_{ik} = \delta_{ik} \tag{65}$$

for all $i = 1, 2, \cdots, n$.

Now, (58), (59) immediately follow from (60), (64), (65). ■

Lemma 4.3 *Suppose that under the assumptions of Lemma 4.2, the coefficients α_{il} and β_{il} are defined via formulae (58) and (59) for all $i = 1, 2, \cdots, n$, Then*

$$\alpha_{il} = -\delta \cdot \sigma_i''(x_l) + O(\delta^2), \tag{66}$$

$$\beta_{il} = O(\delta^2) \tag{67}$$

for all $i \neq l$, $i = 1, 2, \cdots, n$, *and*

$$\alpha_{ll} = 1 - \delta \cdot \sigma_l''(x_l) + O(\delta^2)), \tag{68}$$
$$\beta_{ll} = \delta + O(\delta^2). \tag{69}$$

Proof: Expanding the functions

$$\sigma_i, \eta_i, \sigma_i', \eta_i',$$

into the Taylor series at x_l, we have

$$\begin{cases} \sigma_i(x_l + \delta) = \sigma_i(x_l) + \delta \cdot \sigma_i'(x_l) + O(\delta^2), \\ \eta_i(x_l + \delta) = \eta_i(x_l) + \delta \cdot \eta_i'(x_l) + O(\delta^2), \end{cases} \tag{70}$$

$$\begin{cases} \sigma_i'(x_l + \delta) = \sigma_i'(x_l) + \delta \cdot \sigma_i''(x_l) + O(\delta^2), \\ \eta_i'(x_l + \delta) = \eta_i'(x_l) + \delta \cdot \eta_i''(x_l) + O(\delta^2), \end{cases} \tag{71}$$

for all $i = 1, 2, \cdots, n$.

Evaluating (58) and (59) at $x = (x_l + \delta)$ and using the conditions (39), (40), (62), (70), we obtain

$$\beta_{il} = -\alpha_{il} \cdot \delta + O(\delta^2) \tag{72}$$

for all $i = 1, 2, \cdots, n$.

Differentiating (58) at $x = (x_l + \delta)$ and using conditions (39), (40), (62), (71), we have

$$\begin{aligned} \alpha_{ll} &= \left(1 + \delta \cdot \sigma_l''(x_l)\right)^{-1} \left(1 + O(\delta^2)\right), \\ &= 1 - \delta \cdot \sigma_l''(x_l) + O(\delta^2). \end{aligned} \tag{73}$$

Similarly, differentiating (59) at $x = (x_l + \delta)$ and applying the conditions (39), (40), (62), and (71), we get

$$\alpha_{il} = -\delta \cdot \sigma_i''(x_l) + O(\delta^2) \tag{74}$$

for all $i = 1, 2, d \cdots, n$, and $i \neq l$

Finally, combining (72) with (73), (74), we have

$$\beta_{ll} = \delta + O(\delta^2), \tag{75}$$
$$\beta_{il} = O(\delta^2) \tag{76}$$

for all $i = 1, 2, \cdots, n$, and $i \neq l$ ■

Combining Lemmas 4.2, 4.3, we now obtain the following theorem.

Theorem 4.3 *Under the assumptions of Lemma 4.2,*

$$\tilde{\sigma}_l(x) = \sigma_l(x) - \delta \cdot \sigma_l''(x_l) \cdot \sigma_l(x) - \delta \cdot \eta_l(x) + O(\delta^2) \tag{77}$$
$$\tilde{\sigma}_i(x) = \sigma_i(x) - \delta \cdot \sigma_i''(x_l) \cdot \sigma_l(x) + O(\delta^2) \tag{78}$$

for any $i = 1, 2, \cdots, n$, *and* $i \neq l$.

The following theorem is an immediate consequence of Theorem 4.3. It provides a simple expression for the Jacobian of the mapping (52), showing that the latter is nearly diagonal in the vicinity of the solution of the equation (53).

Theorem 4.4 *Suppose that functions* $\{\varphi_1, \varphi_2, \cdots, \varphi_{2n}\}$ *form an extended Hermite system, and* $\varphi_i \in C^3[a,b]$ *for* $i = 1, 2, \cdots, 2n$. *Suppose further that* x_1, x_2, $\cdots$, x_n *are* n *distinct point on the interval* $[a,b]$, *and functions*

$$\sigma_1, \sigma_2, \cdots, \sigma_n, \eta_1, \eta_2, \cdots, \eta_n$$

are determined by formulae (39) and (40). Then the Jacobian $DF(\mathrm{x})$ *of the mapping* F *defined by (52) is given by the formula*

$$DF(\mathrm{x}) = -\begin{pmatrix} \int_a^b \omega(x)\eta_1(x)dx & 0 & \cdots & 0 \\ 0 & \int_a^b \omega(x)\eta_2(x)dx & \cdots & 0 \\ \vdots & \vdots & & \vdots \\ 0 & 0 & \cdots & \int_a^b \omega(x)\eta_n(x)dx \end{pmatrix} - \mathrm{E}(\mathrm{x}) \quad (79)$$

where $\mathrm{x} = (x_1, x_2, \cdots, x_n)^T$, *and matrix* $E(\mathrm{x})$ *is given by the formula*

$$E(\mathrm{x}) = \begin{pmatrix} \sigma_1''(x_1) & \cdots & \sigma_1''(x_n) \\ \vdots & & \vdots \\ \sigma_n''(x_1) & \cdots & \sigma_n''(x_n) \end{pmatrix} \begin{pmatrix} \int_a^b \omega(x)\sigma_1(x)dx & 0 & \cdots & 0 \\ \vdots & \vdots & & \vdots \\ 0 & 0 & \cdots & \int_a^b \omega(x)\sigma_n(x)dx \end{pmatrix}. \quad (80)$$

Proof: Suppose that l is an integer such that $1 \le l \le n$, and δ is a real number such that

$$x_1, \cdots, x_{l-1}, x_l + \delta, x_{l+1} \cdots, x_n \quad (81)$$

are n distinct points on the interval $[a,b]$. Suppose further that the functions

$$\tilde{\sigma}_1, \tilde{\sigma}_2, \cdots, \tilde{\sigma}_n, \tilde{\eta}_1, \tilde{\eta}_2, \cdots, \tilde{\eta}_n \quad (82)$$

are determined by the set of points (81) via formulae (39) and (40).

Combining (77), (78) with Definition 3.1 of Jacobian matrix, and the definition (52) of the mapping F, we immediately obtain

$$\begin{aligned} (DF(\mathrm{x}))_{il} &= \frac{\partial}{\partial x_l} \int_a^b \omega(x)\sigma_i(x)dx \\ &= \lim_{\delta \to 0} \frac{\int_a^b \omega(x)\tilde{\sigma}_l(x)dx - \int_a^b \omega(x)\sigma_l(x)dx}{\delta} \\ &= -\sigma_l''(x_l) \int_a^b \omega(x)\sigma_l(x)dx - \int_a^b \omega(x)\eta_l(x)dx \end{aligned} \quad (83)$$

for any $i \neq l$, $i = 1, 2, \cdots, n$, and

$$\begin{aligned}(DF(\mathrm{x}))_{il} &= \frac{\partial}{\partial x_l}\int_a^b \omega(x)\sigma_l(x)dx \\ &= \lim_{\delta\to 0}\frac{\int_a^b \omega(x)\tilde{\sigma}_i(x)dx - \int_a^b \omega(x)\sigma_i(x)dx}{\delta} \\ &= -\sigma_i''(x_l)\int_a^b \omega(x)\sigma_l(x)dx. \end{aligned} \tag{84}$$

■

Corollary 4.1 follows immediately from Theorem 2.1 and Theorem 4.4, and corollary 4.2 is the consequence of Corollary 4.1 and Theorem 4.4.

Corollary 4.1 *Suppose that under the assumptions of Theorem 4.4, the function* $F : R^n \to R^n$ *is defined by (52). Then there exists a unique* $\mathrm{x}^* = (x_1^*, x_2^*, \cdots, x_n^*)^T \in R^n$ *such that*

$$F(\mathrm{x}^*) = 0, \tag{85}$$

and the Jacobian matrix

$$DF(\mathrm{x}^*) = -\begin{pmatrix} \int_a^b \omega(x)\eta_1(x)dx & 0 & \cdots & 0 \\ 0 & \int_a^b \omega(x)\eta_2(x)dx & \cdots & 0 \\ \vdots & \vdots & & \vdots \\ 0 & 0 & \cdots & \int_a^b \omega(x)\eta_n(x)dx \end{pmatrix} \tag{86}$$

is nonsingular, where the functions $\eta_1, \eta_2, \cdots, \eta_n$ *are determined by the set of points* $x_1^*, x_2^*, \cdots, x_n^*$ *via the formula (40).*

Corollary 4.2 *Suppose that under the assumptions of Theorem 4.4, the function* $F : R^n \to R^n$ *is defined by (52), and* x^* *is the unique zero of* F. *Then* F *is continuously differentiable, and there exist three positive real numbers* r, β *and* γ *such that*

$$||DF(\mathrm{x}^*)^{-1}|| \leq \beta, \tag{87}$$

and

$$||DF(\mathrm{x}) - DF(\mathrm{y})|| \leq \gamma||\mathrm{x} - \mathrm{y}|| \tag{88}$$

for any x *and* y *such that* $||\mathrm{x} - \mathrm{x}^*|| < r$, $||\mathrm{y} - \mathrm{x}^*|| < r$.

The following theorem is the principal numerical tool of this paper. It shows that an extremely simple iterative scheme converges quadratically for the system of equations (53), and is an immediate consequence of Lemma 3.3, Corollary 4.2, and Theorem 4.4.

Theorem 4.5 *Suppose that functions* $\{\varphi_1, \varphi_2, \cdots, \varphi_{2n}\}$ *form an extended Hermite system, and the mapping* $G : R^n \to R^n$ *is defined by the formula*

$$y_i = x_i + \frac{\int_a^b \omega(x)\sigma_i(x)dx}{\int_a^b \omega(x)\eta_i(x)dx}, \tag{89}$$

with $i = 1, 2, \cdots, n$, *and the functions*

$$\sigma_1, \sigma_2, \cdots, \sigma_n, \eta_1, \eta_2, \cdots, \eta_n$$

defined by the points $x_1, x_2, \cdots, x_n$ *via the formulae (39) and (40). Suppose further that* $\varphi_i \in C^3[a, b]$ *for all* $i = 1, 2, \cdots, 2n$, *and the function* $F : R^n \to R^n$ *is defined by (52). Suppose finally that* x^* *is the unique zero of* F, *that* x_0 *is an arbitrary point in* R^n, *and the sequence* $\mathrm{x}_1, \mathrm{x}_2, \cdots$, *of points in* R^n *is defined by the formula*

$$\mathrm{x}_{k+1} = G(\mathrm{x}_k) \tag{90}$$

for all $k = 0, 1, 2, \cdots$.

Then there exists $\epsilon > 0$ *and* $\alpha > 0$ *such that the sequence* $\mathrm{x}_1, \mathrm{x}_2, \cdots$, *generated by (90) converges to* x^*, *and*

$$||\mathrm{x}_{k+1} - \mathrm{x}^*|| \leq \alpha ||\mathrm{x}_k - \mathrm{x}^*||^2 \tag{91}$$

for any initial point x_0 *such that* $||\mathrm{x}_0 - \mathrm{x}^*|| < \epsilon$.

Remark 4.1 *In Theorem 4.5, we impose the condition*

$$\varphi_i \in C^3[a, b] \tag{92}$$

for all $i = 1, 2, \cdots, 2n$. *However, it can be easily observed that the condition (92) is excessively restrictive, and a somewhat more involved proof shows that as long as* φ_i *are continuously differentiable, and* φ_i' *satisfy the Lipschitz condition for all* $i = 1, 2, \cdots, 2n$, *the modified Newton method (90) will still converge quadratically.*

5 Integration of Singular Functions

In this section, the theory of the generalized Gaussian quadrature rules established in Section 4 will be generalized to a variety of functions with end-point singularities. We will first introduce the concepts of Chebyshev and extended Hermite systems in the case of singular functions. Then we will prove Theorems 5.1 and Theorem 5.2 for the construction of Gaussian quadrature rules, providing effective numerical construction for Gaussian quadratures for functions with end-point singularities.

Definition 5.1 *(Chebyshev System)*

Suppose that $X \subset R^1$ *is either* (a, b), *or* $[a, b)$, *or* $(a, b]$. *Then a finite sequence of functions* $\{\varphi_1, \varphi_2, \cdots, \varphi_n\}$ *will be referred to as a Chebyshev system on* X *if and only if it constitutes a Chebyshev system on every closed subinterval* $[c, d] \subset X$ *(see Definition 2.1).*

Definition 5.2 *(Extended Hermite System)*

Suppose that $X \subset R^1$ is either (a,b), or $[a,b)$, or $(a,b]$. Then a finite sequence of functions $\{\varphi_1, \varphi_2, \cdots, \varphi_n\}$ will be referred to as an extended Hermite system on X if and only if it constitutes an extended Hermite system on every closed subinterval $[c,d] \subset X$ (see Definition 2.3).

The following is an important example of extended Hermite systems.

Example 5.1 *For any natural n, the functions*

$$1, x^\alpha, x, x^{1+\alpha}, x^2, x^{2+\alpha}, \cdots, x^{n-1}, x^{n-1+\alpha} \tag{93}$$

constitute an extended Hermite system on the interval $(0,1]$ with α an arbitrary non-integer real number. (see Example 2.3 and Definition 5.2)

Theorem 5.1 *Suppose that functions $\{\varphi_1, \varphi_2, \cdots, \varphi_{2n}\}$ are all integrable on $[a,b]$, and constitute a Chebyshev system on $(a,b]$. Suppose further that on the interval $[a+\delta, b]$, the n-point Gaussian quadrature (7) is given by the nodes*

$$x_1^{(\delta)}, x_2^{(\delta)}, \cdots, x_n^{(\delta)}, \tag{94}$$

and the weights

$$w_1^{(\delta)}, w_2^{(\delta)}, \cdots, w_n^{(\delta)} \tag{95}$$

for any $\delta \in (0, b-a)$.

Then for any $\epsilon > 0$, there exists $\delta_0 > 0$ such that for all $\delta < \delta_0$,

$$\left| \int_a^b \omega(x)\varphi_i(x)dx - \sum_{j=1}^{n} w_j^{(\delta)} \varphi_i(x_j^{(\delta)}) \right| < \epsilon. \tag{96}$$

for all $i = 1, 2, \cdots, 2n$.

Proof: Due to the Definition 2.4 of the Gaussian Quadratures, we have

$$\int_{a+\delta}^b \omega(x)\varphi_i(x)dx = \sum_{j=1}^{n} w_j^{(\delta)} \varphi_i(x_j^{(\delta)}) \tag{97}$$

for all $i = 1, 2, \cdots, n$. Subtracting

$$\int_a^b \omega(x)\varphi_i(x)dx$$

from both sides of (97), we obtain

$$\begin{aligned} \int_a^b \omega(x)\varphi_i(x)dx - \sum_{j=1}^{n} w_j^{(\delta)} \varphi_i(x_j^{(\delta)}) &= \int_a^b \omega(x)\varphi_i(x)dx - \int_{a+\delta}^b \omega(x)\varphi_i(x)dx \\ &= \int_a^{a+\delta} \omega(x)\varphi_i(x)dx. \end{aligned} \tag{98}$$

Due to the assumption that φ_i are integrable on the interval $[a,b]$ for all $= 1, 2, \cdots, 2n$, for any $\epsilon > 0$, there exists $\delta_0 > 0$ such that for any $\delta < \delta_0$,

$$\left| \int_a^{a+\delta} \omega(x)\varphi_i(x)dx \right| < \epsilon \tag{99}$$

for all $= 1, 2, \cdots, 2n$.

Now, (96) follows immediately from (98), (99). ■

Theorem 5.2 *Suppose that under the assumptions of Theorem 2.2 and Theorem 5.1,*

$$\varphi_1 \equiv 1. \tag{100}$$

Then there exists a unique n-point Gaussian quadrature (7) with respect to the functions

$$\varphi_1, \varphi_2, \cdots, \varphi_{2n} \tag{101}$$

such that all the nodes $x_1, x_2, \cdots, x_n$ lie in the open interval (a,b), and all the weights $w_1, w_2, \cdots, w_n$ are positive. Furthermore, for all $i = 1, 2, \cdots, n$,

$$\lim_{\delta \to 0} x_i^{(\delta)} = x_i \tag{102}$$

and

$$\lim_{\delta \to 0} w_i^{(\delta)} = w_i \tag{103}$$

where the nodes $x_i^{(\delta)}$ and the weights $w_i^{(\delta)}$ are defined in Theorem 5.1.

Proof: Due to Theorem 2.2, there exists a unique Gaussian quadrature (7) with respect to the functions (101) on the interval $[a,b]$ such that all the nodes $x_1, x_2, \cdots, x_n$ lie in the open interval (a,b), and all the weights $w_1, w_2, \cdots, w_n$ are positive.

On the other hand, due to Theorem 2.1, for any $\delta \in (0, b-a)$, there exists a unique Gaussian quadrature (7) with respect to the functions (101) on the interval $[a+\delta, b]$ such that the nodes $x_i^{(\delta)} \in (a+\delta, b)$, and the weights

$$w_i^{(\delta)} > 0 \tag{104}$$

for all $i = 1, 2, \cdots, n$. Combining (100) with Definition 2.4 of the Gaussian quadratures, we obtain

$$\int_{a+\delta}^{b} \omega(x)\varphi_1(x)dx = \sum_{i=1}^{n} w_i^{(\delta)}. \tag{105}$$

Now, for any $\delta \in (0, b-a)$, we will define two vectors $\mathrm{x}_\delta, \mathrm{w}_\delta \in R^n$ via the formulae

$$\mathrm{x}_\delta = (x_1^{(\delta)}, x_2^{(\delta)}, \cdots, x_n^{(\delta)})^T, \tag{106}$$

$$\mathrm{w}_\delta = (w_1^{(\delta)}, w_2^{(\delta)}, \cdots, w_n^{(\delta)})^T, \tag{107}$$

where $x_i^{(\delta)}$ and $w_i^{(\delta)}$ are the Gaussian nodes and weights with respect to functions (101) on the interval $[a+\delta, b]$.

Clearly, for any $\delta \in (0, b-a)$, we have

$$||\mathrm{x}_\delta|| \leq c \cdot \sqrt{n} \tag{108}$$

with $c = \max(|a|, |b|)$.

Combining (105) and (104), we obtain

$$||\mathrm{w}_\delta|| \leq d \cdot \sqrt{n} \tag{109}$$

for any $\delta \in (0, b-a)$, with d given by the formula

$$d = \int_a^b \omega(x)dx. \tag{110}$$

We will show that for all $\delta \in (0, b-a)$, there exists only one limit point for the set of vectors x_δ, and only one limit point for the set of vectors w_δ.

Suppose that there exists a sequence of positive real numbers $\delta_1, \delta_2, \cdots$, such that $\lim_{k\to\infty} \delta_k = 0$,

$$\lim_{k\to\infty} \mathrm{x}_{\delta_k} = \mathrm{y}, \tag{111}$$

$$\lim_{k\to\infty} \mathrm{w}_{\delta_k} = \mathrm{v}, \tag{112}$$

with $\mathrm{y} = (y_1, y_2, \cdots, y_n)^T$, and $\mathrm{v} = (v_1, v_2, \cdots, v_n)^T$.

Due to Theorem 5.1, Definition 2.4 of the Gaussian Quadratures, and conditions (111), (112), we have

$$\begin{aligned} \int_a^b \omega(x)\varphi_i(x)dx &= \lim_{k\to\infty} \int_{a+\delta_k}^b \omega(x)\varphi_i(x)dx \\ &= \lim_{k\to\infty} \sum_{j=1}^n w_j^{(\delta_k)} \varphi_i(x_j^{(\delta_k)}) \\ &= \sum_{j=1}^n v_j \varphi_i(y_j) \end{aligned} \tag{113}$$

for all $i = 1, 2, \cdots, 2n$.

Due to (113) and the uniqueness of the Gaussian quadrature (7) with respect to the functions (101) on the interval $[a, b]$, we have

$$y_j = x_j \tag{114}$$

$$v_j = w_j \tag{115}$$

for all $j = 1, 2, \cdots, n$, where $x_1, x_2, \cdots, x_n$ are the nodes and $w_1, w_2, \cdots, w_n$ are the weights of the Gaussian Quadrature (7) with respect to the functions (101) on $[a, b]$. In other words, the set of vectors x_δ for all $\delta \in (0, b-a)$ has a unique limit point

$$\mathrm{x}_0 = (x_1, x_2, \cdots, x_n)^T,$$

and the set of vectors w_δ for all $\delta \in (0, b-a)$ has a unique limit point

$$\mathrm{w}_0 = (w_1, w_2, \cdots, w_n)^T.$$

Now, the formulae (102) and (103) follow from (108), (109), and the fact that each of the two sets of the vectors x_δ and w_δ possesses only one limit point in R^n. ■

Remark 5.1 *Clearly, the condition $\varphi_1 \equiv 1$ in Theorem 5.2 can be relaxed. To insure the boundedness of the Gaussian weights, we only need to impose the condition that there exists a real $\epsilon > 0$, and $2n$ real numbers α_1, α_2, $\cdots$, α_{2n} such that*

$$\sum_{i=1}^{2n} \alpha_i \cdot \varphi_i(x) \geq \epsilon \tag{116}$$

for all $x \in (a, b)$.

6 The Numerical Algorithm

We can now compute Gaussian quadratures for both smooth functions and functions with end-point singularities using the numerical apparatus developed in Sections 4 and 5. The Gaussian quadrature rules for an extended Hermite system can be obtained by solving a system of non-linear equations (53). Due to Theorems 4.5 and 5.2, the modified Newton's method defined by the formula (90) converges quadratically when it is applied to the system of equations (53).

As is well-known, the Newton method is sensitive to the choice of the initial approximation x_0, and we use the continuation method (see Subsection 3.3 above) to obtain the latter. More specifically, given an extended Hermite system

$$\varphi_1, \varphi, \cdots, \varphi_{2n}, \tag{117}$$

on the interval $[a, b]$, we construct a family of extended Hermite systems

$$\varphi_1^t, \varphi_2^t, \cdots, \varphi_{2n}^t, \tag{118}$$

with $t \in [0, 1]$, and such that

$$\varphi_i^0(x) = x^{i-1}, \tag{119}$$

$$\varphi_i^1(x) = \varphi_i(x), \tag{120}$$

for all $x \in [a, b]$, and $i = 1, 2, \cdots 2n$. For each $t \in [0, 1]$, we construct the system of equations (53) corresponding to the extended Hermite system (118) via the formulae (39), (40). Clearly, for the extended Hermite system (119), the solution of the system of equations (53) is known (see Remark 2.2), and we use the continuation method (see Subsection 3.3) to obtain the solution of (53) for the Hermite system (117).

In the numerical examples of the following section, the one-parameter families of Hermite systems are constructed as follows.

1. For Hermite systems of the form

$$J_0, J_1, \cdots, J_{2n-1}, \tag{121}$$

the one-parameter family of systems is

$$\varphi_i^t(x) = (1-t) \cdot x^{i-1} + t \cdot \varphi_i(x) \tag{122}$$

for $i = 0, 1, \cdots, 2n-1$.

2. For Hermite systems of the form

$$1, \ln x, x, x \ln x, x^2, x^2 \ln x, \cdots, x^{n-1}, x^{n-1} \ln x, \tag{123}$$

the one-parameter family of systems is given by (122).

3. For Hermite systems of the form

$$1, s(x), x, xs(x), x^2, x^2 s(x), \cdots, x^{n-1}, x^{n-1} s(x), \tag{124}$$

with

$$s(x) = x^\alpha, \tag{125}$$

and α an arbitrary non-integer real number, the one-parameter family of systems is

$$1, s(t,x), x, x \cdot s(t,x), x^2, x^2 \cdot s(t,x), \cdots, x^{n-1}, x^{n-1} \cdot s(t,x), \tag{126}$$

with

$$s(t,x) = x^{t \cdot \alpha}. \tag{127}$$

Remark 6.1 *The necessary number m of steps in the continuation process (see Subsection 3.3) is significantly reduced if, prior to the application of the above procedure, the original system (117) is orthonormalied (for example, via the Gram-Schmidt process). To do that, we discretize the original functions φ_i at nested Chebyshev nodes (see Subsection 3.1), and perform the Gram-Schmidt procedure on the obtained finite-dimensional representations.*

The following is the formal description of the numerical algorithm (excluding the continuation process).

Initialization
Comment [Build the structure for integration and interpolation.]

Step 1

do
Subdivide $[a, b]$ into subintervals clustering near end-points (see Figure 3.1).
enddo

Orthogonalization (optional)
Comment [Perform Gram-Schmidt orthogonalization on the given set of functions.]

Step 2

do $i = 1, 2, \cdots, 2n$
  do $j = 1, 2, \cdots, i-1$
    Orthogonalize the i-th function φ_i with respect to j-th function φ_j
  endo
enddo

Nested Chebyshev Approximation (optional)
Comment [Generate the nested Chebyshev expansions for the orthogonalized functions (see Subsection 3.1).]

Step 3

do $i = 1, 2, \cdots, 2n$
  Construct the local Chebyshev expansion of the i-th function φ_i based on Observation 3.1.
enddo

Newton's Iteration
Comment [Conduct Newton's iteration to find Gaussian nodes and weights.]

Step 4

do
  Construct functions σ_i and η_i for $i = 1, 2, \cdots, n$ via formulae (39) and (40).
enddo

Step 5

do
  Adjust Gaussian nodes $\{x_i\}$ via formulae (90).
enddo

Step 6

do
  Compute $error = ||\mathrm{x}_{k+1} - \mathrm{x}_k||$.
  If $error > \epsilon$, Go to Step 4.
enddo

Remark 6.2 *The procedure described above requires the construction of the functions σ_i, η_i, $i = 1, 2, \cdots, n$, given the functions φ_i, $i = 1, 2, \cdots, 2n$. The latter is possible for any extended Hermite systems, and is equivalent to inverting the matrix (3). Obviously, for many choices of functions $\varphi_1, \varphi_2, \cdots, \varphi_{2n}$, the matrix (3) will be ill-conditioned, including the numerical examples given in the following section. Thus, in order to obtain the double precision results presented in this paper, the authors have performed all computations in extended precision (REAL *32).*

7 Numerical Results

We have implemented the numerical algorithm described in Section 6 for the computation of Gaussian quadrature formulae, and tested it on various examples.

Example 7.1 *Gaussian Quadratures with respect to the Bessel Functions*

$$J_0, J_1, \cdots, J_{2n-1} \tag{128}$$

on $[0, 10]$ are given in Table 1, and tested on selected functions in Table 12.

Example 7.2 *Gaussian Quadratures with respect to the Bessel Functions (128) on $[0, 10]$ with the weight function*

$$\omega(x) = \frac{1}{\sqrt{x}} \tag{129}$$

are given in Table 2, and tested on selected functions in Table 13.

Example 7.3 *Gaussian Quadratures with respect to the system of functions*

$$1, \ln x, x, x \ln x, x^2, x^2 \ln x, \cdots, x^{n-1}, x^{n-1} \ln x \tag{130}$$

on $[0, 1]$ are given in Table 3, and tested on selected functions in Table 14.

Example 7.4 *Gaussian Quadratures with respect to the systems of functions*

$$1, x^\alpha, x, x^{1+\alpha}, x^2, x^{2+\alpha}, \cdots, x^{n-1}, x^{n-1+\alpha} \tag{131}$$

on $[0, 1]$ are given respectively in Tables 4-11 for

$$\alpha = \frac{2}{3}, \frac{1}{2}, \frac{1}{3}, \frac{1}{4}, -\frac{1}{4}, -\frac{1}{3}, -\frac{1}{2}, -\frac{2}{3},$$

and tested on selected functions in Tables 15-22 respectively.

Remark 7.1 *Systems of the form (128) are often encountered in physics. It turns out that the system of functions (128) on the interval $[0, B]$ is an extended Hermite system only for certain combinations of B and n. A somewhat subtle analysis shows that the system (128) is an extended Hermite system on the interval $[0, B]$ as long as $\frac{B}{2} \leq n \leq B$.*

8 Conclusions

A numerical algorithm has been presented for the construction of the generalized Gaussian quadrature rules, introduced in [6]. The quadrature rules of this paper possess most of the desirable properties of the classical Gaussian integration formulae, such as positivity of the weights, rapid convergence, mathematical elegance, etc. The algorithm is applicable to a wide class of functions, including smooth functions (not necessarily polynomials), as well as functions with end-point singularities, such as those encountered in the solution of integral equations, complex analysis, potential theory, and several other areas.

References

[1] B. Alpert, *Rapidly-Convergent Quadrature for Integral Operators with Singular Kernels* Lawrence Berkeley Laboratory, University of California at Berkeley, December 1990.

[2] P. Davis and P. Rabinowitz, *Methods of Numerical Integration*, Academic Press, Inc., Orlando, Florida, 1984.

[3] J. E. Dennis, and R. B. Schnabel, *Numerical Methods for Unconstrained Optimization and Nonlinear Equations*, Prentice-Hall, Inc., Englewood Cliffs, New Jersey, 1983.

[4] F. A. Ficken, The Continuation Method for Functional Equations, *Comm. Pure Appl. Math.* 4(1951), pp435-456.

[5] D. Gottlieb, and S. A. Orszag, *Numerical Analysis of Spectral Methods: Theory and Applications*, Regional Conference Series in Applied Mathematics, SIAM, 1977.

[6] S. Karlin and W. Studden, *Tchebycheff Systems with Applications in Analysis and Statistics*, John Wiley (Interscience), New York, 1966.

[7] V. Rokhlin, End-Point Corrected Trapezoidal Quadrature Rules for Singular Functions, *Computers Math. Applic.* Vol.20, No.7, pp.51-62, 1990.

[8] J. Stoer and R. Bulirsch, *Introduction to Numerical Analysis*, Springer-Verlag, New York, 1983.

[9] A. H. Stroud and D. Secrest, *Gaussian Quadrature Formulas*, Prentice-Hall, Inc., Englewood Cliffs, New Jersey, 1966.

Table 1: Gaussian Quadrature for Bessel Functions of the First Kind

$$\int_0^{10} J_{k-1}(x)dx = \sum_{i=1}^{N} w_i J_{k-1}(x_i) \quad \text{for } k = 1, 2, \cdots, 2N$$

N	Nodes x_i	Weights w_i
5	0.469238675868960E+00	0.117179089779279E+01
	0.223157952970870E+01	0.224136849121358E+01
	0.473407702933183E+01	0.266214797121592E+01
	0.735478272434508E+01	0.247001516625585E+01
	0.940238197915203E+01	0.145415103193520E+01
10	0.130535696170244E+00	0.333260223918652E+00
	0.672886387019932E+00	0.742501752317741E+00
	0.159143208236292E+01	0.108005279782693E+01
	0.280041847052746E+01	0.132028812483455E+01
	0.419499640127942E+01	0.144971022336955E+01
	0.566066246651666E+01	0.146169692583314E+01
	0.707810341253441E+01	0.135292016838366E+01
	0.832621870954264E+01	0.112355472887245E+01
	0.928767980905348E+01	0.782143625547308E+00
	0.986125239933237E+01	0.353871429096005E+00

Table 2: Gaussian Quadrature for Bessel Functions with Weight Function

$$\int_0^{10} \frac{1}{\sqrt{x}} J_{k-1}(x)dx = \sum_{i=1}^{N} w_i J_{k-1}(x_i) \quad \text{for } k = 1, 2, \cdots, 2N$$

N	Nodes x_i	Weights w_i
5	0.221525014168133E+00	0.185798994260858E+01
	0.181515943791217E+01	0.162483079218151E+01
	0.434757211490782E+01	0.132302463248861E+01
	0.710741692330460E+01	0.990971542854905E+00
	0.933190129335545E+01	0.527439013034203E+00
10	0.586135127137856E-01	0.966145917958189E+00
	0.517839232816169E+00	0.939662007448660E+00
	0.138739079186343E+01	0.889891823703254E+00
	0.258047692418516E+01	0.821395494863014E+00
	0.398718764645530E+01	0.737970249083253E+00
	0.548586592652336E+01	0.641493179529387E+00
	0.694907018937755E+01	0.531905946105306E+00
	0.824679794056492E+01	0.408087704961759E+00
	0.925206018774378E+01	0.269503595251694E+00
	0.985409749058602E+01	0.118499400771494E+00

Table 3: Gaussian Quadrature for Products of Polynomials and Logarithmic function

$$\int_0^1 \varphi_k(x)dx = \sum_{i=1}^{N} w_i \varphi_k(x_i) \quad \text{for } k = 1, 2, \cdots, 2N$$

$$\text{where } \{\varphi_i\} = \{1, \ln x, x, x \ln x, \cdots, x^{N-1}, x^{N-1} \ln x\}$$

N	Nodes x_i	Weights w_i
5	0.565222820508010E-02	0.210469457918546E-01
	0.734303717426523E-01	0.130705540744447E+00
	0.284957404462558E+00	0.289702301671314E+00
	0.619482264084778E+00	0.350220370120399E+00
	0.915758083004698E+00	0.208324841671986E+00
10	0.482961710689630E-03	0.183340007378985E-02
	0.698862921431577E-02	0.134531223459918E-01
	0.326113965946776E-01	0.404971943169583E-01
	0.928257573891660E-01	0.818223696589036E-01
	0.198327256895404E+00	0.129192342770138E+00
	0.348880142979353E+00	0.169545319547259E+00
	0.530440555787956E+00	0.189100216532996E+00
	0.716764648511655E+00	0.177965753961471E+00
	0.875234557506234E+00	0.133724770615462E+00
	0.975245698684393E+00	0.628655101770325E-01
15	0.105784548458629E-03	0.403217724648460E-03
	0.156624383616782E-02	0.306297843478700E-02
	0.759521890320709E-02	0.978421211876615E-02
	0.228310673939862E-01	0.215587522255813E-01
	0.523886301568200E-01	0.383230673708892E-01
	0.100758685201213E+00	0.588981990263004E-01
	0.170740768849943E+00	0.811170299392595E-01
	0.262591206118993E+00	0.102122101972069E+00
	0.373536505184558E+00	0.118789059030401E+00
	0.497746358414533E+00	0.128210316446694E+00
	0.626789031392373E+00	0.128163327417093E+00
	0.750516103461408E+00	0.117489465888492E+00
	0.858255335207861E+00	0.963230185695904E-01
	0.940141291212346E+00	0.661345398318934E-01
	0.988401595986342E+00	0.296207140035355E-01

Table 3: Gaussian Quadrature for Products of Polynomials and Logarithmic function

$$\int_0^1 \varphi_k(x)dx = \sum_{i=1}^{N} w_i \varphi_k(x_i) \quad \text{for } k = 1, 2, \cdots, 2N$$

where $\{\varphi_i\} = \{1, \ln x, x, x \ln x, \cdots, x^{N-1}, x^{N-1} \ln x\}$

N	Nodes x_i	Weights w_i
20	0.352330453033401E-04	0.134499676467758E-03
	0.526093982517410E-03	0.103477692295062E-02
	0.258751954058141E-02	0.337726367723322E-02
	0.793447194838041E-02	0.767355619359468E-02
	0.186828881374457E-01	0.142054962855420E-01
	0.370976733697505E-01	0.229844384632086E-01
	0.653124886740214E-01	0.337363605577136E-01
	0.105048504711551E+00	0.459147630734522E-01
	0.157359691819002E+00	0.587404799428040E-01
	0.222430062767455E+00	0.712650131611020E-01
	0.299443765654100E+00	0.824518089775832E-01
	0.386542446943882E+00	0.912682015163873E-01
	0.480876453826790E+00	0.967797159091613E-01
	0.578747932205507E+00	0.982381433400897E-01
	0.675835475840038E+00	0.951553030540297E-01
	0.767482460872564E+00	0.873556504104574E-01
	0.849025253970320E+00	0.750027772122717E-01
	0.916133703241664E+00	0.585972958082337E-01
	0.965135427900256E+00	0.389472505496114E-01
	0.993303536456954E+00	0.171372052681059E-01

Table 3: Gaussian Quadrature for Products of Polynomials and Logarithmic function

$$\int_0^1 \varphi_k(x)dx = \sum_{i=1}^{N} w_i \varphi_k(x_i) \quad \text{for} \quad k = 1, 2, \cdots, 2N$$

$$\text{where } \{\varphi_i\} = \{1, \ln x, x, x \ln x, \cdots, x^{N-1}, x^{N-1} \ln x\}$$

N	Nodes x_i	Weights w_i
25	0.148805205646328E-04	0.568460660250201E-04
	0.223091159576411E-03	0.439997585768285E-03
	0.110464364905333E-02	0.145071890475698E-02
	0.341946946887918E-02	0.334401873816821E-02
	0.815052929502022E-02	0.630809954735095E-02
	0.164289374947747E-01	0.104488723103430E-01
	0.294459835598307E-01	0.157795036631243E-01
	0.483575697078870E-01	0.222157908473636E-01
	0.741870939196732E-01	0.295777024140889E-01
	0.107732955883456E+00	0.375970456071727E-01
	0.149486638258006E+00	0.459308515949728E-01
	0.199566730959199E+00	0.541797236656935E-01
	0.257673355831231E+00	0.619100915223039E-01
	0.323066266406625E+00	0.686790748928476E-01
	0.394568512069093E+00	0.740604961651057E-01
	0.470596049553319E+00	0.776705045127697E-01
	0.549212146433099E+00	0.791912877674640E-01
	0.628203942243359E+00	0.783914525088262E-01
	0.705177201069257E+00	0.751418416138657E-01
	0.777664184415768E+00	0.694258212157761E-01
	0.843238762138540E+00	0.613433919048328E-01
	0.899632416106158E+00	0.511088512980136E-01
	0.944844733405702E+00	0.390421895640177E-01
	0.977242575226688E+00	0.255554713626385E-01
	0.995647215456440E+00	0.111503547267104E-01

Table 3: Gaussian Quadrature for Products of Polynomials and Logarithmic function

$$\int_0^1 \varphi_k(x)dx = \sum_{i=1}^{N} w_i \varphi_k(x_i) \quad \text{for} \quad k = 1, 2, \cdots, 2N$$

where $\{\varphi_i\} = \{1, \ln x, x, x \ln x, \cdots, x^{N-1}, x^{N-1} \ln x\}$

N	Nodes x_i	Weights w_i
30	0.732379743551900E-05	0.279892154036191E-04
	0.110044700353982E-03	0.217365526303388E-03
	0.546918325703179E-03	0.720703585941237E-03
	0.170185751774368E-02	0.167446096386701E-02
	0.408386360682336E-02	0.319128240452640E-02
	0.830004117175941E-02	0.535378831096153E-02
	0.150229781480879E-01	0.820962136493378E-02
	0.249539236043865E-01	0.117680292095091E-01
	0.387833861559789E-01	0.159981435010663E-01
	0.571508984622219E-01	0.208290410897408E-01
	0.806057414498694E-01	0.261515976575626E-01
	0.109570394208134E+00	0.318220682660372E-01
	0.144308372971936E+00	0.376672559968915E-01
	0.184897949395368E+00	0.434910622609641E-01
	0.231213001514211E+00	0.490821532269183E-01
	0.282911960162101E+00	0.542224286606307E-01
	0.339435481155556E+00	0.586959442912318E-01
	0.400013113074849E+00	0.622979181160659E-01
	0.463678856906249E+00	0.648434457091797E-01
	0.529295142710295E+00	0.661755598539193E-01
	0.595584395297873E+00	0.661722952804487E-01
	0.661167040372616E+00	0.647524589265887E-01
	0.724604528155535E+00	0.618798583538578E-01
	0.784445734718383E+00	0.575658036673855E-01
	0.839274951465986E+00	0.518697691962532E-01
	0.887759597608297E+00	0.448981784990110E-01
	0.928695795957382E+00	0.368013625032992E-01
	0.961050059184175E+00	0.277688703796847E-01
	0.983995703519948E+00	0.180238737856617E-01
	0.996945958679506E+00	0.782767019615502E-02

Table 4: Gaussian Quadrature for Products of Polynomials and Fractional Powers

$$\int_0^1 \varphi_k(x)dx = \sum_{i=1}^{N} w_i \varphi_k(x_i) \quad \text{for } k = 1, 2, \cdots, 2N$$

where $\{\varphi_i\} = \{1, s(x), x, xs(x), \cdots, x^{N-1}, x^{N-1}s(x)\}$ with $s(x) = x^{\frac{2}{3}}$

N	Nodes x_i	Weights w_i
5	0.111388121461113E-01	0.350341916241438E-01
	0.989954782999841E-01	0.152986023564027E+00
	0.325462965706881E+00	0.293439234461264E+00
	0.650376177175503E+00	0.329423482895757E+00
	0.923830141383311E+00	0.189117067454808E+00
10	0.106075936690850E-02	0.342465634725548E-02
	0.105957835374351E-01	0.179697406786380E-01
	0.419569285287569E-01	0.471712377689652E-01
	0.109001951813403E+00	0.883592422887387E-01
	0.219861071532861E+00	0.132980363859702E+00
	0.372071233678686E+00	0.168929398195588E+00
	0.550779272731362E+00	0.184191248381816E+00
	0.730779332479715E+00	0.170661619172872E+00
	0.881954366270197E+00	0.126951038006216E+00
	0.976639980362546E+00	0.593614553002092E-01
15	0.241818436310427E-03	0.785216839155443E-03
	0.247904422657297E-02	0.428667428787457E-02
	0.102231505109504E-01	0.119847435540932E-01
	0.280798632789153E-01	0.245432960884266E-01
	0.608339281242860E-01	0.416404983681140E-01
	0.112443594490995E+00	0.619571219761760E-01
	0.185105777705090E+00	0.833277026033653E-01
	0.278545764961840E+00	0.103032984392016E+00
	0.389652905586201E+00	0.118190780445325E+00
	0.512532528698514E+00	0.126187019062355E+00
	0.638982003700951E+00	0.125082141394901E+00
	0.759334800695944E+00	0.113931212165169E+00
	0.863560355211660E+00	0.929687707138682E-01
	0.942468575671709E+00	0.636311469832558E-01
	0.988861955722520E+00	0.284506911259040E-01

Table 4: Gaussian Quadrature for Products of Polynomials and Fractional Powers

$$\int_0^1 \varphi_k(x)dx = \sum_{i=1}^{N} w_i \varphi_k(x_i) \quad \text{for } k = 1, 2, \cdots, 2N$$

where $\{\varphi_i\} = \{1, s(x), x, xs(x), \cdots, x^{N-1}, x^{N-1}s(x)\}$ with $s(x) = x^{\frac{2}{3}}$

N	Nodes x_i	Weights w_i
20	0.822258720897910E-04	0.267576170194858E-03
	0.851231173182477E-03	0.148254407742955E-02
	0.356411730804281E-02	0.424221866790033E-02
	0.999446520349904E-02	0.897068317712191E-02
	0.222308791404550E-01	0.158666804741713E-01
	0.424339835363049E-01	0.248722570057384E-01
	0.725741080670503E-01	0.356656880963368E-01
	0.114174415866984E+00	0.476793965125403E-01
	0.168083972212092E+00	0.601415054233364E-01
	0.234302815001518E+00	0.721375449972604E-01
	0.311876663295677E+00	0.826870082942195E-01
	0.398872872080255E+00	0.908280936995649E-01
	0.492442140014574E+00	0.957031990037015E-01
	0.588962927640006E+00	0.966376154468787E-01
	0.684258212417279E+00	0.932044202436777E-01
	0.773867742847468E+00	0.852697379326592E-01
	0.853353935948184E+00	0.730142442020013E-01
	0.918616478895035E+00	0.569289535722086E-01
	0.966190178403627E+00	0.377866171625958E-01
	0.993508545383756E+00	0.166140158404627E-01

Table 5: Gaussian Quadrature for Products of Polynomials and Fractional Powers

$$\int_0^1 \varphi_k(x)dx = \sum_{i=1}^{N} w_i \varphi_k(x_i) \quad \text{for } k = 1, 2, \cdots, 2N$$

where $\{\varphi_i\} = \{1, s(x), x, xs(x), \cdots, x^{N-1}, x^{N-1}s(x)\}$ with $s(x) = x^{\frac{1}{2}}$

N	Nodes x_i	Weights w_i
5	0.970916313338209E-02	0.314958290433846E-01
	0.927420088040289E-01	0.147817740145233E+00
	0.315872313916462E+00	0.292773974169340E+00
	0.643182477910772E+00	0.334349276188739E+00
	0.921965110615521E+00	0.193563180453303E+00
10	0.901742772555592E-03	0.299828120481279E-02
	0.966072992118868E-02	0.168386395659664E-01
	0.396093898716370E-01	0.455491829065261E-01
	0.105011991918026E+00	0.868038128143013E-01
	0.214610971190650E+00	0.132106151126701E+00
	0.366460914978464E+00	0.169114219381655E+00
	0.545885024355929E+00	0.185393787355447E+00
	0.727418879329945E+00	0.172422600578352E+00
	0.880346704943949E+00	0.128574309018165E+00
	0.976306802645093E+00	0.601990160480740E-01
15	0.203617338486320E-03	0.680684768275793E-03
	0.223725122307619E-02	0.397246938629008E-02
	0.954788886412147E-02	0.114344447894424E-01
	0.267548306484035E-01	0.238083807101952E-01
	0.587263787087472E-01	0.408326185452397E-01
	0.109550941121055E+00	0.612195391729371E-01
	0.181570447192808E+00	0.828014703688452E-01
	0.274636464058843E+00	0.102824724623773E+00
	0.385717152459535E+00	0.118348384119426E+00
	0.508930876164803E+00	0.126687910323023E+00
	0.636017805747573E+00	0.125836213297194E+00
	0.757194044089115E+00	0.114797651013883E+00
	0.862273903642310E+00	0.937832798881199E-01
	0.941904608637681E+00	0.642380897499318E-01
	0.988750439427061E+00	0.287341392434250E-01

Table 5: Gaussian Quadrature for Products of Polynomials and Fractional Powers

$$\int_0^1 \varphi_k(x)dx = \sum_{i=1}^{N} w_i \varphi_k(x_i) \quad \text{for } k = 1, 2, \cdots, 2N$$

where $\{\varphi_i\} = \{1, s(x), x, xs(x), \cdots, x^{N-1}, x^{N-1}s(x)\}$ with $s(x) = x^{\frac{1}{2}}$

N	Nodes x_i	Weights w_i
20	0.688907338392845E-04	0.230763814351417E-03
	0.764138398652809E-03	0.136612455217214E-02
	0.331021381556300E-02	0.402291522792898E-02
	0.946809336603785E-02	0.864643822538178E-02
	0.213344721137020E-01	0.154553358601049E-01
	0.410964086262251E-01	0.244080922533623E-01
	0.707645876791935E-01	0.351941337584140E-01
	0.111910522350377E+00	0.472505923470994E-01
	0.165432926252467E+00	0.598034836852591E-01
	0.231376114514019E+00	0.719298383077259E-01
	0.308818842285795E+00	0.826354136333313E-01
	0.395845853335002E+00	0.909411778827062E-01
	0.489607131209166E+00	0.959709232198866E-01
	0.586462066987943E+00	0.970322101197066E-01
	0.682198172145692E+00	0.936833837251139E-01
	0.772307249294583E+00	0.857805916759546E-01
	0.852296694398426E+00	0.735004796732940E-01
	0.918010354508321E+00	0.573364747582598E-01
	0.965932757966444E+00	0.380699389274024E-01
	0.993458519536807E+00	0.167416883525447E-01

Table 6: Gaussian Quadrature for Products of Polynomials and Fractional Powers

$$\int_0^1 \varphi_k(x)dx = \sum_{i=1}^{N} w_i \varphi_k(x_i) \quad \text{for } k = 1, 2, \cdots, 2N$$

where $\{\varphi_i\} = \{1, s(x), x, xs(x), \cdots, x^{N-1}, x^{N-1}s(x)\}$ with $s(x) = x^{\frac{1}{3}}$

N	Nodes x_i	Weights w_i
5	0.831174531456776E-02	0.279778782123048E-01
	0.863966362795308E-01	0.142398935990482E+00
	0.305943516943443E+00	0.291943668689807E+00
	0.635656558720652E+00	0.339447240627363E+00
	0.920004207024857E+00	0.198232276480043E+00
10	0.751897878625465E-03	0.259000938099737E-02
	0.874666094268371E-02	0.157085175605557E-01
	0.372684363855664E-01	0.438972012175236E-01
	0.100986759928202E+00	0.851979518885884E-01
	0.209274931334610E+00	0.131185462315937E+00
	0.360730157291068E+00	0.169279428891491E+00
	0.540868549812902E+00	0.186612247123971E+00
	0.723966527445448E+00	0.174225330076043E+00
	0.878692655294032E+00	0.130242598410538E+00
	0.975963746745065E+00	0.610612531343552E-01
15	0.168121349224655E-03	0.582014429388243E-03
	0.200427399422478E-02	0.366362217710688E-02
	0.888445820257933E-02	0.108842247988913E-01
	0.254380748331252E-01	0.230661756216959E-01
	0.566163366479501E-01	0.400108265603416E-01
	0.106639742234206E+00	0.604643908138577E-01
	0.177998880856086E+00	0.822581407444590E-01
	0.270675783247184E+00	0.102603879506980E+00
	0.381720959785030E+00	0.118500791181315E+00
	0.505267785653412E+00	0.127191992481750E+00
	0.632999186646096E+00	0.126600784497532E+00
	0.755011893747991E+00	0.115679059680403E+00
	0.860961671393287E+00	0.946133646757434E-01
	0.941329076190074E+00	0.648572778769515E-01
	0.988636608057791E+00	0.290234549535849E-01

Table 6: Gaussian Quadrature for Products of Polynomials and Fractional Powers

$$\int_0^1 \varphi_k(x)dx = \sum_{i=1}^{N} w_i \varphi_k(x_i) \quad \text{for } k = 1, 2, \cdots, 2N$$

where $\{\varphi_i\} = \{1, s(x), x, xs(x), \cdots, x^{N-1}, x^{N-1}s(x)\}$ with $s(x) = x^{\frac{1}{3}}$

N	Nodes x_i	Weights w_i
20	0.565910606963981E-04	0.196275471368437E-03
	0.680854395380959E-03	0.125263851254803E-02
	0.306270110956997E-02	0.380561564887333E-02
	0.894917200513315E-02	0.832217213031223E-02
	0.204442383726108E-01	0.150414196754775E-01
	0.397611592475325E-01	0.239388575134562E-01
	0.689512869857525E-01	0.347155654274889E-01
	0.109635234283660E+00	0.468137478429227E-01
	0.162762389006638E+00	0.594574979240510E-01
	0.228422459407150E+00	0.717153419416687E-01
	0.305728258549570E+00	0.825791227715473E-01
	0.392782689780531E+00	0.910522631915573E-01
	0.486735430814252E+00	0.962395518442346E-01
	0.583926798874029E+00	0.974303994336976E-01
	0.680108431067843E+00	0.941680397096348E-01
	0.770723438587922E+00	0.862983560861100E-01
	0.851223225892569E+00	0.739938065555806E-01
	0.917394745239490E+00	0.577502214287376E-01
	0.965671257181204E+00	0.383577114718547E-01
	0.993407695194012E+00	0.168713954188783E-01

Table 7: Gaussian Quadrature for Products of Polynomials and Fractional Powers

$$\int_0^1 \varphi_k(x)dx = \sum_{i=1}^{N} w_i \varphi_k(x_i) \quad \text{for } k = 1, 2, \cdots, 2N$$

where $\{\varphi_i\} = \{1, s(x), x, xs(x), \cdots, x^{N-1}, x^{N-1}s(x)\}$ with $s(x) = x^{\frac{1}{4}}$

N	Nodes x_i	Weights w_i
5	0.762794972812507E-02	0.262298035906717E-01
	0.831895488095584E-01	0.139587984773339E+00
	0.300844037453126E+00	0.291460348074849E+00
	0.631759839813656E+00	0.342065172592006E+00
	0.918985115815450E+00	0.200656690969134E+00
10	0.680661832514276E-03	0.239309679083200E-02
	0.829805126031941E-02	0.151439816123742E-01
	0.361008488950617E-01	0.430595363165574E-01
	0.989606158324035E-01	0.843751810440922E-01
	0.206573413000166E+00	0.130706769333825E+00
	0.357817634747240E+00	0.169354243901417E+00
	0.538312396928998E+00	0.187227677434183E+00
	0.722204307474990E+00	0.175143061430482E+00
	0.877847435011894E+00	0.131094401625182E+00
	0.975788344331792E+00	0.615020505110549E-01
15	0.151429644289982E-03	0.534953080073061E-03
	0.189120816621145E-02	0.351128622129104E-02
	0.855735146816403E-02	0.106091654389163E-01
	0.247829453316383E-01	0.226922601463664E-01
	0.555603949382247E-01	0.395945355599134E-01
	0.105176990238943E+00	0.600799922753622E-01
	0.176199068882164E+00	0.819798274477196E-01
	0.268675523469233E+00	0.102488560198090E+00
	0.379699417736514E+00	0.118574970046103E+00
	0.503412401869408E+00	0.127445268951420E+00
	0.631468760396525E+00	0.126987144614300E+00
	0.753904757831583E+00	0.116125573735615E+00
	0.860295553378594E+00	0.950344508261170E-01
	0.941036823465374E+00	0.651716225755041E-01
	0.988578794355859E+00	0.291703888832093E-01

Table 7: Gaussian Quadrature for Products of Polynomials and Fractional Powers

$$\int_0^1 \varphi_k(x)dx = \sum_{i=1}^{N} w_i \varphi_k(x_i) \quad \text{for } k = 1, 2, \cdots, 2N$$

where $\{\varphi_i\} = \{1, s(x), x, xs(x), \cdots, x^{N-1}, x^{N-1}s(x)\}$ with $s(x) = x^{\frac{1}{4}}$

N	Nodes x_i	Weights w_i
20	0.508401144727475E-04	0.179921229090492E-03
	0.640671409304506E-03	0.119702077067209E-02
	0.294139627824379E-02	0.369773784996860E-02
	0.869257229367654E-02	0.816003283674897E-02
	0.200014921598775E-01	0.148334720914000E-01
	0.390944230688757E-01	0.237022859923791E-01
	0.680431707412333E-01	0.344735758559312E-01
	0.108493186848796E+00	0.465922232807169E-01
	0.161419592745879E+00	0.592814319750155E-01
	0.226935224532033E+00	0.716054742949001E-01
	0.304170319054039E+00	0.825491665123296E-01
	0.391237157031920E+00	0.911070366015320E-01
	0.485285420936866E+00	0.963742175415786E-01
	0.582645888835788E+00	0.976308832970205E-01
	0.679052102488331E+00	0.944125656226918E-01
	0.769922539292854E+00	0.865599052197165E-01
	0.850680233407198E+00	0.742432057258809E-01
	0.917083282994612E+00	0.579594958287601E-01
	0.965538933432666E+00	0.385033140388101E-01
	0.993381975142296E+00	0.169370334348568E-01

Table 8: Gaussian Quadrature for Products of Polynomials and Fractional Powers

$$\int_0^1 \varphi_k(x)dx = \sum_{i=1}^{N} w_i \varphi_k(x_i) \quad \text{for} \quad k = 1, 2, \cdots, 2N$$

where $\{\varphi_i\} = \{1, s(x), x, xs(x), \cdots, x^{N-1}, x^{N-1}s(x)\}$ with $s(x) = x^{-\frac{1}{4}}$

N	Nodes x_i	Weights w_i
5	0.382423605041850E-02	0.159917283936684E-01
	0.634597428923166E-01	0.121052296479220E+00
	0.268079430001204E+00	0.287406177837817E+00
	0.606207314918122E+00	0.358886538601875E+00
	0.912243119495094E+00	0.216663258687420E+00
10	0.311664421263886E-03	0.132408316145357E-02
	0.573840166641843E-02	0.117668861542949E-01
	0.291436456086289E-01	0.378545434895510E-01
	0.865989640195454E-01	0.791317874471543E-01
	0.189850316327027E+00	0.127550269062920E+00
	0.339616983180453E+00	0.169682299097476E+00
	0.522237733374721E+00	0.191015829563274E+00
	0.711076275414628E+00	0.180901690009248E+00
	0.872496278362019E+00	0.136476978227289E+00
	0.974676373102776E+00	0.642956337873400E-01
15	0.671537172803988E-04	0.286236608068052E-03
	0.126348368805257E-02	0.262818581079834E-02
	0.666285677053233E-02	0.895931713383214E-02
	0.208996392447129E-01	0.204062530697822E-01
	0.492092869824728E-01	0.370154044724167E-01
	0.962910504069878E-01	0.576707391266183E-01
	0.165187187294757E+00	0.802098718885372E-01
	0.256372388322078E+00	0.101723142015267E+00
	0.367215812312105E+00	0.118989956384134E+00
	0.491920272820932E+00	0.128983991417795E+00
	0.621967797979428E+00	0.129367050472822E+00
	0.747019986367819E+00	0.118892374347340E+00
	0.856148272384472E+00	0.976520449023468E-01
	0.939215799595110E+00	0.671291997815284E-01
	0.988218403767777E+00	0.300862325687140E-01

Table 8: Gaussian Quadrature for Products of Polynomials and Fractional Powers

$$\int_0^1 \varphi_k(x)dx = \sum_{i=1}^{N} w_i \varphi_k(x_i) \quad \text{for} \quad k = 1, 2, \cdots, 2N$$

where $\{\varphi_i\} = \{1, s(x), x, xs(x), \cdots, x^{N-1}, x^{N-1}s(x)\}$ with $s(x) = x^{-\frac{1}{4}}$

N	Nodes x_i	Weights w_i
20	0.221820235538413E-04	0.946625535057872E-04
	0.420668156388107E-03	0.879580435485498E-03
	0.224897834059227E-02	0.306154371288216E-02
	0.719410590426075E-02	0.718677600572896E-02
	0.173785665899570E-01	0.135708222783955E-01
	0.351053065795165E-01	0.222536266859334E-01
	0.625706338467844E-01	0.329813226328586E-01
	0.101573342538239E+00	0.452169532360338E-01
	0.153248856878474E+00	0.581794488048750E-01
	0.217855193592975E+00	0.709075209058289E-01
	0.294632990834409E+00	0.823427811731510E-01
	0.381755192469280E+00	0.914245608123939E-01
	0.476373817974157E+00	0.971877635212259E-01
	0.574762338493956E+00	0.988547376185605E-01
	0.672543338723645E+00	0.959126372029696E-01
	0.764983189265488E+00	0.881690173465919E-01
	0.847329128952469E+00	0.757803722977461E-01
	0.915160094733383E+00	0.592508853437043E-01
	0.964721591676480E+00	0.394024605588481E-01
	0.993223076818039E+00	0.173425268732812E-01

Table 9: Gaussian Quadrature for Products of Polynomials and Fractional Powers

$$\int_0^1 \varphi_k(x)dx = \sum_{i=1}^{N} w_i \varphi_k(x_i) \quad \text{for } k = 1, 2, \cdots, 2N$$

where $\{\varphi_i\} = \{1, s(x), x, xs(x), \cdots, x^{N-1}, x^{N-1}s(x)\}$ with $s(x) = x^{-\frac{1}{3}}$

N	Nodes x_i	Weights w_i
5	0.325694885051994E-02	0.143436825038591E-01
	0.600861836255002E-01	0.117635462047981E+00
	0.262200689766926E+00	0.286500581347155E+00
	0.601527262010120E+00	0.361906424437754E+00
	0.910998040648555E+00	0.219613849663250E+00
10	0.261010670878138E-03	0.116634009622830E-02
	0.533570406879994E-02	0.112056554482295E-01
	0.279923598777842E-01	0.369538395786576E-01
	0.845001067179312E-01	0.782012224225048E-01
	0.186967540598809E+00	0.126971878207205E+00
	0.336449186747933E+00	0.169715037099809E+00
	0.519422386872603E+00	0.191665171997203E+00
	0.709119391752190E+00	0.181908136234217E+00
	0.871552940481438E+00	0.137424134774237E+00
	0.974480099088773E+00	0.647885841417101E-01
15	0.559212686135403E-04	0.250636999997100E-03
	0.116764741757783E-02	0.248629682453753E-02
	0.635876913141328E-02	0.868418049215750E-02
	0.202601345786029E-01	0.200174031540757E-01
	0.481469972090806E-01	0.365707842279019E-01
	0.947893055727041E-01	0.572506624316614E-01
	0.163312504831184E+00	0.798969454587593E-01
	0.254266678317515E+00	0.101582504459800E+00
	0.365070714120304E+00	0.119053915578673E+00
	0.489939651507906E+00	0.129244090759107E+00
	0.620326692664507E+00	0.129774994114533E+00
	0.745828824368843E+00	0.119369417740098E+00
	0.855429899278146E+00	0.981047682668204E-01
	0.938900129707038E+00	0.674683579975495E-01
	0.988155905432853E+00	0.302450414943277E-01

Table 9: Gaussian Quadrature for Products of Polynomials and Fractional Powers

$$\int_0^1 \varphi_k(x)dx = \sum_{i=1}^{N} w_i \varphi_k(x_i) \quad \text{for} \quad k = 1, 2, \cdots, 2N$$

where $\{\varphi_i\} = \{1, s(x), x, xs(x), \cdots, x^{N-1}, x^{N-1}s(x)\}$ with $s(x) = x^{-\frac{1}{3}}$

N	Nodes x_i	Weights w_i
20	0.184194907598179E-04	0.826457102725699E-04
	0.387587458269692E-03	0.829421040741860E-03
	0.213955259577947E-02	0.295732155968210E-02
	0.695120073310895E-02	0.702434283841401E-02
	0.169467664404234E-01	0.133575962599994E-01
	0.344417452000176E-01	0.220068985356573E-01
	0.616535209242469E-01	0.327254003368527E-01
	0.100407215362434E+00	0.449795404557805E-01
	0.151866019233245E+00	0.579877214786053E-01
	0.216313281828314E+00	0.707843838119479E-01
	0.293009074582624E+00	0.823037488978054E-01
	0.380137222473773E+00	0.914756213036679E-01
	0.474850532149502E+00	0.973244581548574E-01
	0.573412898781505E+00	0.990625442531322E-01
	0.671427980742799E+00	0.961685890414821E-01
	0.764136026657879E+00	0.884443478050775E-01
	0.846753983774620E+00	0.760438602249420E-01
	0.914829857705509E+00	0.594724986507429E-01
	0.964581196697193E+00	0.395568714306716E-01
	0.993195777887590E+00	0.174121882096675E-01

Table 10: Gaussian Quadrature for Products of Polynomials and Fractional Powers

$$\int_0^1 \varphi_k(x)dx = \sum_{i=1}^{N} w_i \varphi_k(x_i) \quad \text{for } k = 1, 2, \cdots, 2N$$

where $\{\varphi_i\} = \{1, s(x), x, xs(x), \cdots, x^{N-1}, x^{N-1}s(x)\}$ with $s(x) = x^{-\frac{1}{2}}$

N	Nodes x_i	Weights w_i
5	0.220055532702321E-02	0.111142584286221E-01
	0.532526444285811E-01	0.110450910249386E+00
	0.250000000000000E+00	0.284444444444444E+00
	0.591721954534264E+00	0.368177760249980E+00
	0.908380401265687E+00	0.225812626627567E+00
10	0.170217313506295E-03	0.869843410720295E-03
	0.455197375232787E-02	0.100832309490842E-01
	0.256945562245545E-01	0.351184957693976E-01
	0.802601948484878E-01	0.762838816843756E-01
	0.181103722710989E+00	0.125764125553643E+00
	0.329978061692620E+00	0.169760099161110E+00
	0.513655588977735E+00	0.192982837625621E+00
	0.705104124523579E+00	0.183967866746584E+00
	0.869615340441312E+00	0.139368118201496E+00
	0.974076745830678E+00	0.658015008979678E-01
15	0.360449058720925E-04	0.184634499540016E-03
	0.983656825228959E-03	0.220691172454993E-02
	0.576031032998391E-02	0.813303209689366E-02
	0.189863966971689E-01	0.192316020292443E-01
	0.460162191690594E-01	0.356670580668843E-01
	0.917631475619828E-01	0.563926955430610E-01
	0.159522718866145E+00	0.792541212080791E-01
	0.250000000000000E+00	0.101289120962781E+00
	0.360716812863579E+00	0.119177364119033E+00
	0.485914494639546E+00	0.129768304472501E+00
	0.616988391777598E+00	0.130602147750110E+00
	0.743404128057339E+00	0.120339075896910E+00
	0.853966893740411E+00	0.990261883702783E-01
	0.938257049225935E+00	0.681591357635582E-01
	0.988028562926358E+00	0.305686074965773E-01

Table 10: Gaussian Quadrature for Products of Polynomials and Fractional Powers

$$\int_0^1 \varphi_k(x)dx = \sum_{i=1}^{N} w_i \varphi_k(x_i) \quad \text{for } k = 1, 2, \cdots, 2N$$

where $\{\varphi_i\} = \{1, s(x), x, xs(x), \cdots, x^{N-1}, x^{N-1}s(x)\}$ with $s(x) = x^{-\frac{1}{2}}$

N	Nodes x_i	Weights w_i
20	0.118040372897702E-04	0.605164515048587E-04
	0.324505506016988E-03	0.731395632734516E-03
	0.192569889609293E-02	0.275022407735182E-02
	0.647083718891321E-02	0.669890718081941E-02
	0.160868754200355E-01	0.129282095841639E-01
	0.331142308281794E-01	0.215082324328235E-01
	0.598127724451431E-01	0.322066292668297E-01
	0.980610158280346E-01	0.444969640416654E-01
	0.149078672924258E+00	0.575967453908003E-01
	0.213200816542450E+00	0.705318509111265E-01
	0.289727337675948E+00	0.822215362195993E-01
	0.376864524065904E+00	0.915762410818034E-01
	0.471767104543454E+00	0.975991452767166E-01
	0.570679774395970E+00	0.994820091823469E-01
	0.669167911554694E+00	0.966862995286949E-01
	0.762418781880186E+00	0.890019102330765E-01
	0.845587809011132E+00	0.765778343958853E-01
	0.914160127147419E+00	0.599218242567572E-01
	0.964296432783931E+00	0.398700341676524E-01
	0.993140403222385E+00	0.175534906876473E-01

Table 11: Gaussian Quadrature for Products of Polynomials and Fractional Powers

$$\int_0^1 \varphi_k(x)dx = \sum_{i=1}^{N} w_i \varphi_k(x_i) \quad \text{for} \quad k = 1, 2, \cdots, 2N$$

where $\{\varphi_i\} = \{1, s(x), x, xs(x), \cdots, x^{N-1}, x^{N-1}s(x)\}$ with $s(x) = x^{-\frac{2}{3}}$

N	Nodes x_i	Weights w_i
5	0.127054140407448E-02	0.798095300782248E-02
	0.462681413226638E-01	0.102702832369157E+00
	0.237083298080667E+00	0.282009089112635E+00
	0.581208702007414E+00	0.374825379887486E+00
	0.905561736397846E+00	0.232481745622901E+00
10	0.945849186124229E-04	0.599207947722056E-03
	0.379603281250484E-02	0.895661938070323E-02
	0.233952614888275E-01	0.332290268550819E-01
	0.759462672091217E-01	0.742813877203913E-01
	0.175082164491838E+00	0.124481407759041E+00
	0.323295565014521E+00	0.169777375189087E+00
	0.507679537823808E+00	0.194331900792034E+00
	0.700934090961697E+00	0.186099994751647E+00
	0.867600470065010E+00	0.141387747529539E+00
	0.973657038209960E+00	0.668553320747537E-01
15	0.197855962731515E-04	0.125556576654582E-03
	0.809581023980278E-03	0.193257660045135E-02
	0.517321860359321E-02	0.757902277249522E-02
	0.177160194789544E-01	0.184325783933937E-01
	0.438708712542835E-01	0.347412411366044E-01
	0.886977166657579E-01	0.555083582856597E-01
	0.155667671624679E+00	0.785867325255755E-01
	0.245646859906903E+00	0.100978745423403E+00
	0.356264972533447E+00	0.119295279382622E+00
	0.481792161982642E+00	0.130299495385019E+00
	0.613565444840732E+00	0.131446824433812E+00
	0.740915815910203E+00	0.121332382739473E+00
	0.852464602157936E+00	0.999716176822775E-01
	0.937596443363357E+00	0.688685445138014E-01
	0.987897722986291E+00	0.309010441487584E-01

Table 11: Gaussian Quadrature for Products of Polynomials and Fractional Powers

$$\int_0^1 \varphi_k(x)dx = \sum_{i=1}^{N} w_i \varphi_k(x_i) \quad \text{for } k = 1, 2, \cdots, 2N$$

where $\{\varphi_i\} = \{1, s(x), x, xs(x), \cdots, x^{N-1}, x^{N-1}s(x)\}$ with $s(x) = x^{-\frac{2}{3}}$

N	Nodes x_i	Weights w_i
20	0.644080669471020E-05	0.408973476604909E-04
	0.265385497209493E-03	0.636150271129477E-03
	0.171795135681289E-02	0.254437715881698E-02
	0.599650565966228E-02	0.637191713688041E-02
	0.152297986688364E-01	0.124939147170132E-01
	0.317830016969808E-01	0.210015095348042E-01
	0.579590115876318E-01	0.316775070055125E-01
	0.956908382982334E-01	0.440030511092655E-01
	0.146256150019543E+00	0.571949651553830E-01
	0.210043256963358E+00	0.702705143585106E-01
	0.286393214270049E+00	0.821337066503373E-01
	0.373535741616497E+00	0.916751595069523E-01
	0.468627945387644E+00	0.978762191044640E-01
	0.567895206083029E+00	0.999075512797006E-01
	0.666863963449413E+00	0.972128770925840E-01
	0.760667402163021E+00	0.895698602397595E-01
	0.844398042013510E+00	0.771222579836698E-01
	0.913476675531666E+00	0.603802128097188E-01
	0.964005785910473E+00	0.401896290968344E-01
	0.993083879404685E+00	0.176977224410030E-01

Table 12: Integration by the Gaussian Quadrature of Bessel Functions in TABLE 1

$$\int_0^{10} f(x)dx \approx \sum_{i=1}^{N} w_i f(x_i)$$

$$f(x) = \sin(x)$$

$\int_0^{10} f(x)dx = 0.183907152907645E+01$			
N	Computed Integral	Absolute Error	Relative Error
5	0.183911205770184E+01	0.40529E-04	0.22038E-04
10	0.183907152907645E+01	0.15543E-14	0.84516E-15

$$f(x) = -\cos(x)$$

$\int_0^{10} f(x)dx = 0.544021110889370E+00$			
N	Computed Integral	Absolute Error	Relative Error
5	0.544074430126847E+00	0.53319E-04	0.98010E-04
10	0.544021110889362E+00	0.77716E-14	0.14285E-13

$$f(x) = -x$$

$\int_0^{10} f(x)dx = 0.500000000000000E+02$			
N	Computed Integral	Absolute Error	Relative Error
5	0.499933635432992E+02	0.66365E-02	0.13273E-03
10	0.499999999999999E+02	0.14921E-12	0.29843E-14

Table 13: Integration by the Gaussian Quadrature of Bessel Functions in TABLE 2

$$\int_0^{10} \frac{1}{\sqrt{x}} f(x)dx \approx \sum_{i=1}^{N} w_i f(x_i)$$

$$f(x) = \sin(x)$$

$\int_0^{10} \frac{1}{\sqrt{x}} f(x)dx = 0.152512353028332E+01$			
N	Computed Integral	Absolute Error	Relative Error
5	0.152515304377709E+01	0.29513E-04	0.19352E-04
10	0.152512353028335E+01	0.33307E-13	0.21839E-13

$$f(x) = 1 - \cos(x)$$

$\int_0^{10} \frac{1}{\sqrt{x}} f(x)dx = 0.522924912143076E+01$			
N	Computed Integral	Absolute Error	Relative Error
5	0.522898009347896E+01	0.26903E-03	0.51447E-04
10	0.522924912142827E+01	0.24931E-11	0.47676E-12

$$f(x) = x$$

$\int_0^{10} \frac{1}{\sqrt{x}} f(x)dx = 0.210818510677892E+02$			
N	Computed Integral	Absolute Error	Relative Error
5	0.210781199174431E+02	0.37312E-02	0.17698E-03
10	0.210818510677890E+02	0.19895E-12	0.94371E-14

Table 14: Integration by the Gaussian Quadrature for the Products of Polynomials and Logarithmic Functions in TABLE 3

$$\int_0^1 f(x)dx \approx \sum_{i=1}^{N} w_i f(x_i)$$

$$f(x) = \sin(17x)$$

$\int_0^1 f(x)dx = 0.750096081206822E\text{-}01$			
N	Computed Integral	Absolute Error	Relative Error
5	-0.445245704584552E+00	0.52026E+00	0.69358E+01
10	0.759657791361190E-01	0.95617E-03	0.12747E-01
15	0.750095713818829E-01	0.36739E-07	0.48979E-06
20	0.750096081208711E-01	0.18893E-12	0.25188E-11
25	0.750096081206832E-01	0.10131E-14	0.13506E-13
30	0.750096081206823E-01	0.11102E-15	0.14801E-14

$$f(x) = x^{45}$$

$\int_0^1 f(x)dx = 0.217391304347826E\text{-}01$			
N	Computed Integral	Absolute Error	Relative Error
5	0.397077526634515E-02	0.17768E-01	0.81734E+00
10	0.206816335417969E-01	0.10575E-02	0.48645E-01
15	0.217347730977134E-01	0.43573E-05	0.20044E-03
20	0.217391290710919E-01	0.13637E-08	0.62730E-07
25	0.217391304347564E-01	0.26222E-13	0.12062E-11
30	0.217391304347826E-01	0.69389E-17	0.31919E-15

$$f(x) = -x^{45} \ln x$$

$\int_0^1 f(x)dx = 0.472589792060492E\text{-}03$			
N	Computed Integral	Absolute Error	Relative Error
5	0.349440397064675E-03	0.12315E-03	0.26058E+00
10	0.554396948210119E-03	0.81807E-04	0.17310E+00
15	0.473519740800504E-03	0.92995E-06	0.19678E-02
20	0.472590360153710E-03	0.56809E-09	0.12021E-05
25	0.472589792079166E-03	0.18675E-13	0.39515E-10
30	0.472589792060492E-03	0.37947E-18	0.80296E-15

Table 15: Integration by the Gaussian Quadrature for the Products of Polynomials and Fractional Power $s(x) = x^{\frac{2}{3}}$ in TABLE 4

$$\int_0^1 f(x)dx = \sum_{i=1}^{N} w_i f(x_i)$$

$$f(x) = \sin(10x)$$

$\int_0^1 f(x)dx = 0.183907152907645E+00$			
N	Computed Integral	Absolute Error	Relative Error
5	0.205829062722746E+00	0.21922E-01	0.11920E+00
10	0.183906457937759E+00	0.69497E-06	0.37789E-05
15	0.183907152908513E+00	0.86728E-12	0.47158E-11
20	0.183907152907645E+00	0.19429E-15	0.10565E-14

$$f(x) = x^{25}$$

$\int_0^1 f(x)dx = 0.384615384615385E-01$			
N	Computed Integral	Absolute Error	Relative Error
5	0.261006235736059E-01	0.12361E-01	0.32138E+00
10	0.384350080122515E-01	0.26530E-04	0.68979E-03
15	0.384615380725112E-01	0.38903E-09	0.10115E-07
20	0.384615384615385E-01	0.69389E-16	0.18041E-14

$$f(x) = x^{25}s(x)$$

$\int_0^1 f(x)dx = 0.377358490566038E-01$			
N	Computed Integral	Absolute Error	Relative Error
5	0.261006235736059E-01	0.12361E-01	0.32138E+00
10	0.384350080122515E-01	0.26530E-04	0.68979E-03
15	0.384615380725112E-01	0.38903E-09	0.10115E-07
20	0.384615384615385E-01	0.69389E-16	0.18041E-14

Table 16: Integration by the Gaussian Quadrature for the Products of Polynomials and Fractional Power $s(x) = x^{\frac{1}{2}}$ in TABLE 5

$$\int_0^1 f(x)dx = \sum_{i=1}^{N} w_i f(x_i)$$

$$f(x) = \sin(10x)$$

$\int_0^1 f(x)dx = 0.183907152907645\text{E+}00$			
N	Computed Integral	Absolute Error	Relative Error
5	0.205245178663791E+00	0.21338E-01	0.11603E+00
10	0.183906379065431E+00	0.77384E-06	0.42078E-05
15	0.183907152908629E+00	0.98405E-12	0.53508E-11
20	0.183907152907645E+00	0.27756E-16	0.15092E-15

$$f(x) = x^{25}$$

$\int_0^1 f(x)dx = 0.384615384615385\text{E-}01$			
N	Computed Integral	Absolute Error	Relative Error
5	0.253967007271653E-01	0.13065E-01	0.33969E+00
10	0.384311761588644E-01	0.30362E-04	0.78942E-03
15	0.384615379738251E-01	0.48771E-09	0.12681E-07
20	0.384615384615383E-01	0.20817E-15	0.54123E-14

$$f(x) = x^{25}s(x)$$

$\int_0^1 f(x)dx = 0.377358490566038\text{E-}01$			
N	Computed Integral	Absolute Error	Relative Error
5	0.243848070841558E-01	0.13351E-01	0.35380E+00
10	0.377002264605833E-01	0.35623E-04	0.94400E-03
15	0.377358483110791E-01	0.74552E-09	0.19756E-07
20	0.377358490566035E-01	0.22898E-15	0.60681E-14

Table 17: Integration by the Gaussian Quadrature for the Products of Polynomials and Fractional Power $s(x) = x^{\frac{1}{3}}$ in TABLE 6

$$\int_0^1 f(x)dx = \sum_{i=1}^{N} w_i f(x_i)$$

$$f(x) = \sin(10x)$$

$\int_0^1 f(x)dx = 0.183907152907645E+00$			
N	Computed Integral	Absolute Error	Relative Error
5	0.203627012649713E+00	0.19720E-01	0.10723E+00
10	0.183906319056362E+00	0.83385E-06	0.45341E-05
15	0.183907152908719E+00	0.10739E-11	0.58396E-11
20	0.183907152907644E+00	0.86042E-15	0.46786E-14

$$f(x) = x^{25}$$

$\int_0^1 f(x)dx = 0.384615384615385E-01$			
N	Computed Integral	Absolute Error	Relative Error
5	0.246599205561149E-01	0.13802E-01	0.35884E+00
10	0.384268064253340E-01	0.34732E-04	0.90303E-03
15	0.384615378508424E-01	0.61070E-09	0.15878E-07
20	0.384615384615384E-01	0.11102E-15	0.28866E-14

$$f(x) = x^{25}s(x)$$

$\int_0^1 f(x)dx = 0.380228136882129E-01$			
N	Computed Integral	Absolute Error	Relative Error
5	0.246599205561149E-01	0.13802E-01	0.35884E+00
10	0.384268064253340E-01	0.34732E-04	0.90303E-03
15	0.384615378508424E-01	0.61070E-09	0.15878E-07
20	0.384615384615384E-01	0.11102E-15	0.28866E-14

Table 18: Integration by the Gaussian Quadrature for the Products of Polynomials and Fractional Power $s(x) = x^{\frac{1}{4}}$ in TABLE 7

$$\int_0^1 f(x)dx = \sum_{i=1}^{N} w_i f(x_i)$$

$$f(x) = \sin(10x)$$

$\int_0^1 f(x)dx = 0.183907152907645E+00$			
N	Computed Integral	Absolute Error	Relative Error
5	0.202354038388179E+00	0.18447E-01	0.10031E+00
10	0.183906300136278E+00	0.85277E-06	0.46370E-05
15	0.183907152908747E+00	0.11020E-11	0.59920E-11
20	0.183907152907645E+00	0.19429E-15	0.10565E-14

$$f(x) = x^{25}$$

$\int_0^1 f(x)dx = 0.384615384615385E-01$			
N	Computed Integral	Absolute Error	Relative Error
5	0.242788857020719E-01	0.14183E-01	0.36875E+00
10	0.384243967690490E-01	0.37142E-04	0.96568E-03
15	0.384615377784612E-01	0.68308E-09	0.17760E-07
20	0.384615384615385E-01	0.41633E-16	0.10825E-14

$$f(x) = x^{25}s(x)$$

$\int_0^1 f(x)dx = 0.380228136882129E-01$			
N	Computed Integral	Absolute Error	Relative Error
5	0.242788857020719E-01	0.14183E-01	0.36875E+00
10	0.384243967690490E-01	0.37142E-04	0.96568E-03
15	0.384615377784612E-01	0.68308E-09	0.17760E-07
20	0.384615384615385E-01	0.41633E-16	0.10825E-14

Table 19: Integration by the Gaussian Quadrature for the Products of Polynomials and Fractional Power $s(x) = x^{-\frac{1}{4}}$ in TABLE 8

$$\int_0^1 f(x)dx = \sum_{i=1}^{N} w_i f(x_i)$$

$$f(x) = \sin(10x)$$

$\int_0^1 f(x)dx = 0.183907152907645E+00$			
N	Computed Integral	Absolute Error	Relative Error
5	0.185981461566628E+00	0.20743E-02	0.11279E-01
10	0.183906491673941E+00	0.66123E-06	0.35955E-05
15	0.183907152908381E+00	0.73541E-12	0.39988E-11
20	0.183907152907644E+00	0.80491E-15	0.43767E-14

$$f(x) = x^{25}$$

$\int_0^1 f(x)dx = 0.384615384615385E-01$			
N	Computed Integral	Absolute Error	Relative Error
5	0.218060230285103E-01	0.16656E-01	0.43304E+00
10	0.384060797524605E-01	0.55459E-04	0.14419E-02
15	0.384615371307963E-01	0.13307E-08	0.34599E-07
20	0.384615384615383E-01	0.19429E-15	0.50515E-14

$$f(x) = x^{25}s(x)$$

$\int_0^1 f(x)dx = 0.380228136882129E-01$			
N	Computed Integral	Absolute Error	Relative Error
5	0.218060230285103E-01	0.16656E-01	0.43304E+00
10	0.384060797524605E-01	0.55459E-04	0.14419E-02
15	0.384615371307963E-01	0.13307E-08	0.34599E-07
20	0.384615384615383E-01	0.19429E-15	0.50515E-14

Table 20: Integration by the Gaussian Quadrature for the Products of Polynomials and Fractional Power $s(x) = x^{-\frac{1}{3}}$ in TABLE 9

$$\int_0^1 f(x)dx = \sum_{i=1}^{N} w_i f(x_i)$$

$$f(x) = \sin(10x)$$

$\int_0^1 f(x)dx = 0.183907152907645\text{E+}00$			
N	Computed Integral	Absolute Error	Relative Error
5	0.181420301850517E+00	0.24869E-02	0.13522E-01
10	0.183906605077266E+00	0.54783E-06	0.29788E-05
15	0.183907152908166E+00	0.52114E-12	0.28337E-11
20	0.183907152907645E+00	0.30531E-15	0.16601E-14

$$f(x) = x^{25}$$

$\int_0^1 f(x)dx = 0.384615384615385\text{E-}01$			
N	Computed Integral	Absolute Error	Relative Error
5	0.213608283352790E-01	0.17101E-01	0.44462E+00
10	0.384022552100793E-01	0.59283E-04	0.15414E-02
15	0.384615369753817E-01	0.14862E-08	0.38640E-07
20	0.384615384615384E-01	0.69389E-16	0.18041E-14

$$f(x) = x^{25}s(x)$$

$\int_0^1 f(x)dx = 0.389105058365759\text{E-}01$			
N	Computed Integral	Absolute Error	Relative Error
5	0.213608283352790E-01	0.17101E-01	0.44462E+00
10	0.384022552100793E-01	0.59283E-04	0.15414E-02
15	0.384615369753817E-01	0.14862E-08	0.38640E-07
20	0.384615384615384E-01	0.69389E-16	0.18041E-14

Table 21: Integration by the Gaussian Quadrature for the Products of Polynomials and Fractional Power $s(x) = x^{-\frac{1}{2}}$ in TABLE 10

$$\int_0^1 f(x)dx = \sum_{i=1}^{N} w_i f(x_i)$$

$$f(x) = \sin(10x)$$

$\int_0^1 f(x)dx = 0.183907152907645E+00$			
N	Computed Integral	Absolute Error	Relative Error
5	0.170313857697349E+00	0.13593E-01	0.73914E-01
10	0.183906941803763E+00	0.21110E-06	0.11479E-05
15	0.183907152907514E+00	0.13078E-12	0.71114E-12
20	0.183907152907644E+00	0.14155E-14	0.76970E-14

$$f(x) = x^{25}$$

$\int_0^1 f(x)dx = 0.384615384615385E-01$			
N	Computed Integral	Absolute Error	Relative Error
5	0.204389144887852E-01	0.18023E-01	0.46859E+00
10	0.383937885473486E-01	0.67750E-04	0.17615E-02
15	0.384615366085782E-01	0.18530E-08	0.48177E-07
20	0.384615384615386E-01	0.11102E-15	0.28866E-14

$$f(x) = x^{25}s(x)$$

$\int_0^1 f(x)dx = 0.392156862745098E-01$			
N	Computed Integral	Absolute Error	Relative Error
5	0.214450816964760E-01	0.17771E-01	0.45315E+00
10	0.391572846318390E-01	0.58402E-04	0.14892E-02
15	0.392156850446440E-01	0.12299E-08	0.31362E-07
20	0.392156862745100E-01	0.16653E-15	0.42466E-14

Table 22: Integration by the Gaussian Quadrature for the Products of Polynomials and Fractional Power $s(x) = x^{-\frac{2}{3}}$
in TABLE 11

$$\int_0^1 f(x)dx = \sum_{i=1}^{N} w_i f(x_i)$$

$$f(x) = \sin(10x)$$

$\int_0^1 f(x)dx = 0.183907152907645\text{E+}00$			
N	Computed Integral	Absolute Error	Relative Error
5	0.156179751994470E+00	0.27727E-01	0.15077E+00
10	0.183907466630775E+00	0.31372E-06	0.17059E-05
15	0.183907152906471E+00	0.11742E-11	0.63847E-11
20	0.183907152907646E+00	0.10825E-14	0.58859E-14

$$f(x) = x^{25}$$

$\int_0^1 f(x)dx = 0.384615384615385\text{E-}01$			
N	Computed Integral	Absolute Error	Relative Error
5	0.194693376078146E-01	0.18992E-01	0.49380E+00
10	0.383840696841997E-01	0.77469E-04	0.20142E-02
15	0.384615361512299E-01	0.23103E-08	0.60068E-07
20	0.384615384615379E-01	0.52042E-15	0.13531E-13

$$f(x) = x^{25}s(x)$$

$\int_0^1 f(x)dx = 0.395256916996047\text{E-}01$			
N	Computed Integral	Absolute Error	Relative Error
5	0.194693376078146E-01	0.18992E-01	0.49380E+00
10	0.383840696841997E-01	0.77469E-04	0.20142E-02
15	0.384615361512299E-01	0.23103E-08	0.60068E-07
20	0.384615384615379E-01	0.52042E-15	0.13531E-13

In the present paper we describe an algorithm for the evaluation of Bessel functions $J_\nu(x)$, $Y_\nu(x)$ and $H_\nu^{(j)}(x)$ $(j = 1, 2)$ of arbitrary positive orders and arguments at a constant CPU time. The algorithm employs Taylor series, the Debye asymptotic expansions and numerical evaluation of the Sommerfeld integral, and is based on the following two observations.
1) The Debye asymptotic expansions, contrary to what appears to be a popular belief, are not expansions in inverse powers of (large) parameter ν but turn out to be uniform expansions in inverse powers of (large) parameter $g_1 = (x - \nu)/x^{1/3}$ for $x > \nu$ and (large) parameter $g_2 = (\nu - x)/\nu^{1/3}$ for $x < \nu$.
2) For x and ν such that both Taylor and Debye expansions do not provide a specified accuracy Bessel functions can be computed at a constant CPU time via (numerical) evaluation of the Sommerfeld integral along contours of steepest descents.
In addition, in Appendix B we obtain certain new estimates concerning decay of the functions $J_\nu(x)$ and $-1/Y_\nu(x)$ of fixed x and large ν, and in Appendix C we show that functions $J_\nu(x)$ of integer ν provide the solution for a certain system of coupled harmonic oscillators.

On the Evaluation of Bessel Functions

Gregory Matviyenko

1. Introduction

Bessel functions of argument x and order ν of the first kind $J_\nu(x)$, second kind $Y_\nu(x)$ and third kind $H_\nu^{(1)}(x)$, $H_\nu^{(2)}(x)$ (Hankel functions), play an important role in physics, mathematics and engineering. Applications of Bessel functions usually require an algorithm for the rapid evaluation of these functions with sufficiently high accuracy.

For arguments $x \sim 1$ and arbitrary ν Bessel functions can be computed via their Taylor expansions (see Subsection 2.2 below). If $x \gg 1$ and $\nu < x^{\frac{1}{2}}$ these functions can be evaluated by means of the Hankel asymptotic expansion (see Subsection 2.3 below). However, there exists a wide region of values of x and ν where both Taylor and Hankel expansions do not provide any reasonable numerical approximation.

Most of the existing algorithms for the evaluation of Bessel functions in this region are based on the recurrence relation (see, for example [1])

$$f_{\nu-1}(x) + f_{\nu+1}(x) = \frac{2\nu}{x} f_\nu(x), \tag{1}$$

where $f_\nu(x)$ denotes one of the functions $J_\nu(x)$, $Y_\nu(x)$ or $H_\nu^{(j)}(x)$ (j=1,2). The asymptotic estimate of the complexity of these algorithms is of order $O(x)$ for functions of the first kind and of order $O(\nu)$ for functions of the second and third kind (see, for example, [1]).

In this paper we present an algorithm for the evaluation of an individual Bessel function of an arbitrary nonnegative order and argument at a constant CPU time. The method is based on the following two observations.

1) The Debye asymptotic expansions [3], proposed in 1909 and since that time considered expansions for large orders (see, for example [1], [4], [5], [6]), are found to have a much wider range of validity. Namely, we show that for $x > \nu$ this expansion for function $H_\nu^{(1)}(x)$ is a *uniform* asymptotic expansion in inverse powers of (large) parameter $g_1 = (x-\nu)/x^{\frac{1}{3}}$ (see Theorem 3.1 and Observation 3.1 below). Moreover, it turns out that for $\nu = 0$ the Debye asymptotic expansion coincides with the Hankel asymptotic expansion (see Theorem 3.2 below). For $x < \nu$ the Debye expansions for functions $J_\nu(x)$ and $Y_\nu(x)$ are proved to be *uniform* asymptotic expansions in inverse powers of (large) parameter $g_2 = (\nu-x)/\nu^{\frac{1}{3}}$ (see Theorem 3.3 and Observation 3.2 below).

2) For the values of x and ν for which both Taylor and Debye expansions do not provide a specified accuracy, Bessel functions can be computed (at a constant CPU time) by means of numerical evaluation of the Sommerfeld integral taken along Debye contours (the definitions of the Sommerfeld integral and Debye contours are presented in Subsection 2.4 below). It is worth noting that Debye contours were extensively investigated in connection with the derivations of various asymptotic expansions for Bessel functions (see, for example, [3], Ch. 8 of [4], [7]). However, the possibility of using them in numerical computations seems to have been overlooked.

The plan of the paper is as follows. In Section 2 we summarize certain mathematical facts to be used in the rest of the paper. In Section 3 we analyze the error terms of the Debye asymptotic expansions. Numerical evaluation of the Sommerfeld integral is discussed in Section 4. In Section 5 we briefly discuss the implementation of our numerical scheme. In Section 6 we present a formal description of the algorithm. In Appendix A we discuss round-off errors. In addition, in Appendix B we obtain asymptotic solutions (with respect to ν) of equations $J_\nu(x) = \epsilon$ and $-1/Y_\nu(x) = \epsilon$ for large fixed positive $x < \nu$ and sufficiently small $\epsilon > 0$. Finally, in Appendix C we show that functions $J_\nu(x)$ of integer ν describe displacements of coupled harmonic oscillators on a line.

2. Relevant mathematical facts

In this section we present a number of well known formulae to be used in the rest of the paper.

2.1 Connections between the three kinds of Bessel functions

All the formulae presented in this subsection can be found, for example, in [1].

Functions $H_\nu^{(j)}(x)$ $(j = 1, 2)$ are expressed through $J_\nu(x)$ and $Y_\nu(x)$ as

$$H_\nu^{(1)}(x) = J_\nu(x) + i\, Y_\nu(x), \tag{2}$$

$$H_\nu^{(2)}(x) = J_\nu(x) - i\, Y_\nu(x). \tag{3}$$

For nonnegative x and ν, both $J_\nu(x)$ and $Y_\nu(x)$ are real. Thus

$$J_\nu(x) = Re\, H_\nu^{(1)}(x), \tag{4}$$

$$Y_\nu(x) = Im\ H_\nu^{(1)}(x), \tag{5}$$

$$H_\nu^{(2)}(x) = H_\nu^{(1)}(x) - 2iIm\ H_\nu^{(1)}(x). \tag{6}$$

2.2 Taylor expansions

For small arguments, function $J_\nu(x)$ is normally evaluated via the formula

$$J_\nu(x) = \left(\frac{x}{2}\right)^\nu \sum_{k=0}^{\infty} \left(-\frac{x^2}{4}\right)^k \frac{1}{k!\ \Gamma(\nu+k+1)}. \tag{7}$$

If ν is not an integer, function $Y_\nu(x)$ is computed as

$$Y_\nu(x) = \frac{J_\nu(x)\ \cos(\pi\ \nu) - J_{-\nu}(x)}{\sin(\pi\ \nu)}. \tag{8}$$

For integer ν the formula (8) can not be used and is replaced by

$$\begin{aligned} Y_\nu(x) \ = \ & -\frac{1}{\pi}\left(\frac{x}{2}\right)^{-\nu} \sum_{k=0}^{\nu-1} \left(\frac{x^2}{4}\right)^k \frac{(\nu-k-1)!}{k!} + \frac{2}{\pi}\ln\left(\frac{x}{2}\right) J_\nu(x) \\ & -\frac{1}{\pi}\left(\frac{x}{2}\right)^{\nu} \sum_{k=0}^{\infty} \left(-\frac{x^2}{4}\right)^k \frac{1}{(\nu+k)!\ k!}\ (\psi(k+1)+\psi(\nu+k+1)), \end{aligned} \tag{9}$$

where $\psi(z) = \frac{d}{dz}\ln(\Gamma(z))$. Formulae (7)-(9) can be found, for example, in [1].

2.3 The Hankel asymptotic expansion

The Hankel asymptotic expansion has the form (see, for example, [1], Ch. 7 of [4] , Ch. 7 of [5])

$$H_\nu^{(1)}(x) = \left(\frac{2}{\pi\ x}\right)^{\frac{1}{2}}\ \exp(i\chi(x,\nu))\ \left(\sum_{n=0}^{N} b_n(\nu)\left(-\frac{i}{x}\right)^n + \theta_{N+1,h}(\nu,x)\right), \tag{10}$$

where

$$\chi(x,\nu) = x - \frac{\pi}{4} - \frac{1}{2}\pi\nu, \tag{11}$$

and $\theta_{N+1,h}(\nu,x)$ is the error term.

Coefficients $b_n(\nu)$ satisfy the recurrence relation

$$b_0(\nu) = 1, \tag{12}$$

$$b_{n+1}(\nu) = \frac{(2n+1)^2 - 4\,\nu^2}{8\,(n+1)}\, b_n(\nu), \quad (n = 0, 1, \cdots), \tag{13}$$

whereas the error term $\theta_{N+1,h}(\nu, x)$ is bounded by (see, for example, Ch. 7 of [5])

$$|\theta_{N+1,h}(\nu, x)| \leq 2\, \frac{b_{N+1}(\nu)}{x^{N+1}} \cdot \exp\left(\frac{|\nu^2 - \frac{1}{4}|}{x}\right). \tag{14}$$

2.4 The Sommerfeld integral

All the formulae, presented in this subsection can be found, for example, in Ch. 8 of [4].

For the values of x and ν for which both Taylor and Debye expansions do not provide a specified accuracy we computed function $H_\nu^{(1)}(x)$ by means of numerical evaluation of the so called Sommerfeld integral:

$$H_\nu^{(1)}(x) = \frac{1}{\pi i} \int_{-\infty}^{\infty+i\pi} \exp(x \sinh(w) - \nu w)\, dw. \tag{15}$$

Following [4] we will write

$$w = u + iv, \tag{16}$$

where both u and v are real. Integration in (15) is performed along an arbitrary contour that has the following asymptotes:

$$\lim_{u \to -\infty} v = 0, \tag{17}$$

$$\lim_{u \to \infty} v = \pi. \tag{18}$$

Observation 2.1

As paths of integration in (15) it is natural to choose the so called Debye contours on which the integrand of (15) does not oscillate (see, for example, Ch. 8 of [4]). We note in passing that the Debye contours are a particular example of contours of steepest descents that are widely used for the evaluation of the asymptotic expansions of certain contour integrals (see, for example, Ch. 8 of [4], [5], [6]).

The Debye contours $u = u(v)$ are curves on the complex w-plane (16) that (generally speaking) are implicitly defined via equations

$$p(u, v) = 0. \tag{19}$$

For $x > \nu$,

$$p(u, v) = \cosh(u) - \frac{\sin(\beta) + (v - \beta)\ \cos(\beta)}{\sin(v)}, \tag{20}$$

where

$$\cos(\beta) = \frac{\nu}{x}. \tag{21}$$

It immediately follows from (21) that for nonnegative x and ν,

$$0 \leq \beta \leq \frac{\pi}{2}. \tag{22}$$

For $x < \nu$,

$$p(u, v) = v, \quad \text{if } u \leq \alpha, \tag{23}$$

and

$$p(u, v) = \cosh(u) - \cosh(\alpha)\ \frac{v}{\sin(v)}, \quad \text{if } u > \alpha, \tag{24}$$

where

$$\cosh(\alpha) = \frac{\nu}{x}. \tag{25}$$

For $x = \nu$,

$$p(u, v) = v, \quad \text{if } u \leq 0, \tag{26}$$

and

$$p(u, v) = \cosh(u) - \frac{v}{\sin(v)}, \quad \text{if } u > 0. \tag{27}$$

Finally we note that all the Debye contours, associated with function $H_\nu^{(1)}(x)$ (of nonnegative x and positive ν) lie within the strip

$$0 \le v \le \pi. \tag{28}$$

Graphs of Debye contours can be found, for example, in Ch. 8 of [4].

2.5 The Debye asymptotic expansions

In this subsection we present formulae for the Debye asymptotic expansions that can be found (in a slightly different form) in Ch. 10 of [5].

For $\nu < x$,

$$H_\nu^{(1)}(x) = \left(\frac{2}{\pi}\right)^{\frac{1}{2}} \frac{1}{(x^2-\nu^2)^{\frac{1}{4}}} \exp(i\eta_1) \left(\sum_{n=0}^{N}(-1)^n \frac{u_n(ip)}{\nu^n} + \tilde{\theta}_{N+1,2}(\nu,p)\right), \tag{29}$$

where

$$\eta_1 = (x^2-\nu^2)^{\frac{1}{2}} - \nu \arccos\left(\frac{\nu}{x}\right) - \frac{\pi}{4}, \tag{30}$$

$\tilde{\theta}_{N+1,2}(\nu,p)$ is the error term, polynomials $u_n(t)$ are defined in (35), (36) below, and

$$p = \frac{\nu}{|x^2-\nu^2|^{\frac{1}{2}}}. \tag{31}$$

For $x < \nu$,

$$J_\nu(x) = \frac{1}{1+\theta_{N+1,1}(\nu,0)} \frac{\exp(-\eta_2)}{(2\pi)^{\frac{1}{2}}\,(\nu^2-x^2)^{\frac{1}{4}}} \left(\sum_{n=0}^{N}\frac{u_n(p)}{\nu^n} + \theta_{N+1,1}(\nu,p)\right), \tag{32}$$

$$Y_\nu(x) = -\left(\frac{2}{\pi}\right)^{\frac{1}{2}} \frac{\exp(\eta_2)}{(\nu^2-x^2)^{\frac{1}{4}}} \left(\sum_{n=0}^{N}(-1)^n\frac{u_n(p)}{\nu^n} + \theta_{N+1,2}(\nu,p)\right), \tag{33}$$

where

$$\eta_2 = \nu \ln\left(\frac{\nu}{x} + \left(\left(\frac{\nu}{x}\right)^2 - 1\right)^{\frac{1}{2}}\right) - (\nu^2-x^2)^{\frac{1}{2}}, \tag{34}$$

and $\theta_{N+1,1}(\nu,p)$ and $\theta_{N+1,2}(\nu,p)$ are the error terms.

Polynomials $u_n(t)$ are defined by the formulae

$$u_0(t) = 1, \quad u_1(t) = \frac{1}{24}\,(3t - 5t^3), \tag{35}$$

$$u_{n+1}(t) = \frac{1}{2}\, t^2\,(1-t^2)\,\frac{du_n(t)}{dt} + \frac{1}{8}\int_0^t (1-5\tau^2)\,u_n(\tau)d\tau,$$
$$(n = 0, 1, \cdots). \tag{36}$$

The error terms in the Debye expansions satisfy the inequalities

$$|\tilde{\theta}_{N,2}(\nu,p)| \le 2\exp\left(\frac{2\tilde{V}_{0,p}(u_1)}{\nu}\right)\,\frac{\tilde{V}_{0,p}(u_{N+1})}{\nu^{N+1}}, \tag{37}$$

$$|\theta_{N+1,1}(\nu,p)| \le 2\exp\left(\frac{2V_{1,p}(u_1)}{\nu}\right)\,\frac{V_{1,p}(u_{N+1})}{\nu^{N+1}}, \tag{38}$$

and

$$|\theta_{N+1,2}(\nu,p)| \le 2\exp\left(\frac{2V_{0,p}(u_1)}{\nu}\right)\,\frac{V_{0,p}(u_{N+1})}{\nu^{N+1}}. \tag{39}$$

In (37) - (39), symbols $V_{a,b}(f)$ and $\tilde{V}_{a,b}(f)$ denote the so called total variations of functions $f(x)$ and $f(ix)$, respectively (see, for example, Ch. 1 of [5]):

$$V_{a,b}(f) = \int_a^b \left|\frac{df(x)}{dx}\right| dx, \tag{40}$$

$$\tilde{V}_{a,b}(f) = \int_a^b \left|\frac{df(ix)}{dx}\right| dx. \tag{41}$$

3. Error terms of the Debye asymptotic expansions

In this section we obtain estimates of the error terms of the Debye asymptotic expansions (29), (32) and (33). We start with a more detailed analysis of the polynomials $u_n(t)$ defined in (35), (36).

3.1 The polynomials $u_n(t)$

Lemma 3.1

For any $n \ge 1$,

$$u_n(t) = t^n\ \tilde{u}_n(t), \tag{42}$$

where

$$\tilde{u}_n(t) = \sum_{k=0}^{n} a_k^n\, t^{2k}. \tag{43}$$

The coefficients a_k^n are defined by the formulae

$$a_0^0 = 1, \tag{44}$$

$$a_k^n = 0 \quad \text{if } k < 0 \text{ or } k > n, \quad (n = 0, 1, \cdots), \tag{45}$$

$$\begin{aligned} a_k^{n+1} &= a_k^n \left(\frac{n+2k}{2} + \frac{1}{8\,(2k+n+1)} \right) - \\ &\quad a_{k-1}^n \left(\frac{n+2k-2}{2} + \frac{5}{8\,(2k+n+1)} \right), \\ &\quad (n = 0, 1, \cdots; \quad k = 0, 1, \cdots, n+1). \end{aligned} \tag{46}$$

Proof

We will prove the lemma by induction. For $n = 1$ the formulae (42)- (46) immediately follow from (35). Suppose now that the formulae (42)-(46) are satisfied for certain $n = m > 1$. Then

$$\begin{aligned} &t^2\,(1-t^2)\,\frac{du_m(t)}{dt} = \\ &\quad t^{m+1} \sum_{k=0}^{m+1} ((m+2k)a_k^m - (m+2k-2)a_{k-1}^m) \cdot t^{2k}, \end{aligned} \tag{47}$$

and

$$\begin{aligned} &\int_0^t (1-5\tau^2)\,u_m(\tau)d\tau = \\ &\quad t^{m+1} \sum_{k=0}^{m+1} \frac{1}{2k+m+1} (a_k^m - 5a_{k-1}^m) \cdot t^{2k}. \end{aligned} \tag{48}$$

Now substituting (47) and (48) into (36) we observe that (42)-(46) hold for $n = m + 1$ which concludes the proof of the lemma. □

The following corollary is an obvious consequence of the lemma and the formulae (12), (13).

Corollary 3.1

For all $n \geq 0$,

$$a_0^n = b_n(0), \tag{49}$$

where the coefficients $b_n(\nu)$ are defined in (12), (13).

Lemma 3.2

For any $t \geq t_1 \geq 0$,

$$\tilde{u}_n(it) \geq \tilde{u}_n(it_1) > 0, \tag{50}$$

$$\frac{\tilde{u}_n(it)}{t^{2n}} \leq \frac{\tilde{u}_n(it_1)}{t_1^{2n}}, \quad \text{if } t \neq 0 \text{ and } t_1 \neq 0, \tag{51}$$

$$\frac{d\tilde{u}_n(it)}{dt} \geq 0, \tag{52}$$

$$\tilde{u}_n(it) \geq \tilde{u}_n(t), \tag{53}$$

$$\frac{d\tilde{u}_n(it)}{dt} \geq \left|\frac{d\tilde{u}_n(t)}{dt}\right|, \tag{54}$$

$$\left|\frac{du_n(it)}{dt}\right| \geq \left|\frac{du_n(t)}{dt}\right|. \tag{55}$$

Proof

It immediately follows from (44)-(46) that for all $n \geq 0$ and $k \leq n$,

$$a_k^n = (-1)^k \tilde{a}_k^n, \tag{56}$$

where

$$\tilde{a}_k^n > 0. \tag{57}$$

Substituting (56) and (57) into (43), we observe that for any real t all the coefficients of the polynomials $\tilde{u}_n(it)$ are positive and therefore the inequalities (50)-(54) are satisfied. The inequality (55) follows from (42), (53) and (54).□

Remark 3.1

While many recurrence relations occurring in mathematical physics are numerically unstable, the recursion (46) is numerically stable since according to (56) and (57), both terms in this relation have the same sign.

The following lemma is an immediate consequence of (42), (52) and (55).

Lemma 3.3

For any $p > 0$ and $n \geq 1$,

$$\tilde{V}_{0,p}(u_n) = \int_0^p \left| \frac{du_n(it)}{dt} \right| dt = p^n \cdot \tilde{u}_n(ip). \tag{58}$$

Furthermore,

$$V_{0,p}(u_n) = \int_0^p \left| \frac{du_n(t)}{dt} \right| dt \leq \tilde{V}_{0,p}(u_n). \tag{59}$$

3.2 Region $x > \nu$

Theorem 3.1

For any

$$x > \nu \geq 0 \tag{60}$$

the error term $\tilde{\theta}_{N+1,2}(\nu, p)$ in the expansion (29) satisfies the inequality

$$|\tilde{\theta}_{N+1,2}(\nu, p)| \leq 2 \exp\left(\frac{2}{3 \cdot g_1^{\frac{3}{2}}}\right) \frac{\tilde{u}_{N+1}(i)}{g_1^{\frac{3}{2}(N+1)}}, \tag{61}$$

where

$$g_1 = \frac{x - \nu}{x^{\frac{1}{3}}}. \tag{62}$$

Proof

The inequality (60) and the definition (62) show that

$$\frac{g_1}{x^{\frac{2}{3}}} \leq 1, \tag{63}$$

and therefore

$$\frac{1}{(x^2 - \nu^2)^{\frac{1}{2}}} \leq \frac{1}{g_1^{\frac{1}{2}} \cdot x^{\frac{2}{3}}}. \tag{64}$$

Now combining (31) with (60) and (64) we observe that

$$p = \frac{\nu}{(x^2 - \nu^2)^{\frac{1}{2}}} \leq \frac{x^{\frac{1}{3}}}{g_1^{\frac{1}{2}}}, \tag{65}$$

and substituting (65) into (50) we obtain

$$\tilde{u}_n(ip) \le \tilde{u}_n\left(i\frac{x^{\frac{1}{3}}}{g_1^{\frac{1}{2}}}\right). \tag{66}$$

Combining the inequalities (51), (63) and (66) we have

$$\tilde{u}_n(ip) \le \tilde{u}_n(i)\left(\frac{x^{\frac{2}{3}}}{g_1}\right)^n. \tag{67}$$

Substitution of (31), (64) and (67) into (58) yields

$$\frac{1}{\nu^n}\,\tilde{V}_{0,p}(u_n) = \frac{\tilde{u}_n(ip)}{(x^2-\nu^2)^{\frac{1}{2}n}} \le \frac{\tilde{u}_n(i)}{g_1^{\frac{3}{2}n}}. \tag{68}$$

Observing that

$$\tilde{u}_1(i) = \frac{1}{3}, \tag{69}$$

and substituting (68) and (69) into (37) we immediately obtain the inequality (61). □

Observation 3.1

Obviously, function $H_\nu^{(1)}(x)$ can be viewed not as a function of x and ν, but as a function of x and the parameter g_1 defined in (62). Then the estimate (61) shows that for $g_1 > 0$ (*i.e.* $x > \nu$) the Debye asymptotic expansion (29) *is not* an asymptotic expansion in inverse powers of (large) parameter ν but it turns out to be *a uniform* (with respect to x) asymptotic expansion in inverse powers of (large) parameter g_1. Moreover, as follows from (61), the error term $\tilde{\theta}_{N+1,2}(\nu,p)$ may be small even if ν is not large. The following theorem describes the behavior of the Debye expansion (29) in the limit $\nu \to 0$.

Theorem 3.2

For any $x > 0$ and $\nu = 0$ the Debye asymptotic expansion (29) *and the Hankel asymptotic expansion* (10) *are identical.*

Proof

From the definitions (11) and (30) we have

$$\lim_{\nu\to 0}\left(\frac{2}{\pi}\right)^{\frac{1}{2}}\frac{1}{(x^2-\nu^2)^{\frac{1}{4}}}\exp(i\eta_1) \;=\; \lim_{\nu\to 0}\left(\frac{2}{\pi x}\right)^{\frac{1}{2}}\exp(i\chi(x,\nu)) = \left(\frac{2}{\pi x}\right)^{\frac{1}{2}}\exp(i(x-\frac{\pi}{4})). \tag{70}$$

Next, combining (31) with (42) and (43) we obtain

$$\lim_{\nu\to 0}\frac{(-1)^n}{\nu^n}u_n(ip)=\lim_{\nu\to 0}\frac{(-i)^n}{(x^2-\nu^2)^{\frac{1}{2}n}}\sum_{k=0}^{n}a_k^n\left(\frac{-\nu^2}{x^2-\nu^2}\right)^k=a_0^n\left(-\frac{i}{x}\right)^n. \tag{71}$$

Now substituting (70) and (71) into (29) and taking into account (49) we see that (for $\nu=0$) the expansions (10) and (29) are identical. □

3.3 Region $x<\nu$

Theorem 3.3

For any

$$\nu>x\geq 0 \tag{72}$$

the error terms $\theta_{N+1,2}(\nu,p)$ of the expansion (32) *satisfies the inequality*

$$|\theta_{N+1,2}(\nu,p)|\leq 2\exp\left(\frac{2}{3\cdot g_2^{\frac{3}{2}}}\right)\frac{\tilde{u}_{N+1}(i)}{g_2^{\frac{3}{2}(N+1)}}, \tag{73}$$

where

$$g_2=\frac{\nu-x}{\nu^{\frac{1}{3}}}. \tag{74}$$

Furthermore, the error term $\theta_{N+1,1}(\nu,p)$ of the expansion (33) *is bounded by*

$$|\theta_{N+1,1}(\nu,p)|\leq 2\exp\left(\frac{2}{3\cdot g_2^{\frac{3}{2}}}\right)\frac{\tilde{u}_{N+1}(i)}{g_2^{\frac{3}{2}(N+1)}}, \tag{75}$$

Proof

Substitution of (59) into (38) yields

$$|\theta_{N,2}(\nu,p)|\leq 2\exp\left(\frac{2\tilde{V}_{0,p}(u_1)}{\nu}\right)\frac{\tilde{V}_{0,p}(u_{N+1})}{\nu^{N+1}}. \tag{76}$$

Now the proof of the inequality (73) becomes almost identical to that of the inequality (61) (see Theorem 3.1) and we omit it.

To prove (75) we observe that for $x<\nu$,

$$p=\frac{\nu}{(\nu^2-x^2)^{\frac{1}{2}}}\geq 1. \tag{77}$$

Therefore

$$V_{1,p}(u_n) = \int_1^p \left|\frac{du_n(t)}{dt}\right| dt \le \int_0^p \left|\frac{du_n(t)}{dt}\right| dt = V_{0,p}(u_n). \tag{78}$$

Substitution of (78) into (38) produces

$$|\theta_{n,1}(\nu, p)| \le 2\exp\left(\frac{2V_{0,p}(u_1)}{\nu}\right) \frac{V_{0,p}(u_n)}{\nu^n}. \tag{79}$$

Comparing (39) and (79) we see that the proof of (75) is reduced to the proof of (73). □

Observation 3.2

Parallel to Observation 3.1, we can view function $H_\nu^{(1)}(x)$ not as a function of x and ν but as a function of ν and the parameter g_2 defined in (74). Then the estimates (73) and (75) mean that the Debye asymptotic expansions (32) and (33) *are not* expansions in inverse powers of (large) parameter ν but turn out to be ***uniform*** (with respect to ν) asymptotic expansions in inverse powers of the (large) parameter g_2 (compare with Observation 3.1).

Observation 3.3

In Appendix B it is shown that for $x \gg 1$ and $\nu > x + \text{const} \cdot x^{\frac{1}{3}}$ function $J_\nu(x)$ becomes small whereas function $|Y_\nu(x)|$ becomes large. Therefore, for sufficiently large x the most important part (in terms of applications of Bessel functions) of the region $x < \nu$ can be estimated as

$$x < \nu < x + \text{const} \cdot x^{\frac{1}{3}}, \tag{80}$$

Combining (62), (74) and (80) we have

$$g_2 = |g_1|\left(1 + O\left(x^{-\frac{2}{3}}\right)\right). \tag{81}$$

The estimate (81) and Observation 3.2 show that in the region (80) for $x \gg 1$ the Debye asymptotic expansions (32) and (33) behave almost like uniform expansions in inverse powers of (large) parameter

$$\frac{\nu - x}{x^{\frac{1}{3}}} = -g_1. \tag{82}$$

4. Certain properties of the Sommerfeld integral

In this section we discuss certain analytical properties of the Sommerfeld integral (15) relevant to its numerical evaluation.

4.1 Region $x > \nu$

It immediately follows from Ch. 8 of [4] that the explicit representation of the Sommerfeld integral (15) on the Debye contours defined by (19) and (20) has the form

$$H_\nu^{(1)}(x) = \frac{1}{\pi i}\ \exp(i(x\sin(\beta) - \nu\beta))\ \int_0^\pi \left(\frac{du}{dv} + i\right)\ \exp(x\phi_1)\ dv, \tag{83}$$

where

$$\phi_1 \equiv \phi_1(v, u(v), \beta) = \cos(v)\cdot\sinh(u) - \cos(\beta)\cdot u, \tag{84}$$

and

$$\frac{du}{dv} = \frac{1}{\sinh(u)\ \sin^2(v)}\cdot(\sin(v-\beta) - (v-\beta)\cdot\cos(\beta)\cdot\cos(v)). \tag{85}$$

In (83)-(85) function $u = u(v)$ is evaluated via (19), (20) and the parameter β is defined in (21).

Theorem 4.1(see §8.31 of [4])

Function $\phi_1(v, u(v), \beta)$, defined in (84), is a nonpositive decreasing function of $|v - \beta|$. It has the only maximum at $v = \beta$ where

$$\phi_1(\beta, u(\beta), \beta) = 0. \tag{86}$$

The following corollary is an immediate consequence the theorem.

Corollary 4.1

The equation

$$x\ \phi_1(\beta, u(\beta), \beta) = \ln(\epsilon). \tag{87}$$

with $\epsilon \in (0,1)$, $v \in (0,\pi)$ and $x > 0$ has two and only two solutions β_1 and β_2 such that

$$\beta_1 < \beta < \beta_2. \tag{88}$$

Theorem 4.2

For any $\beta \neq 0$,

$$\phi_1 = -\sin(\beta)\,(v-\beta)^2 + O((v-\beta)^3). \tag{89}$$

Proof

From (20) for any $\beta \neq 0$ we have

$$u = (v-\beta) + O((v-\beta)^2). \tag{90}$$

Substituting (90) into (84) we immediately obtain (89). □

In the rest of the subsection we will estimate the domain on the $x-\nu$ plane where the integral (83) can be evaluated at a constant CPU time. We start with the following remark.

Remark 4.1

For any $0 < v \ll 1$,

$$\exp(x\phi_1) \sim \exp\left(-\frac{f(x,\nu)}{v}\right), \tag{91}$$

where function $f(x,\nu) > 0$. This formula is an immediate consequence of (19) and (20).

As follows from (19), (20), (84), (85) and Theorems 4.1 and 4.2 the integrand of (83) is a nonoscillatory function of v. Moreover, for small $|v-\beta|$,

$$\left(\frac{du}{dv} + i\right)\,\exp(x\phi_1) = \left(\left.\frac{du}{dv}\right|_{v=\beta} + i\right)\exp\left(-x\sin(\beta)(v-\beta)^2\right)\,(1+\theta_1(v-\beta)), \tag{92}$$

where $\theta_1(v-\beta) = O(v-\beta)$ is the error term.

Next, suppose that

$$x \cdot \sin(\beta) \gg 1, \tag{93}$$

and

$$\beta > \frac{C_1}{(x\sin(\beta))^{\frac{1}{2}}}. \tag{94}$$

where

$$C_1 \sim 1 \tag{95}$$

is a (positive) constant.

Observation 4.1

The condition (93) means that the domain where the integrand of (83) is (numerically) not zero is sufficiently small. The condition (94) shows that the distance between the maximum of the integrand of (83) $v = \beta$ and its singularity at $v = 0$ (see Remark 4.1) is larger than several standard deviations of the Gaussian in (92). Therefore, if the inequalities (93) and (94) are satisfied then the error term $\theta_1(v - \beta)$ in (92) can be approximated (with high accuracy) by a low-degree polynomial of $(v - \beta)$ in the domain, where the integrand of (83) is (numerically) not zero. Thus in this case the evaluation of the integral (83) by means of the trapezoidal rule becomes a superalgebraically convergent procedure. Moreover, the number of nodes of this quadrature formula is (asymptotically for large $x \sin(\beta)$ and C_1) independent of ν and x.

Theorem 4.3

For any

$$x \gg 1 \tag{96}$$

and

$$\nu < x - D_1\, x^{\frac{1}{3}}, \tag{97}$$

where $D_1 \sim 1$ is a (positive) constant, the inequalities (93) *and* (94) *are satisfied.*

Proof

We will prove the inequality (93) first. From the definition (21) we have

$$\sin(\beta) = \left(1 - \frac{\nu^2}{x^2}\right)^{\frac{1}{2}}, \tag{98}$$

and thus

$$x \sin(\beta) = \left(x^2 - \nu^2\right)^{\frac{1}{2}}. \tag{99}$$

Combining (96), (97) and (99) we have

$$x\sin(\beta) > (2D_1)^{\frac{1}{2}} \cdot x^{\frac{2}{3}} \left(1 + O\left(x^{-\frac{2}{3}}\right)\right) \gg 1, \tag{100}$$

which completes the proof of (93). Now we turn to the proof of the inequality (94).

Owing to (22) we have $\beta \geq \sin(\beta)$ and therefore we can replace the inequality (94) by a stronger one

$$\sin(\beta) > \frac{C_1}{(x\sin(\beta))^{\frac{1}{2}}}. \tag{101}$$

Substituting (98) into (101) we have

$$x^{\frac{1}{2}} \cdot \left(1 - \frac{\nu^2}{x^2}\right)^{\frac{3}{4}} > C_1. \tag{102}$$

Using (97) we can estimate the left-hand side of (102) as

$$x^{\frac{1}{2}} \cdot \left(1 - \frac{\nu^2}{x^2}\right)^{\frac{3}{4}} > x^{\frac{1}{2}} \cdot \left(2D_1 \cdot x^{-\frac{2}{3}} - D_1^2 \cdot x^{-\frac{4}{3}}\right)^{\frac{3}{4}} \geq (2D_1)^{\frac{3}{4}}. \tag{103}$$

Now it follows from (101)-(103) that the inequality (94) is satisfied if

$$D_1 > \frac{C_1^{\frac{4}{3}}}{2} + \epsilon \sim 1, \tag{104}$$

where $\epsilon > 0$ is any (small) number. □

The inequalities (96), (97) and the estimate (104) define the domain on the $x - \nu$ plain where the conditions (93) and (94) are satisfied and therefore numerical integration of (83) by means of the trapezoidal formula can be done at a CPU time independent of x and ν (see Observation 4.1).

4.2 Region $x < \nu$

It follows from Ch. 8 of [4] that the explicit representation of the Sommerfeld integral (15) on the contours defined by (19), (23) is

$$I_1 = \frac{1}{\pi i} \int_{-\infty}^{\alpha} \exp(x\phi_2) du, \tag{105}$$

whereas on the contours (19), (24) we have

$$I_2 = \frac{1}{\pi i} \int_0^{\pi} \exp(x\phi_3) \left(i + \frac{du}{dv}\right) dv. \tag{106}$$

Obviously,

$$H_\nu^{(1)}(x) = I_1 + I_2. \tag{107}$$

In (105) and (106),

$$\phi_2 \equiv \phi_2(u, \alpha) = \sinh(u) - \cosh(\alpha)\ u, \tag{108}$$

$$\phi_3 \equiv \phi_3(v, u(v), \alpha) = \sinh(u)\ \cos(v) - \cosh(\alpha)\ u, \tag{109}$$

and

$$\frac{du}{dv} = \cosh(\alpha)\ \frac{(\sin(v) - v\ \cos(v))}{\sin^2(v)\ \sinh(u)}. \tag{110}$$

Function $u = u(v)$ in (106), (109) and (110) is evaluated via (19), (24) and the parameter α is defined in (25).

Observation 4.2

Numerical evaluation of the integral (105) can be performed by means of the Gauss-Legendre quadrature formula with the number of nodes independent of ν and x because its integrand is an analytic nonoscillatory function.

In Theorem 4.4 (see below) it is shown that for any $\alpha > 0$ the integrand of (106) has singularities in the complex v-plane. It turns out (see the estimate (111) below) that for $\alpha \ll 1$ (*i.e.* $\nu/x \sim 1$) these singularities lie close to the domain of integration in (106) which impedes numerical evaluation of this integral. Now we will establish a domain on the $x - \nu$ plane where numerical evaluation of (106) (for example, by means of the Gauss-Legendre quadrature formula) can be performed at a CPU time independent of x and ν; the estimate of this domain is obtained in Theorem 4.7 below.

Theorem 4.4

For any $\alpha > 0$ the integrand of (106) *has two imaginary complex conjugate branch points $\alpha_\pm$. Moreover, for $\alpha \ll 1$,*

$$\alpha_\pm = \pm(3)^{\frac{1}{2}}\alpha i + O(\alpha^3). \tag{111}$$

Proof

For imaginary $v = is$ (s is real) equations (19), (24) become

$$\cosh(u(is)) = \cosh(\alpha)\,\frac{s}{\sinh(s)}. \tag{112}$$

Therefore, for any $\alpha > 0$ there exists a parameter $s = s_0$ such that

$$\cosh(u(is_0)) = 1 \tag{113}$$

and

$$0 < \cosh(u(is)) < 1, \quad |s| > s_0. \tag{114}$$

As follows from (113) and (114) the points $s_\pm = \pm s_0$ (or, equivalently, the points $\alpha_\pm = \pm i s_0$) are the branch points of the function $\sinh(u) = \left(\cosh^2(u) - 1\right)^{\frac{1}{2}}$ and therefore (see (106) and (109)) of the integrand of (106).

To prove (111) we must solve equation (113). Combining (19), (24) and (113) we have

$$\cosh(\alpha) = \frac{\sin(\alpha_\pm)}{\alpha_\pm}. \tag{115}$$

Expanding both parts of (115) in (small) parameters α and $\alpha_\pm$ we immediately obtain estimate (111). □

Theorem 4.5 (see §8.31 of [4]).

Function ϕ_3 from (109) *on the contours defined by* (19), (24) *is a monotonically decreasing function of v with the only maximum at $v = 0$.*

Theorem 4.6

For any $\alpha \neq 0$,

$$\phi_2 = \sinh(\alpha) - \alpha\cosh(\alpha) - \frac{1}{2}\sinh(\alpha)\,v^2 + O(v^4). \tag{116}$$

Proof

For small v and $\alpha \neq 0$ we have from (19), (24)

$$u = \frac{1}{6}\coth(\alpha)v^2 + O(v^4). \tag{117}$$

Substituting (117) into (109) we immediately obtain (116). □

As follows from (19), (24), (109), (110) and Theorems 4.5 and 4.6 the integrand of (106) is a nonoscillatory function of v. Moreover, for small v,

$$\left(\frac{du}{dv} + i\right) \exp(x\phi_3) = \exp(-x \cdot (\alpha\cosh(\alpha) - \sinh(\alpha))) \times$$
$$\left(\left.\frac{du}{dv}\right|_{v=0} + i\right) \exp\left(-\frac{1}{2}x\sinh(\alpha)v^2\right)\ (1 + \theta_2(v)), \tag{118}$$

where $\theta_2(v) = O(v)$ is the error term.

Observation 4.3

The local behavior of the integrands of (106) and (83) is essentially the same (compare (118) and (92)). Therefore the conditions under which the integral (106) can be numerically evaluated at a CPU time, independent of x and ν, are equivalent to the conditions (93) and (94) (see Observation 4.1). These conditions are

$$x\sinh(\alpha) \gg 1, \tag{119}$$

and

$$|\alpha_\pm| > 2^{\frac{1}{2}}\frac{C_2}{(x\sinh(\alpha))^{\frac{1}{2}}}, \tag{120}$$

where the parameters $\alpha_\pm$ are estimated in (111) and

$$C_2 \sim 1 \tag{121}$$

is a (positive) constant. The condition (119) means that the domain where the integrand of (106) is (numerically) not zero is sufficiently small. The condition (120) shows that the distance between the singularities of the integrand of (106) $\alpha_\pm$ and the real axis is larger than several standard deviations of the Gaussian in (118).

Now the proof of the Theorem 4.3 can be repeated almost verbatim yielding the following result:

Theorem 4.7

For any

$$x \gg 1 \tag{122}$$

and

$$\nu > x + D_2\, x^{\frac{1}{3}}, \tag{123}$$

where

$$D_2 \sim 1, \tag{124}$$

is a (positive) constant, the inequalities (119) *and* (121) *are satisfied.*

4.3 Region $x \approx \nu$

In order to construct an algorithm whose complexity does not depend on x and ν in the region

$$|x - \nu| < \text{const} \cdot x^{\frac{1}{3}}, \quad \text{const} \sim 1, \tag{125}$$

(*i.e.* when the conditions (97) and (123) are violated) we will consider numerical integration of (15) along the Debye contours defined in (19), (26) and (27). We note in passing that these contours were extensively used for the derivation of asymptotic expansions of function $H_\nu^{(1)}(x)$ for $x \approx \nu$ (see, for example, Ch.8 of [4], [7]).

Denoting the integral along the contour (19), (26) by J_1 and the integral along the contour (19), (27) by J_2 it can be shown that

$$J_1 = \frac{1}{\pi i} \int_{-\infty}^{0} \exp(x \sinh(u) - \nu u) du, \tag{126}$$

$$J_2 = \frac{1}{\pi i} \int_{0}^{\pi} \exp(x\phi_4)\, (i + \frac{du}{dv}) dv, \tag{127}$$

and

$$H_\nu^{(1)}(x) = J_1 + J_2, \tag{128}$$

where

$$\phi_4 \equiv \phi_4(v, u(v), \tau) = \sinh(u)\ \cos(v) - u + \tau\ (u + i\ v), \tag{129}$$

$$\tau = 1 - \frac{\nu}{x}, \tag{130}$$

$$\frac{du}{dv} = \frac{(\sin(v) - v\ \cos(v))}{\sin^2(v)\ \sinh(u)}. \tag{131}$$

In (127), (129) and (131) function $u = u(v)$ is evaluated via (19), (27).

Observation 4.4

The integral (126) is merely the integral (105) with $\alpha = 0$ and therefore is can be evaluated at a CPU time independent of x and ν (see Observation 4.2).

Observation 4.5

Obviously, the integrand of (127) is an analytic and (for sufficiently small $|\tau|$) nonoscillatory function of v. Therefore the integral (127) can be computed (for example by means of the Gauss-Legendre quadrature formula) at a CPU time independent of ν and x. We will show, however, that for sufficiently large x and $\tau > 0$ the integral (127) can not be evaluated without an unavoidable round-off error (see Observation 4.6 below). The inequalities (141) and (142) below estimate the range of parameters x and ν where this error is small (see also Remark 4.2 below).

Theorem 4.8

For any $0 < \tau \ll 1$ function $Re\phi_4$ has the maximum at

$$v_{max} = \frac{1}{2}(3\tau)^{\frac{1}{2}}(1 + O(\tau)). \tag{132}$$

Moreover,

$$\phi_{max} \equiv Re\ \phi_4(v_{max}, u(v_{max}), \tau) = \frac{1}{3}\ \tau^{\frac{3}{2}}(1 + O(\tau)). \tag{133}$$

Proof

From equations (19), (27) for small v we have

$$u = \frac{1}{3^{\frac{1}{2}}}\, v + \frac{2}{45 \cdot 3^{\frac{1}{2}}}\, v^3 + O(v^5). \tag{134}$$

Therefore

$$\sinh(u)\ \cos(v) = \frac{1}{3^{\frac{1}{2}}}\, v - \frac{2}{5 \cdot 3^{\frac{1}{2}}} v^3 + O(v^5), \tag{135}$$

and

$$\sinh(u)\ \cos(v) - u = -\frac{4}{9 \cdot 3^{\frac{1}{2}}}\, v^3 + O(v^5). \tag{136}$$

Substitution of (134) and (136) into (129) produces

$$Re\ \phi_4 = \frac{1}{3^{\frac{1}{2}}}\, \tau\, v - \frac{4}{9 \cdot 3^{\frac{1}{2}}}\, v^3 + O(\tau\, v^3) + O(v^5). \tag{137}$$

The formulae (132) and (133) are a consequence of (137). □

Theorem 4.9 (see, for example, Ch.8 of [4]).

In the region (125) *for* $x \gg 1$,

$$|H_\nu^{(1)}(x)| = O(x^{-\frac{1}{3}}). \tag{138}$$

Observation 4.6

It follows from the estimate (133) that for sufficiently large x the integrand of (127) may be large whereas, according to Theorem 4.9, the integral itself is (asymptotically) small. Therefore in this case there exist cancellations that account for the round-off errors.

We do not expect significant cancellations if

$$x\phi_{max} < C_3, \tag{139}$$

where

$$C_3 \sim 1 \tag{140}$$

is a (positive) constant and ϕ_{max} is estimated in (133). The condition (139) means that in order to avoid cancellations the maximum of the integrand (127) must be of order $O(1)$.

Using (130) and (133) it is easy to show that for

$$x \gg 1 \tag{141}$$

the condition (139) is equivalent to the condition

$$\nu < x - D_3\, x^{\frac{1}{3}} + O(x^{-\frac{1}{3}}), \tag{142}$$

where

$$D_3 = (3\, C_3)^{\frac{2}{3}} \sim 1, \tag{143}$$

In fact, owing to (138), there must be another condition of the absence of cancellations in addition to (139). Namely, the domain in v where the integrand of (127) is not small must be of order $O(x^{-\frac{1}{3}})$. It can be shown, however, that this condition holds if (142) is satisfied.

We will briefly discuss the case of $\tau < 0$. Now the integrand of (127) does not have a maximum for $v \neq 0$. However, in the vicinity of $v = 0$ this integrand is of order $O(1)$. On the other hand, function $J_\nu(x)$ becomes small if roughly speaking (see Appendix B)

$$\nu > x + \text{const}\; x^{\frac{1}{3}}. \tag{144}$$

Therefore function $J_\nu(x)$ (*i.e.* the real parts of $H_\nu^{(1)}(x)$) can not be evaluated by means of (127) without an unavoidable round-off error if ν satisfies (144) with const $\gg 1$. It can be shown, however, that for

$$\nu < x + D_4 x^{\frac{1}{3}}, \tag{145}$$

where

$$D_4 \sim 1 \tag{146}$$

is a (positive) constant, both real and imaginary parts of function $H_\nu^{(1)}(x)$ can be evaluated without a significant round-off error.

Remark 4.2

The numerical computation of the integrals (126) and (127) provide a method for the evaluation of function $H_\nu^{(1)}(x)$ at a constant CPU time in the region (125) *i.e.* where the algorithms discussed in Subsections 4.1 and 4.2 fail (compare the inequalities (97), (123) and (142), (145), as well as the estimates (104), (124) and (143), (146)). Moreover, for $x \sim 1$ and $x \sim \nu$ the integral (127) can be evaluated without a significant round-off error even if (142) is violated because in this case the maximum of its integrand is of order $O(1)$ (see Theorem 4.8 and inequality (139)).

5. Implementation of the algorithm

In this section we present certain details of the implementation of the algorithm for the evaluation of function $H_\nu^{(1)}(x)$ via the Debye asymptotic expansions (see Section 3) or the contour integration (see Section 4). This scheme was tested to provide double precision accuracy (at least thirteen digits) for

$$2 \leq x \leq 100000 \tag{147}$$

and

$$0 \leq \nu \leq 100000 + 16 \cdot 100000^{\frac{1}{3}}. \tag{148}$$

For

$$\begin{aligned} x &< 2, \\ \nu &\geq 0 \end{aligned} \tag{149}$$

function $H_\nu^{(1)}(x)$ can be evaluated by means of Taylor expansions (see Subsection 2.2). Discussion of the round-off errors for both Taylor expansions and the contour integration is presented in Appendix A.

5.1 Implementation of the Debye asymptotic expansions

Formulae (42)-(46) make numerical evaluation of the Debye asymptotic expansions (29), (32) and (33) fairly straightforward. However, we must estimate the values of parameters x and ν

for which these expansions provide a specified (in our case double precision) accuracy. It is necessary to point out that the computation of a N-term Debye expansion involves evaluation of n-order polynomials $u_n(t)$ for $n = 0, 1, \cdots, N$ (see Lemma 3.1). In other words, the complexity of this procedure is of order $O(N^2)$ operations and therefore for given x and ν it is desirable to choose N as small as possible. The following considerations provide a simple recipe for the optimal (for given x and ν) truncation of the Debye expansions.

The estimates (61), (73), (75) and Observation 3.3 show that for any fixed $x \gg 1$ and given N there exists a constant $g_N \gg 1$ such that the error terms of the expansions (29), (32) and (33) (truncated after N terms) become small if x and ν satisfy the inequality

$$|\nu - x| > g_N \, x^{\frac{1}{3}}. \tag{150}$$

Our numerical experiments showed that for

$$x > 17 \tag{151}$$

and ν satisfying (150) the Debye expansions (29), (32) and (33) provide double precision accuracy. The estimates of constants g_N are presented in Table 1; these values were obtained by means of both analyzing the inequalities (61), (73), (75), and comparing the estimates provided by the Debye expansions with that by contour integration.

The optimal (for given x and ν) truncation of the Debye expansions can be done by the following procedure. First we compute the parameter $g = |x - \nu|/x^{\frac{1}{3}}$, then, using Table 1, find $g_N < g$ closest to g and retain N terms corresponding to this g_N. For example, if $g = 8$ then $g_N = 7$ and thus $N = 13$. As we see from Table 1 the Debye expansions fail to provide double precision accuracy if $g < 6.5$.

Remark 5.1

In addition to the error term $\theta_{N+1,1}(\nu, p)$, estimated in (75), the expansion (32) contains the error term $\theta_{N+1,1}(\nu, 0)$. It can be shown, however, that if the inequalities (150) and (151) are satisfied then (with double precision accuracy) this term can be neglected.

5.2 Numerical integration for $x > \nu$

As follows from (92), for large $x\sin(\beta)$ the integrand of (83) is sharply peaked at $v = \beta$, and thus the interval in v where this integrand is not small may be much narrower than the actual interval of integration $v \in (0, \pi)$. To estimate numerically meaningful domain of integration in (83) we must find (unique) solutions of equation (87) β_1 and β_2 (see Corollary 4.1) with ϵ approximately equal to the absolute value of the (specified) error of the evaluation of (83). After that numerical integration in (83) is restricted to the interval $v \in (\beta_1, \beta_2)$.

In accordance with Observation 4.1 and Theorem 4.3 it was found that for

$$x > 10 \tag{152}$$

and

$$\nu < x - d_1\, x^{\frac{1}{3}} \tag{153}$$

with

$$d_1 \approx 5, \tag{154}$$

the minimal number of nodes of the trapezoidal formula (see Observation 4.1) needed to evaluate (83) with double precision accuracy is

$$n = 25 \tag{155}$$

independent of x and ν. If (152) or (153) are violated then to obtain the same accuracy we have to increase n. Changing the variable of integration (see, for example, [8])

$$v = t^4, \tag{156}$$

it is possible to somewhat improve the estimate (154). It was found that after the change of variable (156) we can evaluate (83) with double precision accuracy in the region (153) where

$$d_1 \approx 1.5, \tag{157}$$

with the number of nodes (of the trapezoidal formula)

$$n = 37 \tag{158}$$

independent of x and ν.

5.3 Numerical integration for $x < \nu$

We will first consider the integral (105) (see Observation 4.2). Function ϕ_2, defined in (108) on the interval $-\infty < u < \alpha$ has the only maximum at $u = -\alpha$. Moreover, for large x this function is not small only for $u \approx -\alpha$. Therefore, we must first estimate the interval $u \in (\alpha_1, \alpha_2)$ $(\alpha_1 < -\alpha < \alpha_2 \leq \alpha)$ where the integrand of (105) is (with given accuracy) not zero and restrict the numerical integration to this interval. We evaluated (105) by means of the Gauss-Legendre quadrature formula. It was found that for

$$x > 1 \tag{159}$$

the minimal number of nodes required to evaluate this integral with double precision accuracy is

$$n = 45 \tag{160}$$

independent of x and ν.

Now we will discuss the computation of the integral (106). As follows from (118) for sufficiently large $x \sinh(\alpha)$ the integrand of (106) is sharply peaked at $v = 0$. Therefore we must first estimate the interval $v \in (0, \alpha_3)$ $(\alpha_3 < \pi)$ where the integrand of (106) is (with given precision) not zero and restrict the numerical integration to this interval (compare with Subsection 5.1).

The integral (106) was evaluated by means of the Gauss-Legendre quadrature formula. In accordance with Observation 4.3 and Theorem 4.7 it was found that this integral can be evaluated with double precision accuracy with the number of nodes

$$n = 45 \tag{161}$$

independent of x and ν, if x satisfies the inequality (159) and

$$\nu > x + d_2\, x^{\frac{1}{3}}, \tag{162}$$

where

$$d_2 \approx 1.5. \tag{163}$$

5.4 Numerical integration for $x \approx \nu$

The problem of the numerical evaluation of the integrals (126) and (127) is essentially the same as that of the integrals (105) and (106) (see Subsection 5.2) and here we will briefly discuss the results of our numerical experiments.

The integrals (126) and (127) were evaluated by means of the Gauss-Legendre quadrature formula. In accordance with Observation 4.6 and the estimates (142), (144) it was found that both real and imaginary parts of these integrals can be computed with double precision accuracy with the number of nodes

$$n = 33 \tag{164}$$

independent of x and ν, if

$$x > 10, \tag{165}$$

and

$$|x - \nu| < d_3 \cdot x^{\frac{1}{3}}, \tag{166}$$

where

$$d_3 \approx 2. \tag{167}$$

In addition (see Remark 4.2), this scheme provides double precision accuracy with n defined in (164) for

$$1 < x < 10 \tag{168}$$

and

$$x \geq \nu. \tag{169}$$

6. Description of the algorithm

In this section we describe the algorithm for the evaluation of an individual function $H_\nu^{(1)}(x)$ (and therefore, according to (4) - (6), all other Bessel functions) of nonnegative x and ν. The final algorithm consists of two parts: algorithm A that combines contour integration and Taylor expansion, and algorithm B that is based on the Debye asymptotic expansions.

6.1 Algorithm A

if $x \le 2$ **then** compute $H_\nu^{(1)}(x)$ via Taylor expansions (see Subsection 2.2).
end if
if $x > 2$ **and** $\nu > x + 1.5 \cdot x^{\frac{1}{3}}$ **then** compute $H_\nu^{(1)}(x)$ by means of evaluation of the Sommerfeld integral along contours (19), (23), (24) (see Subsections 4.2 and 5.3).
end if
if $x > 9$ **and** $\nu < x - 1.5 \cdot x^{\frac{1}{3}}$ **then** compute $H_\nu^{(1)}(x)$ by means of evaluation of the Sommerfeld integral along contours (19), (20). (see Subsections 4.1 and 5.2).
end if
if $x \le 9$ **or** $|\nu - x| \le 1.5 \cdot x^{\frac{1}{3}}$ **then** compute $H_\nu^{(1)}(x)$ by means of evaluation of the Sommerfeld integral along contours (19), (26), (27) (see Subsections 4.3 and 5.4).
end if

6.2 Algorithm B

if $x \ge 17$ **and** $\nu \le x - 6.5 \cdot x^{\frac{1}{3}}$ **then** compute $H_\nu^{(1)}(x)$ by means of evaluation of the Debye expansion (29) (see Subsections 4.1 and 5.1).
end if
if $x \ge 17$ **and** $\nu \ge x + 6.5 \cdot x^{\frac{1}{3}}$ **then** compute $H_\nu^{(1)}(x)$ by means of evaluation of the Debye expansions (32), (33) (see Subsections 4.1 and 5.1).
end if

6.3 The final algorithm

if $x \ge 17$ **and** $|x - \nu| \ge 6.5 \cdot x^{\frac{1}{3}}$ **then** compute $H_\nu^{(1)}(x)$ by means of the algorithm B

else compute $H_\nu^{(1)}(x)$ by means of the algorithm A .

end if

6.4 Timing

A computer (FORTRAN) program using the algorithm described in the preceding sections was implemented and tested on Sun SPARCstation 1. This program consists of approximately 2000 executable lines.

We compared the time for the evaluation of function $H_\nu^{(1)}(x)$ by our algorithm with the time required to compute this function by means of recurrence relation (1) (for increasing orders) in case of integer ν. It was found that in the range of validity of the Debye expansions our algorithm catches up with the recursion for $\nu \approx 10$; in the region where the contour integration is used the same happens for $\nu \approx 800$. For arguments $x < 17$ the algorithm is approximately 20 times slower than the recursion.

8. Conclusions

In the present paper we have shown that the Debye asymptotic expansions, contrary to what appears to be a popular belief, are not expansions in inverse powers of (large) parameter ν but turn out to be uniform expansions in inverse powers of (large) parameter $g_1 = (x-\nu)/x^{\frac{1}{3}}$ for $x > \nu$ and (large) parameter $g_2 = (\nu - x)/\nu^{\frac{1}{3}}$ for $x < \nu$ (see Theorems 3.1, 3.3 and Observations 3.1 and 3.3). For x and ν such that both Taylor and Debye expansions do not provide a specified accuracy we have demonstrated that function $H_\nu^{(1)}(x)$ can be computed at a constant CPU time via (numerical) evaluation of the Sommerfeld integral along contours of steepest descents (the Debye contours). Obviously, numerical integration along contours of steepest descents can be applied for the evaluation of other functions of mathematical physics. In particular, it can be used for the computation of Bessel functions of complex arguments and orders (the classification of the Debye contours in case of complex x and ν can be found, for example, in Ch. 8 of [4]).

In addition, we have obtained new estimates concerning decay of functions $J_\nu(x)$ and $-1/Y_\nu(x)$ of fixed $x > 0$ and large positive ν (see Appendix B). Finally, we have shown that

Bessel functions of the first kind and integer orders provide a solution to a system of differential equations for a chain of coupled harmonic oscillators (see Appendix C).

The author would like to thank Professor Vladimir Rokhlin for useful discussions and for his interest and support.

Appendix A

Round-off errors

In this Appendix we briefly discuss round-off errors that appear (for certain values of x and ν) when function $H_\nu^{(1)}(x)$ is evaluated via either Taylor expansions or contour integration.

A.1 Taylor expansions

It is well known (see, for example, Ch. 3 of [4]) that for

$$\nu = m + \sigma, \tag{170}$$

where m is an integer and $|\sigma| \ll 1$,

$$J_\nu(x)\ \cos(\pi\ \nu) \approx J_{-\nu}(x), \tag{171}$$

and thus in this case formula (8) produces significant round-off error. However, for any fixed $x > 0$ function $Y_\nu(x)$ is an analytic function of ν and therefore it can be evaluated by means of interpolation with respect to the order.

Our experiments showed that that for $|\sigma| > 5 \cdot 10^{-4}$ no significant error occurred. For smaller $|\sigma|$ we used Chebychev interpolation of function $Y_\nu(x)$ on the interval

$$\nu \in [m - 10^{-3}, m + 10^{-3}] \tag{172}$$

with the number of nodes k=6; this number of nodes proves to be sufficient for the evaluation of this function with at least thirteen digits for ν from (172) and $x \leq 2$.

A.2 Numerical integration for $x > \nu$

Our experiments showed that for $x \gg 1$ it is impossible to compute the integral (83) without a round-off error unless function ϕ_1, defined in (84), is carefully evaluated. This error occurs because, as follows from (83), for $x \gg 1$ small errors of the evaluation of function ϕ_1 produce large errors of the integrand of (83).

First of all we observe that for small $|v-\beta|$ there appears a loss of accuracy if we evaluate $\sinh(u)$ by means of the formula

$$\sinh(u) = ((\cosh(u)-1)(\cosh(u)+1))^{\frac{1}{2}} \tag{173}$$

with $\cosh(u)$ computed via (19), (20). Writing

$$\cosh(u) - 1 = \frac{f_1(v,\beta) - f_2(v,\beta)}{\sin(v)} \tag{174}$$

where

$$f_1(v,\beta) = (v-\beta)\ \cos(\beta) \tag{175}$$

$$f_2(v,\beta) = \sin(v) - \sin(\beta) \tag{176}$$

we see that for small $|v-\beta|$ each of the functions $f_1(v,\beta)$ and $f_2(v,\beta)$ are of order $O(v-\beta)$ whereas the numerator of (174) is of order $O((v-\beta)^2)$.

To avoid the round-off error, cased by the cancellation of the leading terms of the Taylor expansions of functions (175) and (176), we can first evaluate the numerator of (174) using its Taylor expansion in (small parameter) $(v-\beta)$ and after that compute $\sinh(u)$ by means of (173), and u via

$$u = \ln(\sinh(u) + \cosh(u)). \tag{177}$$

In addition, a round-off error appears if we evaluate function ϕ_1 itself via the formula (84) Rewriting (84) in an equivalent form

$$\phi_1 = (\cos(v) - \cos(\beta))\ \sinh(u) + (\sinh(u) - u)\ \cos(\beta), \tag{178}$$

we see, that in order to avoid cancellations (and therefore the lost of significant digits in (178)) we can evaluate functions $(\cos(v) - \cos(\beta))$ and $(\sinh(u) - u)$ via their Taylor expansions in (small parameters) $(v-\beta)$ and u, consequently.

Our experiments showed that the integral (83) can be computed without significant round-off error if we use Taylor expansions in (174) and (178) for $|v-\beta| \leq 0.1$.

A.3 Numerical integration for $x \approx \nu$

It was found that the integral (126) can be computed without round-off error for any x and ν. However it turns out that we cannot evaluate of the integral (127) without a round-off error which becomes large for $x \gg 1$. Like in case $x > \nu$, the main source of this error is the sensitivity of the computation of the integrand of (127) (for large x) to small errors of the evaluation of function ϕ_4 defined in (129). To analyze this effect we observe that as follows from (134) and (135) for small v functions u and $\sinh(u) \cdot \cos(v)$ are of order $O(v)$ whereas their difference (136) is of order $O(v^3)$. Therefore the round-off error of the evaluation of (136) (and thus of function ϕ_4 from (129)) appears (for sufficiently small v) due to cancellation of the leading terms of the Taylor expansions of (134) and (135).

It follows from our numerical experiments that if the left-hand sides of (134)-(136) are evaluated via their Tailor expansions for $v < 1$ then the integral (127) can be computed without significant round-off error. These expansions are:

$$\begin{aligned} u \;=\; & 0.57735026918962576\, v + 0.025660011963983367\, v^3 + \\ & 0.0014662863979419067\, v^5 + 0.00009775242652946044 5\, v^7 + \\ & 0.74525058224720925 \cdot 10^{-5}\, v^9 + 0.61544207267743328 \cdot 10^{-6}\, v^{11} + \\ & 0.52905118464628039 \cdot 10^{-7}\, v^{13} + \cdots, \end{aligned} \tag{179}$$

$$\begin{aligned} \sinh(u) \;=\; & 0.57735026918962576\, v + 0.057735026918962576\, v^3 + \\ & 0.0062775386411887880\, v^5 + 0.00065524673408028954\, v^7 + \\ & 0.00006697089225899325 4\, v^9 + 0.67971226373232793 \cdot 10^{-5}\, v^{11} + \\ & 0.68878126140038453 \cdot 10^{-6}\, v^{13} + \cdots, \end{aligned} \tag{180}$$

$$\begin{aligned} u - \sinh(u)\, \cos(v) \;=\; & 0.025660011963983367\, v^3 + \\ & 0.00097752426529460445\, v^7 + \\ & 0.00007240920483663736 8\, v^9 + \\ & 0.74478039260541289 \cdot 10^{-5}\, v^{11} + \\ & 0.74130822294291681 \cdot 10^{-6}\, v^{13} + \cdots. \end{aligned} \tag{181}$$

Appendix B

Decay of functions $J_\nu(x)$ and $-1/Y_\nu(x)$ for the large orders and fixed arguments

In this appendix we discuss the behavior of functions $J_\nu(x)$ and $Y_\nu(x)$ for fixed arguments and large orders. Theorems B1 and B2 and formulae (219) and (222) contain the principal results of this appendix.

B1. Statement of the problem

It is well known that for any fixed $x > 0$ and $\nu \to \infty$ function $J_\nu(x)$ decays rapidly (see, for example, Ch. 10 of [5]) and has an asymptotic behavior defined by the formula

$$J_\nu(x) = \frac{1}{\Gamma(\nu+1)} \cdot \left(\frac{x}{2}\right)^\nu (1 + O(\nu^{-1})). \tag{182}$$

However, this approximation is numerically meaningful only for $\nu \gg x^2/4$ (see, for example, Ch. 10 of [5]). On the other hand, often it is necessary to have an accurate estimate of an order $\nu_j > x > 0$ such that

$$J_\nu(x) < \epsilon, \tag{183}$$

for all $\nu > \nu_j$. In (183) x is fixed and $\epsilon > 0$ is supposed to be sufficiently small. This problem arises, for example, when one implements Miller's algorithm (see, for example, [1], [2]), or sums a Neumann series

$$S_\mu(x) = \sum_{n=0}^{\infty} a_n \, J_{\mu+n}(x). \tag{184}$$

It is well known that the behavior of function $J_\nu(x)$ of fixed positive arguments and large orders is close to that of function $-1/Y_\nu(x)$. For example, for any fixed $x > 0$ and $\nu \to \infty$ this function decays rapidly (see, for example, [1]) and has the following asymptotic representation

$$-\frac{1}{Y_\nu(x)} = \pi \cdot \frac{1}{\Gamma(\nu)} \cdot \left(\frac{2}{x}\right)^\nu (1 + O(\nu^{-1})). \tag{185}$$

In this appendix we prove that functions $J_\nu(x)$ and $-1/Y_\nu(x)$ of any fixed $x > 0$ are monotonically decreasing functions of $\nu > x$ (see Theorems B1 and B2 below). In addition,

in case of large fixed $x > 0$ and sufficiently small $\epsilon > 0$ we present approximate solutions of equations

$$J_{\nu_j}(x) = \epsilon, \tag{186}$$

and

$$-\frac{1}{Y_{\nu_y}(x)} = \epsilon, \tag{187}$$

with respect to ν_j and ν_y for $\nu_j, \nu_y > x$.

B2. Certain properties of function $J_\nu(x)$ for $\nu > x$.

It was proved in Ch. 10 of [4] that the for any $0 < z \leq 1$,

$$J_\nu(\nu z) > 0, \tag{188}$$

and

$$\frac{\partial J_\nu(\nu z)}{\partial \nu} < 0. \tag{189}$$

Similarly, one can prove the following

Theorem B1

For any $\nu \geq x > 0$,

$$\frac{\partial J_\nu(x)}{\partial \nu} < 0. \tag{190}$$

Proof

We start with Schläfli's representation of function $J_\nu(x)$ (see, for example, Ch. 6 of [4]):

$$J_\nu(x) = \frac{1}{2\pi i} \int_{\infty-\pi i}^{\infty+\pi i} \exp(x \sinh(w) - \nu w) dw. \tag{191}$$

Differentiating (191) with respect to ν we have

$$\frac{\partial J_\nu(x)}{\partial \nu} = -\frac{1}{2\pi i} \int_{\infty-\pi i}^{\infty+\pi i} w \ \exp(x \sinh(w) - \nu w) dw. \tag{192}$$

Deforming the contour of integration in (192) into the contour (19), (24) with $v \in (-\pi, \pi)$ we obtain

$$\frac{\partial J_\nu(x)}{\partial \nu} = -\frac{1}{2\pi i} \int_{-\pi}^{\pi} (u + iv) \left(i + \frac{du}{dv} \right) \exp(x \sinh(u) \cos(v) - \nu u) dv, \qquad (193)$$

where the derivative du/dv is defined in (110). On this contour,

$$u > 0, \qquad (194)$$

$$\frac{du(v)}{dv} = -\frac{du(-v)}{dv}. \qquad (195)$$

Combination of (193), (194) and (195) yields

$$\frac{\partial J_\nu(x)}{\partial \nu} = -\frac{1}{\pi} \int_0^{\pi} \left(u + v \frac{du}{dv} \right) \exp(x \sinh(u) \cos(v) - \nu u) dv. \qquad (196)$$

Finally, for $v \in (0, \pi)$ we have from (110)

$$\frac{du}{dv} \geq 0. \qquad (197)$$

The conclusion of the theorem follows from (194), (196) and (197). □

Observation B1

It follows from formula (188) and Theorem B1 that for any $\nu \geq x > 0$ (x is fixed) equation (186) has at most one real solution. Moreover, if such a solution exists, then the inequality (183) is satisfied for all $\nu > \nu_j$.

B3. Certain properties of function $Y_\nu(x)$ for $\nu > x$.

Turning to the discussion of the behavior of function $Y_\nu(x)$ for $\nu > x > 0$ we will first prove the following

Lemma B1

For any $\nu \geq x > 0$,

$$Y_\nu(x) < 0. \qquad (198)$$

Proof

Combining formulae (5), (105) (106) and (107) we have

$$Y_\nu(x) = -\frac{1}{\pi}\int_{-\infty}^{\alpha}\exp(x\phi_2)du - \frac{1}{\pi}\int_0^{\pi}\exp(x\phi_3)\,\frac{du}{dv}dv, \tag{199}$$

where the parameter α and functions ϕ_2 and ϕ_3 are defined in (25), (108) and (109), respectively, and function $u = u(v)$ is evaluated via (19), (23). Now the conclusion of the lemma follows from (197) and (199). □

We will now prove the analogue of Theorem B1 for function $Y_\nu(x)$.

Theorem B2

For any $\nu \geq x > 0$,

$$\frac{\partial Y_\nu(x)}{\partial \nu} < 0. \tag{200}$$

Proof

We start with Nicholson's formula (see, for example, Ch. 9 of [5]):

$$N_\nu(x) \equiv \frac{8}{\pi^2}\int_0^{\infty} K_0(2x\sinh(t))\cdot\cosh(2\nu t)dt = J_\nu^2(x) + Y_\nu^2(x), \tag{201}$$

where

$$K_0(z) = \int_0^{\infty}\exp(-z\cosh(t))dt \tag{202}$$

is Macdonald's function of zero order. It immediately follows from (201) and (202) that for any $x > 0$,

$$\frac{\partial N_\nu(x)}{\partial \nu} > 0. \tag{203}$$

Next, formula (201) yields

$$\frac{\partial Y_\nu(x)}{\partial \nu} = \frac{1}{2Y_\nu(x)}\cdot\left(\frac{\partial N_\nu(x)}{\partial \nu} - 2J_\nu(x)\frac{\partial J_\nu(x)}{\partial \nu}\right). \tag{204}$$

The conclusion of the theorem is a consequence of (188), (190), (198), (203) and (204). □

The following observation is closely related to Observation B1 above.

Observation B2

Lemma B1 and Theorem B2 show that for any fixed positive $x < \nu$ equation (187) has at most one real solution. Moreover, if such a solution exists,

$$-\frac{1}{Y_\nu(x)} < \epsilon \tag{205}$$

for all $\nu > \nu_y$.

In the rest of the appendix we derive approximate (asymptotic) solutions of equations (186) and (187).

B4. Asymptotic solution of equation (186).

We will first prove the following simple

Lemma B2

For any $|z| < 1$,

$$\ln(1+z) = \sum_{n=1}^{\infty} \frac{z^{2n-1}}{2n-1} + \frac{1}{2}\ln(1-z^2). \tag{206}$$

Proof

Expanding left-hand side of (206) into Taylor series we have

$$\ln(1+z) = \sum_{n=1}^{\infty}(-1)^{(n+1)}\frac{z^n}{n} = \sum_{n=1}^{\infty}\frac{z^{2n-1}}{2n-1} - \frac{1}{2}\sum_{n=1}^{\infty}\frac{z^{2n}}{n}, \tag{207}$$

which concludes the proof of the lemma. □

An approximation to ν_j from (186), hereafter denoted by $\tilde{\nu}_j$, will be sought as a solution of the equation

$$\frac{\exp(-\tilde{\eta}_2)}{(2\pi)^{\frac{1}{2}}\ (\tilde{\nu}_j^2 - x^2)^{\frac{1}{4}}} = \epsilon, \tag{208}$$

where the function on the left-hand side of (208) is the leading term of the Debye asymptotic expansion (32) with the change of notation $\nu \to \tilde{\nu}_j$.

Introducing the notation

$$y_j = \frac{\tilde{\nu}_j}{x}, \tag{209}$$

and substituting (209) into (34) we obtain

$$\tilde{\eta}_2 = x \cdot y_j \cdot \left[\ln(y_j) + \ln\left(1 + (1 - y_j^{-2})^{\frac{1}{2}}\right) - (1 - y_j^{-2})^{\frac{1}{2}}\right]. \tag{210}$$

Noticing that for $z = (1 - y_j^{-2})^{\frac{1}{2}}$ equation (206) becomes

$$\ln\left(1 + (1 - y_j^{-2})^{\frac{1}{2}}\right) = (1 - y_j^{-2})^{\frac{1}{2}} + \sum_{n=1}^{\infty} \frac{1}{2n+1}(1 - y_j^{-2})^{\frac{2n+1}{2}} - \ln(y_j), \tag{211}$$

and substituting (211) into (210) we obtain

$$\tilde{\eta}_2 = x\ y_j\ (1 - y_j^{-2})^{\frac{1}{2}}\ \sum_{n=1}^{\infty} \frac{\left(1 - y_j^{-2}\right)^n}{2n+1}. \tag{212}$$

Now, substituting (209) and (212) into (208), we have

$$x \cdot y_j \cdot (1 - y_j^{-2})^{\frac{1}{2}}\ \sum_{n=1}^{\infty} \frac{(1 - y_j^{-2})^n}{2n+1} + \frac{1}{4}\ln(y_j^2 - 1) = -\ln\left((2\pi x)^{\frac{1}{2}}\ \epsilon\right). \tag{213}$$

Finally, introducing a new (unknown) function q_j which is a positive solution of the equation

$$y_j = x^{-\frac{2}{3}}\ q_j^2 + 1, \tag{214}$$

and substituting (214) into (213) we have

$$\frac{2^{\frac{3}{2}}}{3}\ q_j^3\ (1 - \frac{1}{20}\ x^{-\frac{2}{3}}\ q_j^2 + O(x^{-\frac{4}{3}}\ q_j^4)) + \frac{1}{2}\ln q_j + \frac{1}{4}\ln(1 + \frac{1}{2}x^{-\frac{2}{3}}\ q_j^2) = -\ln(2^{\frac{3}{4}}\ \pi^{\frac{1}{2}}\ x^{\frac{1}{3}}\ \epsilon). \tag{215}$$

We seek the asymptotic solution of (215) under the condition

$$x \gg -\ln(2^{\frac{3}{4}}\ \pi^{\frac{1}{2}}\ x^{\frac{1}{3}}\ \epsilon) \gg 1. \tag{216}$$

Taking into account (216), equation (215) immediately yields the leading term of the asymptotic expansion of q_j:

$$q_j \sim \delta_j, \tag{217}$$

where

$$\delta_j = 3^{\frac{1}{3}}\ 2^{-\frac{1}{2}} \left(-\ln(2^{\frac{3}{4}}\ \pi^{\frac{1}{2}}\ x^{\frac{1}{3}}\ \epsilon)\right)^{\frac{1}{3}}. \tag{218}$$

Corrections to (217) can be found by standard methods (see, for example, Ch. 1 of [5]). After some algebra we obtain

$$\begin{aligned} \frac{\tilde{\nu_j}}{x} - 1 \ &= \ \left(\delta_j\ x^{-\frac{1}{3}}\right)^2 \left(1 - \frac{1}{8^{\frac{1}{2}}}\ \ln(\delta_j)\ \delta_j^{-3} + \frac{1}{30}\left(\delta_j\ x^{-\frac{1}{3}}\right)^2 + \right. \\ & \left. O\left(\ln(\delta_j)\ \delta_j^{-6}\right) + O\left(x^{-\frac{2}{3}}\ \delta_j^{-1}\right)\right). \end{aligned} \tag{219}$$

B5. Asymptotic solution of equation (187).

In this subsection we briefly discuss the derivation of the asymptotic solution of equation (187); this approximate solution will be denoted by $\tilde{\nu_y}$. Like in case of equation (186) we seek an approximation to ν_y as a solution (for fixed positive $x < \nu$) of equation

$$\left(\frac{\pi}{2}\right)^{\frac{1}{2}} \exp(-\tilde{\eta}_2)\ (\tilde{\nu}_y^2 - x^2)^{\frac{1}{4}} = \epsilon, \tag{220}$$

where the function on the left-hand side of (220) is the modulus of the inverse of the leading term of the Debye asymptotic expansion (33) with the change of notation $\nu \to \tilde{\nu_y}$. The technique employed for solving equation (220) is the same as that for equation (208) and we omit the computational details. It can be shown that the asymptotic solution of (220) derived under the condition

$$x \gg -\ln(2^{\frac{1}{4}}\ \pi^{-\frac{1}{2}}\ x^{-\frac{1}{3}}\ \epsilon) \gg 1, \tag{221}$$

has the form

$$\begin{aligned} \frac{\tilde{\nu_y}}{x} - 1 \ &= \ \left(\delta_y\ x^{-\frac{1}{3}}\right)^2 \left(1 + \frac{1}{8^{\frac{1}{2}}}\ \ln(\delta_y)\ \delta_y^{-3} + \frac{1}{30}\left(\delta_y\ x^{-\frac{1}{3}}\right)^2 + \right. \\ & \left. O\left(\ln(\delta_y)\ \delta_y^{-6}\right) + O\left(x^{-\frac{2}{3}}\ \delta_y^{-1}\right)\right), \end{aligned} \tag{222}$$

where

$$\delta_y = 3^{\frac{1}{3}}\ 2^{-\frac{1}{2}} \left(-\ln(2^{\frac{1}{4}}\ \pi^{-\frac{1}{2}}\ x^{-\frac{1}{3}}\ \epsilon)\right)^{\frac{1}{3}}. \tag{223}$$

B6. Comparison of exact and asymptotic solutions of equations (186) *and* (187).

Tables 2 and 3 contain approximations $\tilde{\nu_j}$ and $\tilde{\nu_y}$, obtained via (219) and (222), as well as exact numerical solutions of equations (186) and (187) for several values of x and ϵ (when solving equations (186) and (187) their left-hand sides were computed via contour integration for $x > 2$ and Taylor expansion for $x \leq 2$). It is interesting to note, that the formulae (219) and (222) provide reasonable approximations to ν_j and ν_y even for $x \approx 1$, *i.e.* when the conditions (216), (221) are violated.

Remark B1

It is easy to see from (219) and (222), that up to logarithmic (in x) corrections the parameters $\tilde{\nu_j}$ and $\tilde{\nu_y}$ can be estimated as

$$\tilde{\nu_j} \approx x + c_j(\epsilon)\, x^{\frac{1}{3}}, \tag{224}$$

$$\tilde{\nu_y} \approx x + c_y(\epsilon)\, x^{\frac{1}{3}}, \tag{225}$$

where $c_j(\epsilon) \approx c_y(\epsilon) > 0$ are independent of x. In other words, the approximations (224), (225) provide a (rough) estimate of a domain on the $x - \nu$ plane where functions $J_\nu(x)$ and $-1/Y_\nu(x)$ of any fixed $x \gg 1$ are small for all $\nu > \tilde{\nu_j} \approx \tilde{\nu_y}$.

Appendix C

Bessel functions and a chain of harmonic oscillators

In this appendix we show that functions $J_\nu(x)$ of integer ν describe displacements of coupled harmonic oscillators on a line.

Differentiating the formula (see, for example, [1])

$$\frac{df_\nu(x)}{dx} = \frac{1}{2}(f_{\nu-1}(x) - f_{\nu+1}(x)), \tag{226}$$

where $f_\nu(x)$ has the same meaning as in formula (1) we obtain

$$\frac{d^2 f_\nu(x)}{dx^2} = \frac{1}{4}(f_{\nu-2}(x) - 2\, f_\nu(x) + f_{\nu+2}(x)). \tag{227}$$

Equation (227) can be compared with the differential equations for a system of equal point masses on a line which interact with their nearest neighbors via the elastic force. The displacement from the equilibrium $u_n(t)$ (as a function of time t) of an n-th such oscillator satisfies equation (see, for example, [9])

$$M \frac{d^2 u_n(t)}{dt^2} = G\,(u_{n-1}(t) - 2\,u_n(t) + u_{n+1}(t)), \tag{228}$$

where M is the mass and G is the elastic constant.

The analogy between (227) and (228) becomes especially transparent if we rewrite (227) for Bessel functions of the first kind of integer order $\nu = n$. It follows from (227) that these functions of even orders satisfy the system of differential equations

$$\frac{d^2 J_{2n}(x)}{dx^2} = \frac{1}{4}(J_{2n-2}(x) - 2\,J_{2n}(x) + J_{2n+2}(x)), \quad (n = 0, \pm 1, \pm 2, \cdots); \tag{229}$$

with the initial conditions (see, for example, [1])

$$\begin{aligned} &J_0(0) = 1, \quad J_{2n}(0) = 0, \quad (n = \pm 1, \pm 2, \cdots); \\ &\left.\frac{dJ_{2n}(x)}{dx}\right|_{x=0} = 0, \quad (n = 0, \pm 1, \pm 2, \cdots). \end{aligned} \tag{230}$$

For odd orders we have the same system of equations

$$\frac{d^2 J_{2n+1}(x)}{dx^2} = \frac{1}{4}(J_{2n-1}(x) - 2\,J_{2n+1}(x) + J_{2n+3}(x)), \quad (n = 0, \pm 1, \pm 2, \cdots); \tag{231}$$

but the initial conditions in this case are different (see, for example, [1]):

$$\begin{aligned} &J_{2n+1}(0) = 0, \quad (n = 0, \pm 1, \pm 2, \cdots); \\ &\left.\frac{dJ_1(x)}{dx}\right|_{x=0} = \frac{1}{2}, \qquad \left.\frac{dJ_{-1}(x)}{dx}\right|_{x=0} = -\frac{1}{2}, \\ &\left.\frac{dJ_{2n+1}(x)}{dx}\right|_{x=0} = 0, \qquad (n = 1, \pm 2, \cdots). \end{aligned} \tag{232}$$

Comparing (228) with (229) and (231) we see that function $J_{2n}(x)$ (or, equivalently, $J_{2n+1}(x)$) can be viewed as a displacement of an n-th oscillator at a 'time' x in a chain (228) with parameters

$$\begin{aligned} &M = 1, \\ &G = \frac{1}{4}. \end{aligned} \tag{233}$$

It is interesting to observe, that as follows from (229) and (231) the chains of even and odd Bessel function do not interact.

This analogy enables us to give a mechanical interpretation of certain properties of Bessel functions.

1. A zero of a Bessel function can be interpreted as a 'time' at which a corresponding oscillator passes the equilibrium. Therefore, the well known result, that function $J_n(x)$ has infinitely many zeros as $x \to \infty$ reflects the obvious physical property that any oscillator (in a chain with zero friction) passes the equilibrium infinitely many times (as time goes to infinity).

2. The identity (see, for example, [1])

$$\sum_{n=-\infty}^{\infty} J_n^2(x) = J_0^2(x) + 2 \sum_{n=1}^{\infty} J_n^2(x) = 1 \tag{234}$$

means that the oscillators in the chains (229) and (231) under the initial conditions (230) and (232) oscillate in such a way that the sum of squares of the displacements in both of them does not depend on 'time' x.

3. In terms of the mechanical model the approximation (219) (or its simplified version (224)) estimates the range of propagation of the initial perturbation (230) (or (232)) at the 'time' x.

4. It is easy to show that the well known relation (see, for example, [1])

$$\sum_{n=-\infty}^{\infty} J_{2n}(x) = J_0(x) + 2 \sum_{n=1}^{\infty} J_{2n}(x) = 1 \tag{235}$$

is a consequence of the conservation of momentum in the even chain (229). To prove this we observe that according to the initial conditions (230) the total initial momentum of the even chain is zero. Because this system is isolated we can write

$$\sum_{n=-\infty}^{\infty} \frac{dJ_{2n}(x)}{dx} = 0 \tag{236}$$

for any 'time' x. Integrating (236) and observing that due to (230) the constant of integration is equal to unity we immediately obtain (235).

5. An interesting formula can be obtained from the law of conservation of energy in the odd chain (231). Using (233) we find the kinetic K and the potential Π energy of the odd chain (231) (see, for example, [9]):

$$K = \frac{1}{2} \sum_{n=-\infty}^{\infty} \left(\frac{dJ_{2n+1}(x)}{dx} \right)^2 , \tag{237}$$

$$\Pi = \frac{1}{8} \sum_{n=-\infty}^{\infty} (J_{2n+1}(x) - J_{2n-1}(x))^2 . \tag{238}$$

Combining (226) and (238) we obtain

$$\Pi = \frac{1}{2} \sum_{n=-\infty}^{\infty} \left(\frac{dJ_{2n}(x)}{dx} \right)^2 . \tag{239}$$

As follows from (232) and (233) the total initial energy of the odd chain is equal to 1/4 and, the system being isolated, it remains the same at any 'time' x. Therefore from (237) and (239) we have

$$\sum_{n=-\infty}^{\infty} \left(\frac{dJ_n(x)}{dx} \right)^2 = \frac{1}{2}. \tag{240}$$

The formula (240) means that the sum of kinetic energies of the chains (229) and (231) is independent of 'time' x.

Remark C1

As follows from the preceding analysis Bessel functions are a (rare) example of a discrete dynamic interacting system where the coordinate of any particle can be computed at a CPU time independent of the physical time.

References

[1] M. Abramovitz and I.A. Stegun (Eds.), *Handbook of Mathematical Functions,* National Bureau of Standards, 1964. Ch. 9.

[2] W. H. Press, B. P. Flannery, S. A. Teukolsky and W. T. Vetterling, *Numerical Recipes in C,* Cambridge Univ. Press, Cambridge, 1988.

[3] P. Debye *Näherungsformeln für die Zylinderfunktionen für grosse Werte des Arguments und unbeschränkt veränderliche Werte des Index,* Math. Ann., 67, 535-558, 1909.

[4] G. N. Watson, *A Treatise on the Theory of the Bessel Functions,* Cambridge Univ. Press, Cambridge, 1958.

[5] F. W. J. Olver, *Asymptotics and Special Functions,* Academic Press, New York and London, 1974.

[6] N. Bleistein and R. A. Handelsman, *Asymptotic Expansions of Integrals,* Dover, New York, 1986.

[7] F. W. J. Olver, *Some New Asymptotic Expansions for Bessel Functions of Large Orders,* Proc. Cambridge Philos. Soc., 48, 414-427, 1952.

[8] N. S. Bakhvalov, *Numerical Methods,* Nauka, Moscow, 1975. Ch. 3.

[9] J. M. Ziman, *Principles of the Theory of Solids,* Cambridge Univ. Press, Cambridge, 1972. Ch. 2.

Table 1: Numerical estimates of the parameter g_N.

N	5	9	13	17
g_N	23	10	7	6.5

Table 2: Comparison of the numerical solution of (186) with the approximation (219).

	ϵ	$x=1$	$x=2$	$x=10$	$x=50$	$x=100$	$x=1000$	$x=10000$	$x=100000$
ν_0	10^{-5}	6.25	8.37	20.10	66.38	120.2	1040.8	10082.1	100163.9
$\tilde{\nu}$	10^{-5}	6.63	8.61	20.22	66.44	120.3	1040.8	10082.1	100164.0
ν_0	10^{-10}	10.28	13.15	27.60	78.79	135.8	1074.5	10156.0	100326.7
$\tilde{\nu}$	10^{-10}	11.20	13.74	27.83	78.88	135.9	1074.6	10156.0	100326.7
ν_0	10^{-20}	17.18	21.20	39.76	98.33	160.1	1126.2	10267.8	100569.4
$\tilde{\nu}$	10^{-20}	19.73	22.85	40.33	98.53	160.2	1126.2	10267.8	100569.4
ν_0	10^{-30}	23.37	28.34	50.25	114.8	180.5	1169.0	10359.7	100768.1
$\tilde{\nu}$	10^{-30}	28.14	31.47	51.32	115.2	180.7	1169.0	10359.7	100768.1

Table 3: Comparison of the numerical solution of (187) with the approximation (222).

	ϵ	$x=1$	$x=2$	$x=10$	$x=50$	$x=100$	$x=1000$	$x=10000$	$x=100000$
ν_y	10^{-5}	7.42	9.89	23.02	72.26	128.2	1062.5	10139.0	100309.4
$\tilde{\nu}_y$	10^{-5}	7.53	9.88	22.96	72.20	128.1	1062.4	10139.0	100309.4
ν_y	10^{-10}	11.43	14.59	30.18	83.76	142.5	1092.2	10202.1	100443.3
$\tilde{\nu}_y$	10^{-10}	12.06	14.91	30.19	83.70	142.4	1092.2	10202.1	100443.3
ν_y	10^{-20}	18.31	22.57	42.07	102.6	165.7	1140.7	10305.2	100663.6
$\tilde{\nu}_y$	10^{-20}	20.59	23.96	42.40	102.6	165.8	1140.7	10305.2	100663.6
ν_y	10^{-30}	24.48	29.68	52.43	118.7	185.6	1181.9	10392.9	100851.4
$\tilde{\nu}_y$	10^{-30}	29.00	32.56	53.26	118.9	185.6	1181.9	10392.9	100851.4

A group of quadrature formulae is presented applicable to both non-singular functions and functions with end-point singularities, generalizing the classical end-point corrected trapezoidal quadrature rules. We present an algorithm for the construction of very high-order end-point corrected trapezoidal rules, taking advantage of functional information outside the interval of integration. The scheme applies not only to non-singular functions, but also for a wide class of functions with monotonic singularities. Numerical experiments are presented demonstrating the practical usefulness of the new class of quadratures. Tables of quadrature weights are included for singularities of the form $s(x) = log(|x|)$, $s(x) = |x|^\lambda$ for a variety of values of λ.

High-Order Corrected Trapezoidal Rules for Singular Functions

Sharad Kapur and Vladimir Rokhlin

1 Introduction

The trapezoidal rule is known to be an easy and numerically stable means for numerical integration. If a function is periodic and analytic on the interval of integration, the trapezoidal rule converges exponentially fast (see, for example, [7]). However, for non-periodic functions the trapezoidal rule is second order convergent, and end-point corrections are often used to improve the convergence rate. A standard end-point corrected trapezoidal rule is fourth order convergent, and is given by the formula

$$\int_a^b f(x)dx = \sum_{i=1}^{n-2} f(x_i) + \frac{f(x_0)+f(x_{n-1})}{2} + \frac{h}{24}(-f(x_{-1}) + f(x_1) + f(x_{n-2}) - f(x_n)), \tag{1}$$

where, $h = (b-a)/(n-1)$ and $x_i = a + ih$ for $i = 0, 1, 2, ..., n-1$ (see, for example [1]).

More recently, the Euler-Maclaurin formula is used in [4] to obtain a high-order end-point corrected trapezoidal rule of the form

$$T_\alpha^n(f) = \sum_{i=1}^{n-2} f(x_i) + \frac{f(x_0)+f(x_{n-1})}{2} + h\sum_{j=1}^{m} \alpha_j (f(x_{n-j}) - f(x_j)), \tag{2}$$

where $\alpha = (\alpha_1, \alpha_2, ..., \alpha_m)$ are coefficients such that

$$| T_\alpha^n(f) - \int_a^b f(x)dx | < \frac{c}{n^m}. \tag{3}$$

for some $c > 0$.

The scheme of [4] provides satisfactory quadratures upto order 12; for higher orders, the coefficients α grow rapidly, rendering the scheme useless. In this paper we develop a different class of end-point corrected trapezoidal rules, whereby the growth of correction weights is suppressed, enabling the construction of end-point corrected trapezoidal rules of arbitrarily high order for non-singular functions.

In [5], end-point corrected quadrature formulae are developed to approximate definite integrals of singular functions $f : [a, b] \to R^1$ of the form

$$f(x) = \phi(x)s(x) + \psi(x), \tag{4}$$

and

$$f(x) = \phi(x)s(x), \tag{5}$$

where $a \leq 0 \leq b$, $\phi(x), \psi(x) \in c^k[a, b]$, and $s(x) \in c[a, b]$ is an integrable function with a singularity at 0. The procedure developed in [5] provides satisfactory quadratures only upto order 4; for higher orders, the quadrature weights grow rapidly, also rendering the scheme useless. In this paper we construct a different class of end-point corrected trapezoidal rules,

whereby the growth of quadrature weights is partially suppressed for functions of the form (4), obtaining useful quadratures of order upto 12; and completely suppressed for functions of the form (5), providing quadratures of arbitrarily high order. Moreover, we obviate the programming inconvenience associated with the procedure developed in [5], which requires that functional information be tabulated on a grid finer than that required for the uncorrected trapezoidal rule.

Remark 1.1 The approach of this paper is somewhat related to that of [9]. However, [9] constructs quadratures in higher dimensions, and these quadratures are of relatively low order. In this paper, we construct one-dimesional rules of very high order. Furthermore, most rules of this paper are "standard" in the sense that the correction coefficients do not depend on the number of nodes in the trapezoidal rule being corrected, or on the sampling interval.

2 Mathematical Preliminaries

In this section we summarize some well-known results to be used in the reminder of the paper. Lemmas 2.1, 2.2 and 2.3 can be found, for example, in [1].

Definition 2.1 *Suppose that a, b are a pair of real numbers such that $a < b$, and that $n \geq 2$ is an integer. For a function $f : [a,b] \rightarrow R^1$, we define the n-point trapezoidal rule $T_n(f)$ by the formula*

$$T_n(f) = h(\sum_{i=0}^{n-1} f(a+ih) - (\frac{f(a)+f(b)}{2})), \tag{6}$$

with

$$h = (b-a)/(n-1). \tag{7}$$

The following lemma provides an error estimate for the approximation to the integral given by the trapezoidal rule. Along with Lemma 2.2, it can be found, for example in [1].

Lemma 2.1 *(Euler-Maclaurin formula) Suppose that a, b are a pair of real numbers such that $a < b$, and that $m \geq 1$ is an integer. Further, let B_k denote the Bernoulli numbers*

$$B_2 = \frac{1}{6}, B_4 = \frac{-1}{30}, B_6 = \frac{1}{42}, ..., . \tag{8}$$

If $f \in c^{2m+2}[a,b]$ (i.e., f has $2m+2$ continuous derivatives on $[a,b]$), then there exists a real number ξ, with $a < \xi < b$, such that

$$\int_a^b f(x)dx = T_n(f) + \sum_{l=1}^{m} \frac{h^{2l}B_{2l}}{(2l)!}(f^{(2l-1)}(b) - f^{(2l-1)}(a)) - \frac{h^{2m+2}B_{2m+2}}{(2m+2)!}f^{2m+2}(\xi). \tag{9}$$

The following well-known lemma provides an error estimate for Lagrange interpolation.

Lemma 2.2 *(Lagrange interpolation formula) Suppose that a, b are a pair of real numbers such that $a < b$, $m \geq 3$ be an odd integer, and $f \in c^m[a,b]$. Furthermore, let h be defined in (7), and f be tabulated at equispaced points, $x_k = \frac{b-a}{2} + kh$. Then for any real number p there exists a real number ξ, $-mh < \xi < mh$, such that*

$$f(x_0 + ph) = \sum_{k=\frac{-(m-1)}{2}}^{\frac{(m-1)}{2}} A_k^m(p) f(x_k) + R_{m-1}, \tag{10}$$

with

$$A_k^m(p) = \frac{(-1)^{\frac{m-1}{2}+k}}{(\frac{m-1}{2}+k)!(\frac{m-1}{2}-k)!(p-k)} \prod_{t=0}^{m-1} (p + \frac{m-1}{2} - t), \tag{11}$$

and

$$R_{m-1} = \frac{1}{m!} \prod_{k=-\frac{m-1}{2}}^{\frac{m-1}{2}} (p-k) h^m f^{(m)}(\xi). \tag{12}$$

Lemma 2.3 *If $f : [a,b] \rightarrow R^1$ is a function satisfying the conditions of Lemma 2.2, and the coefficients $D_{i,k}^m$ are given by the formula*

$$D_{i,k}^m = \frac{\partial^{(2i-1)}}{\partial p^{(2i-1)}} (A_k^m(p)) \mid^{p=0}, \tag{13}$$

then

$$f^{(2i-1)}(x_0) = \sum_{k=-\frac{m-1}{2}}^{\frac{m-1}{2}} \frac{D_{i,k}^m}{h^{2i-1}} f(x_k) + O(h^m), \tag{14}$$

for any m, i such that $-\frac{m-1}{2} \leq k \leq \frac{m-1}{2}$, and $1 \leq k \leq \frac{m-1}{2}$.

Proof. The proof is as an immediate consequence of (10) and (13). □

Lemma 2.4 *Suppose that m, l, k are integers, and the coefficients $a_{k,l}^m$ are defined by the recurrence relation*

$$a_{1,1}^3 = 1, \tag{15-a}$$

$$a_{1,2}^3 = 1, \tag{15-b}$$

$$a_{k,l}^{2k+1} = (k-k^2) a_{k-1,l}^{2k-1} + a_{k-1,l-1}^{2k-1} + a_{k-1,l-2}^{2k-1}, \tag{15-c}$$

$$a_{k,l}^{m+2} = a_{k,l-2}^m - (\frac{m+1}{2})^2 a_{k,l}^m, \tag{15-d}$$

with $a^m_{k,l} = 0$, *for all* $k \le 0$, *or* $l \le 0$, *or* $m \le 1$. *Then*

$$A^m_k(p) = \frac{(-1)^{\frac{m-1}{2}+k}}{(\frac{m-1}{2}+k)!(\frac{m-1}{2}-k)!} \sum_{l=1}^{\frac{m-1}{2}} a^m_{k,l} p^l, \tag{16}$$

for any odd $m \ge 3$, $1 \le k \le \frac{m-1}{2}$ *and* $A^m_k(p)$ *is defined by (11).*

Proof. Due to (11),

$$A^m_k(p) = \frac{(-1)^{\frac{m-1}{2}+k}}{(\frac{m-1}{2}+k)!(\frac{m-1}{2}-k)!} C^m_k(p), \tag{17}$$

where

$$C^m_k(p) = \frac{1}{(p-k)} \prod_{t=0}^{m-1} (p + \frac{m-1}{2} - t). \tag{18}$$

Thus it is sufficient to show that

$$C^m_k(p) = \sum_{l=1}^{\frac{m-1}{2}} a^m_{k,l} p^l. \tag{19}$$

This will be shown by induction. Indeed, if $m = 3$ then, due to (18),

$$C^3_1(p) = p^2 + p, \tag{20}$$

which is equivalent to (15-a),(15-b).
Assume now that for some m, k such that $-\frac{m-1}{2} \le k \le \frac{m-1}{2}$,

$$C^m_k(p) = \sum_{l=1}^{\frac{m-1}{2}} a^m_{k,l} p^l. \tag{21}$$

Combining (18) and (21), we have

$$\begin{aligned} C^{m+2}_k(p) &= (p + \frac{m+1}{2})(p - \frac{m+1}{2}) \sum_{l=1}^{\frac{m-1}{2}} a^m_{k,l} p^l \\ &= (p^2 - (\frac{m+1}{2})^2) \sum_{l=1}^{\frac{m-1}{2}} a^m_{k,l} p^l \\ &= \sum_{l=1}^{\frac{m-1}{2}} a^m_{k,l} p^{l+2} - (\frac{m+1}{2})^2 \sum_{l=1}^{\frac{m-1}{2}} a^m_{k,l} p^l, \end{aligned} \tag{22}$$

which is equivalent to (15-d).
Now, assume that for some k

$$C^{2k+1}_k(p) = \sum_{l=1}^{k} a^{2k+1}_{k,l} p^l. \tag{23}$$

Combining (23) and (18), we have

$$\begin{aligned} C_k^{2k+3}(p) &= (p-k)(p-(k+1))\sum_{l=1}^{k} a_{k,l}^{2k+1} p^l \\ &= (p^2+p-(k^2+k))\sum_{l=1}^{k} a_{k,l}^{2k+1} p^l \\ &= \sum_{l=1}^{k} a_{k,l}^{2k+1} p^{l+2} + \sum_{l=1}^{k} a_{k,l}^{2k+1} p^{l+1} - (k^2+k)\sum_{l=1}^{k} a_{k,l}^{2k+1} p^l, \end{aligned} \tag{24}$$

which is equivalent to (15-c). □

Lemma 2.5 *Suppose that $m \geq 3$ is odd. Then,*

$$D_{i,k}^m = \frac{(-1)^{\frac{m-1}{2}+k}}{(\frac{m-1}{2}+k)!(\frac{m-1}{2}-k)!} a_{k,2i-1}^m (2i-1)!, \tag{25}$$

for any k, i such that $-\frac{m-1}{2} \leq k \leq \frac{m-1}{2}$, and $1 \leq i \leq \frac{m-1}{2}$,

with the coefficients $a_{k,l}^m$ defined by the recurrence relation in Lemma 2.4.

Proof. Substituting (16) into (13), we immediately obtain

$$\begin{aligned} D_{i,k}^m &= \frac{(-1)^{\frac{m-1}{2}+k}}{(\frac{m-1}{2}+k)!(\frac{m-1}{2}-k)!} \frac{\partial^{(2i-1)}}{\partial p^{(2i-1)}} \sum_{l=1}^{m-1} a_{k,l}^m p^l \mid^{p=0} \\ &= \frac{(-1)^{\frac{m-1}{2}+k}}{(\frac{m-1}{2}+k)!(\frac{m-1}{2}-k)!} a_{k,2i-1}^m (2i-1)!. \end{aligned} \tag{26}$$

□

The following six lemmas provide identities which are used in the proof of Theorem 3.1.

Lemma 2.6 *If $k \geq 2$ is an integer and $a_{k,l}^m$ is defined in Lemma 2.4.*

$$\mid (l)! \cdot a_{k,l}^{2k+1} \mid \; < \; \mid (l+2)! \cdot a_{k,l+2}^{2k+1} \mid, \tag{27}$$

for all $l = 1, 2, ..., 2k-3$.

Proof.
If $k = 2$, and $l = 1$ then $\mid (1)! \cdot a_{2,1}^5 \mid = 2$, $\mid (3)! \cdot a_{2,3}^5 \mid = 12$, and therefore (27) is obviously true.
Now, assume that

$$\mid (l)! \cdot a_{k,l}^{2k+1} \mid \; < \; \mid (l+2)! \cdot a_{k,l+2}^{2k+1} \mid, \tag{28}$$

for some $k \geq 2$ and all $l = 1, 2, ..., 2k-3$.
Now, due to (15-a), (15-b), (15-c), and (15-d),

$$(l)! \cdot a_{k+1,l}^{2k+3} = (((k+1)-(k+1)^2) a_{k,l}^{2k+1} + a_{k,l-1}^{2k+1} + a_{k,l-2}^{2k+1}) \cdot (l!), \tag{29}$$

and

$$(l+2)! \cdot a_{k+1,l+2}^{2k+3} = (((k+1)-(k+1)^2)a_{k,l+2}^{2k+1} + a_{k,l+1}^{2k+1} + a_{k,l}^{2k+1}) \cdot (l+2)!. \tag{30}$$

Finally, combining (28), (29), and (30) we easily obtain

$$|\,(l)! \cdot a_{k+1,l}^{2k+3}\,| \;<\; |\,(l+2)! \cdot a_{k+1,l+2}^{2k+3}\,|, \tag{31}$$

for all $l = 1, 2, ..., 2k-1$. □

Lemma 2.7 *If $k \geq 2$ is an integer, and $a_{k,l}^m$ is defined in Lemma 2.4 then*

$$|\,(l)! \cdot a_{k,l}^m\,| \;<\; |\,(l+2)! \cdot a_{k,l+2}^m\,|, \tag{32}$$

for all $m \geq 2k+1$ and $l = 1, 2, ..., 2k-3$.

Proof. Lemma (2.6) establishes the base case, i.e., that (32) is true when $m = 2k+1$. Now, assume that

$$|\,(l)! \cdot a_{k,l}^m\,| \;<\; |\,(l+2)! \cdot a_{k,l+2}^m\,|, \tag{33}$$

for some odd $m \geq 2k+1$, and all $l = 1, 2, ..., 2k-3$.
Now, due to (15-a), (15-b), (15-c), and (15-d),

$$(l)! \cdot a_{k,l}^{m+2} = (a_{k,l-2}^m - (\frac{m+1}{2})^2 a_{k,l}^m) \cdot (l!), \tag{34}$$

and

$$(l+2)! \cdot a_{k,l+2}^{m+2} = (a_{k,l}^m - (\frac{m+1}{2})^2 a_{k,l+2}^m) \cdot (l+2)!. \tag{35}$$

Finally, combining (33), (34), and (35) we easily obtain

$$(l)! \cdot |\,a_{k,l}^{m+2}\,| \;<\; |\,(l+2)! \cdot a_{k+1,l+2}^{m+2}\,|, \tag{36}$$

for all $l = 1, 2, ..., 2k-3$. □

Lemma 2.8 *If m, k are integers such that $m \geq 3$ is odd, and $-\frac{m-1}{2} \leq k \leq \frac{m-1}{2}$, then*

$$|\,(1)! \cdot a_{k,1}^m\,| < |\,(3)! \cdot a_{k,3}^m\,| < |\,(5)! \cdot a_{k,5}^m\,| < ... < |\,(m-2)! \cdot a_{k,m-2}^m\,|. \tag{37}$$

Proof. This Lemma follows directly from Lemma 2.6 and Lemma 2.7 □

Lemma 2.9 *If $m \geq 3$ is odd, then*

$$\frac{(m-1)(m-2)!}{2((\frac{m-1}{2})!)^2} < \frac{(2\pi)^{m-1}}{4}. \tag{38}$$

Proof. If $m = 3$ then obviously $1 < \frac{(2\pi)^2}{4}$.
Now, assume that for some odd $m \geq 3$,

$$\frac{(m-1)(m-2)!}{2((\frac{m-1}{2})!)^2} < \frac{(2\pi)^{m-1}}{4}. \tag{39}$$

Obviously,

$$\frac{(m+1)(m)}{(\frac{(m+1)}{2})^2} = \frac{4m}{(m+1)} < (2\pi)^2, \tag{40}$$

and combining (39) and (40) we obtain

$$\frac{(m+1)(m)}{(\frac{(m+1)}{2})^2}\frac{(m-1)(m-2)!}{2((\frac{m-1}{2})!)^2} < \frac{(2\pi)^{m-1}}{4}(2\pi)^2, \tag{41}$$

which is equivalent to

$$\frac{(m+1)(m)!}{2((\frac{m+1}{2})!)^2} < \frac{(2\pi)^{m+1}}{4}. \tag{42}$$

Now, the conclusion of the lemma is an immediate consequence of (39) and (42). □

Lemma 2.10 *If $m \geq 3$ is odd then*

$$| D^m_{i,k} | < \frac{(2\pi)^{m-1}}{4}, \tag{43}$$

for any k, i such that $-\frac{m-1}{2} \leq k \leq \frac{m-1}{2}$, and $1 \leq i \leq \frac{m-1}{2}$.

Proof. Combining Lemmas 2.5, 2.6, 2.7, and 2.8, it is easy to see that

$$| D^m_{1,k} | < | D^m_{2,k} | < \ldots < | D^m_{\frac{m-1}{2},k} |. \tag{44}$$

Consequently, it is sufficient to show that

$$| D^m_{\frac{m-1}{2},k} | < \frac{(2\pi)^{m-1}}{4}. \tag{45}$$

First we observe that (obviously) for any k such that $-\frac{m-1}{2} \leq k \leq \frac{m-1}{2}$,

$$\frac{k(m-2)!}{(\frac{m-1}{2}+k)!(\frac{m-1}{2}-k)!} < \frac{(m-1)(m-2)!}{2((\frac{m-1}{2})!)^2}. \tag{46}$$

Then, we combine (15-a), (15-b), (15-c), (15-d), and (25) to obtain

$$| D^m_{\frac{m-1}{2},k} | = \frac{k(m-2)!}{(\frac{m-1}{2}+k)!(\frac{m-1}{2}-k)!}. \tag{47}$$

Now, (45) follows immediately from the combination of (46), (47), and Lemma 2.9. □

Lemma 2.11 *For any $l \geq 1$ the Bernoulli number B_{2l} satisfies the inequality*

$$|\frac{B_{2l}}{(2l)!}| < \frac{4}{(2\pi)^{2l}}. \tag{48}$$

Proof. As is well known (see for example, [1]), for any $l \geq 1$

$$B_{2l} = \frac{(-1)^{l-1}2(2l)!}{(2\pi)^{2l}} \sum_{k=1}^{\infty} \frac{1}{k^{2l}}, \tag{49}$$

and

$$\sum_{k=1}^{\infty} \frac{1}{k^{2l}} < 2. \tag{50}$$

Now, the conclusion of the lemma is an immediate consequence of (49) and (50). □

The proof of the following lemma can be found in [5].

Lemma 2.12 *Suppose that $m \geq 1$, $s \in c^m(0,1]$ possesses a finite integral on the interval $[0,1]$, and that $s^{(m)}(x)$ is monotonic in some neighborhood of 0. Then the product $x \cdot s(x)$ is bounded on $[0,1]$. Suppose further that $w \in c^m[0,1]$ is such that $w(0) = w'(0) = w''(0) = ... = w^{(m)}(0) = 0$. Then the function $\psi(x) = s(x) \cdot w(x)$ is defined on the closed interval $[0,1]$, and $\psi(0) = \psi'(0) = \psi''(0) = ... = \psi^{(m)}(0) = 0$.*

3 End-point Corrections for Non-singular Functions

3.1 End-point corrected trapezoidal rules

While the authors have failed to find the contents of this section in the literature, it is an immediate consequence of well-known facts from classical analysis. We present it here for completeness, and because we found the resulting high-order quadrature rules quite useful (see Section 7.1).

Suppose that n, m, are a pair of integers with $m \geq 3$ and odd, and $n \geq 2$. Further, suppose that a, b are a pair of real numbers such that $a < b$, $h = (b-a)/(n-1)$, and $f : [a-mh, b+mh] \rightarrow R^1$ is an integrable function. We define the corrected trapezoidal rule $T^n_{\beta^m}$ for non-singular functions by the formula

$$T^n_{\beta^m}(f) = T_n(f) + h \sum_{k=-\frac{m-1}{2}}^{\frac{m-1}{2}} (f(b+kh) - f(a+kh))\beta^m_k. \tag{51}$$

The real coefficients β^m_k are given by the formula

$$\beta^m_k = \sum_{l=1}^{\frac{m-1}{2}} \frac{D^m_{l,k} B_{2l}}{(2l)!}, \tag{52}$$

where $D^m_{l,k}$ are defined in (13) (also, see (25)) and B_{2l} are the Bernoulli numbers.

We will say that the rule $T^n_{\beta^m}$ is of order m if for any $f \in c^m[a-mh, b+mh]$, there exists a real number $c > 0$ such that

$$| T^n_{\beta^m}(f) - \int_a^b f(x)dx | < \frac{c}{n^m}. \tag{53}$$

Theorem 3.1 *If $m \geq 3$ is an odd integer then for any k such that $-\frac{m-1}{2} \leq k \leq \frac{m-1}{2}$,*

$$| \beta^m_k | < \frac{m-1}{2}, \tag{54}$$

where the coefficients β^m_k are defined in (52).

Proof. Combining Lemma 2.10 and Lemma 2.11 we immediately observe that

$$| \frac{D^m_{l,k} B_{2l}}{(2l)!} | < 1, \tag{55}$$

and hence

$$| \beta^m_k | = \sum_{l=1}^{\frac{m-1}{2}} \frac{D^m_{l,k} B_{2l}}{(2l)!} < \frac{m-1}{2}. \tag{56}$$

□

Remark 3.1 A somewhat more involved argument shows that in fact $|\beta^m_k| < 1$ for all k, m; empirically this can also be seen from the tables in Section 7.1 below. However, for the purposes of this paper (56) is sufficient.

Theorem 3.2 *Suppose that m, n are a pair of integers with $m \geq 3$ and odd, and $n \geq 2$. Further, suppose that a, b are a pair of real numbers such that $a < b$. Then, the end-point corrected trapezoidal rule $T^n_{\beta^m}$ is of order m, i.e., for any $f : [a-mh, b+mh] \to R^1$ such that $f[a-mh, b+mh] \in c^m[a-mh, b+mh]$, there exists a real number $c > 0$ such that*

$$| T^n_{\beta^m}(f) - \int_a^b f(x)dx | < \frac{c}{n^m}. \tag{57}$$

Proof. Combining (52) and (51), we obtain

$$\begin{aligned} T^n_{\beta^m}(f) &= T_n(f) + h \sum_{k=-\frac{m-1}{2}}^{\frac{m-1}{2}} (f(b+kh) - f(a+kh)) \sum_{l=1}^{\frac{m-1}{2}} \frac{D^m_{l,k} B_{2l}}{(2l)!} \\ &= T_n(f) + \sum_{l=1}^{\frac{m-1}{2}} \frac{h^{2l} B_{2l}}{(2l)!} \Big(\sum_{k=-\frac{m-1}{2}}^{\frac{m-1}{2}} \frac{D^m_{l,k}(f(b+kh) - f(a+kh))}{h^{2l-1}} \Big). \end{aligned} \tag{58}$$

Combining (14) and (58), we have

$$T^n_{\beta^m}(f) = T_n(f) + \sum_{l=1}^{\frac{m-1}{2}} \frac{h^{2l} B_{2l}}{(2l)!}(f^{(2l-1)}(b) - f^{(2l-1)}(a) - 2R^{(2l-1)}_{m-1}). \tag{59}$$

Finally, combining (59) with Lemma 2.1, we observe that for some $a < \xi < b$,

$$T^n_{\beta^m}(f) = \int_a^b f(x)dx + 2R^{(2l-1)}_{m-1} + \frac{h^m B_m}{m!} f^m(\xi), \tag{60}$$

and the theorem immediately follows from (60). □

Remark 3.2 It is easy to see that for $m \geq 3$ and odd, and any k such that $-\frac{m-1}{2} \leq k \leq \frac{m-1}{2}$, $D^m_{i,-k} = -D^m_{i,k}$, and $D^m_{i,0} = 0$ (due to (13)), and hence $\beta^m_{-k} = -\beta^m_k$ and $\beta^m_0 = 0$ (due to 52). Now, instead of (51) one could define the end-point corrected trapezoidal rule by the formula

$$T^n_{\beta^m}(f) = T_n(f) + h \sum_{k=1}^{\frac{m-1}{2}} (f(b+kh) - f(b-kh) - f(a+kh) + f(a-kh))\beta^m_k. \tag{61}$$

4 End-point Corrections for Singular Functions

In this section we construct a group of quadrature formulae for end-point singular functions, generalizing the classical end-point corrected trapezoidal rules. The actual values of end-point corrections are obtained for each singularity as a solution of a system of linear algebraic equations. All the rules developed in this section are simple extensions of the corrected trapezoidal rule $T^n_{\beta^m}$ developed in the preceding section.

A right-end corrected trapezoidal rule $T^n_{R\beta^m}$ is defined by the formula

$$T^n_{R\beta^m}(f) = h(\frac{f(x_{n-1})}{2} + \sum_{i=1}^{n-2} f(x_i)) \quad + \quad h \sum_{k=1}^{\frac{m-1}{2}} (f(b+kh) - f(b-kh))\beta^m_k, \tag{62}$$

where $f(0, b+mh] \rightarrow R^1$ is an integrable function, n, m are a pair of natural numbers with $m \geq 3$ and odd, the coefficients β^m_k are given by (52), and

$$\begin{aligned} h &= \frac{b}{n-1}, \\ x_i &= ih. \end{aligned} \tag{63}$$

We will say that the rule $T^n_{R\beta^m}$ is of right-end order $m \geq 3$ if for any $f \in c^{m+1}[0, b+mh]$ such that $f(0)[214z = f'(0) = ... = f^{(m)}(0) = 0$, there exists $c > 0$ such that

$$| T^n_{R\beta^m}(f) - \int_0^b f(x)dx | < \frac{c}{n^m}. \tag{64}$$

It easily follows from Theorem 3.2 that $T^n_{R\beta^m}$ is of right-end order m.
Similarly, a left-end corrected trapezoidal rule $T^n_{L\beta^m}$ is defined by the formula

$$T^n_{L\beta^m}(f) = h(\frac{f(x_{-(n-1)})}{2} + \sum_{i=1}^{n-2} f(x_{-i})) \quad + \quad h\sum_{k=1}^{\frac{m-1}{2}}(-f(-b+kh) + f(-b-kh))\beta^m_k, \qquad (65)$$

where $f[-b-mh, 0) \to R^1$ is an integrable function, n, m are a pair of natural numbers with $m \geq 3$ and odd, the coefficients β^m_k are given by (52), and h, x_i are defined by (63). We will say that the rule $T^n_{L\beta^m}$ is of left-end order $m \geq 3$ if for any $f \in c^{m+1}[-b-mh, 0)$ such that $f(0) = f'(0) = ... = f^{(m)}(0) = 0$, there exists $c > 0$ such that

$$| T^n_{L\beta^m}(f) - \int_{-b}^{0} f(x)dx | < \frac{c}{n^m}. \qquad (66)$$

It also easily follows from Theorem 3.2 that $T^n_{L\beta^m}$ is of left-end order m.

Suppose now that the function $f(-kh, b+mh] \to R^1$ is of the form

$$f(x) = \phi(x)s(x) + \psi(x), \qquad (67)$$

with $\phi, \psi \in c^k(-kh, b+mh]$, and $s \in c(-kh, b+mh]$ an integrable function with a singularity at 0. For a finite sequence $\alpha = (\alpha_{-k}, \alpha_{-(k-1)}, \alpha_{-1}, \alpha_1, ..., \alpha_k)$ and $T^n_{R\beta^m}$ defined in (62), we define the end-point corrected rule $T^n_{\alpha\beta^m}$ by the formula

$$T^n_{\alpha\beta^m}(f) = T^n_{R\beta^m}(f) + h\sum_{j=-k, j\neq 0}^{k} \alpha_j f(x_j), \qquad (68)$$

with $h = b/(n-1)$, $x_j = jh$.
We will use the expression $T^n_{\alpha\beta^m}$ with appropriately chosen α as quadrature formulae for functions of the form (67), and the following construction provides a tool for finding α once $\beta^m = (\beta^m_1, \beta^m_2, ..., \beta^m_{\frac{m-1}{2}})$ is given, so that the rule is of order k, i.e., there exists a $c > 0$ such that

$$| T^n_{\alpha\beta^m}(f) - \int_0^b f(x)dx | < \frac{c}{n^k}. \qquad (69)$$

For a pair of natural numbers k, m, with $k \geq 1$ and $m \geq 3$ and odd, we will consider the following system of linear algebraic equations with respect to the unknowns α^n_j, with $j = 0, \pm 1, \pm 2, ..., \pm k$:

$$\sum_{j=-k, j\neq 0}^{k} x_j^{i-1}\alpha^n_j = \frac{1}{h}\int_0^b x_j^{i-1}dx - T^n_{R\beta^m}(x^{i-1}), \qquad (70)$$

for $i = 1, 2, ..., k$, and

$$\sum_{j=-k, j\neq 0}^{k} x_j^{i-k-1}s(x_j)\alpha^n_j = \frac{1}{h}\int_0^b x_j^{i-k-1}s(x)dx - T^n_{R\beta^m}(x^{i-k-1}s(x)), \qquad (71)$$

for $i = k+1, k+2, ..., 2k$, with $h = b/(n-1)$, $x_j = jh$ and $T^n_{R\beta^m}$ defined by (62). We denote the matrix of the system (70), (71) by A^{nk}_s, its right-hand side by Y^{nk}_s and its solution by $\alpha_n = (\alpha^n_{-k}, \alpha^n_{-(k-1)}, ..., \alpha^n_{-1}, \alpha^n_1, ..., \alpha^n_k)$. The use of expressions $T^n_{\alpha^n\beta^m}$ as quadrature formulae for functions of the form (67) is based on the following theorem.

Theorem 4.1 *Suppose that a function $s : (-kh, b+mh] \to R^1$ is such that $s \in c^k(-kh, b+mh]$ and s^k is monotonic on either side of 0. Suppose further that the systems (70), (71) have solutions $(\alpha^n_{-k}, \alpha^n_{-(k-1)}, \alpha^n_{-1}, \alpha^n_1, ..., \alpha^n_k)$ for all sufficiently large n, and that the sums*

$$\sum_{j=-k, j\neq 0}^{k} (\alpha^n_j)^2 \tag{72}$$

are bounded uniformly with respect to n. Finally, suppose that the function $f : (-kh, b+mh] \to R^1$ is defined by (67). Then, there exists a real $c > 0$ such that

$$| T^n_{\alpha^n\beta^m}(f) - \int_a^b f(x)dx | < \frac{c}{n^k} \tag{73}$$

for all sufficiently large n.

Proof. Applying the Taylor expansion to the function f at $x = 0$ we obtain

$$f(x) = P(f)(x) + R_k(\phi)(x)s(x) + R_k(\psi), \tag{74}$$

where

$$P(f)(x) = s(x)\sum_{i=0}^{k} \frac{\phi^{(i)}(0)}{(i!)} x^i + \sum_{i=0}^{k} \frac{\psi^{(i)}(0)}{i!} x^i, \tag{75}$$

and $R_k(\phi), R_k(\psi)$ are such functions $[-kh, b+mh] \to R^1$ that

$$R'_k(\phi)(0) = R''_k(\phi)(0) = ... = R^{(k)}_k(\phi)(0) = 0, \tag{76}$$

$$R'_k(\psi)(0) = R''_k(\psi)(0) = ... = R^{(k)}_k(\psi)(0) = 0. \tag{77}$$

Substituting (74) into (73), we obtain

$$\begin{aligned} | T^n_{\alpha^n\beta_m}(f) - \int_0^b f(x)dx | \quad \leq \quad & | T^n_{\alpha^n\beta_m}(P(f)) - \int_0^1 P(f)(x)dx | + \\ | T^n_{\alpha^n\beta_m}((R_k(\phi)\cdot s) + R_k(\psi)) - \int_0^b & ((R_k(\phi(x))s(x))(x) + R_k(\psi(x)))dx | . \end{aligned} \tag{78}$$

Due to (70), (71)

$$T^n_{\alpha^n\beta_m}(P(f)) - \int_0^1 P(f)(x)dx = 0, \tag{79}$$

and we have

$$\begin{aligned} | T^n_{\alpha^n\beta_m}(f) - \int_0^b f(x)dx | \leq \\ | RT^n_{\beta_m k}(s \cdot R_k(\phi)) - \textstyle\int_0^b (s \cdot R_k(\phi))(x)dx | \\ + \quad | RT^n_{\beta_m k}(R_k(\psi)) - \textstyle\int_0^b (R_k(\psi))(x)dx | \\ + \quad | \textstyle\sum_{j=1}^{2k} (R_k(\phi)(jh)s(jh)\alpha_j^n) + (R_k(\psi)(jh)\alpha_j^n) | . \end{aligned} \tag{80}$$

Due to (77) and (64), there exists $c_1 > 0$ such that

$$| RT^n_{\beta_m k}(R_k(\psi)) - \int_0^b (R_k(\psi))(x)dx | < \frac{c_1}{n^k}. \tag{81}$$

Combining (76), (64), and Lemma 2.12 we conclude that for some $c_2 > 0$

$$| RT^n_{\beta_m k}(s \cdot R_k(\phi)) - \int_0^b (s \cdot R_k(\phi))(x)dx | < \frac{c_2}{n^k}. \tag{82}$$

Finally, combining (76), (77) and Lemma 2.12 we conclude that for some $c_3 > 0$,

$$| \sum_{j=-k, j\neq 0}^{k} (R_k(\phi)(jh)s(jh)\alpha_j^n) + (R_k(\psi)(jh)\alpha_j^n) | < \frac{c_3}{n^k}. \tag{83}$$

Now, the conclusion of the theorem follows from the combination of (81), (82), and (83). □

4.1 Convergence Rates for Singularites of the forms $|x|^\lambda$ and $log(|x|)$

For the remainder of the paper, $\phi_1, \phi_2, ..., \phi_{2k}$ will denote functions $(-kh, b+mh] \to R^1$ defined by the formulae

$$\phi_i(x) = x^{i-1}, \tag{84}$$

for $i = 1, 2, ..., k$, and

$$\phi_i(x) = x^{i-k-1}s(x), \tag{85}$$

for $i = k+1, k+2, ..., 2k$. The following lemma is a particular case of a well-known general fact proven, for example, in [8].

Lemma 4.2 *If $s(x) = x^\lambda$ with λ a real number such that $0 < |\lambda| < 1$, then the functions $\phi_1, \phi_2, ..., \phi_{2k}$ constitute a Chebyshev system on the interval $(-kh, b+mh]$ (i.e., the determinant of the $2k \times 2k$ matrix B_{ij} defined by the formula $B_{ij} = \phi_i(t_j)$ is non-zero for any $2k$ distinct points on the interval $(-kh, b+mh]$).*

Theorem 4.3 *If $s(x) = |x|^\lambda$ with $0 < |\lambda| < 1$, then the convergence rate of the quadrature rule $T^n_{\alpha^n\beta_m}$ is at least k.*

Proof. It immediately follows from Lemma 4.2 that the matrix of the system (70), (71) is non-singular. We rescale the system (70), (71) by multiplying its ith equation by $\frac{1}{h^{i-1}}$, for $i = 1, 2, ..., k$, and by $\frac{1}{h^{i-1-k+\lambda}}$, for $i = k+1, k+2, ..., 2k$, obtaining the system of equations

$$\sum_{j=-k, j\neq 0}^{k} j^{i-1}\alpha_k^n = \frac{1}{h^i}\left(\int_0^b x^{i-1}dx - T^n_{R\beta^m}(x^{i-1})\right), \tag{86}$$

$i = 1, 2, ..., k$, and

$$\sum_{j=-k, j\neq 0}^{k} j^{i-k-1+\lambda}\alpha_k^n = \frac{1}{h^{i-k+\lambda}}\left(\int_0^b x^{i-k-1+\lambda}dx - T^n_{R\beta^m}(x^{i-k-1+\lambda})\right), \tag{87}$$

for $i = k+1, k+2, ..., 2k$.
We will denote the matrix of the system (86), (87) by B_k, and its right hand side by Z_k^n. Obviously, B_k is independent of n, and using Theorem 3.2 we observe that if $m > k$ then $|Z_k^n|$ is bounded uniformly with respect to n. Now, due to Theorem 4.1, the convergence rate of $T^n_{\alpha^n\beta^m}$ is at least k. □

The proof of Theorem 4.3 can be repeated almost verbatim with $s(x) = log(|x|)$, instead of $s(x) = |x|^\lambda$, resulting in the following theorem.

Theorem 4.4 *If $s(x) = log(|x|)$ then the convergence rate of the quadrature rule $T^n_{\alpha^n\beta_m}$ is at least k.*

4.2 Asymptotic behaviour of correction coefficients as $n \to \infty$

An obvious drawback of the expressions $T^n_{\alpha\beta^m}$ as practical quadrature rules is the fact that the weights $\alpha^n = (\alpha^n_{-k}, ..., \alpha^n_{-1}, \alpha^n_1, ..., \alpha^n_k)$ have to be determined for each value of n by solving a system of linear algebraic equations. For singularities of the form $s(x) = log(|x|)$, $s(x) = |x|^\lambda$ we eliminate this problem by constructing a new set of quadrature weights $\gamma = (\gamma_{-k}, \gamma_{-(k-1)}, ..., \gamma_{-1}, \gamma_1, ..., \gamma_k)$, independent of n, and such that the quadrature rules $T^n_{\gamma^k\beta^m}$ are still of order not less than k.

Lemma 4.5 *Suppose that $\beta = (\beta_1^m, \beta_2^m, ..., \beta^m_{\frac{m-1}{2}})$ is such that the right-hand order of the quadrature formula $T^n_{R\beta^m}$ is m: Further, let $z > 0$ be some real number. Then for any integers p, q such that $p < q$,*

$$\left|\frac{1}{h_p^{z+1}}(T^p_{R\beta^m}(x^z) - \int_0^b x^z dx) - \frac{1}{h_q^{z+1}}(T^q_{R\beta^m}(x^z) - \int_0^b x^z dx)\right| = O(h_p^{m-z-1}), \tag{88}$$

where $h_p = b/(p-1)$, and $h_q = b/(q-1)$.

Proof. Due to Theorem 3.2, there exist real $c_1, c_2 > 0$ such that

$$(T^p_{R\beta^m}(x^z) - \int_0^b x^z dx) = c_1 h_p^m - h_p \sum_{j=-k}^{k} (jh_p)^z, \tag{89}$$

and

$$(T^q_{R\beta^m}(x^z) - \int_0^b x^z dx) = c_2 h_q^m - h_q \sum_{j=-k}^{k} (jh_q)^z. \tag{90}$$

Now, combining (89), (90) we obtain

$$\begin{aligned}
&| \tfrac{1}{h_p^{z+1}}(T^p_{R\beta^m}(x^z) - \textstyle\int_0^b x^z dx) - \tfrac{1}{h_q^{z+1}}(T^q_{R\beta^m}(x^z) - \textstyle\int_0^b x^z dx) | \\
&= \frac{1}{h_p^{z+1}}(c_1 h_p^m - h_p \sum_{j=-k}^{k} (jh_p)^z) - \frac{1}{h_q^{z+1}}(c_2 h_q^m - h_q \sum_{j=-k}^{k} (jh_q)^z) \\
&= (c_1 h_p^{m-z-1} - \sum_{j=-k}^{k} (j)^z) - (c_2 h_q^{m-z-1} - \sum_{j=-k}^{k} (j)^z) \\
&= c_1 h_p^{m-z-1} - c_2 h_q^{m-z-1} \\
&= O(h_p^{m-z-1}).
\end{aligned} \tag{91}$$

□

Theorem 4.6 *Suppose that k, m are two natural numbers such that $k \leq m-1$ and that $\beta = (\beta_1^m, \beta_2^m, ..., \beta_{\frac{m-1}{2}}^m)$ is such that the right-hand order of the quadrature $T_{R\beta^m}$ is m. Suppose further that $s(x) = |x|^\lambda$ with $0 \leq | \lambda | \leq 1$, and that the coefficients $(\alpha_{-k}^n, \alpha_{-(k-1)}^n, \alpha_{-1}^n, \alpha_1^n, ..., \alpha_k^n)$ are the solutions of the system (70),(71). Then*

1) There exists a limit

$$lim_{n\to\infty} \alpha_i^n = \gamma_i, \tag{92}$$

for each $i = 1, 2, ..., 2k$.
2) For all $i = 1, 2, ..., 2k$,

$$| \alpha_i^n - \gamma_i | = O(\frac{1}{n^{m-k}}). \tag{93}$$

3) γ_i do not depend on m, as long as $m \geq k+1$.
4) The quadrature formulae $T^n_{\gamma\beta^m}$ are of order at least k.

Proof. Suppose that p, q are two natural numbers, and $p < q$. Obviously,

$$\begin{aligned}
\alpha^p &= (B_k)^{-1} Z_k^p, \\
\alpha^q &= (B_k)^{-1} Z_k^q, \\
\alpha^p - \alpha^q &= (B_k)^{-1}(Z_k^p - Z_k^q).
\end{aligned} \tag{94}$$

Due to Lemma 4.5, there exists $c > 0$ such that

$$||Z_k^p - Z_k^q|| < \frac{c}{p^{m-k}}. \tag{95}$$

and by combining (94), (95), we see that for some $d > 0$

$$||\alpha^p - \alpha^q|| < \frac{d}{p^{m-k}}. \tag{96}$$

Since the weights α^n constitute a Cauchy sequence, they converge to some limit $\gamma = (\gamma_{-k}, \gamma_{-(k-1)}, ..., \gamma_{-1}, \gamma_1, ..., \gamma_k)$, which proves 1, and 2, 3, 4 follow easily. □
The proof of the following theorem is a repetition, almost verbatim, of the proofs of the Lemma 4.5 and Theorem 4.6

Theorem 4.7 *If under the conditions of Theorem 4.6 we replace $s(x) = |x|^\lambda$ with $s(x) = log(|x|)$, conclusions 1-4 remain correct.*

For singularities of the form $|x|^\lambda$ and $log(|x|)$, Theorem 4.6 and 4.7 reduce the quadratures $T^n_{\alpha\beta^m}$ to the more "conventional" form

$$\int_0^b f(x)dx \approx T^n_{\gamma^k\beta^m}(f) = T^n_{R\beta^m}(f) + h\sum_{j=-k, j\neq 0}^{k} \gamma_j f(x_j). \tag{97}$$

Remark 4.1 The whole theory in sections 4.1-4.2 has been constructed for functions with a singularity at the left end of the interval. Obviously, an identical theory holds for functions with a singularity at the right end of the interval. However, in all formulae the expression $T^n_{R\beta^m}$ has to be replaced with $T^n_{L\beta^m}$ (see (62), (65)).

4.3 Central Corrections for Singular Functions

In this section, we will be considering functions $f[-b-mh, 0) \cup (0, b+mh] \to R^1$ of the form

$$f(x) = \phi(x)s(x) + \psi(x), \tag{98}$$

with $\phi, \psi \in c^l[-b-mh, b+mh]$, and $s \in c[-b-mh, 0) \cup (0, b+mh]$ an integrable function with a singularity at 0. We will define the central-point corrected trapezoidal rule

$$T^n_{\mu^n\beta^m}(f) = T^n_{R\beta^m}(f) + T^n_{L\beta^m}(f) + h\sum_{j=1}^{l} \mu^n_j(f(x_j) + f(x_{-j})), \tag{99}$$

with h, x_j defined by(63), β^m_i defined by (52), $T^n_{R\beta^m}$, $T^n_{L\beta^m}$ defined by (62) and (65) respectively, and $\mu^n = (\mu^n_1, \mu^n_2, ..., \mu^n_l)$ an arbitrary sequence of length l.
We will use the expression $T^n_{\mu^n\beta^m}$ with appropriately chosen μ^n as quadrature formulae for functions of the form (98), and the following construction provides a tool for finding μ^n once β^m is given, so that the rule is of order $2l$, i.e., there exists some $c > 0$ such that

$$| T^n_{\mu^n\beta^m}(f) - \int_{-b}^{b} f(x)dx | < \frac{c}{n^{2l}}. \tag{100}$$

For a pair of natural numbers l, m, we will consider the following system of linear algebraic equations with respect to the unknowns μ_j^n:

$$\sum_{j=1}^{l} x_j^{2i-2}\mu_j^n = \int_{-b}^{b} x^{2i-2}dx - T^n_{R\beta^m}(x^{2i-2}) - T^n_{L\beta^m}(x^{2i-2}), \tag{101}$$

for $i = 1, 2, ..., l$, and

$$\sum_{j=1}^{l} x_j^{2i-2-2l}s(x_j)\mu_j^n = \int_{-b}^{b} x^{2i-2-2l}s(x)dx - T^n_{R\beta^m}(x^{2i-2-2l}s(x)) - T^n_{L\beta^m}(x^{2i-2-2l}s(x)), \tag{102}$$

for $i = l+1, l+2, ..., 2l$, with $h = b/(n-1)$, $x_j = jh$.
The proofs of Theorem 4.8, 4.9, and 4.10 are almost identical to those of Theorems 4.1, 4.3, and 4.6 respectively, and are thus stated below without proof.

Theorem 4.8 *Suppose that a function $s : [-b - mh, 0) \cup (0, b + mh] \to R^1$ is such that $s \in c^l[-b - mh, 0) \cup (0, b + mh]$ and s^l is monotonic on either side of 0. Suppose further that the systems (101), (102) have solutions $(\mu^n_{-l}, \mu^n_{-(l-1)}, \mu^n_{-1}, \mu^n_1, ..., \mu^n_l)$ for all sufficiently large n, and that the sums*

$$\sum_{j=-l, j\neq 0}^{l} (\mu_l^n)^2 \tag{103}$$

are bounded uniformly with respect to n. Finally, suppose that the function $f : [-b - mh, 0) \cup (0, b + mh] \to R^1$ is defined by (98). Then, there exists such $c > 0$ that

$$| T^n_{\mu^n\beta^m}(f) - \int_a^b f(x)dx | < \frac{c}{n^{2l}} \tag{104}$$

for all sufficiently large n.

Theorem 4.9 *If $s(x) = |x|^\lambda$ with $0 < |\lambda| < 1$, or $s(x) = log(|x|)$, then the convergence rate of the quadrature rule $T^n_{\mu^n\beta_m}$ is at least $2l$.*

Theorem 4.10 *Suppose that k, m are two natural numbers such that $k \leq m - 1$ and that $\beta = (\beta_1^m, \beta_2^m, ..., \beta^m_{\frac{m-1}{2}})$ is such that the right-end order of the quadrature $T_{R\beta^m}$ is m, and the left-end order of the quadrature $T_{L\beta^m}$ is m. Suppose further that $s(x) = |x|^\lambda$, $0 \leq | \lambda | \leq 1$, or $s(x) = log(|x|)$, and that the coefficients $(\mu^n_{-k}, \mu^n_{-(k-1)}, \mu^n_{-1}, \mu^n_1, ..., \mu^n_k)$ are the solutions of the system (70),(71). Then*

1) There exists a limit

$$lim_{n\to\infty}\mu_i^n = \mu_i, \tag{105}$$

for each $i = 1, 2, ..., 2k$.
2) For all $i = 1, 2, ..., 2k$,

$$| \mu_i^n - \mu_i | = O(\frac{1}{n^{m-l}}). \tag{106}$$

3) μ_i do not depend on m, as long as $m \geq l + 1$.
4) The quadrature formulae $T^n_{\mu\beta^m}$ are of order at least $2l$.

For singularities of the form $|x|^\lambda$ and $log(|x|)$, the Theorem 4.10 reduces the quadrature to the more "conventional" form

$$\int_{-b}^{b} f(x)dx \approx T^n_{\mu\beta^m}(f) = T^n_{R\beta^m}(f) + T^n_{L\beta^m}(f) + \sum_{j=1}^{l} \mu_j (f(x_j) + f(x_{-j})). \tag{107}$$

4.4 Central Corrections for Singular Functions $f(x) = \phi(x)s(x)$

In this section we construct a quadrature formula specifically for the purpose of approximating definite integrals of functions of the form

$$f(x) = \phi(x)s(x), \tag{108}$$

where $\phi(x) : c^p[-b - mh, b + mh] \to R^1$, and $s \in c[-b - mh, 0) \cup (0, b + mh]$ an integrable function with a singularity at 0. For a finite sequence $\rho = (\rho_0, \rho_1, \rho_2, ..., \rho_p)$, and $T_{R\beta^m}$, $T_{L\beta^m}$ defined in (62) and (65) respectively, we define the corrected trapezoidal rule $T^n_{\rho^n\beta^m}$ by the formula

$$T^n_{\rho^n\beta^m}(f) = T^n_{R\beta^m}(f) + T^n_{L\beta^m}(f) + h\sum_{j=0}^{p} \rho^n_j(\phi(jh) + \phi(-jh))). \tag{109}$$

For integers n, m, p where $n \geq 2$, $p \geq 1$, $m \geq 3$ and odd, we will consider the following system of equations with respect to the unknowns $\rho^n = (\rho^n_0, \rho^n_1, \rho^n_2, ..., \rho^n_p)$:

$$\sum_{j=0}^{p} x_j^{2i-2}\rho^n_j = \frac{1}{h}\int_{-b}^{b} (x^{2i-2}s(x))dx - T^n_{R\beta^m}(x^{2i-2}s(x)) - T^n_{L\beta^m}(x^{2i-2}s(x)), \tag{110}$$

where, $h = b/(n-1)$, $x_j = jh$, and $i = 1, 2, ..., p+1$.
The proof of the following theorem is almost identical to the proof of Theorem 4.1.

Theorem 4.11 *Suppose that $n > 2$ is an integer, and h, x_i are defined by (63). Further, suppose that $f(x) = \phi(x)s(x)$ where $\phi : [-b - mh, b + mh] \to R^1$, and $s \in c[-b - mh, 0) \cup (0, b + mh]$ is an integrable function with a singularity at 0. Finally, suppose that the system of equations (110) has a solution $(\rho^n_0, \rho^n_1, ..., \rho^n_p)$ for any sufficiently large n and that the sums $\sum_{j=0}^{p}(\rho^n_j)^2)$ are bounded uniformly with respect to n. Then there exists a real $c > 0$ such that*

$$|\, T^n_{\rho^k h}(f) - \int_{-b}^{b} f(x)dx \,| < \frac{c}{n^{2p}}. \tag{111}$$

The proof of the following theorem is almost identical to that of Theorem 4.6, and is omitted.

Theorem 4.12 *Suppose that $s(x) = log(|x|)$. Then for all $n \geq 2p$, the system (110) has a solution $\rho^n = (\rho^n_0, \rho^n_1, \rho^n_2, ..., \rho^n_p)$, and*

$$\rho_0 = \frac{1}{h}\int_{-b}^{b} log(|x|)dx - T^n_{R\beta^m} log(|x|) - T^n_{L\beta^m} log(|x|) - \sum_{j=1}^{p} \rho_j. \tag{112}$$

Furthermore, there exist such real numbers $\rho_1, \rho_2, ..., \rho_p$ *and a real* $d > 0$ *such that*

$$lim_{n\to\infty}\rho_j^n = \rho_j, \tag{113}$$

and

$$| \rho_j^n - \rho_j | < d \cdot h^{m-p} \tag{114}$$

for all $j = 1, 2, ..., p$. *Finally, there exists a real* c_0 *such that*

$$| \rho_0^n - (c_0 + 0.5log(h) - \sum_{j=1}^{p} \rho_j | < d \cdot h^{m-p} \tag{115}$$

for all $n \geq 2p$.

Remark 4.2 Formulae (114), (115) indicate that for sufficiently large m, the convergence of $\rho_1^n, \rho_2^n, ..., \rho_p^n$ to $\rho_1, \rho_2, ..., \rho_p$ is virtually instantaneous, and that (115) is a nearly perfect approximation to ρ_0^n. The numerical values of $\rho_1, \rho_2, ..., \rho_p$ can be found for various values of p in Section 7.4. Also, note that c_0 does not depend on p, and its numerical value (to 16 digits) is $-.9189385332046727$.

The proof of the following theorem is similar to the proof of Theorem 4.6.

Theorem 4.13 *Suppose that* $s(x) = |x|^\lambda$, *with* λ *a real number such that* $0 < |\lambda| < 1$, *and (110) has a solution* $\rho^n = (\rho_0^n, \rho_1^n, \rho_2^n, ..., \rho_p^n)$. *Then for all* $n > 2p$, *the quadrature weights* $\rho_0^n, \rho_1^n, \rho_2^n, ..., \rho_p^n$ *are independent of* n.

4.5 Corrected trapezoidal rules for other singularities

In the preceding sections quadrature formulae are provided for singular functions of the form

$$f(x) = \phi(x)s(x) + \psi(x), \tag{116}$$

and

$$f(x) = \phi(x)s(x), \tag{117}$$

where the singularity $s(x)$ is of the form $log(|x|)$, or x^λ $(0 < |\lambda| < 1)$. Obviously the procedure developed in the preceding sections can be applied to other singularities. As an example, we construct a quadrature formula to approximate the definite integral,

$$\int_{-a}^{a} f(x)dx, \tag{118}$$

where f is of the form (117),

$$s(x) = \frac{1}{\sqrt{a^2 - x^2}}, \tag{119}$$

with $a > 0$, and $\phi(x) \in c^k[-a - kh, a + kh]$ and even (i.e., $\phi(-x) = \phi(x)$).

Remark 4.3 The choice of the singularity (119) is dictated by the frequency with which it is encountered in the numerical solution of partial differential equations, in signal processing, and other areas. Otherwise, almost any integrable, monotone singularity could have been chosen.

We define the corrected trapezoidal rule $T^n_{\nu^n}$ by the formula

$$T^n_{\nu^n}(f) = \sum_{j=-(n-2)}^{n-2} f(x_j) + h\sum_{i=1}^{k} \nu_i^n f(y_i), \tag{120}$$

where $h = a/(n-1)$, $x_j = jh$, $y_i = a - hi$ for $1 \le i \le k/2$, and $y_i = a + h(i - k/2)$ for $k/2 + 1 \le i \le k$. We will use the expression $T^n_{\nu^n}$ with appropriately chosen ν^n as quadrature formulae for functions of the form (117), and the following construction provides a tool for finding ν^n, so that the rule is of order $2k-2$, i.e., there exists a real $c > 0$ such that

$$\mid T^n_{\nu^n}(f) - \int_{-a}^{a} f(x)dx \mid < \frac{c}{n^{2k-2}}. \tag{121}$$

For an even integer $k \ge 2$, we will consider the following system of linear algebraic equations with respect to the unknowns ν_j^n, with $j = 1, 2, ..., k$:

$$\sum_{j=1}^{k} \frac{y_j^{2(i-1)}}{\sqrt{a^2 - x^2}} \nu_j^n = \int_{-a}^{a} \frac{x^{2(i-1)}}{\sqrt{a^2 - x^2}} dx - \sum_{l=-(n-2)}^{n-2} \left(\frac{x_l^{2(i-1)}}{\sqrt{a^2 - x_l^2}}\right), \tag{122}$$

with $h = \frac{a}{n-1}$, $x_j = jh$, $y_j = a - hj$ for all $1 \le j \le k/2$, and $y_j = a + h(j - k/2)$ for all $k/2 + 1 \le j \le k$. It is easy to see that the linear system (122) is independent of the length of the interval a, and the unknowns $\nu_1^n, \nu_2^n, ..., \nu_k^n$ can be determined by solving the system of equations

$$\sum_{j=1}^{k} \frac{y_j^{2(i-1)}}{\sqrt{1 - x^2}} \nu_j^n = \int_{-1}^{1} \frac{x^{2(i-1)}}{\sqrt{1 - x^2}} dx - \sum_{l=-(n-2)}^{n-2} \left(\frac{x_l^{2(i-1)}}{1 - x_l^2}\right), \tag{123}$$

with $h = \frac{1}{n-1}$, $x_j = jh$, $y_j = 1 - hj$ for all $1 \le j \le k/2$, and $y_j = 1 + h(j - k/2)$ for all $k/2 + 1 \le j \le k$.
The proof of the following theorem is quite similar to the proof of Theorem 4.1, and is omitted.

Theorem 4.14 *Suppose that for some $a > 0$, $f(x) = \frac{\phi(x)}{\sqrt{(a^2 - x^2)}}$ with $\phi \in c^k[-a - kh, a + kh]$. Then there exists such $c > 0$ that*

$$\mid T^n_{\nu^n}(f) - \int_{-a}^{a} f(x)dx \mid < \frac{c}{n^{2k-2}} \tag{124}$$

for all sufficiently large n.

The authors have been unable to construct a quadrature rule for singularities of the form (119), which is independent of the number n of points used in the uncorrected trapezoidal rule. However, this is a relatively minor deficiency since the weights in such cases can be precomputed and stored.

5 Numerical Results

Algorithms have been implemented for the construction of the quadratures $T^n_{\beta^m}$, $T^n_{\gamma^k\beta^m}$, $T^n_{\mu^k\beta^m}$, $T^n_{\rho^k\beta^m}$, and $T^n_{\nu^n}$.

The correction coefficients β^m are calculated using (25), and (52). In the tables in Section 7.1 the correction coefficients for orders of convergence upto 43 are tabulated. In Table 1, convergence results are presented for some of the rules $T^n_{\beta^m}$. Column 1 of this table contains the number of nodes discretizing the interval $[0,1]$ was discretized. In column 2 are the relative errors of the standard 1-sided 4th order corrected trapezoidal rule, given here for comparison. Columns 3-9 contain the relative errors for the rule $T^n_{\beta^m}$ for various orders of convergence m. In all cases the integrand was of the form

$$f(x) = \sin(200x) + \cos(201x). \tag{125}$$

The quadrature weights for the rules $T^n_{\gamma^k\beta^m}$, $T^n_{\mu^k\beta^m}$, $T^n_{\rho^k\beta^m}$, and $T^n_{\nu^n}$ are all obtained as solutions of linear systems, and it is easy to see that the linear systems used for determining these weights (see, for example (70), (71)) are very ill-conditioned. In order to combat the high condition number, all systems were solved using the mathematical package MAPLE using 200 significant digits.

In order to evaluate the coefficients γ for singularities of the form $s(x) = |x|^\lambda$ or $s(x) = log(|x|)$, we start with the right-end corrected trapezoidal rule $T^n_{\beta^m}$ of order 40. Under these conditions,

$$| \alpha^n_i - \gamma_i | < O(\frac{1}{n^{40-k}}) \tag{126}$$

for all $-k \leq i \leq k, k \neq 0$ (see Theorem 4.6) and for reasonable k, the convergence of α^n_i to γ_i is almost instantaneous. The construction of the quadrature weights μ_i is performed in a similar manner. In Section 7.2 the coefficients γ_i are listed for the singularities $log(|x|)$, $|x|^{\frac{1}{2}}$, $|x|^{-\frac{1}{2}}$, $|x|^{\frac{1}{3}}$, $|x|^{-\frac{1}{3}}$, $|x|^{-\frac{1}{9}}$ and for the same singularities, the quadrature weights μ_i are listed in Section 7.3. In Table 2, convergence results are presented for some of the rules $T^n_{\gamma^k\beta^m}$ for various singularities. Column 1 of this table contains the number of nodes in the discretization of the interval $[0,1]$. In Table 3, convergence results are presented for some of quadrature rules $T^n_{\mu^k\beta^m}$ for various singularities. Column 1 of this table contains the number of nodes in the discretization of the interval $[-1,1]$. In all cases the integrand was of the form

$$f(x) = (\sin(20x) + \cos(21x)) + (\sin(23x) + \cos(22x))s(x), \tag{127}$$

and the order of convergence used was 10.

Finally, algorithms have been implemented for evaluating quadratures $T^n_{\rho^p h}$, to integrate functions of the form

$$f(x) = \phi(x)log(|x|). \tag{128}$$

The quadrature weights are obtained by solving the linear system (110). Note that the quadrature weights are independent of the discretization h, except for the first weight ρ_0 which is calculated using the formula (115). Presented in Table 4 are convergence results for integrating functions of the form (128) where,

$$\phi(x) = \sin(200x) + \cos(201x). \tag{129}$$

Column 1 shows the number of nodes in the discretization of the interval $[-1, 1]$. Columns 3-6 show the relative errors for the various orders of convergence m as shown.

Table 1: Convergence of quadrature rules $T^n_{\beta m}$ for non-singular functions

N	k=4	m=3	m=9	m=15	m=21	m=27	m=33	m=39
20	.230E-01	.112E-01	.131E-01	.136E-01	.138E-01	.138E-01	.138E-01	.138E-01
40	.132E-01	.120E-01	.122E-01	.122E-01	.122E-01	.122E-01	.122E-01	.122E-01
80	.457E-02	.108E-02	.654E-03	.430E-03	.292E-03	.202E-03	.142E-03	.100E-03
160	.216E-03	.804E-04	.223E-05	.743E-07	.264E-08	.972E-10	.365E-11	.139E-12
320	.310E-05	.522E-05	.292E-08	.199E-11	.116E-14	.304E-15	.306E-15	.306E-15
640	.191E-06	.328E-06	.304E-11	.105E-15	.703E-16	.703E-16	.703E-16	.703E-16
1280	.239E-07	.205E-07	.266E-14	.345E-15	.346E-15	.346E-15	.346E-15	.346E-15

Table 2: Convergence of quadrature rules $T^n_{\gamma^k \beta m}$ for singular functions (10th order)

N	$log(\|x\|)$	$\|x\|^{\frac{1}{2}}$	$\|x\|^{\frac{-1}{2}}$	$\|x\|^{\frac{1}{3}}$	$\|x\|^{\frac{-1}{3}}$
40	0.29128E-03	0.25056E-04	0.11650E-02	0.42510E-04	0.53715E-03
80	0.72599E-07	0.30493E-07	0.98819E-06	0.53217E-07	0.52449E-06
160	0.56928E-10	0.17499E-10	0.10903E-08	0.32715E-10	0.49582E-09
320	0.65586E-13	0.59119E-14	0.76827E-12	0.12962E-13	0.31491E-12
640	0.18596E-14	0.16376E-14	0.66613E-15	0.17208E-14	0.13878E-14

Table 3: Convergence of quadrature rules $T^n_{\mu^k \beta m}$ for singular functions (10th order)

N	$log(\|x\|)$	$\|x\|^{\frac{1}{2}}$	$\|x\|^{\frac{-1}{2}}$	$\|x\|^{\frac{1}{3}}$	$\|x\|^{\frac{-1}{3}}$
40	0.57489E-03	0.49592E-04	0.23137E-02	0.84150E-04	0.10655E-02
80	0.14438E-06	0.60500E-07	0.19680E-05	0.10563E-06	0.10436E-05
160	0.11348E-09	0.34867E-10	0.21762E-08	0.65197E-10	0.98921E-09
320	0.13357E-12	0.13614E-13	0.15360E-11	0.28103E-13	0.62927E-12
640	0.61062E-15	0.16237E-14	0.42188E-14	0.16237E-14	0.50515E-14

Table 4: Convergence of the quadrature rule $T^n_{\rho^k \beta m}$ for functions $f(x) = \phi(x) log(|x|)$

N	m=3	m=9	m=15	m=21	m=27	m=33	m=39
40	.546E-01	.536E-01	.536E-01	.536E-01	.536E-01	.536E-01	.536E-01
80	.291E-03	.764E-03	.265E-03	.129E-03	.640E-04	.300E-04	.107E-04
160	.282E-03	.241E-04	.209E-05	.255E-08	.482E-09	.125E-11	.143E-13
320	.437E-04	.190E-04	.912E-06	.392E-09	.162E-09	.294E-12	.147E-14
640	.573E-05	.315E-05	.468E-06	.166E-07	.108E-09	.583E-13	.119E-14

6 Generalizations and Conclusions

A group of algorithms has been presented for the construction of high-order corrected trapezoidal rules for functions with various types of singularities, both end-point and in the middle of the interval of integration. In many cases, the corrected rule can have effectively an arbitrarily high order, without the attendent growths of correction weights. The drawback of the approach is the need for the integrand to be available in a small area outside the interval of integration, whenever the singularity being corrected is on one of the ends of that interval.
The algorithm of the present paper admits several straightforward generalizations.

1. There are classes of singularities not covered by this paper for which some versions of Theorem 4.1 can be fairly easily proven.
2. The quadratures can be easily modified to handle functions of the form

$$f(x) = \psi(x) + \sum_{i=1}^{m} \phi_i(x) \cdot s_i(x), \tag{130}$$

where ψ, ϕ_1,ϕ_2,...,ϕ_m are smooth functions, and s_1, s_2, ..., s_m are several different singularities.
3. Quadrature rules developed of this paper have fairly obvious analogues in two and three dimensions. However, the proofs of the multidimensional versions of the theorems in this paper are somewhat more involved than those of their one dimesional counterparts. These results will be reported at a later date.
4. High-order corrected trapezoidal rules can be used to approximate integrals

$$\int_0^{\pi} cos(a\cos\theta)d\theta \tag{131}$$

by rewriting the integral as

$$\int_{-a}^{a} \frac{cos(x)}{\sqrt{a^2 - x^2}} dx \tag{132}$$

and using the quadrature rule T_{ν^n} defined in (120). This rule proves to be of fundamental importance in the development of the Fast Bessel Transform (see, for example [10]).
5. Integral equations of the form

$$\int_0^L \sigma(w) log(|z - w|) ds_w = C \tag{133}$$

are encountered in the study of partial differential equations (see, for example [11]). In order to apply the Nystrom algorithm to the integral equation (133), the left-hand side is decomposed into a sum

$$\int_0^L \sigma(w) log(|z - w|) ds_w = I(z) + J(z), \tag{134}$$

where the integral operators I and J are defined by the formulae

$$I(z) = \int_0^L \sigma(w) log(|\frac{z - w}{\gamma^{-1}(z) - \gamma^{-1}(w)}|) ds_w, \tag{135}$$

$$J(z) = \int_0^L \sigma(w) log(|\gamma^{-1}(z) - \gamma^{-1}(w)|) ds_w. \quad (136)$$

Now, the integral operator I can be discretized by the uncorrected trapezoidal rule and the operator J can be discretized by the corrected trapezoidal rule $T^n_{\rho h}$ defined in (109) to a rapidly convergent finite-dimesional approximation to (133).

7 Correction weights for Non-singular and Singular functions

7.1 Quadrature Weights β_k^m for Non-singular Functions

$$\int_a^b f(x)dx \approx T_{\beta^m}^n(f)$$
$$= T_n(f) + h\sum_{k=1}^{\frac{m-1}{2}}(f(b+kh) - f(b-kh) - f(a+kh) + f(a-kh))\beta_k^m.$$

m = 3	m = 5	m = 7
0.4166666666666667D-01	0.5694444444444444D-01	0.6483961640211640D-01
	-0.7638888888888889D-02	-0.1395502645502646D-01
		0.1579034391534392D-02

m = 9	m = 11	m = 13
0.6965636022927690D-01	0.7289995064734647D-01	0.7523240913673701D-01
-0.1877177028218695D-01	-0.2247873075998076D-01	-0.2539430387171893D-01
0.3643353174603175D-02	0.5728518443362193D-02	0.7672233851187638D-02
-0.3440531305114638D-03	-0.9618798768104324D-03	-0.1739366039940610D-02
	0.7722834328737106D-04	0.2539297439987751D-03
		-0.1767014007114040D-04

m = 15	m = 17	m = 19
0.7699017460749256D-01	0.7836226334784643D-01	0.7946301859082432D-01
-0.2773799116605967D-01	-0.2965891540255508D-01	-0.3126001393779562D-01
0.9429999321943197D-02	0.1100166460634853D-01	0.1240262582468400D-01
-0.2591615965155427D-02	-0.3464763345380610D-02	-0.4326893325894750D-02
0.5202578456284055D-03	0.8560837610996297D-03	0.1240963216686299D-02
-0.6683840498737985D-04	-0.1531936403942661D-03	-0.2763550661820004D-03
0.4097355409686621D-05	0.1753039202853559D-04	0.4447195391960246D-04
	-0.9595026156320693D-06	-0.4581897491741901D-05
		0.2263996797568645D-06

m = 21	m = 23	m = 25
0.8036566134581083D-01	0.8111924751518991D-01	0.8175787507251367D-01
-0.3261397807027540D-01	-0.3377334140778168D-01	-0.3477689899786187D-01
0.1365243887004996D-01	0.1477039637407387D-01	0.1577395396415406D-01
-0.5160102022805384D-02	-0.5955094025666833D-02	-0.6707762218226974D-02
0.1657567565141616D-02	0.2092328816706471D-02	0.2535074812330083D-02
-0.4325816968527443D-03	-0.6167158739860944D-03	-0.8233306719437802D-03
0.8735769567235570D-04	0.1470308086322377D-03	0.2231520499850693D-03
-0.1275061020655204D-04	-0.2710805091870410D-04	-0.4885697701951313D-04
0.1193747238089644D-05	0.3616565358265304D-05	0.8277049522724384D-05
-0.5374153101848776D-07	-0.3101244008783459D-06	-0.1016258365190328D-05
	0.1281914349299291D-07	0.8036239225326941D-07
		-0.3070147670921659D-08

m = 27	m = 29	m = 31
0.8230598039728972D-01	0.8278153337505391D-01	0.8319804338077547D-01
-0.3565386751750355D-01	-0.3642664110637037D-01	-0.3711265758638233D-01
0.1667832775003454D-01	0.1749655860883470D-01	0.1823974312884766D-01
-0.7417074991466566D-02	-0.8083781617155592D-02	-0.8709621212955971D-02
0.2978395295604828D-02	0.3417018075663398D-02	0.3847282797776159D-02
-0.1047324179282599D-02	-0.1284180480514226D-02	-0.1530046036007233D-02
0.3146160654817536D-03	0.4198855326958103D-03	0.5372304569083815D-03
-0.7872277799802227D-04	-0.1170025842576793D-03	-0.1636490137583287D-03
0.1591319181836592D-04	0.2714748278587396D-04	0.4245334246577455D-04
-0.2491841417488210D-05	-0.5092371734040995D-05	-0.9173934315347822D-05
0.2832550619442283D-06	0.7409483976575184D-06	0.1604355866780116D-05
-0.2077714429849625D-07	-0.7838889284981948D-07	-0.2179294939201383D-06
	0.5360956533353892D-08	0.2155763344330162D-07
	-0.1778140387386520D-09	-0.1380750254862090D-08
		0.4296200771869423D-10

m = 33	m = 35	m = 37
0.8356586223906441D-01	0.8389305571446765D-01	0.8418600148964681D-01
-0.3772568901686392D-01	-0.3827675171227989D-01	-0.3877475953008444D-01
0.1891730418359046D-01	0.1953724971593344D-01	0.2010640150771007D-01
-0.9296840793733073D-02	-0.9847903489149048D-02	-0.1036531420894598D-01
0.4266725355474089D-02	0.4673760300951798D-02	0.5067442370362510D-02
-0.1781711570625991D-02	-0.2036550840838121D-02	-0.2292444185955085D-02
0.6648868875120992D-03	0.8011551083894191D-03	0.9444553816549185D-03
-0.2183589125884934D-03	-0.2806529564181254D-03	-0.3499410006344108D-03
0.6214890604463385D-04	0.8640764426675015D-04	0.1152776626902024D-03
-0.1506576957398094D-04	-0.2305218544957479D-04	-0.3336290631509345D-04
0.3044582263334879D-05	0.5240846629123186D-05	0.8369617098659884D-05
-0.4984930776645727D-06	-0.9942016492531560D-06	-0.1790615950589770D-05
0.6348092756603319D-07	0.1529838641028607D-06	0.3199739595444088D-06
-0.5895566545002414D-08	-0.1833269916550451D-07	-0.4643199407153423D-07
0.3550460830740161D-09	0.1604311636472664D-08	0.5253570715177823D-08
-0.1040280251184406D-10	-0.9116340394367584D-10	-0.4346230819394555D-09
	0.2523768794744743D-11	0.2337667781591708D-10
		-0.6133208535638922D-12

m = 39	m = 41	m = 43
0.8444980879146044D-01	0.846886187819156OD-01	0.8490582345073519D-01
-0.3922700061890783D-01	-0.3963949060242128D-01	-0.4001723785254232D-01
0.2063059004248263D-01	0.2111481741443320D-01	0.2156339227395194D-01
-0.1085151806728575D-01	-0.1130884391857241D-01	-0.1173947578371039D-01
0.5447289134690455D-02	0.5813149815719777D-02	0.6165108551649863D-02
-0.2547701211583463D-02	-0.2800989375372994D-02	-0.3051271143145499D-02
0.1093355313271473D-02	0.1246579017292300D-02	0.1403005122150116D-02
-0.4255727119317083D-03	-0.5068750854937796D-03	-0.5931791433463679D-03
0.1487041779510615D-03	0.1865518346092672D-03	0.2286250628124040D-03
-0.4617000028477128D-04	-0.6158941596033656D-04	-0.7968542809071795D-04
0.1259595810865357D-04	0.1806736367095093D-04	0.2490991825775139D-04
-0.2980436293579194D-05	-0.4659163000193157D-05	-0.6921164516490830D-05
0.6019365929090900D-06	0.1042814313838009D-05	0.1691476513364548D-05
-0.1016414607443390D-06	-0.1993926296380813D-06	-0.3590633249061523D-06
0.1395254130438025D-07	0.3190683763180230D-07	0.6517156581265044D-07
-0.1495069020432704D-08	-0.4154964772643378D-08	-0.9908863701222516D-08
0.1172703286200068D-09	0.4227988947523140D-09	0.1227209106806963D-08
-0.5987202298631028D-11	-0.3152674188244618D-10	-0.1188835069924533D-09
0.1492744845851982D-12	0.1531756684278896D-11	0.8447500588821128D-11
	-0.3638111051825521D-13	-0.3914899117784468D-12
		0.8877720031504791D-14

7.2 Quadrature Weights γ_j^k for Singular Functions

$$\begin{aligned}\int_0^b f(x)dx &\approx T^m_{\gamma^k\beta^m}(f)\\ &= T^m_{R\beta^m}(f) + h\sum_{j=-k,j\neq 0}^{k}\gamma_j f(x_j)\end{aligned}$$

	$s(x)=log(x)$	$s(x)=x^{\frac{1}{2}}$	$s(x)=x^{-\frac{1}{2}}$
		k= 2	
-1	0.751881233864002SD+00	0.4911169802967502D+00	0.1635135941723353D+01
-2	-0.6032109664493744D+00	-0.3176980828356269D+00	-0.1533115151360971D+01
1	0.1073866830872157D+01	0.7141080571189234D+00	0.2143719446940490D+01
2	-0.7225370982867850D+00	-0.3875269545800468D+00	-0.1745740237302873D+01
		k= 4	
-1	0.1420113571035790D+01	0.8951854542876017D+00	0.3192416400365587D+01
-2	-0.3125287797178819D+01	-0.1631355661694529D+01	-0.8349519005997507D+01
-3	0.2592853861401367D+01	0.1216528022899115D+01	0.7653118908743808D+01
-4	-0.7648698789584314D+00	-0.3318968291168987D+00	-0.2415721426013858D+01
1	0.2027726083620572D+01	0.1323278097869649D+01	0.4127731944814846D+01
2	-0.3730238148796624D+01	-0.1996997843341944D+01	-0.9431538570036398D+01
3	0.2914105643150046D+01	0.1392513231112159D+01	0.8285519053356245D+01
4	-0.8344033342739005D+00	-0.3672544720151524D+00	-0.2562007305232722D+01

k= 6			
-1	0.2051970990601252D+01	0.1265469280121926D+01	0.4710262208645700D+01
-2	-0.7407035584542865D+01	-0.3802563634358600D+01	-0.2025763995934342D+02
-3	0.1219590847580216D+02	0.5639024206133662D+01	0.3690977699143199D+02
-4	-0.1064623987147282D+02	-0.4569107975444730D+01	-0.3458675005305701D+02
-5	0.4799117710681772D+01	0.1943368974038607D+01	0.1646218520818186D+02
-6	-0.8837770983721025D+00	-0.3411137981342110D+00	-0.3167334195084358D+01
1	0.2915391987686506D+01	0.1878261417316043D+01	0.6026290938505443D+01
2	-0.8797979464048396D+01	-0.4649333971499730D+01	-0.2274216675280301D+02
3	0.1365562914252423D+02	0.6444550155059975D+01	0.3978973181300623D+02
4	-0.1157975479644601D+02	-0.5048462684259424D+01	-0.3656337403895339D+02
5	0.5130987287355766D+01	0.2104363245869803D+01	0.1720419649716102D+02
6	-0.9342187797694916D+00	-0.3644552148433214D+00	-0.3285178657691059D+01

k= 8			
-1	0.2661829001135098D+01	0.1616169645940613D+01	0.6202998068889192D+01
-2	-0.1336900704886964D+02	-0.6771767050468779D+01	-0.3714709770899691D+02
-3	0.3292331764210170D+02	0.1503196947284841D+02	0.1012860584122768D+03
-4	-0.4773939140223472D+02	-0.2024989176835058D+02	-0.1577736812789053D+03
-5	0.4288580615706955D+02	0.1717995995110646D+02	0.1497778690096803D+03
-6	-0.2359187584186291D+02	-0.9018058251167396D+01	-0.8617211496827355D+02
-7	0.7312948709041004D+01	0.2686335493243228D+01	0.2773685303768452D+02
-8	-0.9817367313018633D+00	-0.3483500116200692D+00	-0.3846246456428401D+01
1	0.3760781014023317D+01	0.2398992474897278D+01	0.7870429343373961D+01
2	-0.1580903864167977D+02	-0.8260181779465771D+01	-0.4150717430533848D+02
3	0.3674321491528176D+02	0.1714292235263991D+02	0.1088399244984859D+03
4	-0.5179306469244793D+02	-0.2233476105127601D+02	-0.1663887812447046D+03
5	0.4575621781632506D+02	0.1857536706216344D+02	0.1562272759566466D+03
6	-0.2489478606121209D+02	-0.9622728690582360D+01	-0.8923488368760573D+02
7	0.7656685336983747D+01	0.2839683305088209D+01	0.2857613653609836D+02
8	-0.1021900172352320D+01	-0.3656611549965858D+00	-0.3947565212882627D+01

k= 10			
-1	0.3256353919777872D+01	0.1953545360705999D+01	0.7677722423353747D+01
-2	-0.2096116396850468D+02	-0.1050311310076629D+02	-0.5894517227637276D+02
-3	0.6872858265408605D+02	0.3105516048922884D+02	0.2140398605114418D+03
-4	-0.1393153744796911D+03	-0.5850644296241638D+02	-0.4662332548976578D+03
-5	0.1874446431742073D+03	0.7437254291687940D+02	0.6631353162140867D+03
-6	-0.1715855846429547D+03	-0.6498918498319249D+02	-0.6351002576675097D+03
-7	0.1061953812152787D+03	0.3866979933460322D+02	0.4083227672169233D+03
-8	-0.4269031893958787D+02	-0.1502289586232686D+02	-0.1696285390723725D+03
-9	0.1009036069527147D+02	0.3445119980743215D+01	0.4126838241810020D+02
-10	-0.1066655310499552D+01	-0.3544413204640886D+00	-0.4476202232026015D+01
1	0.4576078100790908D+01	0.2895451608911961D+01	0.9675787330957780D+01
2	-0.2469045273524281D+02	-0.1277820188943208D+02	-0.6561769910673283D+02
3	0.7648830198138171D+02	0.3534092272477722D+02	0.2294242274362024D+03
4	-0.1508194558089468D+03	-0.6441908403427060D+02	-0.4907643918974356D+03
5	0.1996415730837827D+03	0.8029833065236247D+02	0.6906485447124722D+03
6	-0.1807965537141134D+03	-0.6926226351772149D+02	-0.6568499770824342D+03
7	0.1110467735366555D+03	0.4083390088012690D+02	0.4202275815793937D+03
8	-0.4438764193424203D+02	-0.1575467189373152D+02	-0.1739340651258045D+03
9	0.1044548196545488D+02	0.3593677332216888D+01	0.4219582451243715D+02
10	-0.1100328792904271D+01	-0.3681517162342983D+00	-0.4566454997023116D+01

	$s(x)=x^{\frac{1}{3}}$	$s(x)=x^{-\frac{1}{3}}$	$s(x)=x^{-\frac{9}{10}}$
		k= 2	
-1	0.5534091724301567D+00	0.1181425202719417D+01	0.9469239981678674D+01
-2	-0.3866961728429464D+00	-0.1060178333186577D+01	-0.9440762908621185D+01
1	0.8032238407479816D+00	0.1613104391254726D+01	0.1027199835611538D+02
2	-0.4699368403351921D+00	-0.1234351260787565D+01	-0.9800475429172870D+01

		k= 4	
-1	0.1020832071388625D+01	0.2282486199885223D+01	0.1887299140127902D+02
-2	-0.1983186102544885D+01	-0.5650813876770368D+01	-0.5533585657332243D+02
-3	0.1533381243224831D+01	0.5015176492677874D+01	0.5446669568113802D+02
-4	-0.4298392181270347D+00	-0.1549698701260824D+01	-0.1798256931439028D+02
1	0.1498331817034082D+01	0.3083643341213459D+01	0.2031702799746152D+02
2	-0.2412699293646369D+01	-0.6532393248536034D+01	-0.5722348457297536D+02
3	0.1747071103625803D+01	0.5514329562635926D+01	0.5565641900092846D+02
4	-0.4738916209550530D+00	-0.1662729769845256D+01	-0.1827122362011895D+02

		k= 6	
-1	0.1453673785846622D+01	0.3345150279872830D+01	0.2823540877500425D+02
-2	-0.4645097217879781D+01	-0.1359274618599862D+02	-0.1374572775395727D+03
-3	0.7134681085431341D+01	0.2395745376553084D+02	0.2701409207262959D+03
-4	-0.5928340311544518D+01	-0.2193610831631847D+02	-0.2668390934875709D+03
-5	0.2571788299099303D+01	0.1025817941642386D+02	0.1321842198719930D+03
-6	-0.4588965281604129D+00	-0.1946039989983884D+01	-0.2624585302793210D+02
1	0.2135823382632839D+01	0.4476264293482232D+01	0.3025125337714398D+02
2	-0.5636852769577275D+01	-0.1561643865091390D+02	-0.1418090842954654D+03
3	0.8109443112743051D+01	0.2622632514046215D+02	0.2756109143783281D+03
4	-0.6522597930471829D+01	-0.2345727234258157D+02	-0.2708086499560764D+03
5	0.2775248991033700D+01	0.1081909216811830D+02	0.1337381187138368D+03
6	-0.4888738991530396D+00	-0.2033859578093758D+01	-0.2650087753598454D+02

	$s(x)=x^{\frac{1}{3}}$	$s(x)=x^{-\frac{1}{3}}$	$s(x)=x^{-\frac{9}{10}}$
		k= 8	
-1	0.1866196808675184D+01	0.4383819645513359D+01	0.3756991225931813D+02
-2	-0.8307135206229368D+01	-0.2478753951112947D+02	-0.2556568200490798D+03
-3	0.1909144688191794D+02	0.6535630997043997D+02	0.7531560640068682D+03
-4	-0.2636153756127239D+02	-0.9943323854718145D+02	-0.1239060653686887D+04
-5	0.2279974850816623D+02	0.9269762740745608D+02	0.1226707735965091D+04
-6	-0.1215894117169713D+02	-0.5255448820422732D+02	-0.7300983324043684D+03
-7	0.3671126621978929D+01	0.1670932578919686D+02	0.2417364444480294D+03
-8	-0.4816958588438264D+00	-0.2292774564229746D+01	-0.3433771074231191D+02
1	0.2736714477854559D+01	0.5819143597164960D+01	0.4011575033483495D+02
2	-0.1004886340865174D+02	-0.2833732911493431D+02	-0.2633133438634569D+03
3	0.2164374286136325D+02	0.7130006863921132D+02	0.7675751360752552D+03
4	-0.2894336017656429D+02	-0.1060508801269256D+03	-0.1256487025699375D+04
5	0.2456068654847544D+02	0.9756101768474124D+02	0.1240341295810031D+04
6	-0.1293400965739323D+02	-0.5482984235409941D+02	-0.7368055436813910D+03
7	0.3870327870200545D+01	0.1732510108672746D+02	0.2436290214530279D+03
8	-0.5044475379801205D+00	-0.2366321397723911D+01	-0.3457193022558553D+02

k= 10			
-1	0.2264788460960479D+01	0.540545463351605 2D+01	0.4688376828974556D+02
-2	-0.1292939169279749D+02	-0.3917131575943378D+02	-0.4098330186123370D+03
-3	0.3957101757244672D+02	0.1375220761115852D+03	0.1609252630383255D+04
-4	-0.7639785056816069D+02	-0.2925218664728695D+03	-0.3705300977598581D+04
-5	0.9898237584503627D+02	0.4085024389395215D+03	0.5500852053333245D+04
-6	-0.8785457780822613D+02	-0.3854463863750540D+03	-0.5454835999290140D+04
-7	0.5297228202020211D+02	0.2447281804852179D+03	0.3611006247703252D+04
-8	-0.2081786990425939D+02	-0.1005754937354166D+03	-0.1538237727142339D+04
-9	0.4823072180507942D+01	0.2423820803863685D+02	0.3825346496620566D+03
-10	-0.5007874588446741D+00	-0.2606987282704575D+01	-0.4230611481851793D+02
1	0.3311620888787288D+01	0.7126578020279918D+01	0.4993063308066224D+02
2	-0.1559126529305869D+02	-0.4460041915515531D+02	-0.4215785445878369D+03
3	0.4475277794263923D+02	0.1496138805763186D+03	0.1638730173971623D+04
4	-0.8371954827689160D+02	-0.3113382992063869D+03	-0.3755162938068600D+04
5	0.1064593309138400D+03	0.4292142311074982D+03	0.5559352058138100D+04
6	-0.9333016061951656D+02	-0.4015725721227424D+03	-0.5502789929350287D+04
7	0.5578209928784346D+02	0.2534431424358416D+03	0.3638060903851112D+04
8	-0.2177894078450347D+02	-0.1036930201058000D+03	-0.1548279140995316D+04
9	0.5020172381264958D+01	0.2490333391795860D+02	0.3847470160018897D+03
10	-0.5191450872697767D+00	-0.2671164050811178D+01	-0.4252574395098780D+02

7.3 Quadrature Weights μ_j^k for Singular Functions

$$\begin{aligned}\int_{-b}^{b} f(x)dx &\approx T^n_{\mu_l\beta^m}(f) \\ &= T^n_{R\beta^m}(f) + T^n_{L\beta^m}(f) + h\sum_{j=1}^{l}\mu_j(f(x_j)+f(x_{-j}))\end{aligned}$$

	$s(x)=log(x)$	$s(x)=x^{\frac{1}{2}}$	$s(x)=x^{-\frac{1}{2}}$
k= 1			
1	0.1825748064736159D+01	0.1205225037415674D+01	0.3778855388663843D+01
2	-0.1325748064736159D+01	-0.7052250374156737D+00	-0.3278855388663843D+01
k= 2			
1	0.3447839654656362D+01	0.2218463552157251D+01	0.7320148345180434D+01
2	-0.6855525945975443D+01	-0.3628353505036473D+01	-0.1778105757603391D+02
3	0.5506959504551413D+01	0.2609041254011273D+01	0.1593863796210005D+02
4	-0.1599273213232332D+01	-0.6991513011320512D+00	-0.4977728731246580D+01
k= 3			
1	0.4967362978287758D+01	0.3143730697437969D+01	0.1073655314715114D+02
2	-0.1620501504859126D+02	-0.8451897605858329D+01	-0.4299980671214643D+02
3	0.2585153761832639D+02	0.1208357436119364D+02	0.7669950880443822D+02
4	-0.2222599466791883D+02	-0.9617570659704153D+01	-0.7115012409201039D+02
5	0.9930104998037539D+01	0.4047732219908410D+01	0.3366638170534288D+02
6	-0.1817995878141594D+01	-0.7055690129775324D+00	-0.6452512852775417D+01

k= 4			
1	0.6422610015158415D+01	0.4015162120837891D+01	0.1407342741226315D+02
2	-0.2917804569054941D+02	-0.1503194882993455D+02	-0.7865427201433540D+02
3	0.6966653255738346D+02	0.3217489182548832D+02	0.2101259829107628D+03
4	-0.9953245609468264D+02	-0.4258465281962659D+02	-0.3241624625236100D+03
5	0.8864202397339461D+02	0.3575532701326990D+02	0.3060051449663269D+03
6	-0.4848666190307500D+02	-0.1864078694174975D+02	-0.1754069986558793D+03
7	0.1496963404602475D+02	0.5526018798331437D+01	0.5631298957378288D+02
8	-0.2003636903654183D+01	-0.7140111666166550D+00	-0.7793811669311027D+01

k= 5			
1	0.7832432020568779D+01	0.4848996969617959D+01	0.1735350975431153D+02
2	-0.4565161670374749D+02	-0.2328131499019837D+02	-0.1245628713831056D+03
3	0.1452168846354678D+03	0.6639608321400605D+02	.0.4434640879476441D+03
4	-0.2901348302886379D+03	-0.1229255269966870D+03	-0.9569976467950934D+03
5	0.3870862162579900D+03	0.1546708735692419D+03	0.1353783860926559D+04
6	-0.3523821383570680D+03	-0.1342514485009140D+03	-0.1291950234749944D+04
7	0.2172421547519342D+03	0.7950370021473013D+02	0.8285503487963169D+03
8	-0.8707796087382989D+02	-0.3077756775605837D+02	-0.3435626041981771D+03
9	0.2053584266072635D+02	0.7038797312960103D+01	0.8346420693053734D+02
10	-0.2166984103403823D+01	-0.7225930366983869D+00	-0.9042657229049132D+01

	$s(x) = x^{\frac{1}{3}}$	$s(x) = x^{-\frac{1}{3}}$
k= 1		
1	0.1356633013178138D+01	0.2794529593974142D+01
2	-0.8566330131781384D+00	-0.2294529593974142D+01

k= 2		
1	0.2519163888422707D+01	0.5366129541098682D+01
2	-0.4395885396191253D+01	-0.1218320712530640D+02
3	0.3280452346850634D+01	0.1052950605531380D+02
4	-0.9037308390820877D+00	-0.3212428471106080D+01

k= 3		
1	0.3589497168479460D+01	0.7821414573355062D+01
2	-0.1028194998745706D+02	-0.2920918483691252D+02
3	0.1524412419817439D+02	0.5018377890599299D+02
4	-0.1245093824201635D+02	-0.4539338065890004D+02
5	0.5347037290133003D+01	0.2107727158454216D+02
6	-0.9477704273134525D+00	-0.3979899568077642D+01

k= 4		
1	0.4602911286529744D+01	0.1020296324267832D+02
2	-0.1835599861488110D+02	-0.5312486862606378D+02
3	0.4073518974328119D+02	0.1366563786096513D+03
4	-0.5530489773783668D+02	-0.2054841186741071D+03
5	0.4736043505664168D+02	0.1902586450921973D+03
6	-0.2509295082909035D+02	-0.1073843305583267D+03
7	0.7541454492179474D+01	0.3403442687592432D+02
8	-0.9861433968239469D+00	-0.4659095961953657D+01

k= 5		
1	0.557640934974767D+01	0.1253203265379597D+02
2	-0.2852065698585619D+02	-0.8377173491458909D+02
3	0.8432379551508595D+02	0.2871359566879038D+03
4	-0.1601173988450523D+03	-0.6038601656792564D+03
5	0.2054417067588763D+03	0.837716670047019 6D+03
6	-0.1811847384277427D+03	-0.7870189584977965D+03
7	0.1087543813080456D+03	0.4981713229210595D+03
8	-0.4259681068876286D+02	-0.2042685138412166D+03
9	0.9843244561772901D+01	0.491415419565954 5D+02
10	-0.1019932546114451D+01	-0.5278151333515754D+01

7.4 Quadrature Weights ρ_j^k for Singular Functions

$$\begin{aligned}\int_{-b}^{b} f(x)dx &\approx T^n_{\rho^p\beta^m}(f) \\ &= T^n_{R\beta^m}(f) + T^n_{L\beta^m}(f) + h\sum_{j=0}^{l}\rho_j(\phi(x_j)+\phi(x_{-j}))\end{aligned}$$

Note: ρ_0 is given for $h = 0.01$, For any other h, the following formula is used to calculate ρ_0.

$$\rho_0 = (-.9189385332046727417803 + 0.5log(h)) - \sum_{j=1}^{p}\rho_j \tag{137}$$

m = 3	m = 5	m = 7
-0.3221523626198730D+01	-0.3191075169140337D+01	-0.3181467102013171D+01
	-0.3044845705839327D-01	-0.4325921322794724D-01
		0.3202689042388491D-02
m = 9	**m = 11**	**m = 13**
-0.3176811195217937D+01	-0.3174071153542312D+01	-0.3172268092036274D+01
-0.5024307342079858D-01	-0.5462714010179898D-01	-0.5763224261186158D-01
0.5996233119529027D-02	0.8188266460029230D-02	0.9905467894350714D-02
-0.4655906795234226D-03	-0.1091885919666338D-02	-0.1735836457536894D-02
	0.7828690501786438D-04	0.2213870245446548D-03
		-0.1431001195267904D-04
m = 15	**m = 17**	**m = 19**
-0.3170992165916170D+01	-0.3170041916020681D+01	-0.3169306861514305D+01
-0.5981954453204053D-01	-0.6148248184914681D-01	-0.6278924541603596D-01
0.1127253159446256D-01	0.1238115647253341D-01	0.1329589096935583D-01
-0.2343420324253269D-02	-0.2897732763288696D-02	-0.3396678852464559D-02
0.4036621845595672D-03	0.6052303442088134D-03	0.8131245480320894D-03
-0.4745095013720858D-04	-0.9784299004952013D-04	-0.1618104373797589D-03
0.2761744848710794D-05	0.1051436637368180D-04	0.2422167651587582D-04
	-0.5537586803550720D-06	-0.2381400032647607D-05
		0.1142275845182835D-06

m = 21	m = 23	m = 25
-0.3168721384920306D+01	-0.3168244070581230D+01	-0.3167847493678468D+01
-0.6384310328523506D-01	-0.6471094753809971D-01	-0.6543800519316396D-01
0.1406233305604607D-01	0.1471321624569456D-01	0.1527249136497475D-01
-0.3843770069700536D-02	-0.4244313571022683D-02	-0.4603847576274231D-02
0.1019474340602541D-02	0.1219746091263614D-02	0.1411497560731106D-02
-0.2355067918692057D-03	-0.3156154921336350D-03	-0.3995067600256630D-03
0.4387403771306165D-04	0.6890800654569580D-04	0.9851668933111745D-04
-0.6066217757119951D-05	-0.1195656336479857D-04	-0.2018119747186014D-04
0.5477355521032650D-06	0.1529459820049702D-05	0.3260961737325821D-05
-0.2408377597694342D-07	-0.1274231726028842D-06	-0.3871484601943021D-06
	0.5166969831297037D-08	0.2990271150667017D-07
		-0.1124351894335142D-08

m = 27	m = 29	m = 31
-0.3167512774719844D+01	-0.3167226492889164D+01	-0.3166978846772530D+01
-0.6605594788600917D-01	-0.6658761414298577D-01	-0.6704988689403577D-01
0.1575801776649599D-01	0.1618335077207727D-01	0.1655894738230538D-01
-0.4927531843955059D-02	-0.5219948285292188D-02	-0.5485075304276741D-02
0.1593569961301572D-02	0.1765579632676354D-02	0.1927601699833581D-02
-0.4851878897058822D-03	-0.5711927253932730D-03	-0.6564674975812873D-03
0.1318371286512027D-03	0.1680496910458935D-03	0.2064233385304999D-03
-0.3070344146767653D-04	-0.4337783830581833D-04	-0.5799637068090648D-04
0.5891522736279919D-05	0.9512778975749005D-05	0.1416413018600433D-04
-0.8882076980903206D-06	-0.1711220479787840D-05	-0.2924616447680532D-05
0.9822897121976360D-07	0.2413616289062888D-06	0.4941524555505996D-06
-0.7065765782430224D-08	-0.2495734799324587D-07	-0.6540388025633560D-07
0.2475589120039617D-09	0.1678885488869214D-08	0.6345793057687260D-08
	-0.5505102218712507D-10	-0.4007478791366100D-09
		0.1234631631962446D-10

m = 33	m = 35	m = 37
-0.3166762511619708D+01	-0.3166571903740287D+01	-0.3166402692325675D+01
-0.6745551530557688D-01	-0.6781430660801560D-01	-0.6813392816895060D-01
0.1689299430945688D-01	0.1719198706148916D-01	0.1746114206017127D-01
-0.5726331418330602D-02	-0.5946641867196491D-02	-0.6148508116208072D-02
0.2079973982393914D-02	0.2223175774156742D-02	0.2357753273497796D-02
-0.7402722529894703D-03	-0.8221018482825148D-03	-0.9016249160749561D-03
0.2463303649153491D-03	0.2872451625618713D-03	0.3287354588014059D-03
-0.7432197238379932D-04	-0.9211101483880897D-04	-0.1111274006152623D-03
0.1984260034353227D-04	0.2651349126416089D-04	0.3412004557474223D-04
-0.4580836910292848D-05	-0.6715522004894009D-05	-0.9348560035479858D-05
0.8916453665775555D-06	0.1466368276662483D-05	0.2246527693132364D-05
-0.1418448246845963D-06	-0.2695610269256914D-06	-0.4646008810431617D-06
0.1767037741742959D-07	0.4047684210333943D-07	0.8082991536902293D-07
-0.1614096203394717D-08	-0.4759815470416764D-08	-0.1148532768136401D-07
0.9602551109604562D-10	0.4105974377982503D-09	0.1278405465017250D-08
-0.2789306492547372D-11	-0.2308426950559283D-10	-0.1044412720573741D-09
	0.6342175941576707D-12	0.5564945021538352D-11
		-0.1450213949229612D-12

m = 39	m = 41	m = 43
-0.3166251466775081D+01	-0.3166115504658825D+01	-0.3166115504658825D+01
-0.6842046079112800D-01	-0.6867878881201404D-01	-0.6867878881201404D-01
0.1770469478902206D-01	0.1792611880692437D-01	0.1792611880692437D-01
-0.6334072100094389D-02	-0.6505172477564357D-02	-0.6505172477564357D-02
0.2484274171602103D-02	0.2603300521146428D-02	0.2603300521146428D-02
-0.9786376366601862D-03	-0.1053029105125390D-02	-0.1053029105125390D-02
0.3704506824517389D-03	0.4121099047922528D-03	0.4121099047922528D-03
-0.1311507079674222D-03	-0.1519803191376791D-03	-0.1519803191376791D-03
0.4259144483911754D-04	0.5184904980367620D-04	0.5184904980367620D-04
-0.1248611531858182D-04	-0.1612303155465844D-04	-0.1612303155465844D-04
0.3255027605557997D-05	0.4509136652480968D-05	0.4509136652480968D-05
-0.7428077534364396D-06	-0.1119040467513331D-05	-0.1119040467513331D-05
0.1457448522607878D-06	0.2428371655709533D-06	0.2428371655709533D-06
-0.2404950901525398D-07	-0.4528845255185268D-07	-0.4528845255185268D-07
0.3241558798437558D-08	0.7103184896000958D-08	0.7103184896000958D-08
-0.3423992518658962D-09	-0.9102854426840433D-09	-0.9102854426840433D-09
0.2656123735758442D-10	0.9146251630822981D-10	0.9146251630822981D-10
-0.1344809528411308D-11	-0.6753249440965090D-11	-0.6753249440965090D-11
0.3332744815245408D-13	0.3256755515337396D-12	0.3256755515337396D-12
	-0.7693711141612778D-14	-0.7693711141612778D-14

References

[1] M. ABRAMOVITZ AND I. STEGUN, *Handbook of Mathematical Functions.* National Bureau of Standards, Washington, DC., 1964.

[2] I. S. GRADSHTEYN AND I. M. RYZHIK, *Table of Integrals, Series and Products*, Academic Press Inc., 1980.

[3] J. STOER AND R. BULIRSCH, *Introduction to Numerical Analysis*, Springer Verlag, New York, 1980.

[4] B. ALPERT, *PhD Thesis*, Yale University, 1989.

[5] V. ROKHLIN, *End-point corrected trapezoidal quadrature rules for singular functions*, Computers and Mathematics with Applications, 1990.

[6] K. E. ATKINSON, *A Survey of Numerical methods for the Solution of Fredholm Integral Equations of the Second Kind*, SIAM, Philadelphia, PA (1976)

[7] G. DAHLQUIST, A. BJORK, *Numerical Methods*, Prentice Hall, NJ (1974)

[8] S. KARLIN AND W.L. STUDDEN, *Tchebycheff Systems with Applications in Analysis and Statistics*, Wiley, NY (1966)

[9] JOHN STRAIN, *Locally-Corrected Multidimensional Quadrature Rules for Singular Functions*, Lawrence Berkeley Laboratory, Berkley, CA, (1993)

[10] SHARAD KAPUR, VLADIMIR ROKHLIN, *The Fast Bessel Transform*, Technical Report 1045, Yale Computer Science Department, New Haven, CT, (1994)

[11] J. MA, *Interpolation on Arbitrary Regions of the Complex Plane*, UCLA, LA, CA, (1994)

The Fast Multipole Method for the Wave Equation: A Pedestrian Prescription

Ronald Coifman[1], Vladimir Rokhlin[1], and Stephen Wandzura[2]

[1]Fast Mathematical Algorithms and Hardware Corporation
1020 Sherman Avenue
Hamden, CT 06514

and

[2]Hughes Research Labs
3011 Malibu Canyon Road
Malibu, CA 90265

1. Introduction

The purpose of this article is to give a practical and complete, but not rigorous, exposition of the Fast Multipole Method (FMM). The aim is to give the computational physicist or engineer a sufficiently clear understanding of the method that he or she will be able to implement it with a minimum of difficulty. For mathematical background and rigor, we refer the reader to Rokhlin's papers [1, 2].

The FMM provides an efficient mechanism for the numerical convolution of the Green's function for the Helmholtz equation with a source distribution. It can be used to radically accelerate the iterative solution of boundary-integral equations. In the simple single-stage form presented here, it reduces the computational complexity of the convolution from $O(N^2)$ to $O(N^{3/2})$, where N is the dimensionality of the problem's discretization. By implementing a multistage FMM [1,2], the complexity can be further reduced to $O(N \log N)$. However, even for problems that have an order of magnitude more variables than those currently tractable using dense-matrix techniques ($N \approx 10^5$), we estimate that the performance of the single-stage algorithm should be near optimal.

Our development is given in terms of the method of moments [3,4] (MoM), rather than the Nyström method [5]. We do this because

- Electrical engineers are more familiar with the MoM, and may therefore be more comfortable with the development.
- The prescription we present is sufficiently simple that it can be easily retrofitted to existing MoM codes.
- When used in the MoM, detailed comparisons to verify that results are identical to dense-matrix techniques are immediately available.
- We avoid all questions of singularity subtraction, as it is required only for matrix elements representing nearby interactions, and the computation of these is unchanged when the FMM is employed.
- The presentation demonstrates the independence of the FMM from the choice of discretization method, boundary-surface model, basis functions, etc.

The reader is cautioned not to interpret our choice of presentation as representing a preference toward the MoM. On the contrary, we think that the Nyström method is the appropriate tool for efficient and accurate boundary-integral-equation solvers.

For the purposes of demonstration, we first consider the MoM for the scalar wave equation, with Dirichlet boundary conditions on the surface of a scatterer. This is done for notational convenience only, the (naive) equivalent application to the electric-field integral equation (EFIE) being straightforward. (One can simply apply the scalar prescription to each Cartesian component of the vector expansion functions, and to their divergences; a more efficient method is described in Section 5.)

If the structure of this article seems somewhat confusing at an initial reading, it is because some considerations are intentionally delayed. We hope that the reasons for this become clear upon subsequent readings. In Section 2, we define notation, introduce the discretization of the scattering problem, relate the FMM to a more familiar fast algorithm, and introduce the fundamental analytic apparatus of the FMM. A detailed prescription for FMM implementation, except for the choice of some important parameters of the algorithm, is given in Section 3. After the structure of the method is exhibited, these parameters (the number of terms used in the multipole expansion, and the directions at which far-field quantities are tabulated) are analyzed in Section 4. The algorithm for the scalar problem then having been being completely defined, we exhibit the minor modifications necessary for application to vector (electromagnetic) scattering in Section 5. Before concluding, a physical interpretation of the analysis behind the FMM is given in Section 6.

2. Basics

2.1 Notation

Vectors in three-dimensional space are represented by boldface type ($\mathbf{x}$). The magnitude of a vector $\mathbf{x}$ is written as $x \equiv |\mathbf{x}|$, unit vectors are written as $\hat{x} \equiv \mathbf{x}/x$, and integrals over the unit sphere are written as $\int d^2\hat{x}$. The imaginary unit is denoted by i.

 1045-9243/93/$03.00©1993 IEEE

2.2 Time-independent scattering and the Method of Moments

A scattering problem [6, 7] can be defined by the scalar wave equation

$$\left(\nabla^2 + k^2\right)\psi = 0, \tag{1}$$

a Dirichlet boundary condition

$$\psi(\mathbf{x}) = 0; \quad \mathbf{x} \text{ on } S, \tag{2}$$

on the surface, S, of a bounded scatterer, and a radiation boundary condition. The method of moments [8] provides a discretization of the first-kind integral equation associated with this problem, giving a set of linear equations with a dense coefficient (impedance) matrix:

$$Z_{nn'} = -i\int_S d^2\mathbf{x}\int_S d^2\mathbf{x}' f_n(\mathbf{x})\frac{e^{ik|\mathbf{x}-\mathbf{x}'|}}{4\pi|\mathbf{x}-\mathbf{x}'|} f_{n'}(\mathbf{x}'). \tag{3}$$

We assume that the basis functions, f_n, are real, and supported on local subdomains. The FMM provides a prescription for the rapid computation of the matrix-vector product

$$B_n = \sum_{n'=1}^{N} Z_{nn'} I_{n'}, \tag{4}$$

for an arbitrary vector I. This rapid computation can then be used in an iterative (e.g., conjugate-gradient) solution of the discretized integral equation $Z \bullet I = V$, where, for an incident wave with wave vector $\mathbf{k}$,

$$V_n(k) = \int_S d^2\mathbf{x} f_n(\mathbf{x}) e^{i\mathbf{k}\cdot\mathbf{x}}. \tag{5}$$

Note that we have chosen to use the same functions for expansion and testing (the Galerkin method). Not only does this simplify the development somewhat, but it also results in superconvergence of the scattering amplitude [9, 10].

2.3 Comparison with the Fast Fourier Transform

A discrete Fourier transform consists of multiplication by a dense $N \times N$ matrix F, with matrix elements

$$F_{kl} = \exp\frac{2\pi ikl}{N}. \tag{6}$$

The fast Fourier transform (FFT) works by using algebraic properties of F to construct a sparse factorization,

$$F = F^{(1)}F^{(2)}\ldots F^{(\log_2 N)}, \tag{7}$$

and applying the sparse factors, $F^{(\alpha)}$, one by one to the vector to be transformed, in lieu of a single multiplication by the matrix F. Because each of the factors has only $O(N)$ non-zero elements, this results in an algorithm that requires $O(N \log N)$ operations. The single-stage FMM works by a similar decomposition of the matrix Z

$$Z = Z' + VTV^{\dagger}, \tag{8}$$

where Z', V, and T are all sparse. As described in detail in this article, this allows computation of the product of Z with an arbitrary vector (corresponding physically to the determination of the fields radiated by a known source distribution), with $O\left(N^{3/2}\right)$ operations. The complexity can be further reduced to $N^{4/3}, N^{5/4}, \ldots$, by recursive decomposition of Z' and V:

$$Z' = Z'' + VT'V'^{\dagger} \tag{9}$$

$$V = V'S. \tag{10}$$

This is entirely analogous to the FFT: if one factors F into only two factors (independent of N), the result would be an $O\left(N^{3/2}\right)$ algorithm. We do not exhibit the details of the multi-stage FMM in this article.

In contrast to the FFT, the FMM decomposition is made possible by analytic rather than algebraic properties of the linear operator. Thus, while the FFT factorization is exact, the FMM decomposition is approximate. However, this does *not* constitute a practical limitation, as it is easy to control the FMM to achieve any desired level of precision (all the way to machine precision).

2.4 Identities

The FMM, as presented here, rests on two elementary identities. They, or formulas from which they may be easily derived, are found in many texts and handbooks on mathematical methods, such as Arfken [11] and Abramowitz and Stegun [12]. The first, an expansion of the kernel in the integral, Equation (3), for the impedance-matrix elements, is a form of Gegenbauer's addition theorem,

$$\frac{e^{ik|\mathbf{X}+\mathbf{d}|}}{|\mathbf{X}+\mathbf{d}|} = ik\sum_{l=0}^{\infty}(-1)^l(2l+1)j_l(kd)h_l^{(1)}(kX)P_l\left(\hat{d}\cdot\hat{X}\right), \tag{11}$$

where j_l is a spherical Bessel function of the first kind, $h_l^{(1)}$ is a spherical Hankel function of the first kind, P_l is a Legendre polynomial, and $d < X$. When using this expansion to compute the field at $\mathbf{x}$ from a source at $\mathbf{x}'$, $\mathbf{X}$ will be chosen to be close to $\mathbf{x}-\mathbf{x}'$, so that d will be small. This relationship of the various vectors is sketched in Figure 1. The special functions are as defined in [12]. The second is an expansion of the product $j_l P_l$ in propagating plane waves:

$$4\pi i^l j_l(kd)P_l\left(\hat{d}\cdot\hat{X}\right) = \int d^2\hat{k}e^{i\mathbf{k}\cdot\mathbf{d}}P_l\left(\hat{k}\cdot\hat{X}\right). \tag{12}$$

Substituting Equation (12) into Equation (11), we get

$$\frac{e^{ik|\mathbf{X}+\mathbf{d}|}}{|\mathbf{X}+\mathbf{d}|} = \frac{ik}{4\pi}\int d^2\hat{k}e^{i\mathbf{k}\cdot\mathbf{d}}\sum_{l=0} i^l(2l+1)h_l^{(1)}(kX)P_l\left(\hat{k}\cdot\hat{X}\right), \tag{13}$$

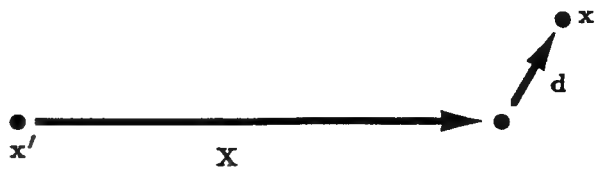

Figure 1. The basic geometry, illustrating the relationship between the locations $\mathbf{x}, \mathbf{x}'$ and the displacements $\mathbf{X}$,$\mathbf{x}$.

where we have performed the illegitimate but expedient interchange of summation and integration. The key point is that we intend to precompute the function

$$\mathcal{T}_L(\kappa,\cos\theta)\equiv\sum_{l=0}^{L} i^l(2l+1)h_l^{(1)}(\kappa)P_l(\cos\theta), \tag{14}$$

for various values of κ. This is not a function in the $L\to\infty$, but that need not concern us, as we obviously intend to truncate the sum in numerical practice. The number of kept terms, $L+1$, will depend on the maximum allowed value of kd, as well as the desired accuracy. The choice of L is discussed in Section 4. It suffices, for the present, to note that, in order to obtain accuracy from Equation (11), it must be slightly greater than κD, where D is the maximum value of d for which the expansion will be used. Ignoring this question for now (except for noting that the required number of terms becomes small as $D\to 0$), we have

$$\frac{e^{ik|\mathbf{X}+\mathbf{d}|}}{|\mathbf{X}+\mathbf{d}|}\approx\frac{ik}{4\pi}\int d^2\hat{k}e^{i\mathbf{k}\cdot\mathbf{d}}\mathcal{T}_L\left(kX,\hat{k}\cdot\hat{X}\right)\ . \tag{15}$$

Using this, the impedance-matrix element, Equation (3), is given by

$$Z_{nn'}\approx\frac{k}{(4\pi)^2}\int_S d^2\mathbf{x}f_n(\mathbf{x})\int_S d^2\mathbf{x}'f_{n'}(\mathbf{x}')\int d^2\hat{k}e^{i\mathbf{k}\cdot(\mathbf{x}-\mathbf{x}'-\mathbf{X})}\mathcal{T}_L\left(kX,\hat{k}\cdot\hat{X}\right) \tag{16}$$

In infinite-precision arithmetic, and in the limit of large L, this result would be independent of the choice of $\mathbf{X}$ (for $X>|\mathbf{x}-\mathbf{x}'-\mathbf{X}|$). In practice, one chooses $\mathbf{X}$ to make $\mathbf{x}-\mathbf{x}'-\mathbf{X}$ relatively small, so that excellent accuracy can be obtained with a modest value of L. (That this can be done by the grouping scheme described below is a consequence of the local support of the basis functions.) Notice that Equation (16) gives the impedance-matrix element (for well-separated interactions) in terms of the Fourier transforms *with wave number k* of the basis functions, i.e. the basis functions' far fields. The acceleration provided by the FMM comes from the fact that these far fields can be grouped together *before* the integral over $\hat{k}$ is performed.

3. Algorithmic prescription

3.1 Setup

1. Divide the N basis functions into M localized groups, labeled by an index m, each supporting about N/M basis functions. (For now, M is a free parameter. Later it will be seen that the best choice will be $M\sim\sqrt{N}$.) Thus, establish a correspondence between the basis-function index, n, and a pair of indices (m,α), where α labels the particular basis function within the mth group. Denote the center of the smallest sphere enclosing each group as $\mathbf{X}_m$. The grouping and index correspondence is shown, for a simple case, in Figure 2.

2. For group pairs (m,m') that contain "nearby" basis functions [defined for now as those whose regions of support are separated by a distance comparable to or smaller than a wavelength, $2\pi/k$, so that Equation (16) is valid], construct the sparse matrix Z', with matrix elements

$$Z'_{m\alpha m'\alpha'}=Z_{n(m,\alpha)n'(m',\alpha')}, \tag{17}$$

by direct numerical computation of the matrix elements, Equation (3). For all other pairs, $Z'_{m\alpha m'\alpha'}=0$.

This part of the matrix computation is identical to what is conventionally done. All matrix elements, the computation of which requires subtraction of singularities, belong to Z'. If the large-N limit is taken with a fixed discretization interval and nearness criterion, this step would require $O(N)$ computations. In Section 4, we define nearby regions precisely, and it turns out that their volume increases as $\sqrt{N}$, so that this step requires $O\left(N^{3/2}\right)$ computations.

3. For K directions $\hat{k}$, compute the "excitation vectors" (Fourier transforms of the basis functions)

$$V_{m\alpha}\left(\hat{k}\right)=\int_S d^2\mathbf{x}\ e^{i\mathbf{k}\cdot(\mathbf{x}-\mathbf{X}_m)}f_{n(m,\alpha)}(\mathbf{x}), \tag{18}$$

where k is considered to be a parameter of the problem, not a variable. Because K needs to be chosen to give accurate numerical quadrature for all harmonics to some order $\propto L\sim kD$, $K\propto L^2\sim(kD)^2$, and because (from geometrical considerations) $kD\propto\sqrt{N/M}$, this step requires $O\left(N^2/M\right)$ computations.

4. For each pair (m,m') for which $Z'_{m\alpha m'\alpha'}=0$ (regions that are not nearby), compute the matrix elements

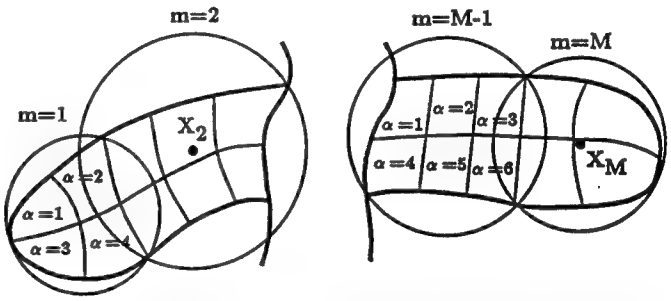

Figure 2. The grouping for a simple surface. It is assumed, for purposes of illustration only, that each patch supports only one basis function. The correspondence $n(m,\alpha)$ is abbreviated in Table 1.

Table 1. The abbreviated correspondence $n\leftrightarrow(m,\alpha)$ for the grouping shown in Figure 2.

m	α	$n(m,\alpha)$
1	1	1
1	2	2
1	3	3
1	4	4
2	1	5
2	2	6
2	3	7
	...	

$$T_{mm'}(\hat{k}) = \frac{k}{(4\pi)^2}\sum_{l=0}^{L} i^l(2l+1)h_l^{(1)}(kX_{mm'})P_l(\hat{k}\cdot\hat{X}_{mm'}) \tag{19}$$

for the same K directions $\hat{k}$ as the previous step, where $L \propto \sqrt{K}$. If done in a naive manner, this computation requires $O(KLM^2 \sim M^{1/2}N^{3/2})$ operations. However, it can be accomplished more rapidly in a number of ways, the most elegant being the fast Legendre expansion [13].

3.2 Fast Matrix-Vector Multiplication

Rapid computation of the vector elements

$$B_{m\alpha} = \sum_{m'\alpha'} Z_{m\alpha m'\alpha'} I_{m'\alpha'} \tag{20}$$

is accomplished by the following steps:

1. Compute the KM quantities

$$s_m(\hat{k}) = \sum_{\alpha} V^*_{m\alpha}(\hat{k}) I_{m\alpha}, \tag{21}$$

which represent the far fields of each group m. This step requires $O(KN \sim N^2/M)$ operations.

2. Compute the KM quantities

$$g_m(\hat{k}) = \sum_{m'} T_{mm'}(\hat{k}) s_{m'}(\hat{k}). \tag{22}$$

These represent the Fourier components of the field in the neighborhood of group m, generated by the sources in the groups that are not nearby. This step requires $O(KM^2 \sim MN)$ operations.

3. Finally, compute

$$B_{m\alpha} = \sum_{m'\alpha'} Z'_{m\alpha m'\alpha'} I_{m'\alpha'} + \int d^2\hat{k} V_{m\alpha}(\hat{k}) g_m(\hat{k}). \tag{23}$$

The first term is the standard MoM computation of near interactions, and the second term gives the far interactions, in terms of the far fields generated by each group. This step requires $O(KN \sim N^2/M)$ operations.

Straightforward substitution of Equations (18), (19), (21), and (22) into Equation (23), and of Equations (14)-(16) into Equation (20), shows that the two expressions for the vector B, Equations (23) and (20), give equal results. Thus, computation of the vector B requires $aNM + bN^2/M$ operations, where a and b are machine and implementation dependent. The total operation count is minimized by choosing $M = \sqrt{bN/a}$; the result is an $O(N^{3/2})$ algorithm.

4. Required number of multipoles and directions

In this section:

- We show how to choose the summation limit in the transfer function $T_{mm'}(\hat{k})$, Equation (19), to achieve the desired accuracy (in the process, giving a precise definition of nearby regions).
- We discuss how to choose the K directions $\hat{k}$, for the tabulation of angular functions.

One must choose L large enough that the multipole expansion of the Green's function, Equation (11), converges to the desired accuracy. As a function of l, the Bessel functions $j_l(z)$ and $h_l^{(1)}(z)$ are of roughly constant magnitude for $l < z$. For $l > z$, $j_l(z)$ decays rapidly and $h_l^{(1)}(z)$ grows rapidly. While one must choose $L > kd = k|\mathbf{x} - \mathbf{x}' - \mathbf{X}_{mm'}|$ (so that the partial-wave expansion has converged), L cannot be taken to be much larger than $kX_{mm'}$, because the transfer function, Equation (14), will oscillate wildly, causing inaccuracies in the numerical angular integrations of Equations (15) and (23). This condition is a consequence of the interchange of summation and integration in Equation (13). An excellent semi-empirical fit to the number of multipoles required for single precision (32-bit reals) is

$$L_s(kD) = kD + 5\ln(kD + \pi), \tag{24}$$

where $D \geq 1/k$ is the maximum d which will be required (the "diameter" of the basis-function groups). For double precision (64-bit reals), our estimate is

$$L_d(kD) = kD + 10\ln(kD + \pi). \tag{25}$$

If the L dictated by the appropriate formula exceeds $kX_{mm'}$, then the groups are too close to use the FMM, and their interaction must be represented in the sparse matrix Z'.

The K directions $\hat{k}$, at which the angular functions are tabulated, must be sufficient to give a quadrature rule that is exact for all spherical harmonics of order $l < 2L$. A simple method [2] for accomplishing this is to pick polar angles θ such that they are zeros of $P_L(\cos\theta)$, and azimuthal angles ϕ to be $2L$ equally spaced points. Thus, for this choice of $\hat{k} = (\sin\theta\cos\phi, \sin\theta\sin\phi, \cos\theta)$, $K = 2L^2$. If more-efficient quadrature rules for the sphere (of the type described by McLaren [14]) are used, then $K \approx (4/3)L^2$. Since $kD \propto \sqrt{N/M}$, this justifies the assertion made in Section 3.1 that $K \propto N/M$.

5. Application to electromagnetic fields

In the solution of the electric-field integral equation, the impedance-matrix elements take the form [15]

$$Z_{mm'} = -i\sum_{j,j'=1}^{3}\int_s d^2\mathbf{x}\int_s d^2\mathbf{x}' f_{mj}(\mathbf{x}) G_{jj'}(\mathbf{x}-\mathbf{x}') f_{m'j'}(\mathbf{x}'), \tag{26}$$

where

$$G_{jj'}(\mathbf{x}-\mathbf{x}') = \left(\delta_{jj'} - \frac{1}{k^2}\frac{\partial}{\partial x_j}\frac{\partial}{\partial x'_{j'}}\right)\frac{e^{ik|\mathbf{x}-\mathbf{x}'|}}{4\pi|\mathbf{x}-\mathbf{x}'|}, \tag{27}$$

and the indices j, j' label Cartesian components. As implied in Section 1, one can integrate by parts, and simply use the scalar prescription, given above, on the three components of $\mathbf{f}$ and the scalar $\nabla \cdot \mathbf{f}$. This is not, however, the most economical procedure. By differentiating with respect to $\mathbf{d}$ under the integral in Equation (15), we get

$$G_{jj'}(\mathbf{X}+\mathbf{d}) \approx \frac{ik}{4\pi}\int d^2\hat{k}\left(\delta_{jj'}-\hat{k}_j\hat{k}_{j'}\right)e^{ik\cdot\mathbf{d}}\mathcal{T}_L\left(kX,\hat{k}\cdot\hat{X}\right) \quad (28)$$

Now it can be easily seen that the scalar prescription presented in Section 3 can be modified to an electromagnetic one, by promoting the quantities $V_{m\alpha}$, $s_m(\hat{k})$, and $g_m(\hat{k})$ to three-dimensional vectors, with

$$\mathbf{V}_{m\alpha}(\hat{k}) = \int d^2\mathbf{x}\, e^{ik\cdot\mathbf{x}}\left[\mathbf{f}_{n(m,\alpha)}(\mathbf{x}) - \hat{k}\,\hat{k}\cdot\mathbf{f}_{n(m,\alpha)}(\mathbf{x})\right], \quad (29)$$

and using a dot product in the $\int d^2\hat{k}$ term of $B_{m\alpha}$, Equation (23). This method can be implemented using about half the storage of the four-fold use of the scalar formula, because the vector $\mathbf{V}_{m\alpha}$ has only two independent components: $\left[\hat{k}\cdot\mathbf{V}(\hat{k})=0\right]$.

6. Physical interpretation

The physics of the FMM rests on the following fact: given a field, $\psi(\mathbf{x})$, which satisfies the wave equation

$$\left(\nabla^2 + k^2\right)\psi(\mathbf{x}) = 0, \quad (30)$$

for all $\mathbf{x}$ outside a given sphere, the field can be reconstructed everywhere outside that sphere from its far field [16, 17]. This means that if the field is radiated by a source density, $\rho(\mathbf{x})$, supported only within a sphere of radius R centered at the origin,

$$\phi(\mathbf{x}) = \int_{x'<R} d^3\mathbf{x}' \frac{e^{ik|\mathbf{x}-\mathbf{x}'|}}{4\pi|\mathbf{x}-\mathbf{x}'|}\rho(\mathbf{x}'), \quad (31)$$

then the contribution of the "off-shell" ($q^2 \neq k^2$) components in the Fourier expansion of the Green's function [11],

$$\frac{e^{ik|\mathbf{x}-\mathbf{x}'|}}{4\pi|\mathbf{x}-\mathbf{x}'|} = \int \frac{d^3\mathbf{q}}{(2\pi)^3}\frac{e^{i\mathbf{q}\cdot(\mathbf{x}-\mathbf{x}')}}{(2\pi)^3 q^2 - k^2 - i\varepsilon}, \quad (32)$$

(where ε is a infinitesimal positive number, prescribing the correct treatment of the singularity at $q^2 = k^2$) are determined for $x > R$ (after integration over $d^3\mathbf{x}'$) by the radiation condition and the "on-shell" components. The on-shell components, coming from the residue of the pole at $q^2 = k^2$, give the imaginary part of the Green's function, and the off-shell components give the real part. It is important that the off-shell part is *not* determined by the on-shell part for $x' < R$. This is related to the divergence of the series in Equation (11) for $d > X$. This interpretation explains why the far interactions can be computed [Equation (23)]from the radiation pattern $s_m(\hat{k})$ of the mth group. It also clarifies why one only need keep two components in $\mathbf{V}$, $\mathbf{g}$, and $\mathbf{s}$ for the electromagnetic case: the electromagnetic far field is transverse, and has only two independent components.

7. Conclusion

Present methods for computing radar and other scattering cross sections are limited by computer-processing and memory requirements. The significance of the increase in problem size made possible by the FMM can be illustrated by considering the calculation of RCS for X-band radar. With current methods, the size of the largest body that can be accurately modeled is a few feet. With the same computing resources, the techniques that we have described will increase this by at least an order of magnitude. Such computational capabilities would significantly reduce the technological risk of expensive projects employing stealth technology. They may likewise revolutionize other applications of scattering computations, such as high-frequency circuit modeling, sonar, and geophysical applications.

Because the FMM accelerates computation of the matrix-vector product $Z \cdot I$, and thus only indirectly solution of $Z \cdot I = V$, we are frequently asked about the relative merits of direct and iterative solutions, and techniques to reduce the iterations required in a conjugate-gradient type of solution. These are important questions, and are under study by us as well as many others. We consider them to be mostly beyond the scope of this article, but note that the FMM is compatible with "complexification," and with preconditioning by a sparse matrix.

Although we have only demonstrated the use of the FMM for surface-scattering problems, its application to volume-integral equations (necessary for the analysis of penetrable inhomogeneous scatterers) is obvious. When comparison to other techniques for computing the fields of volume source distributions is made, it should be noted that in this case the matrix T in Equation (8) is a strict convolution, and as such can be applied by FFT, resulting immediately in an $O(N \log N)$ algorithm, without further decomposition.

8. Acknowledgment

This research was supported by the Advanced Research Projects Agency of the US Department of Defense, and was monitored by the Air Force Office of Scientific Research under Contracts No. F49620-91-C-0064 and F49620-91-C-0084. The United States Government is authorized to reproduce and distribute reprints for governmental purposes notwithstanding any copyright notation hereon.

9. References

1. V. Rokhlin, "Rapid solution of integral equations of scattering theory in two dimensions," *Journal of Computational Physics*, **86**, 2, pp. 414-439, 1990.

2. V. Rokhlin, "Diagonal form of translation operators for the Helmholtz equation in three dimensions," Technical Report YALEU/DCS/RR-894, Yale University, Department of Computer Science, March, 1992, to be published in *Applied and Computational Harmonic Analysis*.

3. R. F. Harrington, *Field Computation by Moment Methods*, New York, Macmillan, 1968.

4. R. F. Harrington, "Origin and development of the method of moments for field computation," *IEEE Antennas and Propagation Society Magazine*, June, 1990, pages 31-35

5. V. Rokhlin, "Solution of acoustic scattering problems by means of second kind integral equations," *Wave Motion*, 5, pp. 257-272, 1983.

6. A. W. Maue, "Toward formulation of a general diffraction problem via an integral equation," *Zeitschrift für Physik*, 126, pp. 601-618, 1949.

7. A. W. Maue, "Toward formulation of a general diffraction problem via an integral equation," in E. K. Miller, L. Medgyesi-Mitschang, and E. H. Newman (eds.), *Computational Electromagnetics*, New York, IEEE Press, pp. 7-14, 1992, (translated into English from [6]).

8. E. K. Miller, L. Medgyesi-Mitschang, and E. H. Newman (eds.), *Computational Electromagnetics, second edition*, New York, IEEE Press, 1992.

9. J. H. Richmond, "On the variational aspects of the moment method," *IEEE Transactions on Antennas and Propagation*, 39, 4, pp. 473-479, April, 1991.

10. S. M. Wandzura, "Optimality of Galerkin method for scattering computations," *Microwave and Optical Technology Letters*, 4, 5, pp. 199-200, April, 1991.

11. G. Arfken, *Mathematical Methods for Physicists, second edition*, New York, Academic Press, 1970.

12. M. Abramowitz and I. A. Stegun, *Handbook of Mathematical Functions*, (Applied Mathematics Series), Cambridge, MA, National Bureau of Standards, 1972.

13. B. K. Alpert and V. Rokhlin, "A fast algorithm for the evaluation of Legendre expansions," *SIAM Journal of Scientific and Statistical Computing*, 12, pp. 158-179, 1991.

14. A. D. McLaren, "Optimal numerical integration on a sphere," *Mathematics of Computation*, 17, pp. 361-383, 1963.

15. S. M. Rao, D. R. Wilton, and A. W. Glisson, "Electromagnetic scattering by surfaces of arbitrary shape," *IEEE Transactions on Antennas and Propagation*, AP-30, 3, pp. 409-418, May, 1982.

16. A. J. Devaney and E. Wolf, "Radiating and nonradiating classical current distributions and the fields they generate," *Physical Review*, D8, 4, pp. 1044-1047, August, 1973.

17. R. Peierls, *Surprises in Theoretical Physics* (Princeton Series in Physics), Princeton, New Jersey, Princeton University Press, 1979.

Introducing Feature Article Authors

Ronald Coifman is a professor of mathematics at Yale University. He received his PhD from the Universityof Geneva, in 1965. He received his License es Sciences Mathematiques in 1962. Prior to coming to Yale, Prof. Coifman was a professor at Washington University, a visiting professor at Tel-Aviv University, and a visiting assistant professor at the University of Chicago. Prof. Coifman's recent publications have been in the areas of scattering and inverse scattering, nonlinear harmonic analysis, and wavelet theory. He was chairman of theYale Mathematics Department from 1986 to 1989.

Vladimir Rokhlin

Vladimir Rokhlin has been a professor of computer science and mathematics at Yale University since 1985. He received a PhD in Applied Mathematics from Rice University, in 1983, and a MS in mathematics from Vilnius University, Vilnius, Lithuania, in 1973. Prior to joining the faculty at Yale, Prof. Rokhlin worked as a Senior Research Specialist at Exxon; a partner in Livshitz and Associates, Houston, TX; a consultant at Computer Systems, Houston, TX; and as a mathematician at the Institute of Arctic Geology, Leningrad, Russia. Prof. Rokhlin's research has been in the areas of numerical-scattering theory, elliptic partial-differential equations, numerical solution of integral equations, quadrature formulas for singular functions, and numerical complex analysis.

Stephen Wandzura

Stephen Wandzura is a Senior Scientist, Optical Physics Labortory, Hughes Research Laboratories. He received his BS in music from UCLA, in 1971, and his PhD in physics from Princeton University, in 1977. His research has been in diverse areas of scattering and propagation His thesis research could be correctly, if somewhat whimsically, characterized as the study of the "impedance matrix of the proton." As a National Research Fellow with the NOAA, he studied scattering of light by atmospheric turbulence, and the occurrence of mountain lee waves. At HRL, he has worked on classical and quantum optics, especially the theoretical and numerical study of stimulated scattering. For the last three years, he has been studying improvements to moment-method techniques He has published articles in *Physical Review*, *Physical Review Letters*, *Physics Letters*, *Optics Letters*, *Nuclear Physics*, *Wave Motion*, and other journals

Annual Technical Report
FMAH Corporation
FAST METHODS FOR SCATTERING COMPUTATIONS
DARPA (AO7894) Sept 30 1993

Fast Electromagnetic scattering algorithm development.

Summary

The purpose of this project is to develop fast algorithms for computations of electromagnetic scattering (radar), and assist in the implementation in software of these algorithms by the team at Hughes Research Laboratories, who are in charge of the software package development. currently it is impossible to perform these computations in a realistic time frame. It is expected that these methods will clear the computational bottleneck. During the last year (9.92 - 9.93), several related efforts were undertaken in connection with the Hughes Scattering Project.

1. We investigated the properties of the three-dimensional version of the FMM for the Helmholtz equation. While the scheme itself was constructed during the preceeding year, it is sufficiently different from its two-dimensional counterpart that a separate investigation had to be performed to determine the various parameters with which it should be implemented.

2. A new version of the two-dimensional FMM has been implemented to test several recent improvements (applicable both in two and three dimensions). The code has been written, and is currently being experimented with. Following is s brief description of these new developments.

3. A competitive Fast Algorithm based on Local Cosine Transform and

Annual Technical Report

FAST METHODS FOR SCATTERING COMPUTATIONS

DARPA (AO7894)

FAST ELECTROMAGNETIC SCATTERING ALGORITHM DEVELOPMENT.

The purpose of this project is to develop fast algorithms for computations of electromagnetic scattering (radar), and assist in the implementation in software of these algorithms by the team at Hughes Research Laboratories, who are in charge of the software package development. currently it is impossible to perform these computations in a realistic time frame. It is expected that these methods will clear the computational bottleneck. During the last year (9.92 - 9.93), several related efforts were undertaken in connection with the Hughes Scattering Project.

1. We investigated the properties of the three-dimensional version of the FMM for the Helmholtz equation. While the scheme itself was constructed during the preceeding year, it is sufficiently different from its two-dimensional counterpart that a separate investigation had to be performed to determine the various parameters with which it should be implemented.

2. A new version of the two-dimensional FMM has been implemented to test several recent improvements (applicable both in two and three dimensions). The code has been written, and is currently being experimented with. Following is s brief description of these new developments.

a. A scheme has been constructed implementing the "sub-wavelength" FMM. As is well-known, on the sub-wavelength scale, the behavior of

unmodified scheme.

c. The above two developments were incorporated into the two-dimensional algorithm; the resulting scheme breaks even with the direct one at $n \sim 500$, which is only a few times worse than the results for the FMM for the Laplace equation in two dimensions. It appears that further improvements in the speed of the two-dimensional FMM for the Helmholtz equation will be very hard to obtain; also the speed of the existing method is quite satisfactory. The improvements easily generalize to the three-dimensional case, and will be tested in that case shortly.

3. One of pervasive problems encountered in the design of boundary integral schemes (both fast and classical ones) is that of quadratures. The Nyquist Theorem demands that at least two points per wavelength on the boundary be employed; for curved boundaries, a more subtle analysis yields an estimate of 3 - 4 nodes per wavelength. In most schemes, the number used is closer to 20 nodes per wavelength, though sometimes 10 are sufficient. The actual number required is determined by the quality of the quadrature formulae employed, and these pose a number of difficulties. Indeed, the solution of the Helmholtz equation in two dimensions requires the integration of functions of the form

$$f(x) = \phi(x) + \psi(x) \cdot log(x),$$

with ϕ, ψ smooth functions.

The problem is that in most cases, the function f can only be evaluated as a whole, while the functions ϕ, ψ are not available separately. Thus, quadratures are required that will integrate with reasonable accuracy functions of the form In [myquad, alperquad], end-point corrected

trapezoidal quadrature rules are derived for functions of that form, but the highest order of convergence they achieve is about 4; for higher orders, the weights of the quadrature begin to grow. Recently, we discovered that Gauss quadrature rules can be generalized to these functions . In fact, a much more extensive generalization of Gauss quadratures has been constructed. Namely, there exists a very wide class W of functions $[0,1] \rightarrow R^1$, such that for any $s \in W$, there exists an n-point quadrature that integrates exactly all functions of the form

$$f(x) = P(x) + Q \cdot s(x),$$

with P, Q arbitrary polynomials of order n-1.

All weights of this quadrature are positive, and all nodes lie on the interval $[0,1]$. While the exact description of W is not available (and not needed), it contains functions of the form x^γ with all $\gamma \in (-1,1)$, functions $(log(x))^\gamma$ with all $\gamma \in (-\infty,\infty)$, all products of such functions, and many others. Applications of such quadrature rules are obviously quite wide, and a report describing a numerical scheme for their evaluation is in preparation.

4. Finally, it appears that fast algorithms are possible for the solution of Boundary Integral equations of scattering theory in the time domain (as opposed to the existing schemes working for the frequency domain scattering, i.e. Helmholtz equation). Such algorithms, if possible, promise to be much faster than the frequency domain ones, whenever the solution is required at many frequencies. They are also likely to be more robust, since in the time domain, scattering problems are hyperbolic, and their numerical treatment does not involve solution of ill-conditioned

systems of linear algebraic equations, which is a major problem with the Helmholtz equation (the notorious "spurious resonances"). This work is very preliminary, and we can not guarantee its success. In a parallel direction we have explored the efficacy of using Local Cosine transform method as a simpler direct approach. While initially this approach did not seem to be competitive it turns out that by further processing with wavelets it could become a viable alternative in smooth geometries. The following is a summary of this effort.

Fast Numerical Computations of Ocsillatory Integrals Related to Acoustic Scattering I

We prove that certain oscillatory boundary integral operators occurring in acoustic scattering computations become sparse when represented in the appropriate local cosine transform orthonormal basis. In a subsequent papers with Yves Meyer, Thierry Paul and Vladimir Rokhlin it is shown that most pseudo differential and Fourier Integral operators are also sparse relative to these bases.

In this paper we relate the location of large coefficients in the matrix realization to the geometry of the boundary on which the integral operator is defined. The sparse matrices obtained here represent the oscillatory (non geometric optic) interactions between regions on the boundary.

The method presented here provides numerical algorithm of asymptotic order $CN \log N$ for the application of an operator to a vector on boundaries with bounded curvature (these algorithms with further processing are almost immediately competitive as demonstrated by Coifman-

Rokhlin).

We refer to work by V. Rokhlin where faster algorithms are obtained for solutions of the Helmholtz equation with no regularity assumptions. His work is specific to solutions of Helmholtz equation and relies on specific properties of such solutions. While ours is simpler in nature viewing the operators as "perturbations" of convolutions, and is essentially dependent on the smoothness of underlying structures.

We also mention that computations for acoustic scattering based on the LCT bases where carried out by F. Canning with good results.

§1. A Model Operator.

For simplicity we treat a model oscillatory operator in $\mathbf{R}^2$. This treatment will enable us to concentrate fully on the oscillatory nature of the integral (the mild singularity occurring in the Green's function of the Helmholtz is a distraction). The extension to higher dimensions is straightforward (and will be described).

Let Γ be a closed curve of length L and bounded curvature (say both bounded by 2), and s be arc length parametrization, $z(s) \in \Gamma \qquad 0 \leq s \leq L$. We consider

$$H_\nu(f)(s) = \int_0^L e^{i\nu|z(s)-z(t)|} f(t)dt$$

where ν is a large constant $\nu \geq 100$. In order to discretize this integral we need to resolve the oscillation, i.e. to have N discretization points with $N \geq 2\nu L$, in order to construct appropriate quadrature formulas to convert H to a discrete sum. An equivalent method consists of finding a finite orthonormal basis with N elements and with the same resolution

and consider the operator $H_N = P_N H P_N$ where P_N is the orthogonal projection on the span of the basis function.

§2. The Local Trigonometric Basis Functions on Γ.

We pick a partition of Γ into M intervals $I_i = (a_i, a_{i+1}), a_{M+1} = a_0$ and a collection of smooth window functions $b_i(s)$ supported in $I_{i-1} \cup I_i \cup I_{i+1}$ such that

1^0 $\sum_{i=1}^{M} b_i^2(s) = 1.$

2^0 $b_i(s) = b_{i-1}(2a_i - s).$

It is proved in [CM] that the functions

$$C_k^i(s) = b_i(s) \left(\frac{2}{a_{i+1} - a_i} \right)^{1/2} \cos \left((k + \frac{1}{2}) \pi \frac{s - a_i}{a_{i+1} - a_i} \right)$$

form an orghonormal basis of $L^2(\Gamma, ds)$. It is also clear that the real discrete version, where s form N equispaced discrete set of points and $0 \leq k \leq N-1$ form an orthonormal basis of $\mathbf{R}^N$ (provided the a_i are midpoints between adjacent s).

In our treatment we will discuss only the continuous version, having in mind the discretization for which the oscillation range is limited. In particular, we will pick the points a_i to be equispaced with $a_i - a_{i+1} = \frac{L}{\sqrt{N}} = \eta$ and on each I_i we will consider only $k < \sqrt{N}$. This corresponds to a discrete basis for Γ with N discrete equispace points and each I_i having $\sqrt{N}$ points. In this case, if we let $\alpha_i = \frac{a_i + a_{i+1}}{2}$ we can take the basis to have the form

$$C_k^i(s) = \left(\frac{2}{\ell} \right)^{1/2} b \left(\frac{s - \alpha_i}{\eta} \right) \cos \left((k + \frac{1}{2}) \pi \frac{s - a_i}{\eta} \right) \qquad 0 \leq i, k < \sqrt{N}$$

where $\eta = \frac{L}{\sqrt{N}}$.

If we let P_N be the orthogonal projection on the span of these functions, it is obvious that $P_N \to$ Identity ad $N \to \infty$. It is also clear that the basis functions themselves do not converge to a basis as $N \to \infty$.

We would like to point out that we are forced to segment the curve in at least $\sqrt{N}$ windows if we want to restrict the frequencies to be less than $\sqrt{N}$.This restriction is necessary if we wish to have some freedom in choosing a parametrization of a curve (or allow mildly non equispace points). Such a constraint will be a requirement in surfaces where we do not dispose of a natural arc length parametrization. These choices guarantee that the transition matrix among the basis given in different, smoothly related parametrizations, is sparce [CM].

§3. The Matrix Estimates.

We fix $I_i, I_j \qquad i \neq j$ and consider the block of coefficients representing the interaction between these windows

$$\begin{aligned} A^{i,j}_{k,\ell} &= \langle H_N C^i_k, C^j_\ell \rangle \\ &= N \int_0^L \int_0^L e^{i\nu|z(s)-z(t)|} b\left(\frac{t-\alpha_i}{\eta}\right) b\left(\frac{s-\alpha_j}{\eta}\right) \\ &\qquad \cos\left[(k-\frac{1}{2})\pi\frac{t-a_i}{\eta}\right] \cos\left((\ell+\frac{1}{2})\pi\frac{s-a_j}{\eta}\right) dsdt \\ 0 \leq k < \sqrt{N} &\qquad 0 \leq \ell < \sqrt{N} \end{aligned}$$

Given a precision threshold ε we would like to find all k, ℓ for which

$$|A_{k,\ell}{}^{i,j}| < \varepsilon.$$

We change variables $s - a_j = \eta u \qquad (t - a_i) = \eta v$

$$= \int_{\mathbf{R}} \int_{\mathbf{R}} e^{iN|z(a_j+\eta u)-z(a_i+\eta v)|} b(v-\frac{1}{2}) b(u-\frac{1}{2}) \cos\left[(k+\frac{1}{2})\pi v\right] \cos\left[(\ell+\frac{1}{2})\pi u\right].$$

We represent cos as a combination of exponentials leading us to estimate the integrals.

$$\int_{-1}^{1}\int_{-1}^{1} e^{i\nu|z(a_j+\eta u)-z(a_i+\eta v)|}\beta(v)\beta(u)e^{i\pi(\mp kv\pm \ell u)}dudv$$

where $\beta(u) = b(u-\frac{1}{2})e^{\pm i\pi\frac{1}{2}u}$ or

$$(*) \qquad \iint \beta(u)\beta(v)e^{i\emptyset_N(u,v,k,\ell)}dudv.$$

Thus

$$\frac{\partial \emptyset_N}{\partial u} = \nu\eta\frac{z'(a_j+\eta u)\cdot(z(a_j+\eta u)-z(a_i+\eta v)}{|z(a_j+\eta u)-z(a_i+\eta v)|}\pm\pi\ell$$
$$\frac{\partial \emptyset_N}{\partial v} = -\nu\eta\frac{z'(a_i+\eta v)\cdot(z(a_j+\eta u)-z(a_i+\eta v)}{|z(a_j+\eta u)-z(a_i+\eta v)|}\pm\pi k.$$

But

$$z'(a_j+\eta u) = z'(a_j)+O((\eta u)) = z'(a_j)+O(\left(\frac{1}{\sqrt{N}}\right)$$
$$z'(a_i+\eta v) = z'(a_i)+O\left(\frac{1}{\sqrt{N}}\right)$$

if we write

$$\Delta(u,v) = \frac{z(a_j+\eta u)-z(a_i+\eta v)}{|z(a_j+\eta u)-z(a_i+\eta v)|}$$

then

$$\frac{\partial \emptyset_N}{\partial u} = \sqrt{\nu}\left\{z'(a_j)\cdot\Delta(u,v)\pm\pi\frac{\ell}{\sqrt{N}}\right\}+O(1) \qquad |O(1)|\le 1$$
$$\frac{\partial \emptyset_N}{\partial v} = +\sqrt{\nu}\left\{-z'(a_i)\Delta(u,v)\pm\pi\frac{k}{\sqrt{N}}\right\}+O(1).$$

We observe that, as u,v vary so as to parametrize I_iI_j, $\Delta(u,v)$ describes a unit vector on an arc of the unit circle whose length is of the order $\frac{1}{r_{i,j}}$ where $r_{i,j} = 1+$ distance between the windows in units of η.

Therefore the set of points $(z'(a_j)\cdot\Delta(u,v), -z'(a_i)\cdot\Delta(u,v))$ describe an arc of an ellipse of length $\leq \frac{c}{r_{i,j}}$.

If the distance of $\left(\pm\frac{k}{\sqrt{N}}, \pm\frac{\ell}{\sqrt{N}}\right)$ to this arc exceeds $\delta + 1/\sqrt{N}$ then

$$|\nabla\emptyset(u,v)| \geq \delta.$$

A simple integration by part argument proves that $*$ is dominated by $\frac{c_j}{\delta_j}$ for all j and some constants c_j depending only on the function $b(u)$. Fixing j, picking ν so that $\left(\frac{c_j}{\delta j}\right) < \epsilon$ we find that all grid points $\frac{1}{\sqrt{N}}(k,\ell)$ in the square $[-1,1]\times[-1,1]$ whose distance from the arc of ellipse of length $\frac{1}{r_{ij}}$ exceeds $\delta/\sqrt{N}$ give rise to a matrix entry less than ϵ.

The number of grid points not satisfying this condition is $\delta\frac{\sqrt{N}}{r_{ij}}$

We observe that $r_{ij} \cong |i-j|+1$ (with possibly a few exceptions) permitting us to estimate the total number of coefficients $|A^{i,j}_{k,\ell}| > \epsilon$ by

$$C\delta\sqrt{N}\cdot\sqrt{N}\sum_{d=1}^{\sqrt{N}}\frac{1}{d} \leq C\delta N\log N.$$

We remark also that if the curve has a corner or an irregular region of size $\frac{1}{\sqrt{N}}$ with $\sqrt{N}$ discretization points, we can take on such a window basis of $\sqrt{N}$ step functions leading to an estimate a $\left|\frac{\partial\emptyset_N}{\partial u}\right| > \delta$ for all windows ℓ outside an interval of length $\frac{1}{r_{ij}}$, giving the count of entries (k,ℓ) for which $|A^{i,j}_{k,\ell}| \geq \epsilon$ as $\delta\frac{\sqrt{N}}{r_{ij}}\sqrt{N}$ where i_0 denotes the index of a bad window.

Summation over j leads to

$$C\delta N\log N.$$

See enclosed figures where the matrix of interactions of two windows is represented at different level of precision.

§4. Higher Dimensions.

We observe that in $\mathbf{R}^2$ we can take any collection of nonoverlapping rectangles with sides parallel to the axis and with some care construct an orthonormal basis of LCT where orthogonality is maintained by picking the basis to be odd on the southern and western edges and even on the northern and eastern edges, i.e. if

$$R_i = (\alpha_i \beta_i) \times (\gamma_i, \delta_i)$$

then

$$S^i_{k,\ell}(x_1, x_2) = \beta_i(x_1, x_2) \sin\left[(k + \frac{1}{2})\pi \frac{x_1 - \alpha_i}{\beta_i - \alpha}\right] \sin\left[(\ell + \frac{1}{2})\pi \frac{x_2 - \gamma_i}{\delta_i - \gamma_i}\right]$$

where $\Sigma B_i^2 = 1$ and $B_i B_j$ are mirror images of each other around a common edge of R_i and R_j.

For a closed surface Γ on which a global parametrization does not exist, in general, the simplest approach is to decompose Γ into patches of roughly the same size on which an orthogonal basis can be taken. This leads to a number of exceptional regions which can be handled separately. We illustrate these issues for the sphere on which we take the natural "geographic coordinates". With the exception of the polar caps it is easy to obtain a "rectangular" patching by patches of roughly the same size on which a local cos basis exists. On the poles we can take a basis of simple bump functions and count their contributions in the same way we handled corners on curves.

The geometry of a cap of radius η and orthogonal bump function bases on it can be obtained as follows: Let $\eta = 2^{-j}$, consider radial

functions $b_i(r)$ such that $\sum_1^j b_i^2 = 1$. b_i is supported in $\left(\frac{3\eta}{2^{i+1}}, \frac{3\eta}{2^i}\right)$ and $b_i(r) = b_{i+1}\left(2\frac{\eta}{2^i} - r\right)$.

Clearly the functions

$$b_i(r)\sin\left[(k+\frac{1}{2})\pi\left(\frac{r-\eta/2^i}{\eta/2^i}\right)\right]e^{i\ell\theta} \qquad k \le 2^{j-i}, \ell \le 2^{j-i}$$

form an orthogonal set of functions resolving a discretization of resolution η^2 with total number of functions $2^{2j} = \eta^2$. Moreover, they are orthogonal to the basis function on the complement of the cap, provided these are even in r around the cap's circumference.

It is quite clear that, with the exception of a few cap-like exceptional regions, each surface can be treated by a similar procedure by slicing it into parallel "circular" slices whose boundaries are in turn windowed as curves.

§5..

We now wish to describe the analysis for the Helmholtz operator on a surface S.

$$\mathcal{H}_\nu(f) = \int_S \frac{e^{i\nu|s-y|}}{|x-y|} f(y) d\sigma(y)$$

where $d\sigma(y)$ is surface measure on S. Since the sparcity of the matrix of $\mathcal{H}_\nu$ is due to oscillation where $|x-y|$ is "large" we could, in this case, only consider interactions between non-neighboring patches on which $|x-y|$ is smooth, and we can essentially ignore the "singularity" in this analysis.

As before, the unit of discretization is $\approx \frac{6}{\nu}$ resulting in roughly $\frac{1}{\nu 2} = N^2$ points. The window size for a patch is $\eta \times \eta$ with $\eta \simeq \frac{1}{\nu^{\frac{1}{2}}}$ $\eta^{-2} \cong N$, each patch has $\frac{1}{\eta} \times \frac{1}{\eta} \cong N$ points.

Let Q_iQ_j be two non-neighboring patches at distance $\simeq r_{ij}\eta$ from each other. Assume that S is a parametrization of Q_i, t of Q_j. As before we need to estimate

$$\frac{1}{\eta^4}\int_{Q_1}\int_{Q_j} e^{i\nu|x(s)-x(t)|}b_i(s)b_j(t)e^{(ik\cdot s/\eta+\ell\cdot t/\eta)}d\sigma(s)d\sigma(t).$$

By rescaling to the product of unit squares we get

$$\iint e^{i\nu|(x(a_i+\eta u))-x(a_j+\eta v)|}b(u)b(v)e^{i(ku\pm\ell v)}dudv.$$

As before, let $\Phi = N|(a_i+\eta u)-x(a_j+\eta v)|+k\cdot u\pm\ell\cdot v$, and for simplicity we write

$$x(a_i+\eta u) = x(a_i)+u\cdot\eta(u_1\cdot\overrightarrow{T}_1+u_2\overrightarrow{T}_2)+O(\eta^2u^2)$$

$$\frac{\partial x}{\partial u_i} = \eta\overrightarrow{T}_i+O(\eta^2u)$$

$$\frac{1}{\sqrt{N}}\frac{\partial\emptyset}{\partial u_i} = \frac{\nu\eta}{\sqrt{N}}T_i\cdot\frac{(x(a_i+\eta u)-x(a_j+\eta v)}{|x(a_i+\eta u)-x(a_j+\eta v)|}+O\left(\frac{1}{\sqrt{N}}\right)\pm\frac{k_i}{\sqrt{N}}.$$

As u_1u_2 vary the first terms are the coordinates of points on an ellipse of length $\approx\frac{1}{r_{ij}}$. Therefore, the number of grid points k such that $\frac{k}{\sqrt{N}}$ is at distance $\leq\frac{\delta}{\sqrt{N}}$ from the ellipse is $\delta\frac{\sqrt{N}}{r_{ij}}$. If we include the v coordinates the number of pairs $\left(\frac{k}{\sqrt{N}},\frac{\ell}{\sqrt{N}}\right)$ at distance $\leq\frac{\delta}{\sqrt{N}}$ from the corresponding surface is $\delta^2\frac{N}{r_{ij}^2}$. For all other pairs $(k,\ell)\frac{1}{\sqrt{N}}$, the gradient of the phase function exceeds δ.

The number of matrix entries resulting from all non-neighbor interaction kept is

$$N\delta^2\sum_j\frac{N}{r_{ij}^2}\leq c\delta^2N^2\log N.$$

For the contribution of the interaction of the polar caps basis with the more regular basis functions we only use the gradient of the phase in u

or v (as we did for corners on a curve) leading to a total matrix having $CN^2 \log N$ entries.

We remark that we can, as in one dimensions, allow conical singularities around which we place caps. For corner singularities along a smooth curve we can introduce a local basis, smooth in directions parallel to the wedge and non smooth transversally, leading to small estimates in three of the coordinates and again leading to $N^2 \log N$ algorithms.

We now need to deal with the singularity effect on the interaction of a window with its close neighbor, or with itself. This leads to a computation of

$$\iint \frac{e^{i\nu|x(a+\eta u)-x(a+\eta v)|}}{|x(a+\eta u)-x(a+\eta v)|} b(u)b(v)e^{i\pm(ku+lv)}dudv.$$

This integral can be easily estimated by parametrizing the surface in terms of its tangent plane at the center of the box. This parametrization permits us to write

$$|x(a+\eta u)-x(a+\eta v)| = \eta|u-v|\{1+\eta\emptyset_\eta(u,v)\}$$

where the "remainder" $\emptyset_\eta(u,v)$ has bounded derivatives.

We are therefore led to compute

$$\sqrt{N}\iint \frac{e^{i\sqrt{N}|u-v|}}{|u-v|}\beta_N(u,v)e^{i\pm k\cdot u\pm \ell v}dudv$$

where $\beta_N(u,v)$ is supported in $|u| \le 1$ $|v| \le 1$ has derivatives bounded independently of N.

We can use the following lemma to prove that the matrix is concentrated near the entries $k = \pm\ell$.

LEMMA. *Let* $k(u) \in L^1(\mathbf{R}^2)\beta \in L^1(\mathbf{R}^4)$ *then*

$$\iint_{\mathbf{R}^4} k(u-v)\beta(u,v)e^{iku+\ell v}dudv = \int_{\mathbf{R}^2} \hat{k}(\xi)\hat{\beta}(k-\xi,\ell+\xi)d\xi$$

where $\hat{k}$ *is the Fourier transform in* $\mathbf{R}^2$ *of* k *and* $\hat{\beta}$ *is the Fourier transform in* $\mathbf{R}^4$ *of* β.

In our case $|\hat{\beta}_N(\xi,\eta)| \leq \frac{C_M}{(1+|\xi|+|\eta|)^{M+1}}$ for each $M > 0$ (since the derivatives of β_N are bounded uniformly in N. Also

$$k_N(u) = \sqrt{N}\frac{e^{i\sqrt{N}|u|}}{|u|}\chi_2(u) \text{ where } \chi_2 = \begin{cases} 1 & |u| < 2 \\ 0 & |u| > 2 \end{cases}$$

is such that $|\hat{k}_N(\xi)| \leq C\sqrt{N}$, leading us to estimate the k,ℓ entry by

$$\sqrt{N}\int_{\mathbf{R}^1} \frac{C_M}{(1+|\xi-\ell|+|\xi-k|)^{M+1}}d\xi \leq \frac{C_M\sqrt{N}}{1+|k\pm\ell|^M}$$

Again counting the total number of terms in self window interactions leads to N^2 terms.

Altogether, for N^2 discretisation points we obtain a matrix having order $CN^2 \log N$. These estimates are asymptotique in nature ,their usefullness depends on the desired precision ,as is obvious from the figures . V Rokhlin and the authors have shown that with further processing these algorithms are competetive for relatively small values of N starting at about 1000.

REFERENCES

1. R. Coifman, Y. Meyer, and V. Wickerhauser, ***Wavelet Analysis and Signal Processing Proceeding conference on Wavelets Lowell Mass 1991.***
2. R. Coifman and Y. Meyer, *Remarques sur l'analyse de Fourier à fenêtre*, série I, C. R. Acad. Sci. Paris **312** (1991), 259–261.
3. V.Rokhlin, *Diagonal forms of translation operators for the Helmholtz equation in three Dimensionsand Computational Harmonic Analysis 1. 1993..*

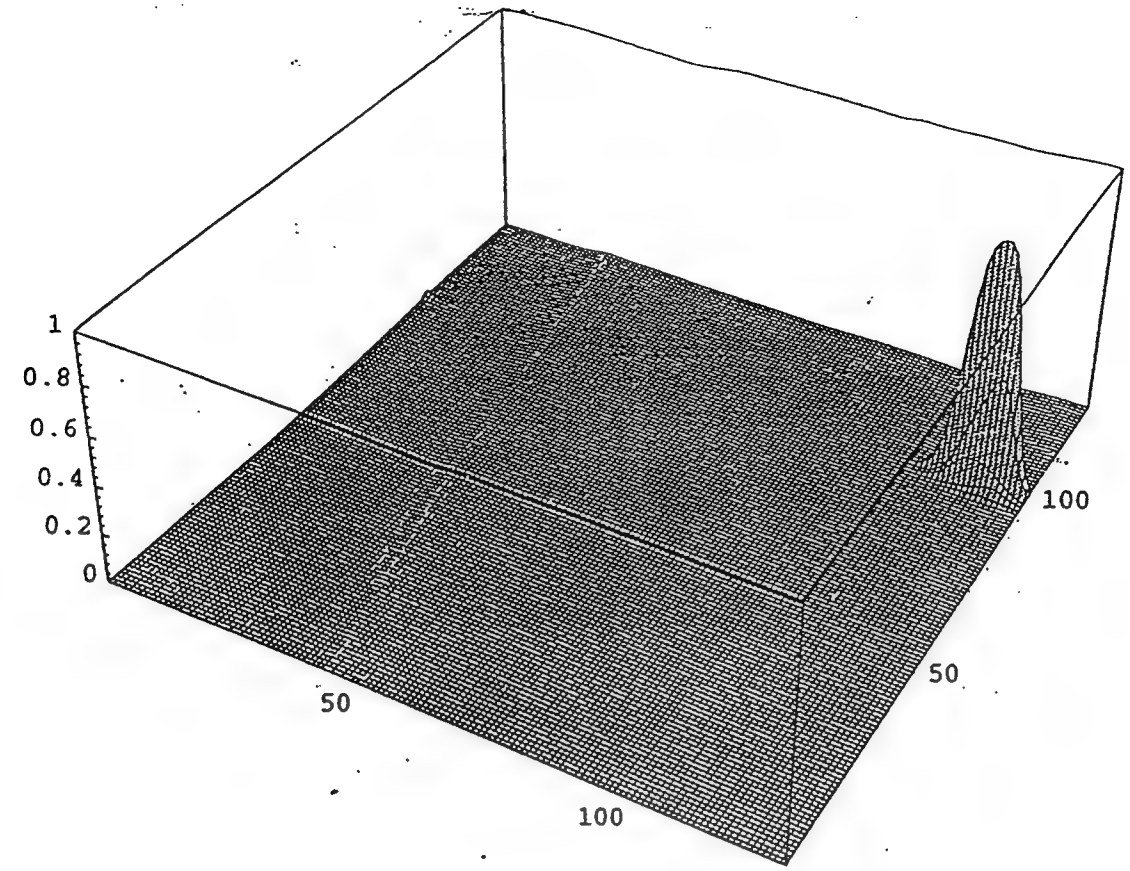
1
0.8
0.6
0.4
0.2
0
50
100
50
100

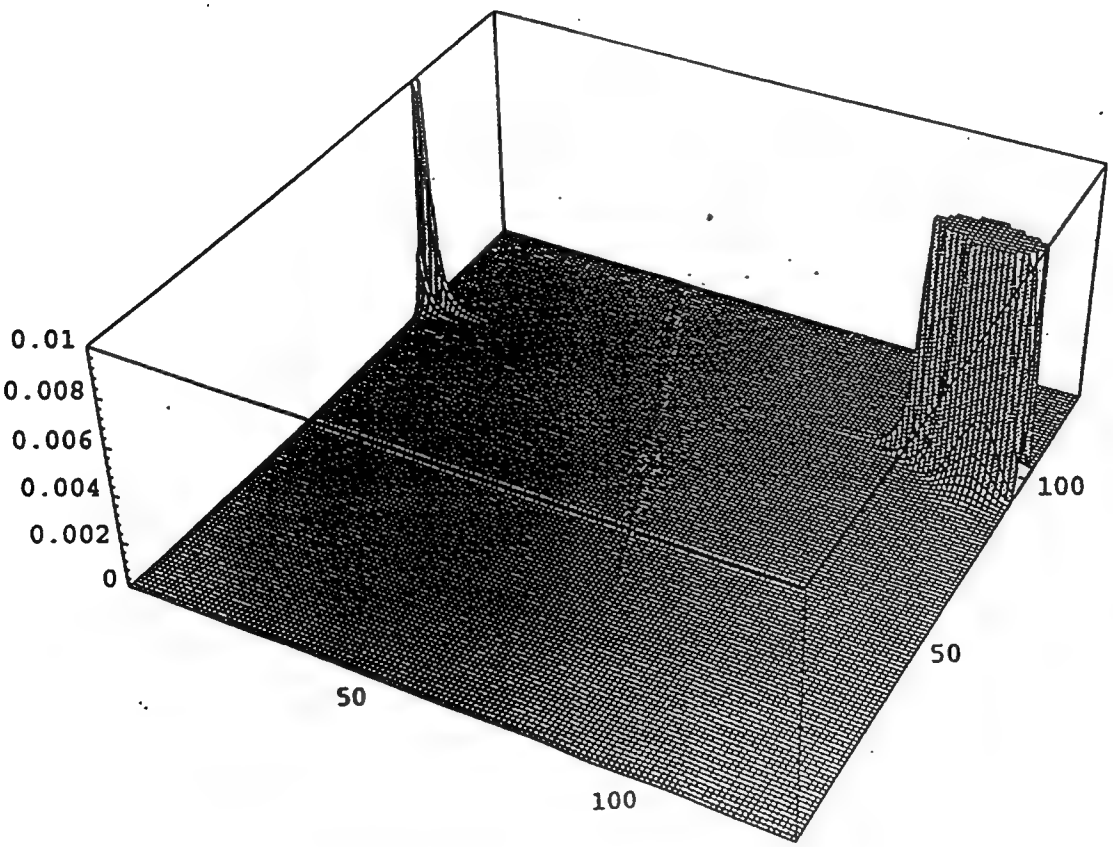
0.01
0.008
0.006
0.004
0.002
0
50
100
50
100

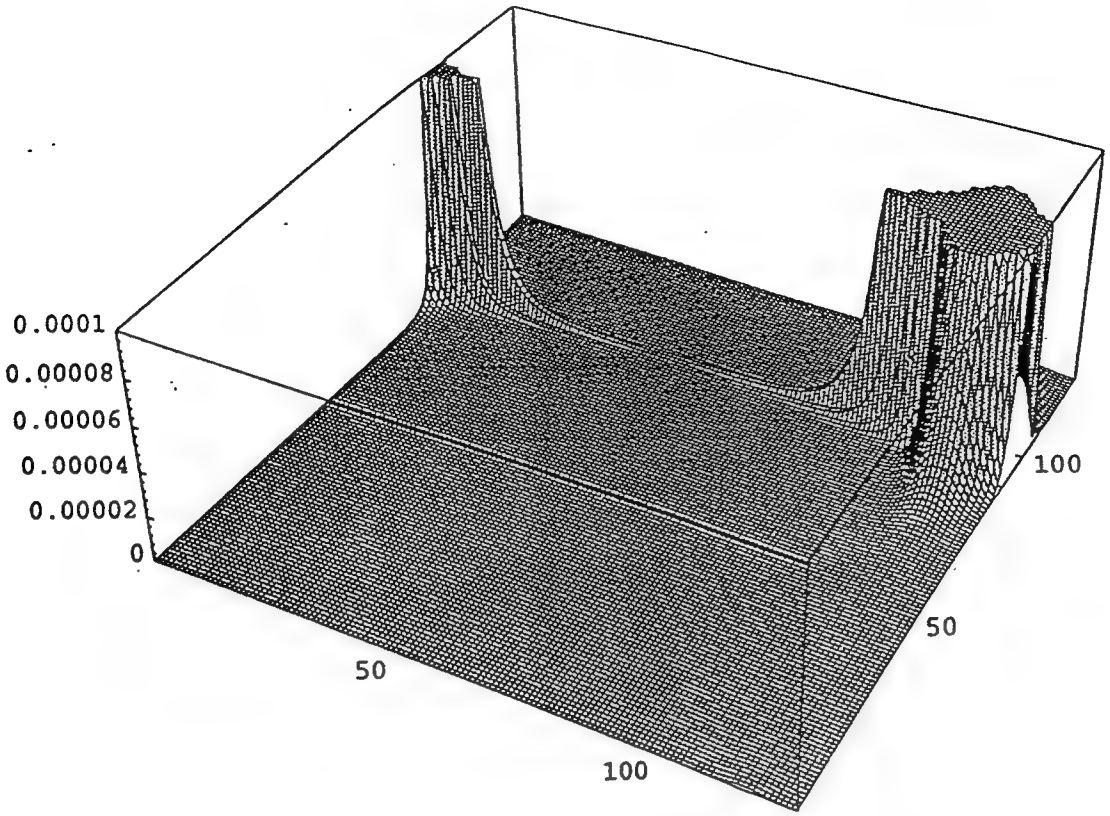
0.0001
0.00008
0.00006
0.00004
0.00002
0
50
100
50
100

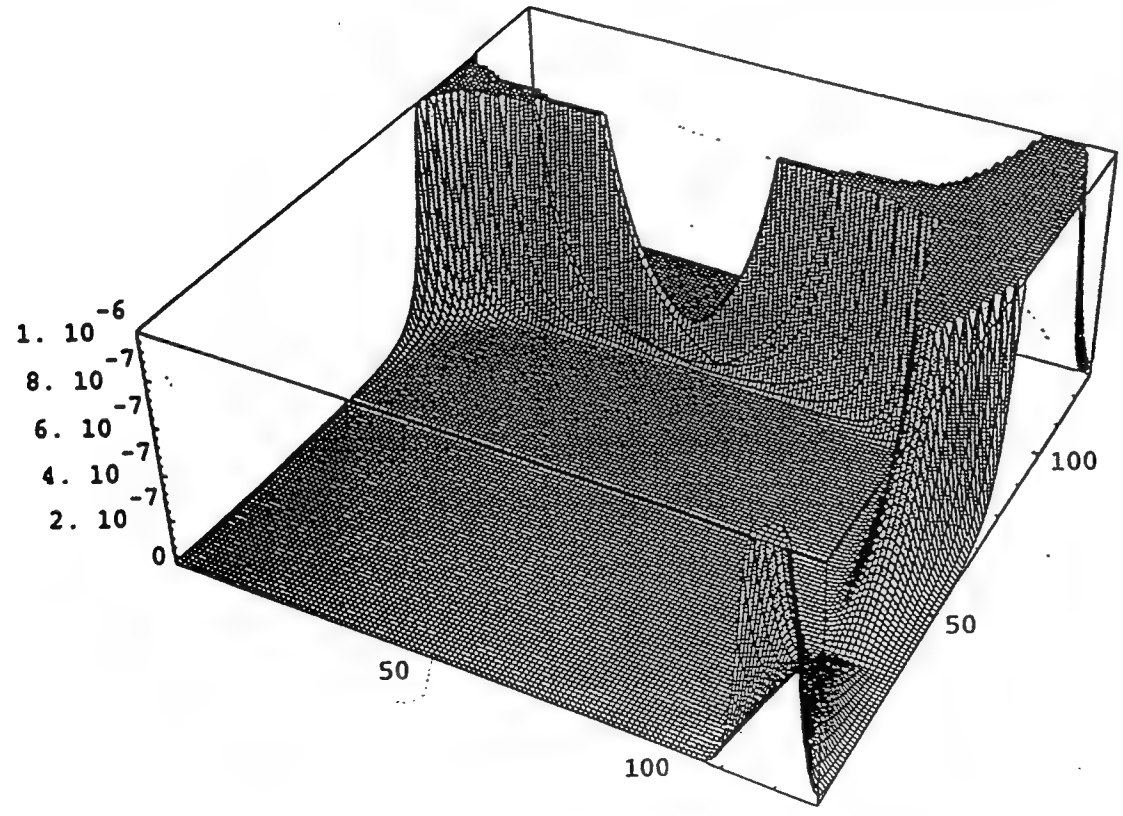
1. 10^-6
8. 10^-7
6. 10^-7
4. 10^-7
2. 10^-7
0
50
100
50
100

The diagonal forms are constructed for the translation operators for the Helmholtz equation in three dimensions. While the operators themselves have a fairly complicated structure (described somewhat incompletely by the classical addition theorems for the Bessel functions), their diagonal forms turn out to be quite simple. These diagonal forms are realized as generalized integrals, possess straightforward physical interpretations, and admit stable numerical implementation. This paper uses the obtained analytical apparatus to construct an algorithm for the rapid application to arbitrary vectors of matrices resulting from the discretization of integral equations of the potential theory for the Helmholtz equation in three dimensions. It is an extension to the three-dimensional case of the results of [13], where a similar apparatus is developed in the two-dimensional case.

Diagonal Forms of Translation Operators for the Helmholtz Equation in Three Dimensions

V. Rokhlin
Fast Mathematical Algorithms and Hardware Corporation
May 5, 1992

This research was performed under DARPA Contract F49620/91/C/0084

Diagonal Forms of Translation Operators for the Helmholtz Equation in Three Dimensions

1. Introduction

One of standard approaches to numerical treatment of boundary value problems for elliptic partial differential equations (PDEs) calls for converting them into second kind integral equations (SKIEs) with subsequent discretization of the latter via appropriate quadrature formulae. Discretization of the resulting SKIEs usually leads to dense large-scale systems of linear algebraic equations, which are in turn solved by means of some iterative technique, such as Generalized Conjugate Residual algorithm. Most iterative schemes for the solution of linear systems of this type require application of the matrix of the system to a sequence of recursively generated vectors. Applying a dense matrix to a vector is an order n^2 procedure, where n is the dimension of the matrix, which in this case is equal to the number of nodes in the discretization of the domain of the integral equation. As a result, the whole process is at least of the order n^2, and for many large scale problems, this estimate is prohibitively large.

During the last several years, a group of algorithms has been introduced for the rapid application to arbitrary vectors of matrices resulting from the discretization of integral equations from several areas of applied mathematics. The schemes include the Fast Multipole Method for the Laplace equation in two and three dimensions (see, for example, [6]), the fast Gauss transform (see [8]), the Fast Laplace Transform (see [12, 15]), and several other schemes. In all cases, the resulting algorithms have asymptotic CPU time estimates of either $O(n)$ or $O(n \cdot log(n))$, and are a dramatic improvement over the classical ones for large-scale problems.

All such schemes are based on one of two approaches.

1. The first approach utilizes the fact that the kernel of the integral operator to be applied is smooth (away from the diagonal or some other small part of the matrix), and decomposes it into some appropriately chosen set of functions (Chebychev polynomials in [12] and [2], wavelets in [4], wavelet-like objects in [3], etc.). This approach is extremely general and easy to use, since a single scheme is applicable to a wide class of operators.

2. The second approach is restricted to the cases when the integral operator has some special analytical structure, and uses the corresponding special functions (multipole expansions for the Laplace equation in [6], [7], Hermite polynomials in [8], Laguerre polynomials in [15], etc.

In this approach, a special-purpose algorithm has to be constructed for each narrow class of kernels, and in each case the appropriate special functions and translation operators for them (historically known as Addition Theorems) have to be available. However, once constructed, such algorithms tend to be extremely efficient. In addition, there are several important situations where the first approach fails, but the second can be used (a typical example is the n-body graviational problem with a highly non-uniform distribution of particles, as in [5]).

Both of the above approaches fail when the kernel is highly oscillatory, and simple counter-examples show that it is impossible to construct a scheme that would work in the general oscillatory case (the Nyquist theorem being the basic obstacle). However, several oscillatory problems are of sufficient importance that it is worth-while to construct special purpose methods for them. A typical example are kernels satisfying the Helmholtz equation in two and three dimensions, since this is the equation controlling the propagation of acoustic and electromagnetic waves, and many quantum-mechanical phenomena. Unlike the non-oscillatory case, the oscillatory one requires a fairly subtle mathematical apparatus, and for the Helmholtz equation in two dimensions, such an apparatus is constructed in [13].

The present paper presents an extension of the results of [13] to the three-dimensional case, and a description of an algorithm for the rapid application to arbitrary vectors of matrices resulting from the discretization of integral equations of the potential theory for the Helmholtz equation in three dimensions. The principal purpose of this paper are Theorems 3.1 - 3.3, describing the diagonal forms of the well-known translation operators for the Helmholtz equation in three dimensions.

2. Analytical and Numerical Preliminaries

2.1. Notation. We will be denoting by (ρ, θ, ϕ) the spherical coordinates in R^3, with the Euclidean coordinates denoted by (x, y, z). Given a point s on the two-dimensional sphere S^2, we will denote its spherical coordinates by $(\theta(s), \phi(s))$, and note that the north pole s_N has the coordinates $(\pi, *)$, while the coordinates of the south pole s_S are $(0, *)$.

We will denote by E the natural embedding $S^2 \to R^3$, defined by the formula

$$E(s) = (cos(\theta(s)) \cdot cos(\phi(s)), cos(\theta(s)) \cdot sin(\phi(s)), sin(\theta(s))). \tag{1}$$

For a non-zero vector $u \in R^3$, we will denote by $P(u)$ the point on S^2 defined by the formula

$$P(u) = E^{-1}(\frac{u}{\|u\|}). \tag{2}$$

Sometimes, we will use a more invariant notation, saying that the pair $(r \in R^1, s \in S^2)$ is the spherical coordinates of the point $u \in R^3$, with r, s defined by the formulae

$$r = \|u\| \tag{3}$$

$$s = P(u). \tag{4}$$

For a pair of points $s_0, s \in S^2$, we will denote by $A_{s_0}(s)$ the angle between the vectors $E(s_0)$, $E(s)$.

Finally, for any $s_0, s \in S^2$, we will denote by $c(s_0, s)$ the cosine of the angle between the vectors $E(s_0)$, $E(s)$, so that

$$c(s_0, s) = (E(s_0), E(s)) = cos(A_{s_0}(s)). \tag{5}$$

2.2. Charges and dipoles. For a Helmholtz equation

$$\nabla^2 f + k^2 f = 0 \tag{6}$$

we will define the potential $f^k_{x_0} : R^3 \setminus \{x_o\} \to C^1$ of a unit charge located at the point $x_0 \in R^3$ by the formula

$$f^k_{x_0}(x) = h_0(k\|x - x_0\|), \tag{7}$$

where h_0 denotes the spherical Hankel function of order zero (see (16) below). For any $h \in R^3$ such that $\|h\| = 1$, we will define the potential $f^k_{x_0,h}$ of a unity dipole located at x_0 and oriented in the direction h by the formula

$$f^k_{x_0,h}(x) = -h_1(k\|x - x_0\|) \cdot \frac{k(x - x_0, h)}{\|x - x_0\|}. \tag{8}$$

As is well known, both potentials $f^k_{x_0}$, $f^k_{x_0,h}$ (as well as most other physically meaningful potentials for the equation (6)), satisfy the radiation condition at ∞, i.e., for any $x \in R^3$, there exists $c \in C^1$ such that when $t \to \infty$,

$$\psi(t \cdot x) = c \cdot \frac{e^{ikt \cdot |x|}}{t} + O(\frac{1}{t^2}). \tag{9}$$

The following theorem is well-known, and is a direct consequence of the Gauss theorem.

Theorem 2.1

Suppose that $\tilde{D} \subset D$ are two balls in R^3, and that D is bounded by a sphere S. Suppose further that $f : R^3 \setminus \tilde{D} \to C$ is a radiation field satisfying the equation (6)) in $R^3 \setminus \tilde{D}$ and the radiation condition (9)) at ∞. Then there exist two analytical functions $\sigma, \eta : S \to C$, such that for all $x \in R^3 \setminus D$,

$$f(x) = \int_S \sigma(s) \cdot f^k_s(x) ds, \tag{10}$$

and

$$f(x) = \int_S \eta(s) \cdot f^k_{s,N(s)}(x) ds, \tag{11}$$

where $N(s)$ denotes the exterior normal to S at the point s.

2.3. Spherical Bessel and Hankel functions. In agreement with standard practice, we will denote by j_m the spherical Bessel function of the first kind of order m, and by h_m, the spherical Hankel function of order m. As is well known (see, for example [17]), j_m are analytic on the whole complex plane for all values of m, while h_m have a branch cut along the negative real axis, and become infinite at the origin. The asymptotic behaviour of the functions j_m, h_m for large m is given by the formulae

$$\lim_{m \to \infty} j_m(z) \cdot \frac{2 \cdot (2n+1)^{n+1}}{z^n \cdot e^{n+\frac{1}{2}}} = 1, \tag{12}$$

and

$$\lim_{m \to \infty} h_m(z) \cdot \frac{e^{n+\frac{1}{2}} \cdot z^{n+1}}{\sqrt{2} \cdot (2n+1)^n} = 1 \tag{13}$$

(see [1], 9.3.1, 9.3.2, 9.1.3). For large z and fixed m, the asymptotic behavior of $j_m(z)$, $h_m(z)$ is given by the formulae

$$z \cdot j_m(z) - \cos(z - \frac{m\pi}{2} - \frac{\pi}{2}) = O(\frac{e^{|Im(z)|}}{|z|^2}), \tag{14}$$

$$z \cdot h_m(z) - e^{i\cdot(z-\frac{m\pi}{2}-\frac{\pi}{2})} = O(\frac{e^{-Im(z)}}{|z|^2}) \tag{15}$$

when $z \to \infty$, as long as $Im(z) \geq 0$ (see [1], 9.2.5, 9.2.7).

All spherical Bessel functions are 'elementary functions'. In particular,

$$\begin{aligned}
j_0(z) &= \frac{sin(z)}{z}, \\
h_0(z) &= -\frac{i \cdot e^{i\cdot z}}{z}, \\
j_1(z) &= \frac{sin(z)}{z^2} - \frac{cos(z)}{z}, \\
h_1(z) &= -(\frac{1}{z} + \frac{i}{z^2}) \cdot e^{i\cdot z}, \\
\frac{d}{dz} j_0(z) &= -j_1(z), \\
\frac{d}{dz} h_0(z) &= -h_1(z).
\end{aligned} \tag{16}$$

The following theorem is known as the Addition Theorem for spherical Bessel functions, and is one of principal analytical tools of this paper. It can be found, for example, in [1].

Theorem 2.2

Suppose that r, ρ, θ, λ are arbitrary complex numbers, $\eta = \pi - \theta$, and that $R \in C$ is defined by the formula

$$R = (r^2 + \rho^2 - 2 \cdot r \cdot \rho \cdot cos(\theta))^{\frac{1}{2}} = (r^2 + \rho^2 + 2 \cdot r \cdot \rho \cdot cos(\eta))^{\frac{1}{2}} \tag{17}$$

(see Figure 1). Then

$$\begin{aligned}
&\sum_{n=0}^{\infty} (2n+1) \cdot j_n(\lambda \cdot r) \cdot j_n(\lambda \cdot \rho) \cdot P_n(cos(\theta)) = \\
&\sum_{n=0}^{\infty} (-1)^n \cdot (2n+1) \cdot j_n(\lambda \cdot r) \cdot j_n(\lambda \cdot \rho) \cdot P_n(cos(\eta)) = \\
&j_0(\lambda \cdot R) = \frac{sin(\lambda \cdot R)}{\lambda \cdot R}.
\end{aligned} \tag{18}$$

and

$$\sum_{n=0}^{\infty}(2n+1)\cdot e^{\frac{1}{2}\cdot n\pi\cdot i}\cdot j_n(\rho)\cdot P_n(cos(\theta)) =$$

$$\sum_{n=0}^{\infty}(2n+1)\cdot i^n\cdot j_n(\rho)\cdot P_n(cos(\theta)) = e^{i\cdot\rho\cdot cos(\theta)}. \tag{19}$$

If, in addition, $|\, r\cdot e^{\pm i\cdot\theta}\,| < |\,\rho\,|$, then

$$\sum_{n=0}^{\infty}(2n+1)\cdot j_n(\lambda\cdot r)\cdot h_n(\lambda\cdot\rho)\cdot P_n(cos(\theta)) =$$

$$\sum_{n=0}^{\infty}(-1)^n\cdot(2n+1)\cdot j_n(\lambda\cdot r)\cdot h_n(\lambda\cdot\rho)\cdot P_n(cos(\eta)) = \tag{20}$$

$$h_0(\lambda\cdot R) = \frac{-i\cdot e^{i\cdot\lambda\cdot R}}{\lambda\cdot R}.$$

2.4. Integrals of spherical harmonics.

A function $\omega : S^2 \to C$ is referred to as a spherical harmonic of degree n if the function $f : R^3 \to C$ defined by the formula

$$f(x,y,z) = \omega(\theta,\phi)\cdot\rho^m \tag{21}$$

satisfies the Laplace equation in R^3 (see, for example, [9]).

Remark 2.1

As is well-known (see, for example, [10]), for any integer $n \geq 0$, there exist exactly $2n+1$ linearly independent spherical harmonics of order n, and a standard representation of a spherical harmonic of order n is by an expression

$$\omega(\theta,\phi) = \sum_{m=-n}^{n}\gamma_i\cdot P_n^m(cos(\theta))\cdot e^{i\cdot m\cdot\phi}, \tag{22}$$

with P_n^m the associated Legendre function of degree n and order m (see, for example, [1]), and $\gamma_i, i = 0, \pm1, \pm2, \cdots, \pm n$ a finite sequence of complex numbers. However, in this paper we will not be using the representation (22), remembering only that the spherical harmonics of order n constitute a complex linear space of dimension $2n+1$.

We will need the following three well-known lemmas involving the integration of spherical harmonics over the surface of the sphere. Lemmas 2.1, 2.2 below can be found, for example, in [9]), [1], respectively. Lemma 2.3 is a simple consequence of Lemma 2.2, and can be found in [1].

Lemma 2.1.

For any spherical harmonic Y of degree $n \geq 0$,

$$\int_{S^2} Y(s) \cdot P_n(cos(\theta(s)))ds = \frac{4 \cdot \pi}{2n+1} \cdot Y(s_N) \tag{23}$$

Lemma 2.2.

For any $n \geq 0$ and $z \in C$,

$$j_n(z) = \frac{(-i)^n}{2} \cdot \int_{S^2} e^{i \cdot z \cdot cos(\theta(s))} \cdot P_n(cos(\theta(s)))ds. \tag{24}$$

The following theorem is a simple consequence of the preceeding two lemmas, Theorem 2.2, and the formulae (12), (13).

Theorem 2.3.

Suppose that $\rho \in R$, n is a natural number, and $k \in C$ is such that $Im(k) \geq 0$. Suppose further that $u \in R^3$ is such that $\|u\| < \rho$, and that the functions $T_n : S^2 \rightarrow C$, $F_n : R^3 \rightarrow C$ are defined by the formulae

$$T_n(s) = T_n(\theta, \phi) = \sum_{m=0}^{n} i^m \cdot (2m+1) \cdot h_m(k \cdot \rho) \cdot P_m(cos(\theta)), \tag{25}$$

$$F_n(u) = \frac{1}{4 \cdot \pi} \cdot \int_{S^2} T_n(s) \cdot e^{i \cdot k \cdot (E(s),u)} ds. \tag{26}$$

Then

$$\lim_{n \rightarrow \infty} F_n(u) = h_0(k \cdot (\rho^2 + \|u\|^2 + 2 \cdot \rho \cdot \|u\| \cdot cos(\eta))^{\frac{1}{2}}), \tag{27}$$

with η the angle between the vector u and the z axis. Furthermore, for large n,

$$| F_n(u) - h_0(k \cdot (\rho^2 + \|u\|^2 + 2 \cdot \rho \cdot \|u\| \cdot cos(\eta))^{\frac{1}{2}}) = O((\frac{\|u\|}{\rho})^n). \tag{28}$$

Proof.

Combining (25) with (26), we have

$$F_n(u) = \frac{1}{4\cdot\pi}\cdot\sum_{m=0}^{n} i^m\cdot(2m+1)\cdot h_m(k\cdot\rho)\cdot\int_{S^2} T_n(s)\cdot P_m(cos(\theta))\cdot e^{i\cdot k\cdot(E(s),u)}ds, \quad (29)$$

and, substituting (19) into (29), obtain

$$F_n(u) = \frac{1}{4\cdot\pi}\cdot\sum_{m=0}^{n} i^m\cdot(2m+1)\cdot h_m(k\cdot\rho)\cdot \quad (30)$$
$$\int_{S^2} P_m(cos(\theta(s))) \cdot \sum_{l=0}^{\infty}(2l+1)\cdot e^{l\frac{\pi}{2}i}\cdot j_l(k\cdot\|u\|)\cdot P_l(c(P(u),s))ds$$

For any $m \neq l$,

$$\int_{S^2} P_m(cos(\theta(s)))\cdot P_l(c(P(u),s))ds = 0, \quad (31)$$

since in this case $P_m(cos(\theta(s)))$, $P_l(c(P(u),s))$ are two spherical harmonics of different degrees, and, therefore, orthogonal on S^2. Combining (30) with (31), we have

$$F_n(u) = \frac{1}{4\cdot\pi}\cdot\sum_{m=0}^{n}(2m+1)^2\cdot h_m(k\cdot\rho)\cdot j_m(k\cdot\|u\|) \quad (32)$$
$$\cdot\int_{S^2} P_m(cos(\theta(s)))\cdot P_m(c(P(u),s))ds.$$

Due to Lemma 2.1,

$$\int_{S^2} P_m(cos(\theta(s)))\cdot P_m(c(P(u),s))ds = \frac{4\cdot\pi}{(2m+1)}\cdot P_m(cos(\theta(P(u)))), \quad (33)$$

and (32) assumes the form

$$F_n(u) = \sum_{m=0}^{n}(2m+1)\cdot h_m(k\cdot\rho)\cdot j_m(k\cdot\|u\|)\cdot P_m(cos(\theta(P(u)))). \quad (34)$$

Now (27) follows from the combination of (34) and Theorem 2.2, and (28) follows from the combination of (27) with (12), (13).

2.5. Partial wave expansions of radiating fields. Suppose that the function $\phi : R^3 \to C^1$ satisfies the Helmholtz equation (1) outside an open ball D of radius R with the center at the point $x_0 \in R^3$, and also satisfies the radiation condition (9) at ∞. Then there

exists a unique sequence of spherical harmonics $\alpha = \{\alpha_m\}$, $m = 0, 1, 2, \cdots$, such that for any $x \in R^3 \setminus \bar{D}$,

$$\phi(x) = \sum_{m=0}^{\infty} \alpha_m(s) \cdot h_m(k\rho), \tag{35}$$

with (ρ, s) the spherical coordinates of the vector $x - x_0$, and for each $m \in [0, \infty)$, α_m a spherical harmonic of degree m.

If a function ψ satisfies the equation (6) inside D, then there exists a unique sequence of spherical harmonics $\beta = \{\beta_m\}, m = 0, 1, 2, \cdots$, such that for each m, β_m is a harmonic of degree m, and for any $x \in D$,

$$\psi(x) = \sum_{m=0}^{\infty} \beta_m(s) \cdot j_m(k\rho). \tag{36}$$

A derivation of the formulae (35), (36) can be found, for example, in [10], and we will refer to functions satisfying the Helmholtz equation as radiation fields, to expansions of forms (35), (36) as h-expansions and j-expansions respectively, and to the point x_0 as the center of the expansions (35) (36).

The following lemma is a direct consequence of the formulae (12), (13). It establishes the convergence rates of the expansions (35), (36).

Lemma 2.4

If $D_1 \subset D$ is a ball of radius $R_1 < R$ with the center at x_0 then there exists $c > 0$ such that for any $x \in D_1$ and $N > |k| \cdot R_1$,

$$|\phi(x) - \sum_{m=0}^{N} \alpha_m(\theta, \phi) j_m(k\rho)| < (\frac{R_1}{R})^N. \tag{37}$$

If $D_2 \supset D$ is a ball of radius $R_2 > R$ with the center at x_0 then there exists $c > 0$ such that for any $x \in R^2 \setminus \bar{D}_2$ and $N > |k| \cdot R$,

$$|\psi(x) - \sum_{m=0}^{N} \beta_m(\theta, \phi) h_m(k\rho)| < c(\frac{R}{R_2})^N. \tag{38}$$

Remark 2.2

In numerical calculations, expansions (35), (36) are truncated after a finite number of terms, and the resulting expressions are viewed as approximations to the fields ϕ, ψ. If we want to approximate ϕ by an expansion of the form (37) with an accuracy ϵ then according to the above lemma, we have to choose

$$N \geq \max(|k| \cdot R_1, \frac{-\ln(\epsilon) + \ln(c)}{\ln(R) - \ln(R_1)}). \tag{39}$$

Since logarithm is a very slowly growing function, for medium and large scale problems,

$$\max(R_1 \cdot |k|, \frac{-\ln(\epsilon) + \ln(c)}{\ln(R) - \ln(R_1)}) \sim R_1 \cdot |k|, \tag{40}$$

i.e. the number of terms in the approximation is almost independent of ϵ, and must be roughly equal to $|k|\ R_1$. A similar calculation shows that for medium to large scale problems, the expansion (36) can be truncated after approximately $N \geq |k|R$ terms.

2.6. Numerical integration on S^2.

In this subsection we formulate two lemmas describing the optimum quadrature formulas for two situations: smooth functions on a circle, and smooth functions on an interval. Then, we use these lemmas to construct a high-order quadrature formula on S^2 (Theorem 2.4 below). Both Lemmas 2.5, 2.6 are well-known, and can be found, for example, in [14].

Lemma 2.5

For any integer m, n such that $n \geq 2|m|$, the n-point trapezoidal quadrature rule on the interval $[0, 2\pi]$ integrates the function e^{imx} exactly.

Lemma 2.6

For any natural n, there exist a unique pair of finite sequences $\{\chi_i^n\}$, $\{w_i^n\}, i = 1, 2, \cdots, n$, such that for any integer $k \in [1, 2n-1]$,

$$\sum_{i=1}^{n} w_i^n \cdot (\chi_i^n)^k = \int_{-1}^{1} t^k dt. \tag{41}$$

Furthermore, $\chi_i^n \in [-1, 1]$ and $w_i^n \in [0, 1]$ for all $i = 1, 2, \cdots n$.

The points χ_i^n and the coefficients w_i^n are known as the nodes and coefficients of the n-point Gaussian quadrature rule, which is the unique n-point quadrature rule that integrates exactly all polynomials of order up to $2n-1$.

For a natural n, we will define a finite sequence $\phi_1, \phi_2, \cdots, \phi_n$ by the formula

$$\phi_j = \frac{2 \cdot \pi}{n} \cdot (j-1), \tag{42}$$

and the finite sequence $\theta_1, \theta_2, \cdots, \theta_n$ by the formula

$$\theta_j = arccos(w_j^n). \tag{43}$$

Now, we define a discretization of S^2 as a collection of n^2 points $s_{j,k}^n$ on it defined by the formula

$$s_{j,k}^n = (\theta_j, \phi_k), \tag{44}$$

and given a function $f : S^2 \to C$, will be approximately representing it by a table of n^2 values

$$f_{j,k}^n = f(\theta_j, \phi_k). \tag{45}$$

Our choice of this discretization scheme is motivated by the following theorem, which is an immediate consequence of Lemmas 2.5, 2.6.

Theorem 2.4.

Suppose that the function $f : S^2 \to C$ is a spherical harmonic of degree n. Then

$$\int_{S^2} f(s)ds = \sum_{j,k=1}^{n} w_{j,k}^n \cdot f_{j,k}^n, \tag{46}$$

with the coefficients $w_{j,k}$ defined by the formula

$$w_{j,k}^n = \frac{2 \cdot \pi}{n} \cdot w_j^n. \tag{47}$$

Furthermore, the condition (46) defines the nodes $s_{j,k}^n$ and the weights $w_{j,k}^n$ uniquely, except for obvious transpositions and rotations.

3. Translation Operators For h and j Expansions.

3.1. Sequences of spherical harmonics and functions on S^2. We will denote by Y the set of all sequences $\alpha = \{\alpha_m\}, \quad m = 0, 1, 2, \cdots$, such that for each m, α_m is a spherical harmonic of degree m. We will define a norm on Y via the formula

$$\|\alpha\| = \sqrt{(\sum_{m=0}^{\infty} \|\alpha_m\|^2)}, \tag{48}$$

denote by X the subspace of Y consisting of such sequences α that $\|\alpha\| < \infty$, and observe that the norm (48) converts X into a Hilbert space. For a real number $r > 0$, we will denote by X_r the subspace of X consisting of all sequences $\alpha = \{\alpha_m\}, m = 0, 1, 2, \cdots$, such that

$$\|\alpha_m\| \cdot (\frac{2m}{er})^m \cdot \sqrt{m} < c \tag{49}$$

for all $m \geq r$. We will denote by Y_r the subspace of Y consisting of all complex sequences $\beta = \{\beta_m\}, m = 0, 1, 2, \cdots$, such that for some $c > 0$,

$$\|\beta_m\| \cdot (\frac{er}{2m})^m \cdot \sqrt{m} < c \tag{50}$$

for all $m \geq r$. It is easy to see that $X_r \subset Y_r$, and that the condition (49) is a very restrictive one, since in order to satisfy it, the elements of the sequence $\{\alpha_m\}$ must decay roughly as $(r/2)^m/m!$, while the condition (49) is a very mild one - it prohibits the elements of $\{\beta_m\}$ from growing faster than approximately $(2/r)^m \cdot m!$. By applying formulae (9.3.1), (9.3.2) from [1], it is easy to show that in (35) (36), $\alpha \in Y_{|k|R}$ and $\beta \in Y_{|k|\ R}$. Conversely, for any sequence $\alpha \in Y_{|k|\ R}$, the expansion (35) converges inside D, and for any $\beta \in Y_{|k|\ R}$, the expansion (36), converges outside D. For a natural n, we will denote by T_n a linear mapping $Y_r \to Y_r$ converting a sequence $\alpha = \{\alpha_m\}, m = 0, 1, 2, \cdots$ into a sequence $\tilde{\alpha} = \{\tilde{\alpha}_m\}, m = 0, 1, 2, \cdots$, defined by the formulae

$$\begin{aligned} \tilde{\alpha}_m &= \alpha_m \quad for \quad |m| \leq n \\ \tilde{\alpha}_m &= 0 \quad for \quad |m| \geq n+1. \end{aligned} \tag{51}$$

Clearly, $T_n(Y_r) \subset X_r$, and for obvious reasons, we will refer to T_n as truncation.

We will define the mapping $F : X \to L^2(S^2)$ by the formula

$$F(\alpha)(s) = \sum_{m=0}^{\infty} \alpha_m(s) \cdot e^{-i \cdot \frac{(m+1) \cdot \pi}{2}}, \tag{52}$$

with $\alpha = \{\alpha_0, \alpha_1, \cdots\} \in X$, and the mapping $F_- : X \to L^2(S^2)$ by the formula

$$F_-(\alpha)(s) = \sum_{m=0}^{\infty} \alpha_m(s) \cdot e^{i \cdot \frac{(m+1)\cdot\pi}{2}}. \tag{53}$$

It is easy to see that the mappings F, F_- are unitary in the norm on X defined by (48), since the expansion into spherical harmonics is a unitary transformation, and any two spherical harmonics of different degrees are orthogonal to each other (see, for example, [9])).

The following lemma can be found (in a slightly different form) in [????]. It connects the speed of convergence of an expansion of the form (52) with the analyticity of its sum.

Lemma 3.1

Suppose that $\alpha \in X_r$ with some (arbitrarily large) r. Then $F(\alpha) : S^2 \to C$ is an analytic function on S^2.

While the definitions (52), (53) might seem arbitrary, they are motivated by the following two lemmas, which are a direct consequence of the formulae (14), (15).

Lemma 3.2

If $\phi : R^3 \setminus \bar{D} \to C^1$ is defined by (35), then

$$\lim_{t\to\infty} \phi(x_0 + t \cdot E(s)) \cdot t \cdot e^{-i\cdot k\cdot t} = F(\alpha)(s). \tag{54}$$

Lemma 3.3

Suppose that $\psi : D \to C^1$ is defined by (36), and that, in addition, $\beta \in X_a$ for some (arbitrarily large) a. Then

$$\lim_{t\to\infty} t \cdot (\psi(x_0 + t \cdot E(s)) - (F(\beta)(s) \cdot e^{i\cdot k\cdot t}) + F_-(\beta)(s) \cdot e^{-i\cdot k\cdot t}). \tag{55}$$

Remark 3.1

The above two lemmas can be viewed as describing the far-field behavior of the potentials ϕ, ψ in terms of the mappings $F(\alpha), F(\beta) : S^2 \to C$, and we will refer to $F(\alpha), F(\beta)$ as far-field

representations of ϕ, ψ, respectively. Alternatively, we will be calling $F(\alpha), F(\beta)$ far-field forms of expansions (35), (36).

For a point $s_0 \in S^2$, a natural n, and a complex z, we will define the function $\lambda_{s_0}^{z,n} : S^2 \to C^1$ by the formula

$$\lambda_{s_0}^{z,n}(s) = \sum_{m=0}^{n} i^m \cdot (2m+1) \cdot P_m(c(s_0, s) \cdot j_m(z). \tag{56}$$

It immediately follows from (19) that

$$\sum_{m=0}^{\infty} i^m \cdot (2m+1) \cdot P_j(c(s_0, s)) \cdot j_m(z) = e^{i \cdot z \cdot c(s_0, s)}, \tag{57}$$

and for $n = \infty$, (56) assumes the form

$$\lambda_{s_0}^{z,\infty}(s) = e^{i \cdot z \cdot c(s_0, s)}. \tag{58}$$

For a point $s_0 \in S^2$, a natural n, and a complex z, we will define the function $\mu_{s_0}^{z,n} : S^2 \to C^1$ by the formula

$$\mu_{s_0}^{z,n}(s) = \sum_{m=0}^{n} i^m \cdot (2m+1) \cdot P_m(c(s_0, s)) \cdot h_m(z), \tag{59}$$

and observe that no analogue of the formula (58) is possible in this case (at least in the proper sense), since the series

$$\sum_{m=0}^{\infty} i^m \cdot (2m+1) \cdot P_j(c(s_0, s)) \cdot h_m(z) \tag{60}$$

does not converge.

Finally, we will define mappings $\Lambda_{s_0}^{z,n}, M_{s_0}^{z,n} : L^2(S^2) \to L^2(S^2)$ via the formulae

$$\Lambda_{s_0}^{z,n}(f)(s) = \lambda_{s_0}^{z,n}(s) \cdot f(s), \tag{61}$$

$$M_{s_0}^{z,n}(f)(s) = \mu_{s_0}^{z,n}(s) \cdot f(s) \tag{62}$$

respectively, with $f \in L^2(S^2)$.

3.3. Definition of translation operators. For the remainder of this section, D_1, D_2, D_3 will denote three balls in R^3 such that $D_2 \subset D_1$ and $D_1 \cap D_3 = \emptyset$ (see Figure 3). The

centers and radii of these disks will be denoted by c_1, c_2, c_3 and R_1, R_2, R_3 respectively. We will denote the spherical coordinates of the vector $c_2 - c_1$ by (ρ_{12}, s_{12}), the spherical coordinates of the vector $c_1 - c_2$ by (ρ_{21}, s_{21}), the spherical coordinates of the vector $c_3 - c_1$ by (ρ_{13}, s_{13}), and the spherical coordinates of the vector $c_1 - c_3$ by (ρ_{31}, s_{31}). For a point $x \in R^3$, we will denote by (ρ_1, s_1), (ρ_2, s_2), (ρ_3, s_3) its spherical coordinates with respect to the centers c_1, c_2, c_3 respectively.

Suppose now that $\psi : R^3 \to C^1$ is a radiation field analytical in $R^3 \setminus \bar{D}_2$ and satisfying the radiation condition (9) at ∞. Suppose further that ψ is represented by an expansion

$$\psi(x) = \sum_{m=0}^{\infty} \beta_m(s_2) \cdot h_m(k\rho_2) \tag{63}$$

valid in $R^3 \setminus \bar{D}_2$, and by an expansion

$$\psi(x) = \sum_{m=0}^{\infty} \tilde{\beta}_m(s_1) \cdot h_m(k\rho_1) \tag{64}$$

valid in $R^3 \setminus \bar{D}_1$. It is easy to see that $\tilde{\beta} \in X_{|k|\cdot R_1}$ depends linearly on $\beta \in X_{|k|\cdot R_2}$, and we will denote by $U_{c2,c1}$ the operator $X_{|k|\cdot R_2} \to X_{|k|\cdot R_1}$ such that

$$\tilde{\beta} = U_{c2,c1}(\beta). \tag{65}$$

Suppose that $\phi : R^3 \to C^1$ is a radiation field analytical in D_1 and represented by an expansion

$$\phi(x) = \sum_{m=0}^{\infty} \alpha_m(s_1) \cdot j_m(k\rho_1) \tag{66}$$

valid in D_1, and by an expansion

$$\phi(x) = \sum_{m=0}^{\infty} \tilde{\alpha}_m(s_2) \cdot j_m(k\rho_2), \tag{67}$$

valid in D_2. Again, it is easy to see that $\tilde{\alpha} \in Y_{|k|\cdot R_2}$ depends linearly on $\alpha \in Y_{|k|\cdot R_1}$, and we will denote by $V_{c1,c2}$ the operator $Y_{|k|\cdot R_1} \to Y_{|k|\cdot R_2}$ such that

$$\tilde{\alpha} = V_{c1,c2}(\alpha). \tag{68}$$

For any $r > 0$, we will denote by $V^r_{c1,c2}$ the restriction of $V_{c1,c2}$ on the subspace X_r of $Y_{|k|\cdot R_1}$, so that

$$V^r_{c1,c2} = (V_{c1,c2})_{|X_r}. \tag{69}$$

Finally, suppose that $\psi : R^3 \setminus \bar{D}_1 \to C^1$ is a radiation field analytical outside the ball D_1 and satisfying the radiation condition (9) and that it is represented in $R^3 \setminus \bar{D}_1$ by the expansion (63). Then inside the ball D_3, the function ψ can be represented in the form

$$\psi(x) = \sum_{m=0}^{\infty} \gamma_m(s_3) \cdot j_m(k\rho_3) \tag{70}$$

with $\gamma \in Y_{|k|\cdot R_3}$ a linear function of $\alpha \in X_{|k|\cdot R_2}$, and we define the operator $W_{c1,c2} : X_{|k|\cdot R_1} \to Y_{|k|\cdot R_3}$ via the formula

$$\gamma = W_{c1,c3}(\alpha). \tag{71}$$

3.4. Diagonal Forms of Translation Operators. This subsection describes the diagonal forms of the translation operators U, V, W for the Helmholtz equation. These diagonal forms are provided by the Theorems 3.1 - 3.3 below, and are the principal purpose of this paper.

Theorem 3.1.

If the operator $U_{c2,c1} : X_{|k|\cdot R_2} \to X_{|k|\cdot R_1}$ is defined by the formula (65), then

$$U_{c2,c1} = F^{-1} \circ \Lambda_{s_{12}}^{k\cdot\rho_{12},\infty} \circ F. \tag{72}$$

Proof.

We will prove (72) by showing that

$$F \circ U_{c2,c1} = \Lambda_{s_{12}}^{k\cdot\rho_{12},\infty} \circ F. \tag{73}$$

Suppose that $s \in S^2$, and $\beta \in X_{kR_2}$. Combining (61) with (58), we have

$$\Lambda_{s_{12}}^{k\cdot\rho_{12},\infty}(s) = F(\beta(s) \cdot e^{i\cdot k\cdot R_{21}\cdot c(P(c_1-c_2),s)}. \tag{74}$$

On the other hand, due to Lemma 3.1,

$$\begin{aligned} F(\tilde{\beta})(s) &= \lim_{t\to\infty} \phi(c_1 + t\cdot E(s)) \cdot t \cdot e^{-i\cdot k\cdot t} \\ &= \lim_{t\to\infty} \phi(c_2 + (c_1 - c_2) + t\cdot E(s)) \cdot t \cdot e^{-i\cdot k\cdot t} \\ &= \lim_{t\to\infty} \phi(c_2 + \frac{u + t\cdot v}{\|u + t\cdot v\|} \cdot \|u + t\cdot v\|) \cdot t \cdot e^{-i\cdot k\cdot t}, \end{aligned} \tag{75}$$

with $u = c_1 - c_2$, and $v = E(s)$. Denoting $\|u + t \cdot v\|$ by τ, we obtain after simple analysis

$$t = \tau - (u,v) + O(\frac{1}{\tau}), \tag{76}$$

and (75) assumes the form

$$\begin{aligned} F(\tilde{\beta})(s) &= \lim_{\tau\to\infty} \phi(c_2 + \frac{u + (\tau - (u,v) + O(\frac{1}{\tau}))\cdot v}{\|u + (\tau - (u,v) + O(\frac{1}{\tau}))\cdot v\|} \cdot \tau) \\ &\cdot \ (\tau - (u,v) + O(\frac{1}{\tau}))\cdot e^{-i\cdot k\cdot(\tau - (u,v) + O(\frac{1}{\tau}))}, \end{aligned} \tag{77}$$

which, due to the radiation condition (9) can be reduced to

$$\begin{aligned} F(\tilde{\beta})(s) &= \lim_{\tau\to\infty} \phi(c_2 + \frac{u + (\tau - (u,v))\cdot v}{\|u + (\tau - (u,v))\cdot v\|} \cdot \tau) \\ &\cdot \ \tau \cdot e^{i\cdot k\cdot(u,v)} \cdot e^{-i\cdot k\cdot\tau}. \end{aligned} \tag{78}$$

Finally, combining Lemma 3.1 with (78) yelds

$$\begin{aligned} F(\tilde{\beta})(s) &= \lim_{\tau\to\infty} \phi(c_2 + \frac{v}{\|v\|} \cdot \tau)\cdot\tau\cdot e^{-i\cdot k\cdot\tau}\cdot e^{i\cdot k\cdot(u,v)} \\ &= \lim_{\tau\to\infty} \phi(c_2 + E(s)\cdot\tau)\cdot\tau\cdot e^{-i\cdot k\cdot\tau}\cdot e^{i\cdot k\cdot(c_1 - c_2, E(s))} \\ &= F(\beta)(s)\cdot e^{i\cdot k\cdot(c_1 - c_2, E(s))}. \end{aligned} \tag{79}$$

Now, the conclusion of the theorem follows from the combination of (79) with (74).

The above theorem provides the diagonal form of the operator U_{c_2,c_1} shifting the origin of an h - expansion. Theorem 3.2 below is the analogue of of Theorem 3.1 for the case of j-expansions. Since the proofs of the two theorems are virtually adentical, we omit the proof of the following theorem.

Theorem 3.2.

If the operator $V_{c1,c2} : Y_{|k|\cdot R_1} \to Y_{|k|\cdot R_2}$ is defined by the formula (68), then for any $\tau > 0$,

$$V_{c1,c2} = F^{-1} \circ \Lambda_{s_{12}}^{k\cdot\rho_{12},\infty} \circ F. \tag{80}$$

The following two lemmas are an immediate consequence of Theorems 3.1, 3.2. Lemma 3.4 provides the far-field representations of the potentials (7), (8) of charge and dipole. Given a

far-field representation of a potential of the form (36), Lemma 3.5 provides an expression of its value (and the value of its gradient) at any point within the region of its validity.

Lemma 3.4

Suppose that in (35),

$$\phi = \phi^k_{x_1}, \tag{81}$$

with x_1 an arbitrary point in R^3. Then for any $s \in S^2$,

$$F(\alpha)(s) = \lambda^{k\cdot\|x_0-x_1\|,\infty}_{P(x_0-x_1)}(s) = e^{i\cdot k\cdot(x_0-x_1,E(s))}. \tag{82}$$

If $h \in R^3$ is such that $\|h\| = 1$, and

$$\phi = \phi^k_{x_1,h}, \tag{83}$$

then for any $s \in S^2$,

$$\begin{aligned} F(\alpha)(s) &= \lambda^{k\cdot\|x_0-x_1\|,\infty}_{P(x_0-x_1)}(s)\cdot i\cdot k\cdot\frac{(x_0-x_1,E(s))}{\|x_0-x_1\|} \\ &= e^{i\cdot k\cdot(x_0-x_1,E(s))}\cdot i\cdot k\cdot c(P(x_0-x_1),s). \end{aligned} \tag{84}$$

Lemma 3.5

Suppose that the potential ψ is defined by (36), and that $\beta \in X_r$, with some $0 < r < \infty$. Then for any $x \in D$ and $h \in R^3$ such that $\|h\| = 1$,

$$\psi(x) = \int_{S^2} F(\beta)(s)\cdot\lambda^{k\cdot\|x_0-x\|,\infty}_{P(x_0-x)}(s)ds = \int_{S^2} F(\beta)(s)\cdot e^{i\cdot k\cdot(x_0-x,E(s))}ds. \tag{85}$$

and

$$\begin{aligned} \frac{d}{dt}\psi(x+t\cdot h)|_{t=0} &= \int_{S^2} F(\beta)(s)\cdot\lambda^{k\cdot\|x_0-x\|,\infty}_{P(x_0-x)}(s)\cdot i\cdot k\cdot\frac{(x_0-x,E(s))}{\|x_0-x\|}ds \\ &= \int_{S^2} F(\beta)(s)\cdot e^{i\cdot k\cdot(x_0-x,E(s))}\cdot i\cdot k\cdot c(P(x_0-x),s)ds. \end{aligned} \tag{86}$$

While the preceeding two theorems are fairly obvious, and appear to be known (though in a somewhat different form) among certain groups of physicists, the following theorem is considerably more technical, and appears to be quite new.

Theorem 3.3.

Suppose that the operator $W_{c1,c3} : X_{|k|\cdot R_1} \to Y_{|k|\cdot R_3}$ is defined by the formula (71). Suppose further that $\psi : R^3 \setminus \bar{D}_1 \to C$ is a radiation field represented by the expansion (64) outside D_1, and by the expansion (70) inside D_3. For any $n \geq 1$, we will denote by ψ_n the radiation field $D_3 \to C$ defined by the formula

$$\psi_n(x) = \sum_{m=0}^{\infty} \gamma_m^n(s_3) \cdot j_m(k\rho_3), \tag{87}$$

with $\gamma^n = \{\gamma_1^n, \gamma_2^n, \gamma_3^n, \cdots\}$ defined by the formula

$$\gamma^n = F^{-1} \circ M_{s_{13}}^{k\cdot\rho_{13},n} \circ F(\alpha). \tag{88}$$

Then for any $x \in D_3$,

$$\lim_{n\to\infty} \psi_n(x) = \psi(x). \tag{89}$$

Furthermore,

$$\max_{D_3} | \psi_n(x) - \psi(x) | = O((\frac{R_1 + R_3}{R_{13}})^n \cdot \|\alpha\|). \tag{90}$$

Proof.

Due to Theorem 2.1, it is sufficient to prove (90) in the special case of

$$\psi = f_{x_0}^k, \tag{91}$$

with X_0 an arbitrary point in D_1. Combining (91) with (82), we have

$$F(\beta)(s) = e^{i\cdot k\cdot(x_0 - c_1, E(s))} \tag{92}$$

for all $s \in S^2$, and combining (92) with (62), (59), obtain

$$M_{s_{1,3}}^{k\cdot\rho_{13},n} \circ F(\beta)(x) = \tag{93}$$

$$e^{i\cdot k\cdot(x_0 - c_1, E(s))} \cdot \sum_{m=0}^{n} i^m \cdot (2m+1) \cdot P_m(c(s_{13}, s)) \cdot h_m(k \cdot \rho_{13}). \tag{94}$$

Now, combining (93) with (85), (87), we have

$$\psi_n(x) = \int_{S^2} e^{i\cdot k\cdot(x_0-c_1,E(s))} \cdot e^{i\cdot k\cdot(x-c_3,E(s))} \cdot \sum_{m=0}^{n} i^m \cdot (2m+1) \cdot P_m(c(s_{13},s)) \cdot h_m(k\cdot\rho_{13}), \tag{95}$$

and (90) follows from the combination of (95) and Theorem 2.3.

3.5. Numerical evaluation of translation operators. For the rest of this paper, we will view the asymptotic representations $F(\alpha)$, $f(\beta)$ defined by (52 (as opposed to the expansions of the forms (35, (36) as our principal tool for representing radiation fields. Lemma 3.4 permits one to calculate asymptotic representations of fields of distributions of charges and dipoles without evaluating the coefficients of their h-expansions, and Lemma 3.5 provides a tool for calculating the fields and derivatives of the fields with given asymptotic representations without having to evaluate the coefficients of j-expansions of these fields.

For a radiation field $\psi : R^3 \to C^1$ analytical outside D_1 given by the expansion (35), and an integer $n \geq 2$, we will denote by F^n_{ψ,c_1} the function $F(\alpha)$ tabulated at the n^2 nodes $s^n_{j,k}$ defined by the formulae (42) - (44), so that

$$F_{\phi,c_1}(j,k) = F(\alpha)(s^n_{j,k}). \tag{96}$$

Similarly, for a radiation field ϕ analytical inside D_1 and possessing an asymptotic representation $F(\beta)$, we will denote by G^n_{ϕ,c_1} the table of n^2 complex numbers defined by the formula

$$G_{\phi,c_1}(j,k) = F(\beta)(s^n_{j,k}). \tag{97}$$

and view F^n_{ψ,c_1}, G^n_{ϕ,c_1} as finite-dimensional projections of the asymptotic representations of the radiation fields ψ, ϕ.

Given a discretization G^n_{ϕ,c_1}, we will consider a radiation field $\tilde{G}^n_{\psi,c_1} : R^3 \to C^1$ defined by the formula

$$\tilde{G}^n_{\phi,c_1}(x) = \sum_{j,k=1}^{n} w^n_{j,k} G^n_{\phi,c_1}(j,k) \cdot e^{i\cdot k\cdot(x_0-x,E(s^n_{j,k}))}. \tag{98}$$

Clearly, (98) is a quadrature formula approximating the integral (85) and we will look upon (98) as an approximation to the field ϕ. Differentiating (98) with respect to x, we obtain the formula

$$\frac{d}{dt}\bar{G}^n_{\phi,c_1}(x+th)_{|t=h} =$$
$$i\cdot k\cdot\|h\|\cdot\sum_{j,k=1}^{n} w^n_{j,k}G^n_{\phi,c_1}(j,k)\cdot c(P(x_0-x),s)\cdot e^{i\cdot k\cdot(x_0-x,E(s^n_{j,k}))}. \tag{99}$$

Finally, we will define mappings $P^{mn}_{c_2c_1}, Q^{mn}_{c_1c_2}, S^{mn}_{c_1c_3} : C^n \to C^n$ by the formulae

$$P^{mn}_{c_2c_1}(z_1,z_2,\cdots,z_n) = (\lambda_m(w_1)\cdot z_1, \lambda_m(w_2)\cdot z_2,\cdots,\lambda_m(w_n)\cdot z_n), \tag{100}$$

$$Q^{mn}_{c_1c_2}(z_1,z_2,\cdots,z_n) = (\mu_m(w_1)\cdot z_1, \mu_m(w_2)\cdot z_2,\cdots,\mu_m(w_n)\cdot z_n), \tag{101}$$

$$S^{mn}_{c_1c_3}(z_1,z_2,\cdots,z_n) = (\nu_m(w_1)\cdot z_1, \nu_m(w_2)\cdot z_2,\cdots,\nu_m(w_n)\cdot z_n), \tag{102}$$

with the functions λ_m, μ_m, defined by (56), (59). It is easy to see from the Theorems 3.1, 3.2, 3.3 that

$$P^{mn}_{c_2c_1}(F^m_{\psi,c_2}) = F^m_{U,c_1}, \tag{103}$$

$$Q^{mn}_{c_1c_2}(G^n_{\psi,c_1}) = G^n_{V,c_2}, \tag{104}$$

$$S^{mn}_{c_1c_3}(F^m_{\psi,c_1}) = G^n_{W,c_3}, \tag{105}$$

with $U = \psi^m_{c_2c_1}$, $V = \phi^m_{c_1c_2}$, $W = \bar{\psi}^m_{c_1c_3}$ and we will look upon the operators $P^{mn}_{c_2c_1}, Q^{mn}_{c_1c_2}, S^{mn}_{c_1c_3}$ as discretizations of diagonal forms of the operators $U^{mn}_{c_2c_1}, V^{mn}_{c_1c_2}, W^{mn}_{c_1c_3}$.

Remark 3.5

By combining the above lemma with Remark 3.1, it is easy see that the number n of nodes in the discretization G^n_{ϕ,c_1} of the function $G_{\phi,c_1} : [0,2\pi] \to C^1$ has to be approximately equal to $2|k|R_1$, and is almost independent of the accuracy ϵ with which the field ϕ is being calculated.

Lemmas 3.5 - 3.7 provide a tool for shifting the origins of asymptotic expansions of radiation fields, and for converting asymptotic representations of the form (3.32) into asymptotic representations of the form (3.38) for a cost proportional to n, where n is the number of nodes

in the discretization (3.48) of the interval $[0, 2\pi]$. In the following two sections, this apparatus is used to construct an algorithm for rapid evaluation of integral operators of Section 2.

4. Rapid Evaluation of Radiation Fields of Charge Distributions

In this section, we describe an algorithm for rapid evaluation of the field and the normal derivative of the field created on a surface $\Gamma \subset R^3$ by charge and dipole distributions on that same curve. For definitiveness, we will be discussing the evaluation of the field created by a charge distribution. The algorithms evaluating the normal derivative of the field created by a charge distribution, and the field and the normal derivative of the field created by a dipole distribution are quite similar.

4.1. Notation. We will consider the situation depicted in Figure 4. The surface $\Gamma \subset R^3$ is discretized into N equispaced nodes $x_1, x_2, \cdots, x_N$, and we will assume that these nodes are distributed on the surface in a roughly uniform manner. Suppose that for each $i = 1, 2, \cdots, N$, a charge a_i of strength σ_i is located at the point x_i. In this section, we describe an algorithm for rapid calculation of approximations $g_i = 1, 2, \cdots, N$ to the sums

$$G_\sigma(x_i) = \sum_{j=1,\ j\neq i}^{N} \sigma_j \phi^k_{x_j}(x_i) \tag{106}$$

for $i = 1, 2, \cdots, N$. Clearly, this is an order N^2 process (evaluating N fields at n points). However, if we are interested in evaluating (106) with a finite accuracy (which is always the case in practical calculations), Theorem 3.1 and Lemmas 3.7, 3.8, 3.9 can be used to speed up the process.

For an integer $m \geq 2$, we will define the points $t_1, t_2, \cdots, t_{m+1}$ on the interval $[0, L]$ by the formula $t_i = (i-1)L/m$, subdividing the interval $[0, L]$ into m segments of equal length, and denote the center of the i-th segment by z_i, so that $z_i = t_i + L/(2m)$. For each natural $j = 1, 2, \cdots, m$, we will denote by A_j the set of all charges a_i such that $x_i \in \gamma([t_j, t_{j+1}])$, and by D_j the circle of radius $r = L/(2m)$ with the center at $\gamma(z_j)$. We will denote by W_j the union of all A_i such that $\|z_j - z_i\| > 3r$, and by $\bar{W}_j$ the union of all A_i such that $\|z_j - z_i\| \leq 3r$. Obviously, $A_j \subset D_j$ for any $j = 1, 2, \cdots, m$. Also, it follows from the triangle inequality that

$$\min_{x\in A_i,\ y\in A_j} \|x - y\| \geq r \tag{107}$$

for any i, j such that $A_i \subset W_j$. Finally, we will denote by ϕ_j the field of all charges a_i such that $x_i \subset A_j$ and observe that if $x_p \in A_j$ then

$$G_\sigma(x_p) = \sum_{A_i \subset W_j} \phi_i(x_p) + \sum_{x_i \in \bar{W}_j} \sigma_i \phi^k_{x_i}(x_p). \tag{108}$$

4.2. Detailed description of an order $N^{3/2}$ algorithm. In this subsection, M, N will denote "sufficiently large" integer numbers. The actual choice of the numbers M, N is discussed in the following subsection.

We will evaluate the fields (106) in five steps.

Step 1.

Using Lemma 3.4, obtain discretized asymptotic representations $F^N_{\phi_j, \gamma(z_j)}$ of the fields ϕ_j for all $j = 1, 2, \cdots, m$.

Step 2

For every pair of natural numbers $i, j \in [1, m]$ such that $A_i \subset W_j$, calculate the representation

$$G^N_{\psi_{ij}, \gamma(z_j)} = S^{M,N}_{\gamma(z_i), \gamma(z_j)}(F^N_{\phi_j, \gamma(z_j)}) \tag{109}$$

of the field $\psi_{ij} = \bar{\phi}^M_{\gamma(z_i), \gamma(z_j)}$ and view it as a finite- dimensional approximation to the asymptotic representation of the field ϕ_i on D_j.

Step 3

For each natural $j \in [1, m]$, calculate the sum

$$G^N_{\psi_j, \gamma(z_j)} = \sum_{A_i \subset W_j} G^N_{\psi_{ij}, \gamma(z_j)}, \tag{110}$$

and view the field $\psi_j = \sum_i \psi_{ij}$ as an approximation to the field $\sum_{A_i \subset W_j} \phi_i$, and $G^N_{\psi_j, \gamma(z_j)}$ as a finite-dimensional approximation to the asymptotic representation of ψ_j on D_j.

Step 4

For each natural $j \in [1, m]$, evaluate

$$\tilde{\psi}_j(x_i) = \tilde{G}_{\psi_j, \gamma(z_j)}(x_i) \tag{111}$$

for all i such that $x_i \in \gamma([t_j, t_{j+1}])$ and look upon (111) as an approximation to $\psi_j(x_i)$.

Step 5.

For each $j = 1, 2, \cdots, m$, evaluate the sum

$$\tilde{\psi}_j(x_i) + \sum_{x_p \in \tilde{W}_j} \sigma_p \phi^k_{x_p}(x_i) \tag{112}$$

for all i such that $x_i \in \gamma([t_j, t_{j+1}])$, and view (112) as an approximation to $G_\sigma(x_i)$.

4.3. Choice of parameters and CPU time estimate. In the estimates below, a, b, c, d, e are coefficients determined by the computer system, language, particular implementation of the algorithm, etc.

Step 1

Obviously, this step will require order $n \cdot N$ operations (tabulating $F^N_{\phi_j, \gamma(x_j)}$ at N nodes on the interval $[0, 2\pi]$ for each of the nodes $x_1, x_2, \cdots, x_n$). According to the Remark 3.5, $N \sim |k| \cdot L/m$, and the CPU time estimate for this step becomes $a \cdot n \cdot |k| \cdot L/m$.

Step 2

For each of the pairs i, j such that $A_j \subset W_i$, evaluating (4.3) will require order N operations (see (3.54)), and the total number of such pairs is less than m^2, which results in the CPU time estimate of $b \cdot m^2 \cdot n \sim b \cdot m^2 \cdot |k| \cdot L/m = b \cdot m \cdot |k| \cdot L$ for this step.

Step 3

Obviously, evaluating the sums (4.4) for all $j = 1, 2, \cdots, m$ is an order $c \cdot m \cdot N \sim c \cdot m \cdot |k| \cdot L/m = c \cdot |k| \cdot L$ procedure.

Step 4

Evaluating (4.5) for each $i = 1, 2, \cdots, n$ is an order N procedure, resulting in the total CPU time estimate for this step of $d \cdot n \cdot N \sim d \cdot n \cdot |k| \cdot L/m$.

Step 5

Evaluating the sum (4.6) for each $i = 1, 2, \cdots, n$ is an order n/m procedure, with the resulting CPU time estimate of $e \cdot n^2/m$ for this step.

Summing up the time estimates for the steps 1-5, we obtain the following time estimate for the whole process:

$$T = A \cdot n \cdot |k| \cdot L/m + b \cdot m \cdot |k| \cdot L + c \cdot |k| \cdot L + \frac{e \cdot n^2}{m}, \tag{113}$$

with $A = a+d$, and we would like to choose m in such a manner that (4.7) would be minimized. Differentiating (4.7) with respect to m, and setting the resulting derivative to zero, we obtain

$$m_{\min} = \sqrt{\frac{A \cdot n \cdot |k| \cdot L + e \cdot n^2}{b \cdot |k| \cdot L}} \tag{114}$$

and the corresponding minimum of (4.7) is equal to

$$T_{\min} = 2\sqrt{A \cdot n \cdot |k| \cdot L + e \cdot n^2} \cdot \sqrt{b \cdot |k| \cdot L} + c \cdot |k| \cdot L. \tag{115}$$

If the calculations are performed with a fixed number of nodes per wavelength (which is often a reasonable assumption), n is proportional to $|k|L$, and (4.9) assumes the form

$$T_{\min} \sim (|k| \cdot L)^{\frac{3}{2}}, \tag{116}$$

or

$$T_{\min} \sim n^{\frac{3}{2}}, \tag{117}$$

which for large n is considerably smaller than N^2.

4.4. Further reduction of the CPU time estimate of the process. The approach of the above subsection can be used recursively by subdividing each of the sets A_i into subsets $\{B_{ij}\}, j = 1, 2, \cdots, \bar{m}$ with appropriately chosen $\bar{m}$ and representing the fields ϕ_i as sums $\phi_i = \sum_i \phi_{ij}$ where ϕ_{ij} is the field created by all charges a_p such that $a_p \in B_{ij}$. A calculation similar to the one in the preceeding section shows that such an algorithm will have an asymptotic CPU time estimate of $n^{4/3}$.

In [11], such subdivision process is used recursively to obtain an order n algorithm for numerical evaluation of integral operators of classical potential theory (Laplace's equation). By reproducing the construction of Section VII of [11] almost literally, one can obtain an order $n\log(n)$ algorithm for evaluating (4.1). However, our estimates indicate that for problems of practicable size ($n \leq 1000,000$), the improvement in actual computation times obtained by replacing an order $n^{4/3}$ algorithm with an order $n \log n$ algorithm would not be very significant.

References

[1] M. Abramovitz, I. Stegun, *Handbook of Mathematical Functions*, Applied Math. Series (National Bureau of Standards), Washington, DC, 1964.

[2] B. Alpert and V. Rokhlin, *A fast algorithm for the evaluation of Legendre expansions*, SIAM J. Sci. Stat. Comput., 12:158-179 (1991).

[3] B. Alpert, G. Beylkin, R. Coifman, V. Rokhlin, *Wavelets for the fast solution of second-kind integral equations*, Technical Report 837, Yale University, Department of Computer Science, 1990, (to appear SIAM J. Sci. Stat. Comput.)

[4] G. Beylkin, R. Coifman, and V. Rokhlin, *Fast wavelet transforms and numerical algorithms I*, Communications on Pure and Applied Mathematics, 14:141-183 (1991).

[5] J. Carrier, L. Greengard and V. Rokhlin, *A fast adaptive multipole algorithm for particle simulations*, SIAM J. Sci. Stat. Comput., 9(4), 1988.

[6] L. Greengard and V. Rokhlin, *A fast algorithm for particle simulations*, Journal of Computational Physics, 73:325-348 (1987).

[7] L. Greengard and V. Rokhlin, *On the Efficient Implementation of the Fast Multipole Algorithm*, Technical Report 602, Yale University, Department of Computer Science, 1988.

[8] L. Greengard, J. Strain, *The Fast Gauss Transform*, SIAM J. Sci. Stat. Comput., 12:79-94 (1991).

[9] E. W. Hobson, *The Theory of Spherical and Ellipsoidal Harmonics*, Chelsea, New York, 1955.

[10] N.S. Koshliakov, M.M. Smirnov, E.B. Gliner, *Differential Equations of Mathematical Physics*, North-Holland, Amsterdam, 1964.

[11] V. Rokhlin, *Rapid Solution of Integral Equations of Classical Potential Theory*, Journal of Computational Physics, 60(2) : 187 (1985).

[12] V. Rokhlin, *A Fast Algorithm for the Discrete Laplace Transformation* , Journal of Complexity, v. 4 pp. 12-32 (1988).

[13] V. Rokhlin, *Rapid Solution of Integral Equations of Scattering Theory in Two Dimensions*, Journal of Computational Physics, 86(2) : 414 (1990).

[14] J. Stoer and R. Bulirsch, *Introduction to numerical analysis*, Springer-Verlag, New York, 1980.

[15] J. Strain, *The Fast Laplace Transform Based on Laguerre Functions*, to appear in Math. Comp.

[16] J. Strain, *The Fast Gauss Transform with Variable Scales*, SIAM J. Sci. Stat. Comput., 12 : 1131-1139 (1991).

[17] G.N. Watson, *A Treatise on the Theory of Bessel Functions*, Cambridge University Press, Cambridge, 1980.

FIGURE 1

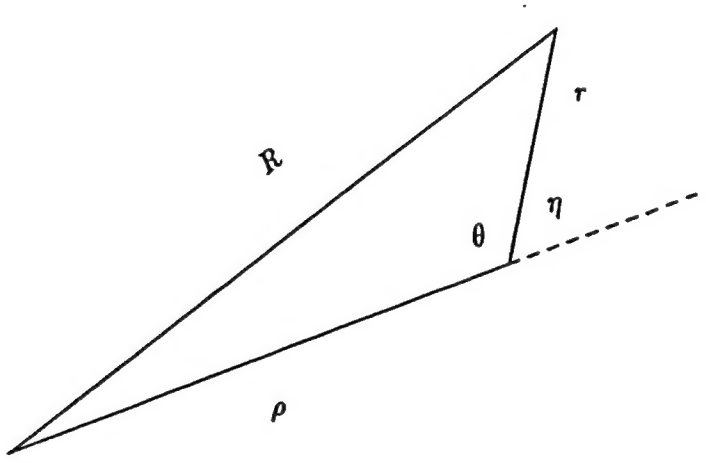

FIGURE 2

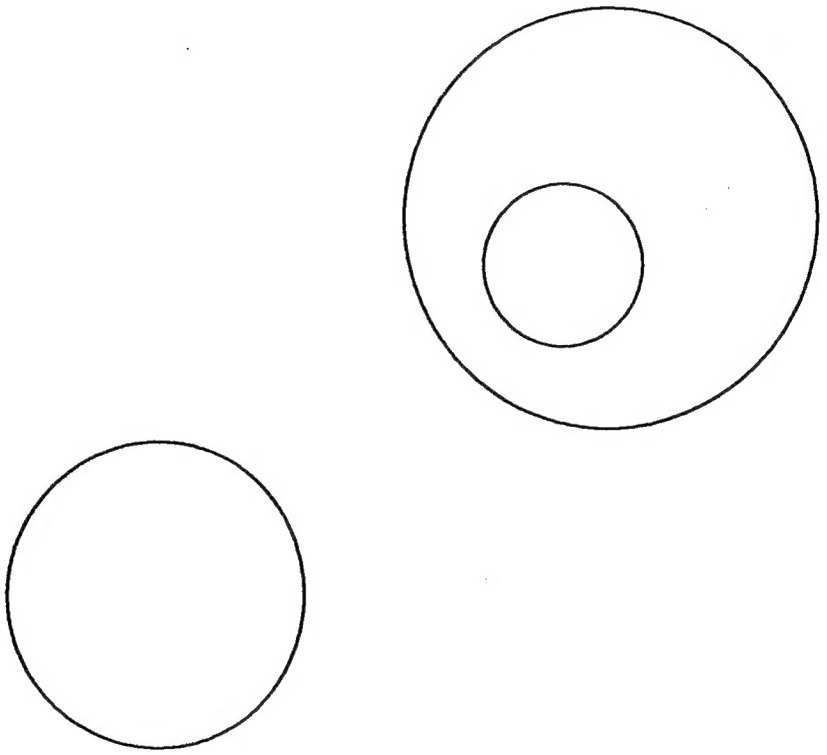

FIGURE 3

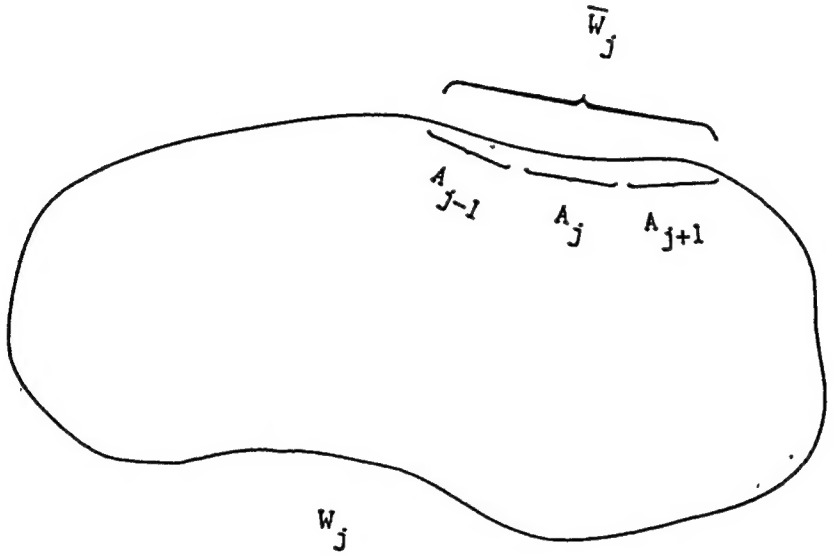

Definition of the Sets A_j, $\bar{W}_j$, W_j